Resource utilisation and the evolution of antifungal resistance in *Candida* species

Submitted by Sarah Jennifer Nicola Duxbury to the University of Exeter as a thesis for the degree of Doctor of Philosophy in Biological Sciences in September 2017.

I certify that all material in this thesis which is not my own work has been identified and that no material has previously been submitted and approved for the award of a degree by this or any other University.

Signature……

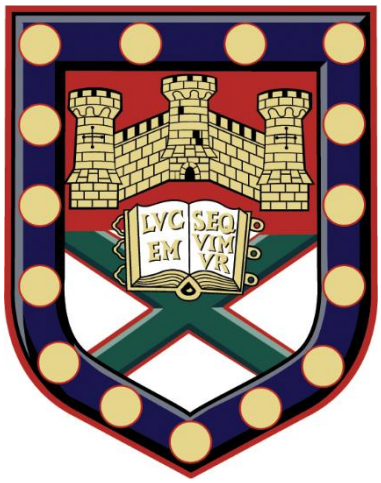

Abstract

Fungal pathogens, particularly species of the *Candida* genus, are responsible for superficial infections and invasive disease in humans, the latter of which is responsible for more deaths than tuberculosis or malaria. Despite this, fungal infections receive considerably less research attention than those of bacteria. Mixed-*Candida* species infections are increasing in prevalence, and occur as secondary infections in HIV and cancer patients. Resources are important in infection environments, in which competition between species and interactions with the host can influence community composition. After *C. albicans, C. glabrata* is the second most commonly isolated species, which colonises different host sites and patients and rapidly develops drug resistance. In this thesis, we investigate competition between *C. albicans* and *C. glabrata* in clinically-relevant *in vitro* cultures and in an invertebrate model. We then measure *in vitro* growth of *C. glabrata* strains over different glucose concentrations and the influence on virulence and antifungal adaptation. Following culture propagation in environments containing antifungal drug, we analyse *C. glabrata* fitness in evolved populations.

We found that outcomes of short and long-term competition between *C. albicans* and *C. glabrata* were dependent on resource level in clinically-relevant media, with *C. albicans* favoured at low and *C. glabrata* favoured at high glucose (Chapter 2). *C. glabrata* clinical strains varied in competitive abilities (Chapter 2), and in their strength of interaction with *C. albicans* evidenced by differing levels of host survival in dual-species infections of the wax moth *Galleria mellonella* (Chapter 3). For growth on glucose, we identified a strain of *C. glabrata* (3605) isolated from a diabetic patient that had a significantly greater growth rate but lower final growth density than a lab reference strain (2001) (Chapter 4). We found that a higher growth density was correlated with greater virulence and adaptability to the antifungal caspofungin (Chapters 4 and 5). Finally, we found that caspofungin resistance could incur fitness costs and that sub-population variation in phenotypic adaptations evolved in parallel populations. These results improve understanding of microbial species interactions in infections by considering effects of resource levels and pathogen growth strategies on competitive abilities, virulence and antifungal resistance.

This could lead to better characterisation of fungal infections and evolutionary adaptations in different host environments.

Acknowledgements

My PhD has been a challenging yet rewarding and invaluable opportunity to develop as an independent scientist over the past four years and for this I would like to thank a number of people. My greatest thanks go to my primary supervisor Professor Ivana Gudelj for all her guidance and support and the inspiration drawn from our many discussions. I would also like to thank my seconday supervisors Professor Ken Haynes for his advice on my research during the early part of my PhD, and Dr. Steve Bates for training in the use of the wax moth *Galleria mellonella* as an infection model and for his continued support. Thanks also go to Professor Rob Beardmore for all his valuable research advice during my presentations in the Gudelj/Beardmore group meetings.

I would also like to thank all past and present members of the Gudelj, Beardmore and Haynes groups in Lab 309 and Office 322 for help with experimental work and data analysis and for their companionship. In particular, I would like to thank Emily Cook for training me in *Candida* species culturing and competition experiments. Thanks also go to Dr. Carlos Reding-Roman for all his help and discussions on Matlab data analysis and for the model fits for my data. Thank you to Dr. Richard Lindsay for all his guidance with molecular techniques and gene sequencing and for our many informal discussions.

Thanks also to BBSRC for providing the funding for my research and the fantastic opportunities to attend national and international meetings and meet many inspirational scientists. Thanks to the University of Exeter for providing the research facilities and opportunities to attend several interesting seminars.

Last but not least, I would also like to thank my parents for all their support and encouragement and my sister, Elizabeth, for all her invaluable advice on the PhD process.

Table of Contents

Abstract 2
Acknowledgements 4
Table of Contents 5
List of Figures 10
List of Tables 15
List of Abbreviations 18
Publications 20
1. Chapter 1: Introduction 21
1.1 Fungi as Pathogens of Humans 21
1.2 Microbial Species Interactions in Infections 22
1.3 Laboratory Evolution of Microbial Species 24
1.4 *Candida* Species Biology and Epidemiology 24
1.5 Thesis Aims and Outline 28
2. Chapter 2: Population Dynamics of *In vitro* Resource Competition between *C. glabrata* and *C. albicans* in Clinically Relevant Environments 31
2.1 Introduction 31
2.2 Aims of the Chapter 34
2.3 Materials and Methods 35
2.3.1 *Candida* Strains and Growth Conditions 35
2.3.2 One-Season Resource Competition in Synthetic Urine Media 36
2.3.3 Long-Term Competition in Synthetic Urine Media 37
2.3.3.1 Volumetric Serial Transfers 37
2.3.3.2 Cell Density Serial Transfers 37
2.3.4 Clinical Strain Competitions 38
2.3.5 Competitions in Sterile Culture Tubes 38
2.3.6 Data Analysis and Statistics 39
2.4 Results 41
2.4.1 One-Season Glucose Competitions in Mixed-*Candida* Species Environments 41
2.4.2 Competition in SU Media: CHROMagar Plating 43
2.4.3 Long-Term Competition Dynamics in Clinically Relevant SU Media 46
2.4.4 Influence of Small Frequency and Density Changes on Long-Term Competition Dynamics 49

2.4.5 Influence of Larger Density Changes on One Season Competition Dynamics 50
2.4.6 Influence of Larger Competition Volumes on One Season Population Dynamics 53
2.4.7 Competitions between *C. albicans* and Clinical Isolates of *C. glabrata* 56
2.5 Discussion 59
2.6 Conclusions of the Chapter 65
3. Chapter 3: Dual *Candida* Species Interactions in the Host Model *Galleria mellonella* 66
3.1 Introduction 66
3.2 Aims of the Chapter 70
3.3 Materials and Methods 72
3.3.1 *Galleria mellonella* Larvae 72
3.3.2 Single *Candida* Species Infection in *G. mellonella* 72
3.3.3 Dual *Candida* Species Infection in *Galleria mellonella*: Replication of Experiments Described by Rossoni *et al.* (2015) 73
3.3.4 Dual Species *G. mellonella* Infection with Different Doses and Strains 74
3.3.5 Host Melanisation Response 75
3.3.6 Statistical Analyses 76
3.4 Results 77
3.4.1 Single *Candida* Species Infection of *G. mellonella*: Dose and Temperature-Dependent Effects 77
3.4.2 Dual *Candida* Species Infection in *Galleria mellonella*: Replication of Experiments from Rossoni *et al.* (2015) 78
3.4.3 Dual *Candida* Species Infection of *G. mellonella*: Manipulating Species Ratio, Total Infective Dose and Species Strains 80
3.4.4 Strain-Dependent Dual *Candida* Species Interactions in *G. mellonella* 85
3.4.5 Comparative Virulence and Host Melanisation Response across *C. glabrata* Strains 89
3.5 Discussion 91
3.6 Conclusions of the Chapter 95

4. Chapter 4: Growth Kinetics of *C. glabrata* Clinical Strains and the Evolution of Antifungal Resistance 96
4.1 Introduction 96
4.2 Aims of the Chapter 100
4.3 Materials and Methods 102
4.3.1 Cell Growth in Synthetic Complete Medium at Different Glucose Concentrations 102
4.3.1.1 Media and Stock Solutions 102
4.3.1.2 *Candida glabrata* Strains 102
4.3.1.3 Single Season Cell Growth Assays 103
4.3.1.4 Data Analysis and Statistics 104
4.3.2 Comparative Virulence of *C. glabrata* Strains 105
4.3.3 *In vitro* Experimental Evolution of Populations of *C. glabrata* Strains 2001 and 3605 on a Gradient of Caspofungin Concentrations 106
4.4 Results 109
4.4.1 Resource-Dependent Growth Kinetic Relationships across and within *C. glabrata* Strains 109
4.4.2 Comparative Virulence of *C. glabrata* Strains 2001 and 3605 117
4.4.3 Experimental Evolution of Populations of *C. glabrata* Strains 2001 and 3605 Across a Gradient of Caspofungin Concentrations 118
4.5 Discussion 125
4.6 Conclusions of the Chapter 131
5. Chapter 5: Fitness Costs and Adaptations in Experimental Evolution of Caspofungin Resistance in *C. glabrata* Strain 2001 132
5.1 Introduction 132
5.2 Aims of the Chapter 136
5.3 Materials and Methods 137
5.3.1 Revival of Experimentally-Evolved Populations of *C. glabrata* Strain 2001 from Caspofungin Dosing 137
5.3.2 Growth Profiling of Single Colonies in the Absence of Caspofungin 138
5.3.3 Data Analysis and Statistics 139
5.3.4 Phenotyping of Caspofungin-Evolved Colony Variants 140
5.3.4.1 Colony Morphology 140
5.3.4.2 Growth on Different Carbon Substrates 140

5.3.4.3 *Galleria mellonella* Survival Assay 140
5.3.4.4 Dose Response Profiling 141
5.3.5 Genotyping of Caspofungin Resistance Targets in Single Colonies 142
5.3.5.1 Genomic DNA Extraction 142
5.3.5.2 PCR Amplification of Gene Targets and Gel Electrophoresis 142
5.3.5.3 Sanger Sequencing Sample Preparation and Data Analysis 144
5.4 Results 144
5.4.1 Fitness Costs of Caspofungin Adaptation Between and Within Evolved Replicate Populations of *C. glabrata* Strain 2001 in Experiment 1 144
5.4.2 Phenotyping of Sub-Population Colony Diversity in a Single Caspofungin-Evolved Replicate Population in Experiment 1 147
5.4.3 Independent Evolution of Fitness Costs and Adaptations within Populations in Experiments 2 and 3 of the 14-Day Caspofungin Evolution 150
5.4.4 Characterising Caspofungin Susceptibility of Small and Large Colony Variants in Independent 14-Day Caspofungin Evolution Experiments 155
5.4.5 Genetic Characterisation of Common Caspofungin Resistance Targets in Small and Large Colony Variants 161
5.5 Discussion 164
5.6 Conclusions of the Chapter 172
6. Chapter 6: Discussion 173
6.1 Thesis Overview 173
6.2 Competition for Resources in Dual Species *in vitro* and *in vivo* Environments 173
6.3 *C. glabrata* Clinical Strain Variation in Competitive Abilities, Species Interactions and Growth Kinetics 176
6.4 Influence of Pathogen Growth Strategies on Virulence and Antifungal Adaptation 178
6.5 Conclusions 182
6.6 Future Perspectives 182
Appendices 185
A.1. Chapter 2 Appendix 185
A.1.1 Supplementary Materials and Methods 185

A.1.2 Supplementary Figures and Tables 186
A.2 Chapter 3 Appendix 194
A.2.1 Supplementary Tables 194
A.3. Chapter 4 Appendix 200
A.3.1 Supplementary Figures and Tables 200
A.4 Chapter 5 Appendix 222
A.4.1 Supplementary Materials and Methods 222
A.4.2 Supplementary Figures and Tables 224
Bibliography 237

List of Figures

Figure 1.1. Phylogeny of the Saccharomycotina subphylum of the hemiascomycetes (yeasts). 26
Figure 1.2. Colony morphology of *C. glabrata* (left) and *C. albicans* (right) on SDA (Sabouraud Dextrose Agar). 27
Figure 2.1. Example plot of negative frequency-dependent selection and predicted species co-existence. 33
Figure 2.2. One-season competition between *C. glabrata* and *C. albicans* at low glucose concentration in Synthetic Complete (SC) medium. 42
Figure 2.3. One-season competitions between *C. glabrata* and *C. albicans* at 6 different glucose concentrations in Synthetic Urine (SU) media. 45
Figure 2.4: Long-term competition of a high initial fraction of *C. albicans* with *C. glabrata* at low and intermediate glucose concentrations in Synthetic Urine media, via volumetric serial transfers. 47
Figure 2.5: Long-term competition of a high initial fraction of *C. albicans* with *C. glabrata* at intermediate glucose concentration (1% w/v) in Synthetic Urine media, via cell density serial transfers. 48
Figure 2.6: Long-term competitions between *C. glabrata* and *C. albicans* for different initial frequencies of C. albicans and co-culture initial densities. 49
Figure 2.7: One-season competition between *C. glabrata* and *C. albicans* at different glucose concentrations in Synthetic Urine medium, for large changes in initial cell densities of competition suspensions. 51
Figure 2.8. One-season competition between *C. glabrata* and *C. albicans* at a 50:50 ratio in 0.05 % w/v glucose media, for different volumes of competition suspension in culture tubes. 56
Figure 2.9: One-season competition between *C. glabrata* clinical strains and *C. albicans* at low glucose concentration in SC medium. 57
Figure 3.1. Survival of *G. mellonella* infected with *C. glabrata* or *C. albicans* at two different temperatures. 78
Figure 3.2. Survival curves for single and dual *Candida* species *G. mellonella* infection. 80

Figure 3.3. Survival curves for single species *C. albicans* and *C. glabrata* infections and dual *C. albicans*-*C. glabrata* infection of *G. mellonella*, with different *C. glabrata* strains. 87
Figure 3.4. Survival curves for single species *C. albicans* and *C. krusei* infections and dual *C. albicans*-*C. krusei* infection of *G. mellonella*. 88
Figure 3.5. Survival curves of *G. mellonella* infection for doses of *C. glabrata* strains BG2 and 1184 with comparative virulence to *C. albicans*. ... 89
Figure 3.6. Melanisation response in *G. mellonella* with single species *C. glabrata* strain or *C. krusei* infection. 90
Figure 4.1. Logistic population growth described by the Verhulst equation. 98
Figure 4.2. Experimental design for populations of *C. glabrata* strains 2001 and 3605 evolving on a gradient of caspofungin concentrations. 106
Figure 4.3. Growth kinetics of five *C. glabrata* strains measured over a range of glucose concentrations. 110
Figure 4.4. Relationship between growth rate (r) and carrying capacity (K) in five *C. glabrata* strains. 112
Figure 4.5. Relationship between growth rate (r) and yield (OD mg ml^{-1} glucose) in five *C. glabrata* strains. 113
Figure 4.6. Comparison of r/K and r/yield relationships across *C. glabrata* strains. 114
Figure 4.7. Growth rates, carrying capacities (K) and yields across *C. glabrata* strains at low and intermediate glucose concentrations. 117
Figure 4.8. Survival of *Galleria mellonella* infected with *C. glabrata* strain 2001 or 3605 at 30ºC. 118
Figure 4.9. Evolution of populations of *C. glabrata* strains 2001 and 3605 on a gradient of caspofungin concentrations in three independent experiments. 123
Figure 5.1. Fitness costs of caspofungin adaptation in individual colonies of parallel-evolved populations of *C. glabrata* strain 2001 in Experiment 1 (E1) of the 14-day evolution. 146
Figure 5.2. Growth profiling, substrate usage and colony morphology of individual colonies revived from a single 0.78 µg/ml caspofungin-adapted population of *C. glabrata* strain 2001. 148

Figure 5.3. Comparative survival of Galleria mellonella with injection of *C. glabrata* strain 2001 WT and 0.78 µg/ml caspofungin-evolved colonies. 150
Figure 5.4. Fitness costs of caspofungin adaptation in colonies of day 14 populations of *C. glabrata* strain 2001 from Experiment 2 (E2) of the 14-day evolution. 151
Figure 5.5. Fitness costs and caspofungin adaptations in colonies of day 14 populations of *C. glabrata* strain 2001 evolved at 0.00 or 0.78 µg/ml from Experiment 3 (E3) of the 14-day evolution. 154
Figure 5.6. Dose response profiles for *C. glabrata* strain 2001 WT ancestor and colony variants from day 14 of Experiment 1 of the 14-day evolution of caspofungin resistance. 157
Figure 5.7. Dose response profiles for *C. glabrata* strain 2001 WT ancestor and colony variants from day 14 of Experiment 3 of the 14-day evolution of caspofungin resistance……..160
Figure 5.8. Genomic DNA extraction, PCR amplification and Sanger sequencing of caspofungin resistance gene targets in colony variants of *C. glabrata* strain 2001. 162
Figure A.1.2.S1: *C. glabrata* (left) and *C. albicans* (right) monocultures on CHROMagar plates. 186
Figure A.1.2.S2: Layout of 96-well plate for one-season and serial transfer competitions for a range of initial species ratios. 186
Figure A.1.2.S3. One-season competitions between *C. glabrata* and *C. albicans* for five initial fractions of *C. albicans* and each of six different glucose concentrations in SU media. 187
Figure A.3.1.S1. Growth rate (r) for five *C. glabrata* strains measured over a range of glucose concentrations in Synthetic Complete medium. . 200
Figure A.3.1.S2. OD at carrying capacity (K) for five *C. glabrata* strains measured over a range of glucose concentrations in Synthetic Complete medium. 201
Figure A.3.1.S3. Yield for five *C. glabrata* strains measured over a range of glucose concentrations in Synthetic Urine medium. 202
Figure A.3.1.S4. Growth curves of *C. glabrata* strains 2001 and 3605 at low and intermediate glucose concentrations, with fitted logistic models and calculated growth parameters..... 203

Figure A.3.1.S5 Relative growth of populations of *C. glabrata* strains 2001 and 3605 evolving on a gradient of caspofungin concentrations over 14 days. 204
Figure A.3.1.S6. Evolution of caspofungin dose response profile of *C. glabrata* strains 2001 and 3605 in three independent experiments. 205
Figure A.3.1.S7. Caspofungin IC estimates from dose-response fits across populations of *C. glabrata* strain 2001 evolving on a gradient of caspofungin concentrations in three 14-day experiments..... 207
Figure A.3.1.S8. Evolution of *C. glabrata* strain 2001 dose response profile in 1% w/v (10 mg ml^{-1}) glucose SC medium- Experiment 1. 209
Figure A.3.1.S9. Evolution of *C. glabrata strain* 3605 dose response profile in 1% w/v (10 mg ml^{-1}) glucose SC medium- Experiment 1. 210
Figure A.3.1.S10. Evolution of *C. glabrata* strain 2001 dose response profile in 1% w/v (10 mg ml^{-1}) glucose SC medium- Experiment 2. 211
Figure A.3.1.S11. Evolution of *C. glabrata* strain 3605 dose response profile in 1% w/v (10 mg ml^{-1}) glucose SC medium- Experiment 2. 212
Figure A.3.1.S12. Evolution of *C. glabrata* strain 2001 dose response profile in 1% w/v (10 mg ml^{-1}) glucose SC medium- Experiment 3. 213
Figure A.3.1.S13. Evolution of *C. glabrata* strain 3605 dose response profile in 1% w/v (10 mg ml^{-1}) glucose SC medium- Experiment 3. 214
Figure A.3.1.S14. Strain 2001 growth kinetics- Experiment 3, day 1..... 216
Figure A.3.1.S15. Strain 3605 growth kinetics- Experiment 3, day 1..... 216
Figure A.3.1.S16. Strain 2001 growth kinetics- Experiment 3, day 7..... 217
Figure A.3.1.S17. Strain 3605 growth kinetics- Experiment 3, day 7..... 217
Figure A.3.1.S18. Strain 2001 growth kinetics- Experiment 3, day 14..... 218
Figure A.3.1.S19. Strain 3605 growth kinetics- Experiment 3, day 14..... 218
Figure A.4.2.S1. Dose response model predictions with confidence regions for *C. glabrata* strain 2001 WT ancestor and colony variants from day 14 of Experiment 1 of caspofungin evolution. 230
Figure A.4.2.S2. Dose response profile predictions with confidence regions for *C. glabrata* strain 2001 WT ancestor and colony variants from day 14 of Experiment 3 of caspofungin evolution. 231
Figure A.4.2.S3. Caspofungin IC estimates over a range of inhibitory levels from dose-response fits to sensitivity tests of the wild-type ancestral strain of *C. glabrata* 2001, media-adapted and large colony variants. 233

Figure A.4.2.S4. Dose response profiles for the *C. glabrata* ATCC 2001 WT ancestor and a single colony from each of three replicate populations founded from the SCV from Experiment 3 after 14 days propagation without caspofungin. 234
Figure A.4.2.S5. Pilot dose response assays for the revived population colonies of C. glabrata strain 2001 evolved at 0.78 µg/ml for 14 days in three independent experiments……236

List of Tables

Table 2.1: Statistical comparisons of initial and final *C. albicans* fractions over one-season competition between *C. glabrata* 2001 and *C. albicans* GFP in 0.05 % w/v glucose Synthetic Urine medium at ten times greater competition density. 52

Table 2.2: Statistical comparisons of initial and final *C. albicans* fractions over one-season competition between *C. glabrata* 2001 and *C. albicans* GFP in 0.1 % glucose Synthetic Urine medium, for initial competition cell densities of approximately 10^6 and 10^3 cells/ml. 52

Table 2.3: Change in *C. albicans* fraction over one-season competition between *C. glabrata* 2001 and *C. albicans* GFP in 5-ml culture tubes. 55

Table 3.1. *Candida* strains used in single and dual species infections. 74

Table 3.2. Comparison of *G. mellonella* survival between single species *C. glabrata* and *C. krusei* strain infections..... 82

Table 3.3. Comparison of *G. mellonella* survival between single species *C. albicans* strain infections. 83

Table 3.4. Comparison of *G. mellonella* survival between single species strain *C. albicans* infections and dual infection of *C. albicans* with different strains of *C. glabrata* and *C. krusei*. 83

Table A.1.2.S1. *C. glabrata* Strains. 188

Table A.1.2.S2. Statistical results from Wilcoxon signed-rank tests to determine significant deviation of *C. albicans* relative fitness from 1 in one-season competition in 0.1% w/v glucose SC media. 188

Table A.1.2.S3. Statistical results from Wilcoxon signed-rank tests or one-sample t-tests to determine significant deviation of *C. albicans* relative fitness from 1 in one-season competition for glucose concentrations in SU media..... 189

Table A.1.2.S4. Statistical results from t-tests for significance of the slope of the negative frequency-dependent relationship for one-season competitions between *C. albicans* and *C. glabrata* at different glucose concentrations and competition cell densities. 192

Table A.1.2.S5: Statistical results of significant pairwise comparisons from Tukey *post hoc* tests following one-way ANOVA tests on daily *C.*

albicans fractions during long-term competition in 1% w/v glucose SU media. 193
Table A.2.1.S1. Statistical results from log-rank tests for survival curve comparisons between infective doses and temperatures for single species *C. albicans* and *C. glabrata* infections of *G. mellonella*. ... 194
Table A.2.1.S2. Results from survival analyses of single and dual species *Candida* infections of *G. mellonella*, using infective doses from Rossoni *et al.* (2015). 195
Table A.2.1.S3. Statistical results from log-rank tests for survival curves of single species *C. albicans* infection and dual species *C. albicans-C. glabrata* strain infections of *G. mellonella*. 196
Table A.2.1.S4. Statistical results from log-rank tests for single species *C. albicans* infection and dual species *C. albicans-C. krusei* strain infections of *G. mellonella.* 198
Table A.2.1.S5. Statistical results from log-rank tests for single species *C. albicans* and *C. glabrata* strain infections of *G. mellonella* at equally virulent doses. 199
Table A.3.1.S1. Statistical results for Strain 2001 dose response slope comparisons during caspofungin evolution. 219
Table A.3.1.S2. Statistical results for Strain 2001 IC50 comparisons during caspofungin evolution. 220
Table A.3.1.S3. Statistical results for Strain 3605 dose response slope comparisons during caspofungin evolution. 220
Table A.3.1.S4. Statistical results for Strain 3605 IC50 comparisons during caspofungin evolution. 221
Table A.4.1.S1. Primers for PCR amplification and Sanger sequencing of caspofungin resistance gene targets. 224
Table A.4.2.S1. Comparison of growth rate (1/h) and final OD (24 hours) across population colonies at different caspofungin concentrations, revived from day 14 of the first experimental 14-day caspofungin evolution. 224
Table A.4.2.S2. Significant pairwise differences in growth rate (h^{-1}) and final OD (24 hours) between population colonies revived from day 14 following evolution at 0.78 225

Table A.4.2.S3. Significant pairwise differences in relative growth rate (h^{-1}) and relative OD (24 hours) between population colonies revived from day 14 in Experiment 2 of 14-day caspofungin evolution. 226
Table A.4.2.S4. Significant pairwise differences in growth rate (h^{-1}) and OD (24 hours) between population colonies revived from day 14 from Experiment 3 of caspofungin evolution. 227
Table A.4.2.S5. Comparison of IC50 and slope (gradient) parameters for the 4-parameter logistic dose response model fit for colony variants from Experiment 1. 228
Table A.4.2.S6. Comparison of IC50 and slope (gradient) parameters for the 4-parameter logistic dose response model fit for colony variants from Experiment 3. 229

List of Abbreviations

ATCC	American Type Culture Collection
ATP	Adenosine Triphosphate
CFU	Colony Forming Unit
E	Experiment
GFP	Green Fluorescent Protein
HS	Hotspot region of a gene
ICx	Inhibitory Concentration: lowest concentration of drug required to inhibit microbial growth to a certain percentage (x), relative to a non-drug-treated control
K	Carrying Capacity
LCV	Large Colony Variant
MIC	Minimum Inhibitory Concentration: lowest concentration of drug required to substantially inhibit microbial growth, usually to 50 or 90% inhibition
MSC	Multi-Species Candidemia
NCPF	National Collection of Pathogenic Fungi
OD	Optical Density
PxCy	Population (x) Colony (y): notation for a specific colony (y) from a replicate population (x)
PBS	Phosphate Buffered Saline
PCR	Polymerase Chain Reaction
r	Exponential phase intrinsic growth rate (h^{-1})
SC	Synthetic Complete medium
SCV	Small Colony Variant

SDA	Sabouraud Dextrose Agar
SE	Standard Error
SU	Synthetic Urine
TCA	Tricarboxylic Acid Cycle
WHO	World Health Organisation
WT	Wild-Type or Wild Type
YNB	Yeast Nitrogen Base
YPD	Yeast Peptone Dextrose
YPG	Yeast Peptone Glycerol

Publications

Ames, L., **Duxbury, S.,** Pawlowska, B., Ho, H. L., Haynes, K., & Bates, S. (2017). *Galleria mellonella* as a host model to study *Candida glabrata* virulence and antifungal efficacy. *Virulence*, 8(8), 1909-1917.

Reding-Roman, C., Hewlett, M., **Duxbury, S.,** Gori, F., Gudelj, I. & Beardmore, R. (2017). The unconstrained evolution of fast and efficient antibiotic-resistant bacterial genomes. *Nature Ecology & Evolution,* 1(3), 0050.

Data from Chapter 3 on *Galleria mellonella* survival with single species *C. albicans* infection and brief commentary on the relationship between *C. glabrata* clinical strain growth strategies and virulence, is presented in Ames *et al.* (2017).

Data from Chapter 4 on comparative growth kinetics of five different *C. glabrata* strains is presented in Reding-Roman *et al.* (2017).

1. Chapter 1: Introduction

1.1 Fungi as Pathogens of Humans

Fungal pathogens are emerging as major causes of severe, invasive disease in humans with a particularly dramatic rise of bloodstream infections (Brown *et al.,* 2012). Annually, fungi are responsible for greater than one billion skin and mucosal infections and more than one million deaths from invasive disease (Gow and Netea, 2016). Given that mortality rates from invasive disease parallel those of tuberculosis and malaria and 2 million people worldwide are affected annually, surprisingly the severity of fungal disease is poorly recognised and under researched amongst the scientific community (Brown *et al.,* 2012; Barnes *et al.,* 2014). Research funding for fungal diseases comprises less than 5% of UK budgets on infection biology (Head *et al.,* 2014; Fisher *et al.,* 2016) and there is minimal reporting of fungal epidemiology worldwide, with the exception of surveillance by the US Centers for Disease Control and Prevention (CDC) (Brown *et al.,* 2012). There is now an important need to research fungal disease prevention and control strategies due to the threats posed to crops, wildlife and human health from a variety of animal and plant pathogens (Fisher *et al.,* 2016).

Fungi are healthy components of human microbial communities (Underhill and Iliev, 2014) but cause infection due to pathogenic overgrowth. This results in superficial infections of the skin and nails in otherwise healthy individuals or those on antibiotic treatment, or invasive disease in patients with severe underlying disease such as HIV (Segal, 2005; Brown *et al.,* 2012; Kumar and Singhi, 2013). Opportunistic species of the *Candida* genus are the “fourth most common cause of nosocomial bloodstream infections” in the United States (Wisplinghoff *et al.* 2004) and are responsible for a worldwide 46-75% mortality rate (Brown *et al.* 2012). *Candida* species are carried in approximately a third to a half of human oral cavities (Ito-Kuwa *et al.,* 1997; Thein *et al.* 2009) and in many other host sites, existing as healthy commensals (Fidel *et al.,* 1999). Often, more than one species is found in commensal carriage and a study of oral sites found that 31% of colonised individuals had mixed-*Candida* species carriage, with *C. albicans* and *C. glabrata* most common (Lockhart *et al.* 1999).

Infections occur due to immune compromise and range from superficial mucosal to invasive candidiasis involving respiratory, gastrointestinal and urino-genital tracts, due to pathogenic overgrowth (Segal 2005; Kumar and Singhi, 2013).

Invasive candidiasis affects greater than 250,000 people worldwide annually and includes bloodstream infections (candidemia) and lesions in organs such as the kidneys and lungs and other sites including the bones and eyes (Kullberg and Arendrup, 2015). The most common risk factors for infection include intravenous catheters, surgery and widespread antibiotic usage. Broad-spectrum antibiotics promote *Candida* species colonization, and dissemination into the bloodstream in severe infection, as antibiotics eliminate healthy intestinal bacteria that are important in maintaining microbial balance and act as a physical barrier against infection (colonisation resistance) (Saiman *et al.*, 2001; Kumar and Singhi, 2013).

1.2 Microbial Species Interactions in Infections

Infections consisting of more than one *Candida* species are increasing in prevalence and have been isolated in the bloodstream (Nace *et al.,* 2009) and oral cavities (Soll, 2002; Coco *et al.,* 2008), often occurring alongside serious pathologies such as HIV (Junqueira *et al.,* 2011) and cancer (Boktour *et al.,* 2004). Often, *C. albicans* and *C. glabrata* are the most common species co-isolated (Coco *et al.,* 2008; Nace *et al.,* 2009). Mixed *Candida* species infections are more difficult to treat than single-species infections due to combined pathogenic effects on the host (Silva *et al.,* 2011) and the presence of drug-resistant species (Mikulska *et al.,* 2012). Multi-species infections derive from the presence of multiple commensal *Candida* species, as the causative species are entirely endogenous (Jenkinson and Douglas, 2002).

Mixed species carriage has been described in oral cavities (Lockhart *et al.* 1999) but *Candida* species are carried at a range of diverse sites including the intestinal tract and the vagina (Underhill and Iliev, 2014), and in patients with different underlying risk factors (Li *et al.,* 2007). This indicates that *Candida* species will form ecological interactions in a range of different host

environments under different abiotic conditions, which are likely to impact on pathogenesis and the evolution of drug resistance (Jenkinson and Douglas, 2002). Inter-specific competition in host niches usually occurs for limiting resources and for space (Payne *et al.,* 2003). Differences in pathogen glucose metabolism have influenced competition outcomes in mixed *Candida*-bacterial species environments (Basson, 2000), but the effects of resources on mixed *Candida* species interactions in host environments were not explored.

Resources are important in host environments as host diet has been shown to cause rapid changes in commensal microbial community structure (David *et al.,* 2014) and competition for resources can occur between host cells, pathogens and commensals (Smith and Holt, 1996). Ecological interactions that are influenced by spatially and temporally heterogeneous resource levels in different host sites and patients, can influence pathogenesis. In competition between commensal bacterial species, species abundance is controlled by resource use efficiency and the number of resources available (Freter *et al.,* 1983). Bacteria can evolve strategies to become better competitors in natural communities, for example through toxin production, a mechanism of interference competition (Hibbing *et al.,* 2010). Competitive interactions can also be described as exploitative due to differential rates of resource uptake and growth rates of competitors. These types of interactions are antagonistic as competitor growth is inhibited; alternatively, microbial species can interact synergistically by production of growth-promoting molecules that increase pathogenesis (Harrison, 2007).

Species interactions may be modulated by the host immune response (Pedersen and Fenton, 2007; Smith, 2007), affecting pathogen community structure and the outcome of infections if competitors differ in virulence or drug resistance (Lello *et al.,* 2004). Reciprocally, pathogen interactions can influence host fitness and affect activation of host immunity, as well as depleting host resources to indirectly affect growth of microbial competitors (Pedersen and Fenton, 2007). The interactions between pathogen resource competition, metabolism and host immunity remain to be studied in detail for mixed-species fungal infections.

1.3 Laboratory Evolution of Microbial Species

Experimental evolution has been used to study long-term adaptation of model bacterial and yeast species, but laboratory evolution of non-model pathogenic fungal species lacks research. Experiments with *Escherichia coli* and yeast have studied adaptation to defined nutrient environments (Lenski *et al.,* 1991; Ferea *et al.,* 1999) and evolution of competitor interactions (Turner *et al.,* 1996). Yeast can be evolved under controlled experimental conditions via sequential batch cultivation to generate mutants resistant to stresses such as high concentrations of nickel (Küçükgöze *et al.,* 2013), salt and oxidative stress (Dhar *et al.,* 2012). Some model bacterial species (*E. coli, Pseudomonas aeruginosa and Salmonella typhimurium* (Buckling *et al.,* 2009)) that have well characterised genetics and molecular biology are also human pathogens (MacLean *et al.,* 2010).

A few studies have described evolution of antibiotic resistance in non-model pathogenic bacteria, such as *Mycobacterium tuberculosis (*Gagneux *et al.,* 2006)*, Staphylococcus aureus* (Nagaev *et al.,* 2001) and *Streptococcus pneumoniae* (Rozen *et al.,* 2007), and evolution of fungal pathogens of amphibians, plants and insects via *in vitro* (Jeon *et al.,* 2013; Voyles *et al.,* 2014) or *in vivo* serial passaging (Valero-Jiménez *et al.,* 2017). Experimental evolution of fungal human pathogens is limited, apart from a few studies of antifungal resistance evolution in *Saccharomyces cerevisiae* (Anderson *et al.,* 2003) and *C. albicans* (Cowen *et al.,* 2000; Vincent *et al.,* 2013). More research is needed to understand adaptation of fungal human pathogens under different environmental conditions of relevance to the host.

1.4 *Candida* Species Biology and Epidemiology

For completeness, we now provide more details on the biology, epidemiology and drug resistance of *Candida* species. The *Candida* genus is composed of more than 150 yeast species with 15 of these identified as pathogens of humans (Henry-Stanley *et al.,* 2005; Yapar, 2014). *C. albicans* is responsible for approximately 75% of infections (Jenkinson and Douglas, 2002), particularly systemic infections (candidemia), but *C. glabrata* is the second most commonly

identified *Candida* species in intensive care units and candidemia surveys (Odds, 1996; Henry-Stanley *et al.* 2005). Recently, *C. auris* has been classified as an important emerging pathogen due to its global spread and multi-drug resistance (Chowdhary *et al.,* 2017). *C. albicans* and *C. glabrata* are classified in the subphylum Saccharomycotina of the hemiascomycetous yeasts (Diezmann *et al.,* 2004) (phylum Ascomycota (Hendriks *et al.,* 1989)), but are distantly related, as *C. albicans* is classified as a CTG clade yeast, whilst *C. glabrata* (formally denoted *Torulopsis glabrata*) and *S. cerevisiae* are post-whole genome duplication (WGD) yeasts (**Figure 1.1**) (Barns *et al.,* 1991; Marcet-Houben and Gabaldón, 2009; Roetzer *et al.,* 2011). CTG clade fungal species use the CUG codon to encode serine instead of the universally-coded leucine (Sugita and Nakase, 1999; Santos *et al.,* 2011). A whole genome duplication event occurred in the ancestor of *C. glabrata* and *S. cerevisiae,* followed by subsequent loss of paralogous genes in the two species (Dujon *et al.,* 2004).

C. glabrata shares a close evolutionary relation to the non-pathogenic yeast *Saccharomyces cerevisiae* (Barns *et al.,* 1991; Dujon *et al.,* 2004) but has evolved adaptations to survive in the human host and exist as an opportunistic pathogen, due to prolonged starvation survival, shorter generation times, stress resistance and loss of metabolic genes due to its obligate association with the host (Roetzer *et al.,* 2011; Rodrigues *et al.,* 2014). Unlike *S. cerevisiae, C. glabrata* is not known to undergo sexual reproduction (Dujon *et al.,* 2004).

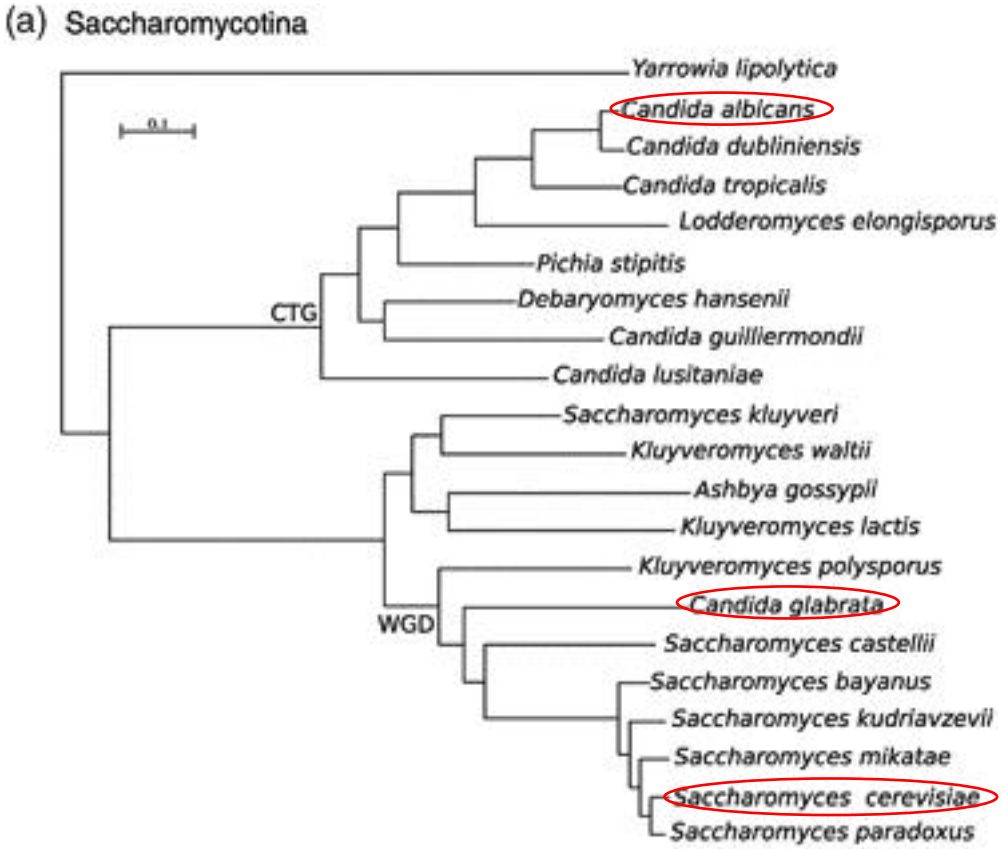

Figure 1.1. Phylogeny of the Saccharomycotina subphylum of the hemiascomycetes (yeasts). This figure is taken from Figure 1a of Roetzer *et al.* (2011) and shows evolutionary distance between *C. albicans*, *C. glabrata* and *S. cerevisiae* (circled in red). *C. albicans* is found in a separate branch of the tree with CTG clade yeasts, including other species of the *Candida* genus. *C. glabrata* shows a closer evolutionary relation to species of the *Saccharomyces* genus than those of the *Candida* genus as it is descended from an ancestor that underwent a random whole genome duplication (WGD) event.

C. albicans and *C. glabrata* show distinct differences in their biology and virulence (Fidel *et al.,* 1999). Both species form yeast cells but those of *C. glabrata* are significantly smaller than *C. albicans.* On SDA (Sabouraud Dextrose Agar), *C. glabrata* forms smooth, shiny colonies whereas *C. albicans* forms flatter, larger colonies with a rougher morphology (**Figure 1.2**). *C. albicans* is a diploid species that exhibits dimorphic growth due to formation of yeast cells and filamentous hyphal elements, as well as pseudohyphae (elongated cells) (Brunke and Hube, 2013) that aid its tissue colonisation and invasion stages during infection (Sudbery, 2011). In contrast, *C. glabrata* is a haploid species (Whelan *et al.,* 1984) and grows only as yeast cells (Fidel *et al.,* 1999). The two species differ in their virulence factors and infection strategies

as both species produce adhesins for attachment to host cells, but *C. albicans* causes greater host damage, triggers a greater host inflammatory response and has greater metabolic flexibility (Brunke and Hube, 2013). In contrast, *C. glabrata* shows greater intracellular survival and persistence but is more metabolically specialised to specific host niches in *in vitro* studies. Co-infection by the two species may allow *C. glabrata* to access a greater range of nutrients due to tissue destruction by *C. albicans,* or allow systemic dissemination.

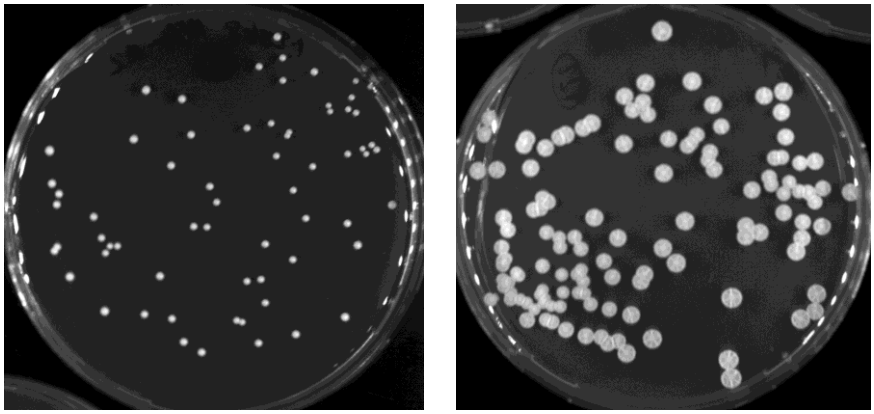

Figure 1.2. Colony morphology of *C. glabrata* (left) and *C. albicans* (right) on SDA (Sabouraud Dextrose Agar).

Candida glabrata is a pathogen of great clinical importance, as it is associated with a greater than 50% death rate and high resistance to the antifungal drug fluconazole (Fidel *et al.,* 1999; Gudlaugsson *et al.,* 2003; Pfaller *et al.,* 2012). Although Fidel *et al.* (1999) described fluconazole use as a main cause of increased prevalence, Diekema *et al.* (2012) reported increased *C. glabrata* prevalence in hospital-associated candidemia without increased resistance over a three-decade study. *C. glabrata* is a non-pathogenic component of the healthy microbiota (Fidel *et al.* 1999; Li *et al.* 2007) although increased *C. glabrata* commensal colonisation and infections have been associated with immunosuppression, antibiotic usage, dentures and aging (Li *et al.* 2007; Malani *et al.* 2010), with *C. glabrata*-associated candidemia exhibiting global geographical variation (Guinea, 2014). *C. glabrata* affects a diverse range of clinical patients including those with cancer (Farmakiotis *et al.,* 2014), HIV (Diamond, 1991) and diabetes (Goswami *et al.,* 2006). Diabetes is a common risk factor for *C. glabrata* infections (Fidel *et al.,* 1996), which is concerning as diabetes now affects nearly 1 in 11 adults (WHO, 2016)

Antifungal resistance across the main classes of antifungals is increasing in *Candida* species infections and poses challenges to clinical therapy (Sanglard, 2016). As human and fungal cells share structural similarities due to their close evolutionary relation within the eukaryotes (Baldauf *et al.,* 2000), it remains a challenge to identify novel antifungal drug targets to specifically target fungal cells (Anderson, 2005). The main classes of antifungal drugs include the azoles (fluconazole), echinocandins, polyenes and nucleoside analogues (flucytosine) which all target the fungal cell wall or membrane sterol and ergosterol components and slow growth (fungistatic agents: fluconazole and flucytosine) or kill cells (fungicidal agents: echinocandins and polyenes) (Odds *et al.* 2003; Mikulska *et al.,* 2012). The main mechanisms of drug resistance amongst *Candida* species include drug efflux, altered expression or affinity of the drug target, or changes in cell metabolism (Sanglard, 2016). Azoles have the greatest use in the clinic, which has led to widespread emergence of non-*albicans* species with intrinsic resistance (Mikulska *et al.,* 2012).

C. albicans is intrinsically susceptible to the azole drug fluconazole and the echinocandins and has low levels of resistance (Cleveland *et al.,* 2012). In contrast, *C. glabrata* has intrinsic fluconazole resistance and rates of acquired resistance have increased over time (Pfaller *et al.,* 2009; Sanglard, 2016). As a result, echinocandins are often used as a first-line therapy, but acquired resistance in the clinic is increasing (Alexander *et al.,* 2013). This poses an important clinical challenge, so the dynamics of adaptation and mechanisms of resistance require further study.

1.5 Thesis Aims and Outline

In this thesis, we investigated the influence of resource levels and pathogen metabolism on the ecology and evolution of single and mixed-species *Candida* infections, using *C. albicans* and *C. glabrata,* which are the species most commonly isolated in infections.

Firstly, in Chapter 2, we investigated whether resource levels impact on the outcomes of mixed-species competition in clinically relevant environments limited by a single carbon source. *C. albicans* and *C. glabrata* are co-isolated as

commensals and in mixed-species infections in different body sites and host patients, but ecological interactions and their stability have not been explored at different resource levels in physiological conditions. We studied how resources influence species' competitive abilities in short and long-term competition experiments in synthetic urine media and variation in competitive outcomes with different clinical species strains.

Next, in Chapter 3, we investigated the types of interactions formed between *C. albicans* and *C. glabrata* clinical strains in an invertebrate host infection model. Microbial competitors can interact antagonistically or synergistically in infections but the diversity of interactions and impact on host survival have not been fully characterised in mixed-species fungal infections. We studied mixed-species *Candida* interactions for a set of clinical strain combinations, monitoring host survival, pathogenicity and virulence in the wax moth larval model *Galleria mellonella.*

We then focused, in Chapter 4, in more detail on different clinical strains of *C. glabrata* and explored growth properties at different resource levels and the influence on evolution of antifungal resistance. *C. glabrata* is known to colonise multiple body sites and patients with different underlying risk factors, therefore different strains are likely exposed to different resource environments. As a consequence, different pathogen growth strategies may influence antifungal susceptibility and adaptability. We measured growth kinetic parameters across a set of *C. glabrata* clinical strains and compared the virulence of contrasting strains and their abilities to adapt to antifungal caspofungin treatment over laboratory experimental evolution.

Finally, in Chapter 5, we explored the fitness costs and adaptations to antifungal treatment in *C. glabrata. C. glabrata* is known to develop antifungal resistance in the clinic but the dynamic process of adaptation and repeatability across replicate populations under controlled conditions is unknown. We studied phenotypic adaptations in experimentally-evolved populations of a lab reference strain of *C. glabrata* and investigated the presence of sub-population heterogeneity in resistant populations.

This thesis will end with a discussion in Chapter 6, describing the overall results of the thesis and their significance, as well as perspectives on future research directions.

2. Chapter 2: Population Dynamics of *In vitro* Resource Competition between *C. glabrata* and *C. albicans* in Clinically Relevant Environments

2.1 Introduction

The human body is host to several microbial communities, collectively known as the microbiota, consisting of bacterial and fungal commensals across sites including the gastrointestinal, oral and urino-genital tracts (Pelag *et al.* 2010; Saleem 2015). This community is vital in maintaining human health and performs several important functions of which "colonisation resistance", a physical barrier against invading pathogens, is particularly important (Payne *et al.* 2003). Although studies of the human microbiota largely focus on bacterial species, there remains an important, largely under-studied part consisting of fungal commensals: the 'mycobiota' (Underhill and Iliev 2014), which colonise the skin, mucosal surfaces and a range of organs. *Candida* species make up a large component of the mycobiota, composing approximately 25% of all fungal genera in the colon and 50% in the vagina (Underhill and Iliev 2014; Figure 1) and fungal dysbiosis has also been attributed to diseases such as IBD (Inflammatory Bowel Disease) (Ott *et al.,* 2008). The ecological dynamics of these mixed-species fungal communities remain to be fully characterised.

It is important to study ecology and evolution of the human microbiome as competition for resources occurs during niche construction and dynamic community changes can predispose infection (Dethlefsen *et al.,* 2006; Peleg *et al.,* 2010). The microbiota differs between individuals due to various host-related factors; recent studies have detected rapid changes in community structure due to diet (David *et al.,* 2014). Community dynamics may not be stable over short and long-term timescales due to changes in resource supply and consequent selection for strains with growth advantages. Changes in communities can cause shifts in microbial species or abundances that can lead to disease (Marchesi *et al.,* 2016).

Previous studies to investigate microbial community dynamics in the lab have

focused on competition for resources between non-pathogenic strains of *Escherichia coli* (Turner *et al.,* 1996; Elena and Lenski, 1997) or *Saccharomyces cerevisiae* (MacLean and Gudelj, 2006) in simple, resource-limited environments. These experiments studied competition between genotypes on a single limiting resource in minimal media and described stable co-existence. This was possible in seasonal environments maintained in batch cultures, whereby resources are supplied and are then depleted throughout a defined competition period (Rainey *et al.,* 2000).

During competition for a limiting resource, selection can maintain diversity through a mechanism know as negative frequency dependence or balancing selection. Genotypes are selected when they are at low frequency in a population but are disadvantaged when common (Haldane and Jayakar, 1963; Feldgarden *et al.,* 2003). Stable co-existence is predicted at the genotypic frequency at which fitness of the two genotypes is equal, a stable equilibrium point (Antonovics and Kareiva, 1988); this is presented graphically in **Figure 2.1**. Several studies have described short-term negative frequency dependence as a predictor of long-term, stable co-existence (Ayala and Campbell, 1974; Rainey *et al.,* 2000; Feldgarden *et al.,* 2003; Vellend, 2010) and stable polymorphism maintenance has been experimentally verified over serial transfers (Turner *et al.,* 1996) and in long-term experimental evolution (Elena and Lenski, 1997). It remains to be investigated whether negative frequency dependence allows stable co-existence of pathogenic species in clinically-relevant environments.

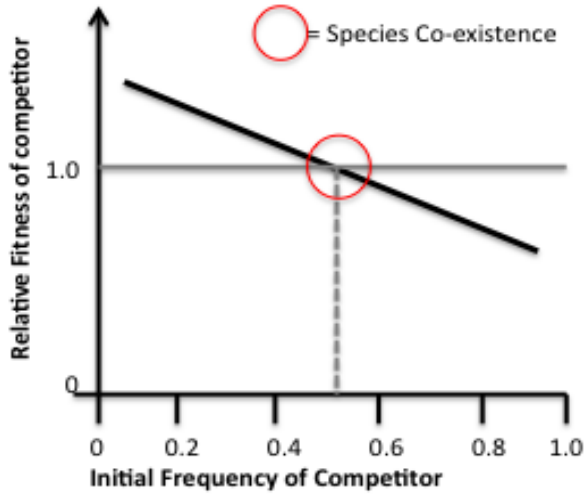

Figure 2.1. Example plot of negative frequency-dependent selection and predicted species co-existence. Relative fitness of one competitor against another in a single resource environment is usually described by the ratio of the Malthusian parameters (logarithmic changes in densities of the two competitors) over a single season (24 hours) of competition (Lenski *et al.,* 1991). This is calculated for competition mixtures of two competitors mixed together in different ratios. The relationship between fitness and competitor frequency is described by a negative linear relationship shown by the black line (Turner *et al.,* 1996; Rainey *et al.,* 2000) as competitors are selected for when rare but are less fit when common. Co-existence is predicted for the competitor frequency when neither competitor has a fitness advantage (relative fitness = 1.0; grey horizontal line), shown by the dotted grey line and red circle. It is predicted that competitor frequencies in mixed suspensions will converge towards the predicted stable co-existence point when serially transferred over multiple seasons.

Species interactions and ecological dynamics are particularly important to study in *Candida* species infections due to the rise of multi-species infections. Multi-species candidemia (MSC) has been reported as representing 2.8-8.0% of all bloodstream candidemias, of which the most common species combination (37.5% of patients with MSC) was *Candida albicans/ Candida glabrata* (Nace *et al.,* 2009). These infections pose a great threat to healthcare, particularly as they occur alongside serious pathologies such as cancer (Boktour *et al.,* 2004) and HIV (Patel *et al.,* 2012). In addition, bloodstream infections can form polymicrobial communities including more than one *Candida* species alongside bacterial species (Klotz *et al.,* 2007). It is within these environments that competitive interactions occur that contribute to pathogenesis. Kirkpatrick *et al.* (2000) studied interactions between

clinical isolates of two similar species - *C. dubliniensis* and *C. albicans*- that occur together in oropharyngeal candidiasis, using *in vitro* broth and biofilm conditions. Another study (Thein *et al.,* 2007) investigated competitive interactions between *C. albicans* and *C. krusei* in dual-species biofilms. These studies show that competitive interactions can be quantified in dual *Candida* species competitions, which can be applied to investigate the effect of resource levels on competition dynamics between *C. glabrata* and *C. albicans.*

2.2 Aims of the Chapter

In this chapter, we aim to extend the work of Nilsson (2012) and Beardmore *et al.* (in prep), which addressed short term *in vitro* resource competition between drug-resistant *C. glabrata* and drug-sensitive *C. albicans* in a simple medium. We focus on resource competition between these two species at different glucose concentrations in the absence of drug and explore the population dynamics of short and long-term competition in clinically relevant media. We address three aims:

1) To test whether variation in environmental resources in clinically relevant environments affects ecological dynamics within dual *Candida* species environments.

2) To investigate whether short-term negative frequency-dependent changes in community composition are predictive of long-term population dynamics.

3) To test whether competitive abilities for resources are ubiquitous across strains of a species.

We studied *in vitro* competitions between *C. glabrata* and *C. albicans* for a range of limiting glucose concentrations and initial species ratios in Synthetic Urine media (Domergue *et al.,* 2005; Uppuluri *et al.,* 2009) over one-season to investigate competition dynamics in clinically-relevant media. *Candida* species are increasingly the cause of urinary tract infections in hospitals for which non-*albicans Candida* species, particularly *C. glabrata,* compose approximately half of *Candida* urinary isolates (Fidel *et al.,* 1999). Multi-species infections

containing *C. glabrata* and *C. albicans* are particularly prevalent, but the competitive dynamics within this environment have not been characterised. Whilst virulence of the individual species has been studied in SU media (Domergue *et al.,* 2005; Uppuluri *et al.,* 2009), here we study inter-specific competition in a "nutritionally poor medium supplemented with urine-specific salts and urea" (Domergue *et al.,* 2005), in which the sole carbon source is glucose. We compare short-term competitions with long-term competitions extended via serial transfers and also test for frequency and density dependence of competitive outcomes. Finally, we test a set of *C. glabrata* clinical strains in competition with *C. albicans,* for ubiquity of the species-specific resource responses.

2.3 Materials and Methods

2.3.1 *Candida* Strains and Growth Conditions

Wild-Type reference strains used were *Candida glabrata* ATCC 2001 (**Table A.1.2.S1**) and *Candida albicans* ACT1-GFP (SBC153) (Milne *et al.,* 2011) (Nilsson 2012, 12.1; Beardmore *et al.* (in prep)). *C. albicans* SBC153 has a GFP-tagged *ACT1* gene and integrated nourseothricin resistance cassette but is otherwise isogenic to the clinical strain SC5314 from a "patient with disseminated candidiasis" (Gillum *et al.,* 1984). See **Table A.1.2.S1** for *C. glabrata* clinical strains. Glycerol stocks (15% v/v) of each strain were maintained at -80^{o}C and were streaked on YPD (yeast peptone dextrose) agar plates (2% w/v bacteriological peptone, 1% w/v yeast extract, 1.8 % w/v agar, 2% w/v glucose (**A.1.1 Supplementary Materials and Methods**)) and maintained at room temperature. Overnight cultures were prepared as previously described (Nilsson 2012, 12.1; Beardmore *et al.* (in prep)) via inoculation of a single colony into YPD broth per culture, and were grown in an orbital shaking incubator at 30^{o}C and 180 rpm for 18-24 hours.

Overnights were centrifuged and washed once in autoclaved distilled, de-ionised water before re-suspension in the assay medium, to prepare growth assays. Synthetic Complete media (yeast nitrogen base (YNB) supplemented with amino acids: **A.1.1 Supplementary Materials and Methods**) was

sterilised by autoclaving and Synthetic Urine, as prepared previously (Griffith *et al.,* 1976, cited by Martino *et al.,* 2003; Domergue *et al.,* 2005: Supplementary Materials; Uppuluri *et al.,* 2009), was filter-sterilised. Filter-sterilised glucose in water was later added to media to prepare final glucose concentrations.

2.3.2 One-Season Resource Competition in Synthetic Urine Media

Competition between *C. glabrata* 2001 and *C. albicans* GFP in Synthetic Complete (SC) medium at 0.1% w/v glucose was performed as previously described (Nilsson, 2012, 12.3; Beardmore *et al.* (in prep)). We used ready-plated CHROMagar *Candida* medium (BD Biosciences, Oxford, UK: Product code 257480; Nilsson, 2012, 12.6) for species identification (**Figure A.1.2.S1**).

Synthetic Urine media (Griffith *et al.,* 1976, cited by Martino *et al.,* 2003; Domergue *et al.,* 2005: SOM; Uppuluri *et al.,* 2009), a "nutritionally-poor medium supplemented with urine-specific salts and urea" (Domergue *et al.,* 2005), was prepared as previously described but was supplemented with glucose at 6 different concentrations: 0.05, 0.1, 0.5, 1, 2 and 4% w/v. Overnight cultures of the reference strains were each diluted in the assay medium to approximately 6-8x10^6 cells/ml, estimated via haemocytometer colony counts. Initial cell densities were two times the desired starting density for competition, as cell suspensions were diluted by a factor of two within the assay medium in the 96-well plate. Five species ratios were prepared as previously described for SC media: %*C. glabrata*: %*C. albicans*- 90:10, 70:30, 50:50, 30:70, 10:90 (Nilsson, 2012, 12.3).

Competition experiments were run in sterile 96-well flat-bottom polystyrene microtiter plates (Greiner BioOne; Product code: 655161) (see **Figure A.1.2.S2a** for details on plate set-up). The plate was sealed with transparent film with sterile holes punctured for aeration (Nilsson, 2012; 12.3) and was incubated in an orbital shaking incubator (180 rpm) for 24 hours at 30^{o}C. Competition for ten times initial cell density was performed as above for 0.05, 1 and 4% w/v glucose concentrations with initial cell density set to approximately 6x10^7 cells/ml. Competition for one thousand times lower initial cell density was performed in 0.1% w/v glucose with initial cell density set to 6.5 x 10^3 cells/ml.

Initial *C. albicans* fractions were determined via dilution in PBS and plating on each of three CHROMagar plates (100-200 colonies per plate). After 24 hours, cells within triplicate wells were re-suspended and mixed via multi-channel pipetting, prior to dilutions. 9 CHROMagar plates were spread per species ratio (3 plates per replicate well). Plates were incubated at 30^{o}C for 48-72 hours before colony counting and calculation of *C. albicans* fractions and viable CFU/ml counts.

2.3.3 Long-Term Competition in Synthetic Urine Media

2.3.3.1 Volumetric Serial Transfers

Competition between *C. glabrata* and *C. albicans* was extended over time in low glucose (0.1% w/v) and intermediate glucose (1% w/v) for a high initial fraction (0.70) of *C. albicans.* Each species was diluted in the assay medium to approximately 5-6 x10^{6} cells/ml. Long-term competitions were run in intermediate glucose (1% w/v), for initial *C. albicans* fractions of 0.20, 0.50 and 0.80. For 0.20, three approximate initial densities were prepared: 3.25 x 10^{6} cells/ml, 6.50 x 10^{6} cells/ml and 1.30 x 10^{7} cells/ml. See **Figure A.1.2.S2b** for set-up. Growth conditions over the first season matched those of one-season competitions. After 24 hours, fresh media/ water was added to the subsequent row of the 96-well plate (**Figure A.1.2.S2b**). Overnight cells were re-suspended, mixed and serially diluted (1 in 30) for transfer to the next season (E. Cook, 2014, *pers.comm.*). Monocultures and co-cultures were plated on CHROMagar (same replication as one-season) from initial until day 5, then approximately every 2 days until *C. albicans* was excluded. After 10 seasons, cell suspensions from the frequency/density-dependent experiment were frozen at -80^{o}C in 15% v/v glycerol.

2.3.3.2 Cell Density Serial Transfers

Long-term competition in 1% w/v glucose was run in an independent experiment where initial cell density of each season was controlled via haemocytometer counts (total cell count). The same high initial fraction of *C. albicans* was set as in the volumetric transfers (0.70) and initial cell density of

each species was set to 6.5 x 10^6 cells/ml, prior to 2-fold dilution in the assay medium within the 96-well plate. The 96-well plate was set up in the same way as described above. After 24 hours of competition, the competition suspensions within the 3 replicate wells of the 96-well plate were thoroughly re-suspended and mixed via scraping the well bases with the pipette tip and pipette mixing. An appropriate aliquot of cells from each well was diluted in PBS, counted with the haemocytometer and diluted to a final concentration of 3.25 x 10^6 cells/ml within the assay medium in fresh wells of the plate for transfer to the next season. This protocol was repeated every 24 hours up until day 7 so that each season began with a constant density. As above, monocultures and co-cultures were plated on CHROMagar at the end of each season from days 1-5 and day 7. Viable end-of-season colony counts were compared with haemocytometer cell counts.

2.3.4 Clinical Strain Competitions

One-season and serial transfer competitions were performed as above, but just for one initial species ratio. Competitors were diluted to an initial cell density of approximately 6.5 x 10^6 cells/ml. Initial and final competition suspensions were plated on CHROMagar as described above because all *C. glabrata* strains formed similar pink colonies, distinguishing them from *C. albicans.*

One-season competitions involved all 5 strains in **Table A.1.2.S1**, paired with *C. albicans* GFP set to 10:90 initial ratio. The assay medium was 0.05% w/v glucose SC, instead of SU medium as strains were isolated from different host sites. *C. glabrata* NCPF 3605 and 3309 were competed against *C. albicans* GFP at 4% w/v glucose for five seasons of volumetric serial transfers.

2.3.5 Competitions in Sterile Culture Tubes

One-season and serial-transfer competitions in 0.05% w/v glucose SC and SU medias used 5-ml sterile culture tubes with two-position cap (Greiner BioOne; Product code 115 261). The tubes were incubated under the same conditions as for 96 well plates, with caps loosened. Change in *C. albicans* fraction was measured over one-season competition between the reference strains at different final tube volumes, representing fold increases in 96-well plate

volumes (**Table 2.3**). The tubes were set up as of wells of a 96-well plate (described above) using scaled volumes of the two species but with the same initial cell densities. Initial species ratio was set to 50:50. Long-term competition was run for 5 times the final 96-well plate volume over serial transfers (1 in 30 dilution maintained).

2.3.6 Data Analysis and Statistics

Data was plotted in Excel and statistical analyses were completed in Excel or R (R version 3.3.2; R Core Team, 2016). *C. albicans* relative fitness in one-season competitions was calculated as the log ratio of the strains' Malthusian parameters as described previously using competition plating (Lenski *et al.,* 1991; Turner *et al.,* 1996) by the following equation:

$$\text{Relative fitness of } C.\ albicans = \frac{LN\left(\frac{final\ density\ C.a.}{initial\ density\ C.a.}\right)}{LN\left(\frac{final\ density\ C.g.}{initial\ density\ C.g.}\right)}$$

This was calculated for five initial fractions of *C. albicans* (competition ratios of the two species) using initial and final densities of each species calculated from colony counts on CHROMagar plates. Initial density was fixed as the average of the three initial CHROMagar plates, for each initial competition ratio. CHROMagar medium has previously been verified (Odds and Bernaerts, 1994) as a reliable method of detecting *Candida* species from clinical samples, due to differential enzymatic reactions with chromogenic substrates in the agar.

We used a general linear model in R (R version 3.4.3; R Core Team, 2017) to test the main effects of *C. albicans* fraction, glucose concentration and their interaction on relative fitness of *C. albicans,* when in competition with *C. glabrata* in Synthetic Urine media, followed by model reduction to include only the significant effects. We used the R-package 'plotrix' (Lemon, 2006) to show all data in a single plot with fitted linear trendlines (**Figure A.1.2.S3**). We checked that the assumptions of normality and homoscedasticity were met by visualising the distribution of standardised residuals and plotting residuals against model fitted values.

The least-squares linear regression of relative fitness of *C. albicans* against initial fraction, was plotted in Excel and the slope and R-squared correlation co-efficient were calculated for competition in each glucose concentration. Using the equation of the regression line, the *C. albicans* competitor fraction at which co-existence was predicted was calculated when relative fitness was equal to one. The significance of the regression slope was calculated in Excel (Zaiontz, 2015). When co-existence was not predicted (the regression line did not intersect relative fitness = 1) the significance of *C. albicans* relative fitness above or below a relative fitness of 1 was calculated in one-sample tests in R. Samples were first tested for normality using a Shapiro-Wilk test and if found to be normally distributed then a one-sample t-test was used, otherwise a Wilcoxon signed-rank test was used. Both one sample tests were two-tailed to robustly test for changes in *C. albicans* relative fitness in either direction.

To detect significant differences between initial and end *C. albicans* fractions in single-season competition experiments, two-sample, two-tailed unpaired t-tests were used (as in Beardmore *et al.* (in prep)) when initial and end fraction populations were normally distributed (Shapiro-Wilk test) and population variances were equal. When variances were not equal, Welch's two-sample t-test was run instead. When populations were non-normally distributed, non-significant skew or kurtosis results justified use of t-tests (Crawley *et al.,* 2007). Detection of significant skew in a small number of populations was due to random measurement error within small samples and would not be expected to occur in infinitely large populations. In addition, the t-test has been reported to be robust to non-normality (McDonald, 2014, pp.126-130).

One-way ANOVA followed by Tukey's *post hoc* test was used to deduce significant daily changes in *C. albicans* fraction in long-term competitions of *C. glabrata* and *C. albicans* at 1% w/v glucose.

To test for significant differences in *C. albicans* relative fitness between different strains of *C. glabrata,* we used R (R version 3.4.3; R Core Team, 2017) and the package 'plotrix' (Lemon, 2006) to compare one-way ANOVA and Kruskal-Wallis tests and to use Tukey's HSD *post hoc* test to deduce significant pairwise

differences. The data was presented in box-plots with means and standard error bars overlain.

2.4 Results

2.4.1 One-Season Glucose Competitions in Mixed-*Candida* Species Environments

Firstly, we replicated one-season competition between *C. glabrata* strain ATCC 2001 and *C. albicans* ACT1-GFP in low glucose (0.1% w/v) Synthetic Complete (SC) medium, to ensure that we could replicate the results of Nilsson (2012) and Beardmore *et al.* (in prep). Previously, a significant increase in *C. albicans* frequency for five initial starting fractions was described over 24-hour competition. In support, we found that fitness of *C. albicans* relative to *C. glabrata* was significantly greater than 1 for all initial fractions (**Figure 2.2(a); Table A.1.2.S2**), meaning that *C. albicans* was consistently fitter than *C. glabrata* in short-term competition at this glucose concentration. The increase in *C. albicans* density in each competition mixture determined by CHROMagar plating (green colonies) is shown in **Figure 2.2(b)**. We fitted a least-squares linear regression to the relative fitness data to see whether our data showed frequency-dependence and found that relative fitness was significantly negatively correlated with initial *C. albicans* fraction (**Figure 2.2(a)**), although co-existence was not predicted to occur at any species ratio.

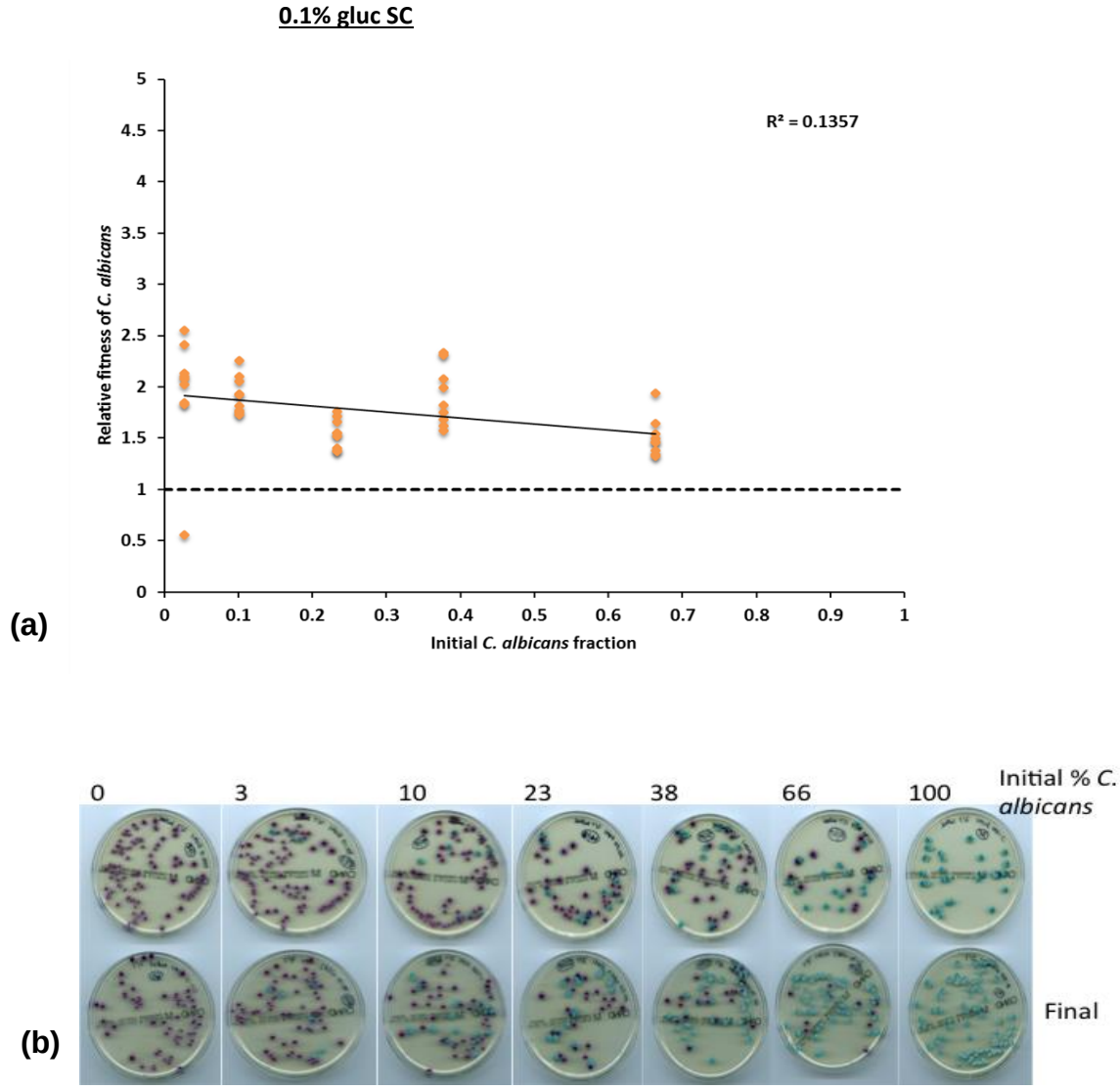

Figure 2.2. One-season competition between *C. glabrata* and *C. albicans* at low glucose concentration in Synthetic Complete (SC) medium. (a) Fitness of *C. albicans* relative to *C. glabrata* over one season (24 hours) of competition in 0.1% w/v glucose SC is calculated as the ratio of their Malthusian parameters (Lenski *et al.,* 1991). Relative fitness assays were performed for mixtures of the two species at five different ratios (initial *C. albicans* fractions plotted). N = 9 for each initial fraction. The black continuous line is the best-fit least-squares linear regression, with the R-squared correlation coefficient shown. The slope of the line is significant (slope = -0.58, t = -2.60, df = 43, *P* = 0.01279). The dotted line indicates a relative fitness of 1 and would predict stable co-existence if the regression line intersected this line at a specific fraction (see **Figure 2.1**). Relative fitness of *C. albicans* is significantly greater than 1 for all species mixtures (Wilcoxon signed-rank test: *P* < 0.01; see **Table A.1.2.S2** for full statistics). **(b)** CHROMagar plates showing change in *C. albicans* fraction for five initial frequencies. 1 plate is shown for each initial and final competition suspension. *C.*

glabrata colonies are purple and *C. albicans* colonies are green. Mean frequencies (%) of *C. albicans* for initial populations are shown.

2.4.2 Competition in SU Media: CHROMagar Plating

To investigate whether these competitive outcomes are applicable to *Candida* species competitions in more clinically relevant environments, we completed competitions between *C. glabrata* and *C. albicans* in Synthetic Urine medium at each of six different glucose concentrations, starting with five initial fractions of *C. albicans*. We used CHROMagar plating to determine species densities. Firstly, we tested whether initial *C. albicans* fraction, glucose concentration and their interaction had a significant effect on relative fitness of *C. albicans,* using a general linear model. Overall, the model was significant (adjusted $R^2 = 0.2258$, $F_{3, 259} = 26.48$, $P = 5.699e\text{-}15$) but the interaction term was non-significant ($P = 0.2090$). This showed that the trend in *C. albicans* relative fitness across different initial fractions was not significantly influenced by glucose concentration **(Figure A.1.2.S3).** We removed the interaction term from the model to achieve an improved fit for the data (adjusted $R^2 = 0.2241$, $F_{2, 260} = 38.84$, $P = 1.744e\text{-}15$; AIC (main effects model) = 679.21, AIC (main effects and interaction model) = 679.61) and found significant independent effects of initial *C. albicans* fraction ($P = 7.131e\text{-}10$) and glucose concentration ($P = 4.826e\text{-}09$) on relative fitness of *C. albicans* **(Figure 2.3).**

At low glucose concentrations (0.05% and 0.1% w/v), *C. albicans* relative fitness was significantly greater than 1 over one-season competition, for all initial fractions apart from the highest at 0.05% (**Figure 2.3; Table A.1.2.S3**), and at the lowest two fractions and the highest fraction at 0.1%. This shows that *C. albicans* was more fit than *C. glabrata* for competition at low glucose. Relative fitness was a significant negative function of *C. albicans* fraction at 0.05%, but not at 0.1%, glucose.

As glucose concentration was increased (0.5-2% w/v), *C. albicans* was less fit than *C. glabrata*, when starting from a high frequency in the population. Relative fitness was a significant decreasing function of *C. albicans* fraction for all three

glucose concentrations (**Figure 2.3; Table A.1.2.S4**) and species co-existence could be predicted for the *C. albicans* fraction at which the regression line intersected with a relative fitness of 1 meaning that both species were equally fit, as described previously (Turner *et al.,* 1996). This *C. albicans* equilibrium fraction was 0.59 for 0.5% glucose, 0.49 for 1% glucose and 0.32 for 2% glucose (**Figure 2.3**). The fitted regression line shows that *C. albicans* is respectively more or less fit than *C. glabrata* at respective frequencies below or above the equilibrium fractions.

At the highest glucose concentration (4% w/v), *C. albicans* relative fitness was significantly lower than 1 for the highest three initial fractions, meaning that *C. glabrata* was fitter than *C. albicans* in competition at these species ratios (**Figure 2.3; Table A.1.2.S3**). Relative fitness was significantly negatively correlated with *C. albicans* fraction.

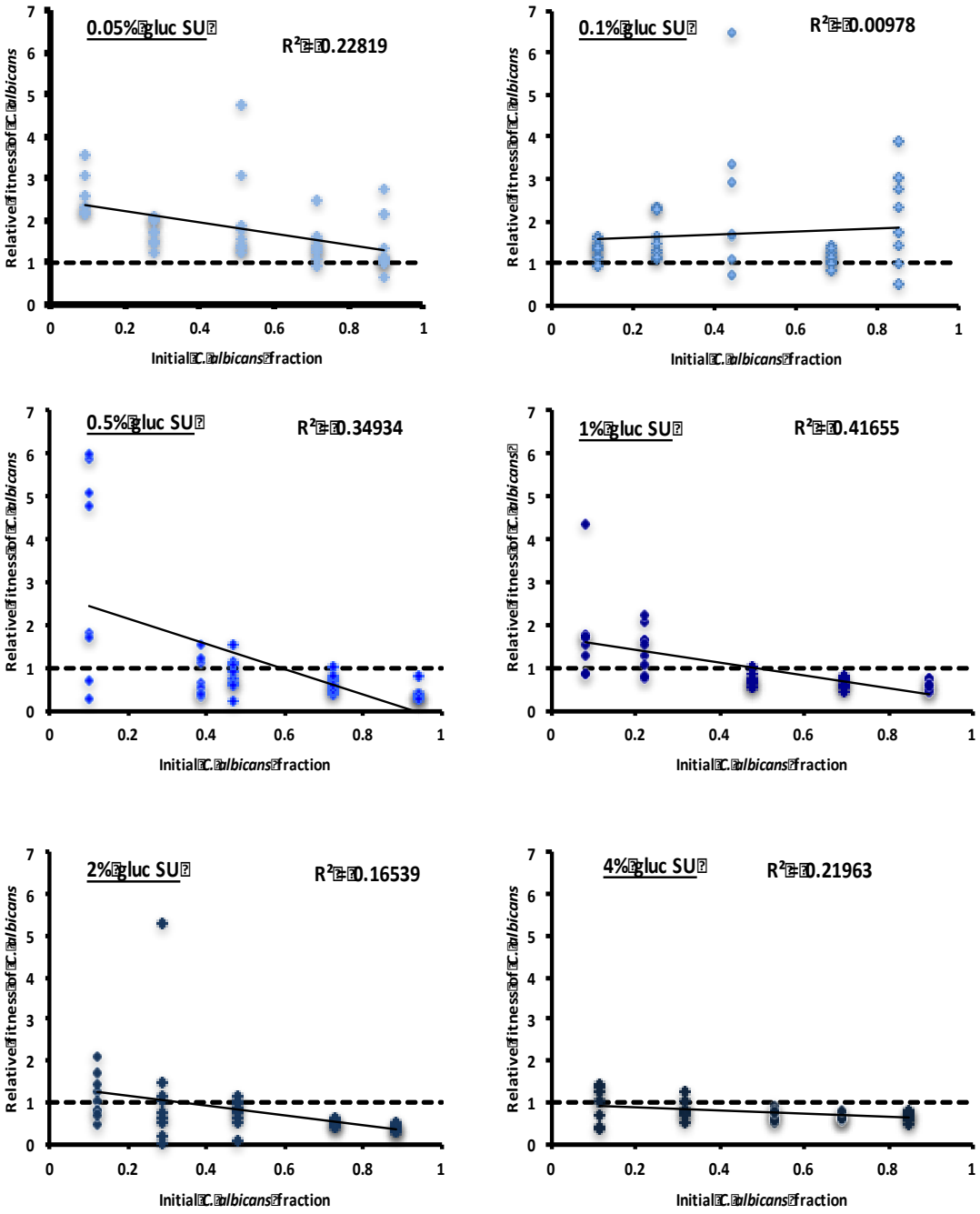

Figure 2.3. One-season competitions between *C. glabrata* and *C. albicans* at 6 different glucose concentrations in Synthetic Urine (SU) media. Single season competitions in glucose concentrations ranging 0.05-4% w/v were completed over single 24-hour periods for five mixtures of the two species (initial *C. albicans* fractions). Relative fitness of *C. albicans* is calculated as the ratio of the two species' Malthusian parameters, as in **Figure 2.2**. N = 9 for each initial fraction at each glucose concentration. The black continuous line on each plot is the linear least-squares regression with the R-squared correlation coefficient shown for each. The slope of each regression is significant for all glucose concentrations, except 0.1% w/v (0.05%: *P* = 0.0009453; 0.1%: *P* = 0.5333; 0.5%: *P* = 3.005e-05; 1%: *P* = 1.696e-06; 2%: *P* = 0.005566; 4%: *P* = 0.001166; **Table A.1.2.S4**). The dotted line on each plot indicates a

relative fitness of 1 and predicts stable species co-existence at 0.5 - 2% w/v glucose, when *C. albicans* has a relative fitness of 1 (see **Figure 2.1**). For plots in which co-existence is not predicted: 0.05% glucose- relative fitness is significantly greater than 1 ($P < 0.05$) for all initial *C. albicans* fractions, except 0.89; 0.1% glucose- relative fitness is significantly greater than 1 ($P < 0.05$) for the lowest two fractions and the highest initial fraction ($P < 0.05$); 4% glucose- relative fitness is significantly lower than 1 for the highest three initial fractions ($P < 0.0001$) (**Table A.1.2.S3**).

2.4.3 Long-Term Competition Dynamics in Clinically Relevant SU Media

We tested whether our short-term results, which show that *C. albicans* is fitter than *C. glabrata* at low glucose concentration, would lead to *C. glabrata* exclusion over long-term competition. We then investigated whether our predicted species co-existence, in an intermediate glucose concentration from one-season competition, resulted in stable equilibrium frequencies long-term. We selected a high initial fraction (0.70) of *C. albicans* for competitions with *C. glabrata* over daily transfers of a constant volume of cells into fresh media and plating of competition suspensions on CHROMagar. We found that *C. albicans* increased and excluded *C. glabrata* after 11 seasons at low glucose (0.1% w/v) (**Figure 2.4(a) and (c)**), as predicted from one-season data. At intermediate glucose (1% w/v), instead of reaching stable coexistence at a predicted *C. albicans* fraction of 0.49 (**Figure 2.3**), *C. albicans* rapidly decreased and was excluded from the population by *C. glabrata* after 11 days (**Figure 2.4(b) and (d)**).

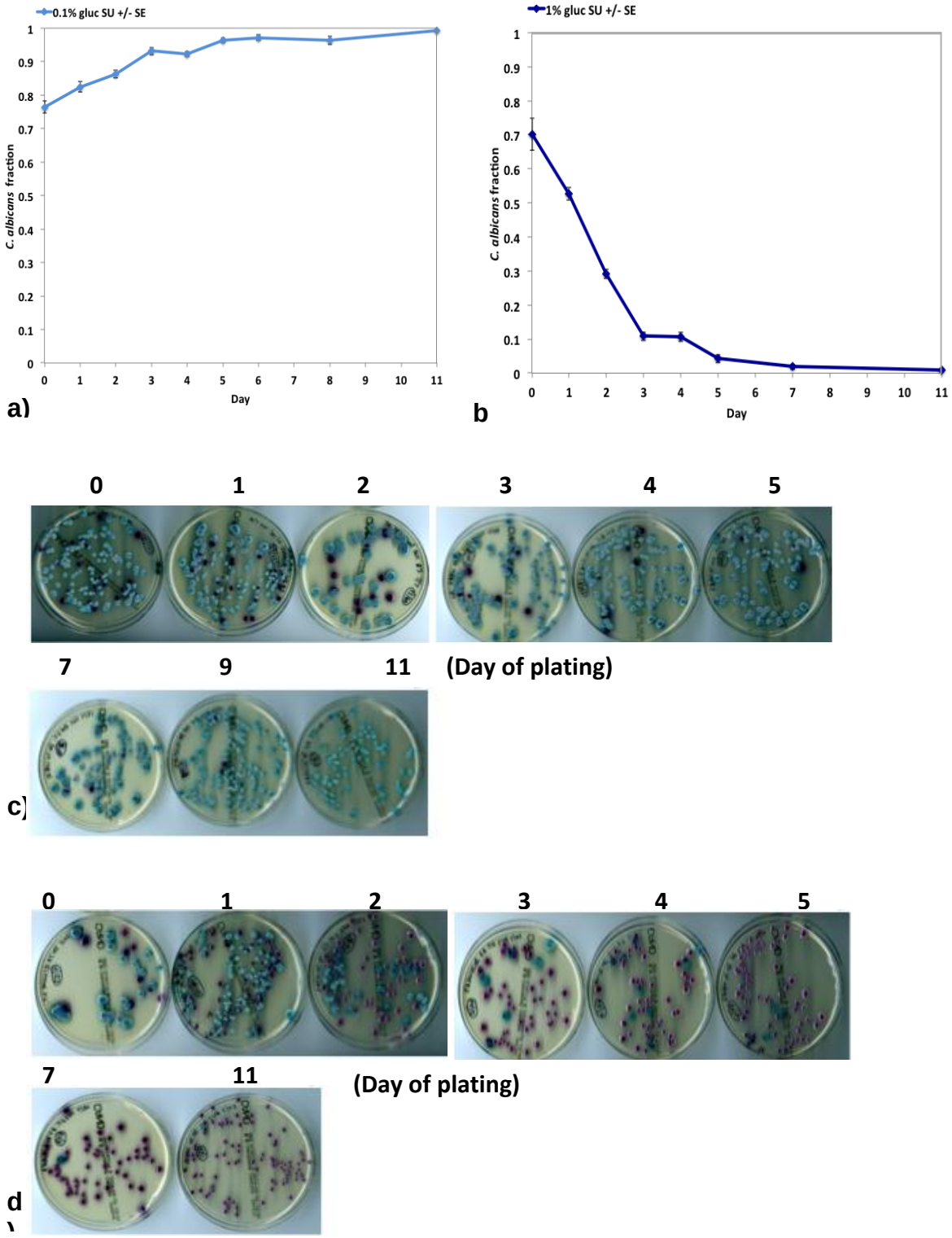

Figure 2.4: Long-term competition of a high initial fraction of *C. albicans* with *C. glabrata* at low and intermediate glucose concentrations in Synthetic Urine media, via volumetric serial transfers. a) Low glucose concentration (0.1% w/v); **b)** Intermediate glucose concentration (1% w/v); **c)** Increase in *C. albicans* fraction on CHROMagar (1 replicate per day plated); **d)** Decrease in *C. albicans* fraction on CHROMagar. Initial *C. albicans* fraction was taken as the average of 3 CHROMagar plates, as for one-season competitions. End-of-season populations were plated daily

on CHROMagar (9 replicates) until day 5, after which plating was done every 2-4 days until day 11. SE bars are shown. Initial cell density at day 0 was 2.2 x 10^6 cells/ml for 0.1% glucose and was 1.7 x 10^6 cells/ml for 1% w/v glucose.

As *C. albicans* was excluded from the populations at 1% w/v glucose rather than co-existing with *C. glabrata* as predicted, we repeated the experiment with daily transfers of a constant density of cells. This was performed, as any deviation in initial cell density between seasons could have affected competitive pressures, meaning that initial season competition dynamics were not predictive of later seasons. Again, by starting with a high initial *C. albicans* fraction and plating end of season competition suspensions on CHROMagar, *C. albicans* was excluded from the populations after 7 days (**Figure 2.5**).

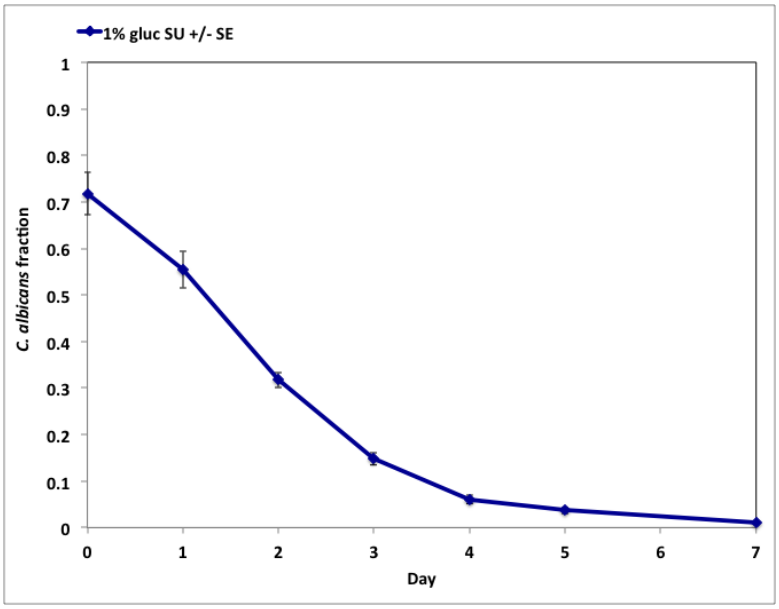

Figure 2.5: Long-term competition of a high initial fraction of *C. albicans* with *C. glabrata* at intermediate glucose concentration (1% w/v) in Synthetic Urine media, via cell density serial transfers. Initial *C. albicans* fraction was taken as the average of 3 CHROMagar plates, as for one-season competitions. End-of-season populations were plated daily on CHROMagar (9 replicates) until day 5 and then on day 7. Initial cell density at day 0 was 3.5 x 10^6 cells/ml.

2.4.4 Influence of Small Frequency and Density Changes on Long-Term Competition Dynamics

Firstly, we selected three initial frequencies of *C. albicans* (approximately 0.20, 0.50 and 0.80) to compete against *C. glabrata* in Synthetic Urine media at 1% w/v glucose over daily serial transfers of a constant volume of cells. *C. albicans* decreased in fraction and was excluded by *C. glabrata* from all 3 populations after 9 seasons of competition (**Figure 2.6(a); Table A.1.2.S5**). Next, we found that over small changes in initial cell density (a doubling and halving of that used above) for a low initial fraction, *C. albicans* was again excluded from the populations after 9 seasons of competition with *C. glabrata* (**Figure 2.6(b); Table A.1.2.S5**). These results support the long-term exclusion of *C. albicans* at intermediate glucose concentration.

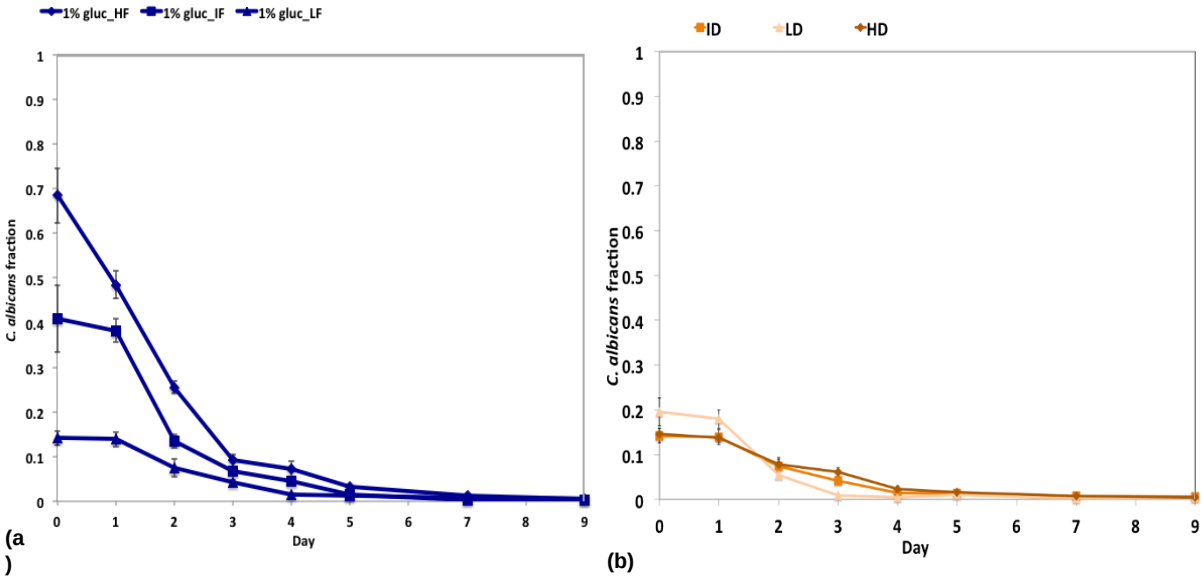

Figure 2.6: Long-term competitions between *C. glabrata* and *C. albicans* for different initial frequencies of C. albicans and co-culture initial densities. a) Competition at 3 different initial fractions. LF (triangles)=0.14 (initial density = 2.35 x 10^6 cells/ml), IF (squares)= 0.41 (initial density = 1.9 x 10^6 cells/ml), HF (diamonds)= 0.68 (initial density = 1.45 x 10^6 cells/ml): determined from viable counts on 3 CHROMagar plates per ratio. One-way ANOVA tests on daily *C. albicans* fraction changes: HF: $F_{7, 58}$ = 183.6, *P* < 2e-16 ***; IF: $F_{7, 58}$= 134.3, *P* < 2e-16 ***; LF: $F_{7, 58}$ = 27.23; *P* = 3.87e-16 ***. **b)** Competition at 3 different initial densities. LD (light orange, triangles) =9 x 10^5 cells/ml (initial frac = 0.20), ID (bright orange, squares) =2.35 x10^6 cells/ml (initial frac = 0.14), HD (brown, diamonds) =5.05 x 10^6 cells/ml (initial frac =

0.15): determined from viable counts on CHROMagar. One-way ANOVAs: HD: $F_{7, 58}$ = 54.08; *P* < 2e-16 ***; ID (same as LF); LD: $F_{7, 58}$ = 71.25; *P* < 2e-16 ***. Competition suspensions were plated on days 1 - 5, 7 and 9 in both experiments. Points plotted are averages from 9 CHROMagar plates with SE bars shown. See **Table A.1.2.S5** for significant pairwise comparisons.

2.4.5 Influence of Larger Density Changes on One Season Competition Dynamics

Firstly, we investigated whether a ten-fold increase in initial cell density could affect one-season competition dynamics over the same set of five initial *C. albicans* fractions. By measuring the change in *C. albicans* and *C. glabrata* cell densities at the beginning and end of 24-hour competition, unexpectedly we found that at 0.05% glucose only, both species' final densities were lower than their initial densities. This was likely due to error in dilution plating rather than cell death occurring during the experiment. This did not allow plotting of *C. albicans* relative fitness but we found that *C. albicans* decreased in frequency at all five initial fractions and this was significant for the lowest three fractions (**Table 2.1**), therefore *C. albicans* became less fit than *C. glabrata* in low glucose.

A ten-fold higher cell density for competition at intermediate (1% w/v) (**Figure 2.7(a)**) and high (4% w/v) (**Figure 2.7(b)**) glucose concentrations resulted in *C. albicans* relative fitness significantly lower than 1 (**Table A.1.2.S3**) for all initial *C. albicans* fractions, except for the lowest fraction in 1% glucose, so *C. glabrata* was more fit than *C. albicans*. For 1% glucose, these results contrast to those from ten times lower cell density (**Figure 2.3**), because relative fitness is not significantly negatively correlated with initial fraction and the regression line does not predict co-existence at any fraction, at ten times greater density (**Figure 2.7(a); Table A.1.2.S4**). The results at 4% glucose are similar to those at ten times lower density (**Figure 2.3**) and a significant negative frequency-dependent effect is still observed, as the slope of the regression was significant (**Figure 2.7(b)**).

In contrast to a large increase in competitor density, we also tested whether one-thousand times decrease in initial competition density affected one season competition dynamics. Starting with an initial density of 10^3 cells/ml, *C. albicans* had a relative fitness significantly greater than 1 for all initial fractions (**Figure 2.7(c); Table A.1.2.S3**), which was a stronger effect than that found at one-thousand times higher cell density (**Figure 2.3**) and *C. albicans* showed larger and more significant increases in frequency at lower density (**Table 2.2**). There was no significant negative frequency-dependent effect on relative fitness and the regression line did not predict co-existence (**Figure 2.7(c); Table A.1.2.S4**).

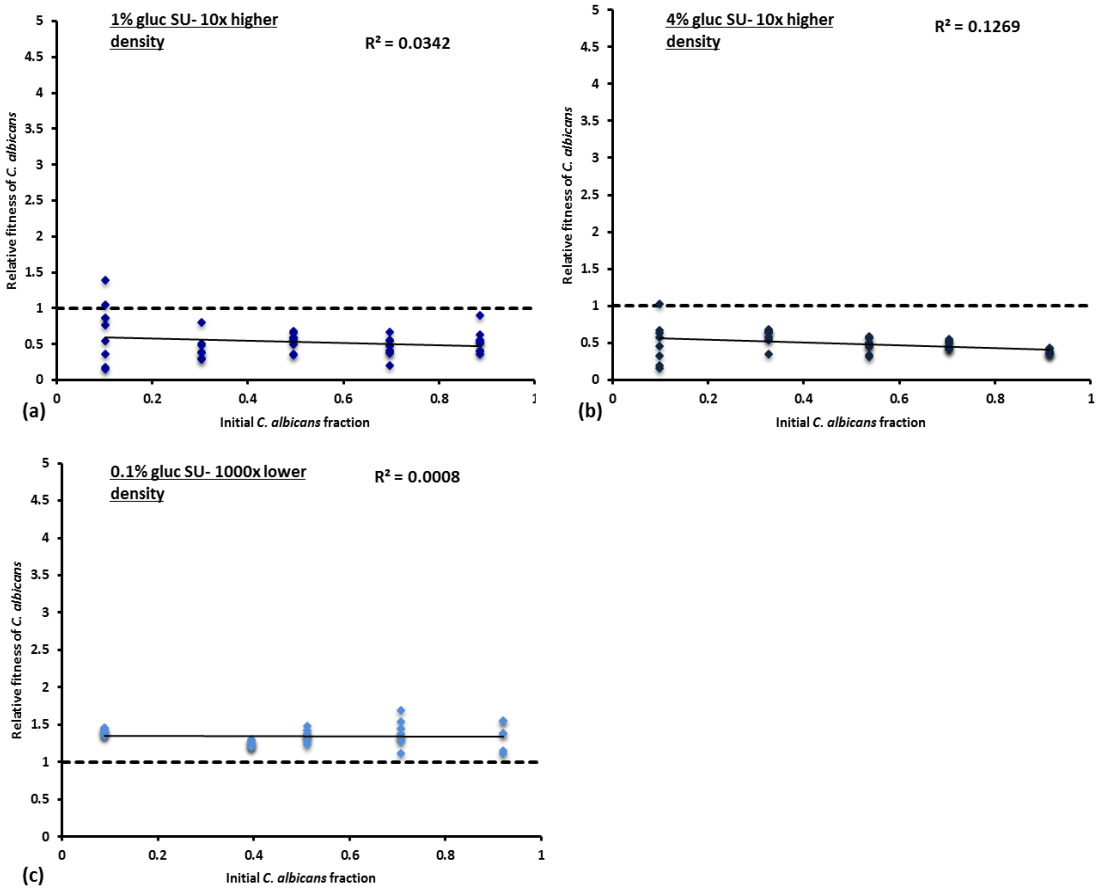

Figure 2.7: One-season competition between *C. glabrata* and *C. albicans* at different glucose concentrations in Synthetic Urine medium, for large changes in initial cell densities of competition suspensions. Competition was tested at ten times the initial cell density used in **Figure 2.3** and is shown for two different glucose concentrations: **(a),** intermediate (1% w/v) **(b)** high (4% w/v). Competition at one thousand times lower initial density was tested for 0.1% w/v glucose **(c).** Initial and end ratios were plated on CHROMagar. Initial cell densities (from viable colony counts) for all mixed species ratios were between 2.33 and 2.67 x 10^7 cells/ml for 0.05% w/v

glucose, between 2.32 and 2.71 x 10^7 cells/ml for 1% w/v glucose, and between 2.15 and 2.52 x 10^7 cells/ml for 4% w/v glucose. Average initial cell density of co-cultures for one thousand times lower cell density for 0.1% glucose was 2.35 x 10^3 cells/ml. Data is plotted as relative fitness of *C. albicans* over 24 hours of competition and correlation coefficients are shown, as in **Figure 2.3.** The slope of each regression line is not significant, except for 4% glucose at ten times initial cell density (P = 0.01760; **Table A.1.2.S4**). Significance tests for *C. albicans* relative fitness significantly different from 1 (**Table A.1.2.S3**): 1% glucose- lower than 1 for all initial fractions apart from the lowest (P < 0.0001); 4% glucose- lower than 1 for all initial fractions (P < 0.05); 0.1% glucose at one thousand times lower initial cell density- greater than 1 for all initial fractions (P < 0.01).

Table 2.1: Statistical comparisons of initial and final *C. albicans* fractions over one-season competition between *C. glabrata* 2001 and *C. albicans* GFP in 0.05 % w/v glucose Synthetic Urine medium at ten times greater competition density. Initial and final *C. albicans* fractions were determined from CHROMagar plating and averages are shown. Fractions are presented in ascending order. Values in bold show significance with asterisks indicating significance level: * = P < 0.05; ** = P < 0.01; P < 0.001.

0.05 % w/v glucose: 2-tailed, 2-sample t-tests				
Average initial *C. albicans* fraction	**Average final *C. albicans* fraction**	**df**	**t-value**	***P*-value**
0.136315176	0.080803335	10	2.6715	**0.02343 ***
0.368573461	0.259124652	10	3.0119	**0.01308 ***
0.583120393	0.398088425	10	3.0819	**0.0116 ***
0.768867294	0.684041314	10	1.4942	0.166
0.918357488	0.895937455	10	0.78295	0.4518

Table 2.2: Statistical comparisons of initial and final *C. albicans* fractions over one-season competition between *C. glabrata* 2001 and *C. albicans* GFP in 0.1 % glucose Synthetic Urine medium, for initial competition cell densities of approximately 10^6 and 10^3 cells/ml. Initial and final *C. albicans* fractions were determined from colony counts on CHROMagar plates and averages are shown. Values in bold show significance with asterisks indicating significance level: * = P < 0.05; ** = P < 0.01; P < 0.001.

0.1% w/v glucose: 2-sample, 2-tailed test: 10^6 cells/ml				
Initial *C. albicans* fraction	**Final *C. albicans* fraction**	**df**	**t-value**	***P*-value**
0.112864672	0.16459501	10	-2.0833	0.06385
0.2590261	0.3645866	10	-2.9794	**0.01382 ***
0.4420522	0.5415211	10	-1.821	0.09862
0.6883541	0.7164979	10	-1.0422	0.3219
0.8499979	0.8944496	10	-1.2329	0.2458

0.1% w/v glucose: 2-tailed, 2-sample t-tests: 10^3 cells/ml				
Average initial *C. albicans* fraction	**Average final *C. albicans* fraction**	**df**	**t-value**	***P*-value**
0.088525531	0.491319381	10	-13.605	**8.899e-08 *** **
0.39497314	0.730916927	10	-10.81	**7.748e-07 *** **
0.511993024	0.871003859	10	-16.552	**1.353e-08 *** **
0.706162137	0.936851406	10	-8.0934	**1.064e-05 *** **
0.920388091	0.987537691	10	-7.4151	**2.275e-05 *** **

2.4.6 Influence of Larger Competition Volumes on One Season Population Dynamics

To investigate the possibility of oxygen limitation causing downward shifts in *C. albicans* relative fitness, we reduced the surface area to volume ratio in the competition mixture by competing *C. glabrata* and *C. albicans* over single seasons in 5 ml culture tubes, in low glucose (0.05% w/v) SU (**Table 2.3a**) and SC (**Table 2.3b**) media (see Methods). This was used as a proxy for reduced oxygen availability with more competitors, occurring at ten times the initial cell density. Tubes with larger competition mixture volumes have a smaller surface area to volume ratio so have less capacity for gaseous exchange.

Measuring change in *C. albicans* frequency over a single season starting from 0.50 fraction, the largest frequency increases were seen for the smallest competition suspension volumes with the biggest surface area to volume ratios. In SU media, *C. albicans* frequency increased by 13% for a 1.5-fold greater volume than in the microtiter plate whereas a 5-fold greater volume only resulted in a 7% increase (**Table 2.3a**). When the competition suspension volume was increased to 10 or 15 times the volume used in 96-well plate wells, *C. albicans* frequency decreased by 7%. These trends were also seen in SC media, as a 1.5-fold increase in volume resulted in a 19% increase in *C. albicans* frequency, compared with a 3% increase for a 3.5-fold greater final volume (**Table 2.3b**).

We conclude that *C. albicans* is fitter in more aerobic environments, which is supported by the negative correlation we find between *C. albicans* relative fitness and culture tube volume in 0.05% w/v glucose media (**Figure 2.8**). Co-existence is predicted when *C. albicans* fitness is equal to that of *C. glabrata,* which occurs in a competition volume of 1616 µl in SU (**Figure 2.8a**) and 545 µl in SC (**Figure 2.8b**), suggesting that *C. albicans* is fitter in the nutritionally poorer SU medium.

Table 2.3: Change in *C. albicans* fraction over one-season competition between *C. glabrata* 2001 and *C. albicans* GFP in 5-ml culture tubes. A range of final volumes was tested, representing fold increases in the final volume (150 µl) used in the 96-well plate for competitions. A larger range was tested for SU media and the 3 volumes with results most comparable to one-season 96-well plate data were selected for confirmation in SC media. Initial species ratio was set to 50:50 and initial cell density added to tubes was set to approximately 6.5 x 10^6 cells/ml (diluted 2-fold in media). Media glucose concentration was 0.05% w/v. **a)** Competition in SU media. **b)** Competition in SC media.

a)

Fold increase in final volume	***C. albicans* fraction change**
1.5	13% increase
2.5	8% increase
3.5	10% increase
4	6% increase
5	7% increase
10	7% decrease
15	7% decrease

b)

Final increase in final volume	***C. albicans* fraction change**
1.5	19% increase
2.5	8% increase
3.5	3% increase

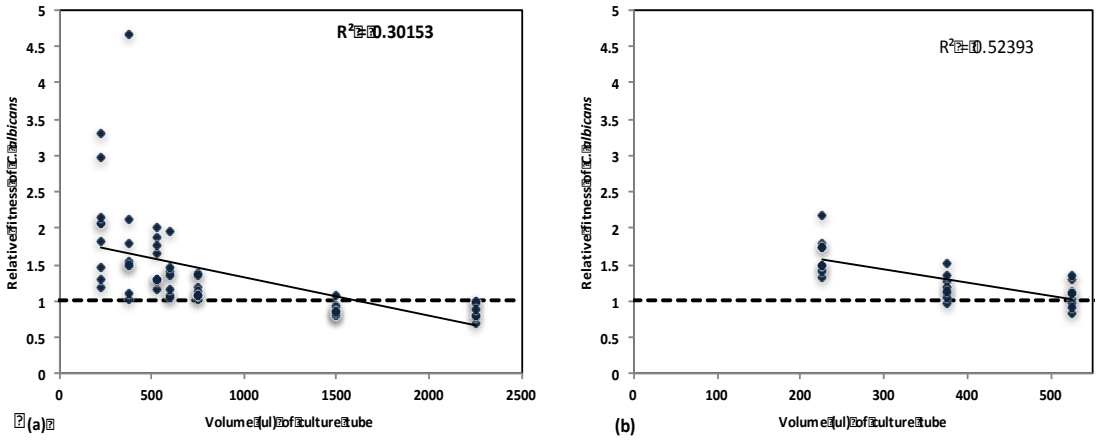

Figure 2.8. One-season competition between *C. glabrata* and *C. albicans* at a 50:50 ratio in 0.05 % w/v glucose media, for different volumes of competition suspension in culture tubes. 5-ml culture tubes were used for competitions with 7 different final volumes in SU media **(a)** and 3 different final volumes in SC media **(b).** N = 9 for each tube volume. Relative fitness of *C. albicans* is calculated as the ratio of the two species' Malthusian parameters. The slope of the least-squares linear regression line on each plot is significant (**(a)** slope = -0.00053, t = -5.13, df = 61, *P* = 3.159e-06; **(b)** slope = -0.0018, t = -5.25, df = 25, *P* = 1.978e-05). Co-existence is predicted for competition volumes at which the regression line intersects with relative fitness of 1.

2.4.7 Competitions between *C. albicans* and Clinical Isolates of *C. glabrata*

To test whether *C. albicans* relative fitness in glucose competition is dependent on *C. glabrata* strain, we competed clinical strains of *C. glabrata* (**Table A.1.2.S1**) against the *C. albicans* reference strain in 0.05 % w/v glucose in microtiter plates over one season, plating the competition suspensions on CHROMagar. Using standard SC medium as strains were isolated from different host sites, we found that *C. albicans* relative fitness significantly varied in competition with different strains of *C. glabrata* (**Figure 2.9**; One-way ANOVA: $F_{4, 40} = 11.94$, *P* = 1.78e-06). *C. albicans* relative fitness was significantly greater in competition with *C. glabrata* strain 3605 (mean *C. albicans* relative fitness = 1.599 +/- 0.1275) than in competition with each of the other strains (Tukey HSD *post hoc* tests: 3605:2001, *P* = 0.0422; 3605:BG2, *P* = 0.000225; 3605:BG2Δ*ssk2*, *P* = 0.00231; 3605:3309, *P* = 0.0000007). This showed that *C. glabrata* 3605 was a poorer competitor than the other strains. *C. albicans* relative fitness was significantly greater in competition with strain

ATCC 2001 than NCPF 3309 (mean relative fitness: 1.273 +/- 0.1132; 0.8650 +/- 0.0183 respectively; Tukey HSD *post hoc* test: *P* = 0.00614). *C. albicans* relative fitness was not significantly different between competitions with strains BG2 or BG2Δ*ssk2,* or between either of these strains and strain 2001 or 3309 (Tukey HSD *post hoc* tests: *P* > 0.05). *C. albicans* was significantly more fit (relative fitness > 1.0) with all strains (one-sample, two-tailed t-tests: ATCC 2001: t(8) = 2.412, *P* = 0.0424; BG2: t(8) = 2.4917, *P* = 0.0374; BG2Δ*ssk2:* t(8) = 5.2061, *P* = 0.000816; NCPF 3605: t(8) = 4.6975, *P* = 0.00155), except strain 3309, with which *C. albicans* was less fit (relative fitness < 1.0) (one-sample, two-tailed t-test: t(8) = -7.3862, p = 7.721e-05).The two *C. glabrata* strains most contrasting in competitive abilities were NCPF 3605 as the poorest competitor (*C. albicans* mean relative fitness: 1.599 +/- 0.1275) and NCPF 3309 as the best competitor (*C. albicans* mean relative fitness: 0.8650 +/- 0.0183).

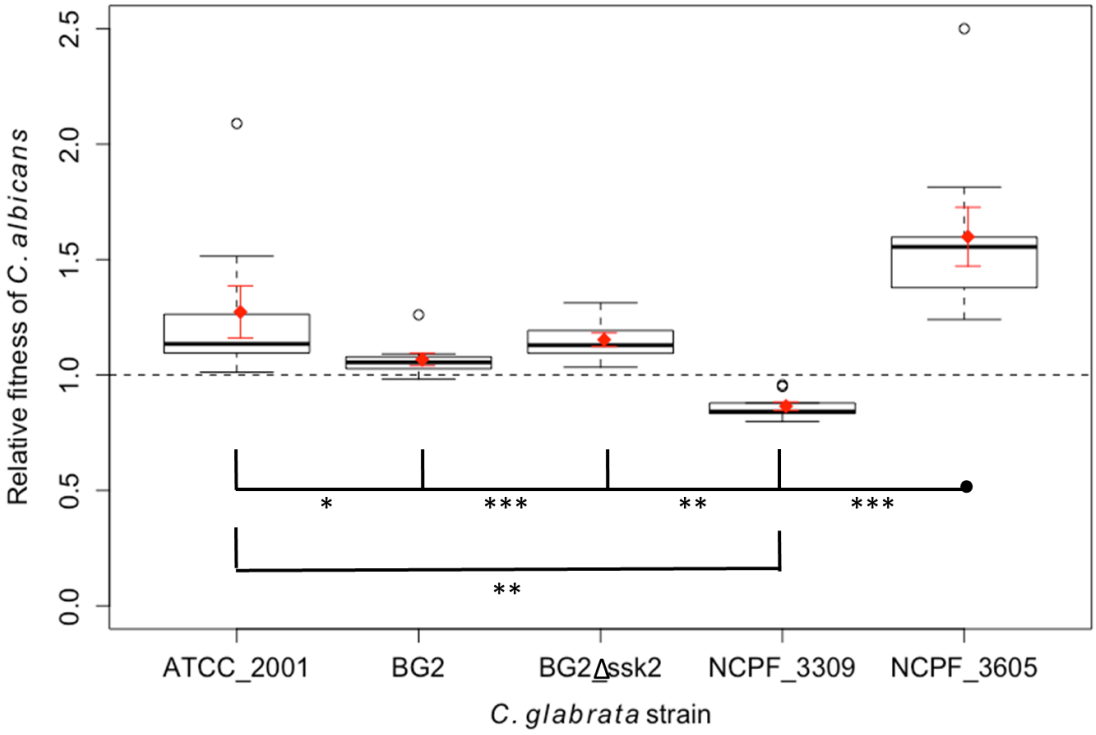

Figure 2.9: One-season competition between *C. glabrata* clinical strains and *C. albicans* at low glucose concentration in SC medium. A set of 4 clinical isolates (**Table A.1.2.S1**), in comparison with the reference *C. glabrata* strain (ATCC 2001) were competed against a single high initial fraction of *C. albicans* GFP (~0.80 - 0.90). The assay medium was 0.05 % w/v SC medium. Relative fitness of *C. albicans* was calculated from the ratio of Malthusian parameters. N=9 for each species. The dotted line passing through relative fitness = 1.0 indicates no change in *C. albicans* fitness

during one-season competition. Box-plots show the median value as a horizontalline, 1st and 3rd quartiles as box limits, whiskers marking 1.5 x interquartile range in both directions and empty plotted points as outliers. Red points and error bars overlaying each box represent mean and standard error. Relative fitness of *C. albicans* was significantly different in competition with different *C. glabrata* strains: One-way ANOVA ($F_{4, 40}$ = 11.94, *P* = 1.78e-06) and Kruskal-Wallis test ($\chi^2(4)$ = 33.743, *P* = 8.413e-07). Significant pairwise differences identified by Tukey HSD *post hoc* tests are shown by connecting lines. Asterisks represent significance level: * *P* < 0.05; ** *P* < 0.01; *** *P* < 0.001. Mean (+/- SE) relative fitness of *C. albicans* in competition with each *C. glabrata* strain: ATCC 2001- 1.273 +/- 0.1132; BG2- 1.0674 +/- 0.027; BG2Δ*ssk2*- 1.153 +/- 0.0294; NCPF 3309- 0.8650 +/- 0.0183; NCPF 3605- 1.599 +/- 0.1275.

To determine whether differing strain competitive abilities were also present at high glucose and maintained long-term, we individually competed strains NCPF 3605 and NCPF 3309 with *C. albicans* in high glucose (4% w/v) SC media (see Methods; data not shown). *C. albicans* greatly decreased in frequency in competition with each strain over five seasons (initial-end: 0.47 - 0.06 for 3605; initial-end: 0.72 - 0.02 for 3309). This equated to an 87% proportional decrease in *C. albicans* fraction in competition with strain 3605 compared with a 97% proportional decrease in *C. albicans* in competition with strain 3309. These results support the decrease in *C. albicans* fraction in long-term competition seen with strain 2001 in SU media at intermediate glucose (1% w/v: **Figure 2.4b**), suggesting that long-term outcomes in this *in vitro* system are broadly conserved across strains.

2.5 Discussion

The human microbiota is composed of a diversity of bacterial species, but fungal species also have an important role in health and disease, often interacting in mixed-species communities (Underhill and Iliev, 2014). The eco-evolutionary dynamics of standard bacterial (Turner *et al.,* 1996) and yeast (MacLean and Gudelj, 2006) laboratory species have been studied in *in vitro* simple nutrient environments, but competitive interactions between clinical fungal species have not been explored in depth. It is important to understand the ecological dynamics in clinical environments, as mixed-species infections make up a significant proportion of *Candida* species infections (Nace *et al.,* 2009). We investigated short and long-term resource competition between *C. albicans* and *C. glabrata* in clinically relevant environments, testing different species frequencies, densities and clinical strains. We found that outcomes of species competition were dependent on resources and that discrepancy occurred between short and long-term outcomes. These findings contribute to understanding fungal interactions that underlie mixed-species clinical infections.

During short-term competitions in Synthetic Urine (SU) media, we found that *C. albicans* had a greater fitness than *C. glabrata* in low glucose concentrations (0.05 - 0.1% w/v) but was less fit in high glucose (4% w/v). This correlates with the findings of Nilsson (2012) and Beardmore *et al.* (in prep), who described a shift from *C. albicans* to *C. glabrata* with increasing glucose concentration, over competitions in the standard Synthetic Complete (SC) minimal medium. These results are similar to those from glucose competition between *Saccharomyces cerevisiae* and *Candida utilis* (Postma *et al.,* 1989a) in which *C. utilis* dominated under glucose-limited conditions due to the presence of high affinity transporters, compared with low affinity transporters in *S. cerevisiae*. Similar to *C. utilis, C. albicans* may dominate in low glucose due to its high affinity glucose sensor encoded by *HGT4* (Brown *et al.,* 2006) and efficient glucose utilisation from transcriptomic regulation of respiratory genes (Rodaki *et al.,* 2009). *C. glabrata* may dominate under glucose excess due to lower affinity glucose transport and less-efficient utilisation for growth, due to up-regulation of fermentative genes, as described for *S. cerevisiae.*

The shift towards *C. glabrata* with increasing glucose is consistent with detection of *C. glabrata* infections in diabetics (Fidel *et al.,* 1996; Malani *et al.,* 2011) and is of clinical concern as multi-drug resistant *C. glabrata* infections are common (Farmakiotis *et al.,* 2014). The glucose concentrations we use are physiologically relevant as glucose is not normally present in the urine of healthy patients, but can be detected at concentrations of 11 mmol/l (0.2 % w/v) in the urine or blood of diabetics (WHO Committee on Diabetes Mellitus, 1980; Gibson *et al.,* 1990).

In short-term competitions in SU media at intermediate glucose concentrations (0.5-2% w/v) we found that *C. albicans* relative fitness was a decreasing function of its initial frequency, such that species co-existence occurred at an intermediate species frequency. *C. albicans* was fitter than *C. glabrata* when at low frequency but was less fit than *C. glabrata* when common. Negative frequency-dependent selection has been observed in single-season competition between two different *Eschericia coli* metabolic genotypes in single resource environments (Turner *et al.,* 1996) and in glucose competition between socially interacting co-operator and cheat *S. cerevisiae* strains (MacLean and Gudelj, 2006). In these systems, co-existence via negative frequency dependence occurred due to temporal heterogeneity in resource levels during the season: resources change from high to low (Levin, 1972; Rainey *et al.*, 2000). Under competition for a single resource, if one competitor grows faster at higher resource concentrations and the other grows faster at lower resource levels then a balance between the two strategies will result in stable co-existence (Stewart and Levin, 1973). This may be the mechanism for co-existence in our system as it is likely that *C. albicans* grows faster at lower resources and *C. glabrata* grows faster at higher resources.

Our work shows that negative frequency-dependent selection can occur in competition for a single carbon source between clinical species in more complex clinically-relevant media. By using synthetic urine medium, we could mimic *Candida* species interactions that occur in urinary tract infections, which are commonly composed of *C. glabrata* and *C. albicans* (Fidel *et al.,* 1999). SU is a “nutritionally poor medium supplemented with urine-specific salts and urea”

(Domergue *et al.,* 2005) and it is possible that amino acid deficiencies or differential species abilities to utilise nitrogen (a large component of the media) could also influence competition dynamics, as these have previously affected virulence and drug resistance in biofilms (Domergue *et al.,* 2005; Uppuluri *et al.,* 2009).

We implemented growth conditions that encouraged the two competitors to grow as single yeast cells (non-adherent microplates, 30^0C and orbital agitation), rather than allowing *C. albicans* to form hyphae, which would have complicated evaluation of species competitive abilities via colony counts. This allowed us to better study interactions amongst fungal commensals (existing in yeast form) within the human microbiota, an area lacking in research (Krom *et al.,* 2014), and to predict interactions that may occur in multi-species infections. We do not claim that the outcomes of our competition experiments will match species interactions in host infections, particularly as fungi naturally co-exist with bacterial species in human environments (Jenkinson and Douglas, 2002) and context-dependent competition can alter competitive outcomes (de Muinck *et al.,* 2013).

CHROMagar plating has been used to measure competition dynamics between *C. albicans* and *C. dubliniensis* in *in vitro* broth and biofilm studies and *C. albicans* dominated in both environments (Kirkpatrick *et al.,* 2000). In contrast, another biofilm study showed that *C. albicans* could be inhibited by *C. krusei* (Thein *et al.,* 2007). Support for antagonistic *C. glabrata*-*C. albicans* interactions was provided in a recent study by Rossoni *et al.* (2015) who found a 77% reduction in *C. albicans* density in dual-species compared with single species biofilms. Alternatively, co-existence and apparent lack of competition between *C. glabrata* and *C. albicans* has been described *in vitro,* likely due to biochemical and morphological differences between the two species (Silva *et al.,* 2011) and may occur *in vivo* due to spatial structuring. Co-existence between *S. cerevisiae* strains has been described in spatially structured environments (MacLean *et al.,* 2010).

For longer term competitions in SU media extended via seasonal batch culturing, *C. albicans* dominated the populations at low glucose (0.1% w/v) but

was excluded at intermediate glucose (1% w/v) concentration. In one-season competition at 0.1% glucose, as *C. albicans* was significantly fitter than *C. glabrata* for most initial fractions and fitness was not a significant decreasing function of *C. albicans* fraction, our long-term results supported our prediction that *C. albicans* would dominate over time. In contrast, at 1% glucose we predicted from one-season competition that stable co-existence would occur long-term for a *C. albicans* fraction of approximately 0.49, but instead *C. albicans* was excluded.

Previous studies have commonly described negative frequency dependence as a predictor of long-term stable co-existence in bacterial and yeast studies (Stewart and Levin, 1973; Ayala and Campbell, 1974; Lunzer *et al.,* 2002; MacLean *et al.,* 2006), in the absence of experimental verification. Some studies have verified that negative frequency dependence maintains stable co-existence via serial batch culturing, for example in competition between *E. coli* genotypes (Turner *et al.,* 1996) or in stable maintenance of polymorphisms in Lenski's long-term *E. coli* evolution experiment (Lenski *et al.,* 1991; Elena and Lenski, 1997). These studies used a constant daily volumetric transfer of cells in order to maintain the same environment each season. In our work, we employed this volumetric transfer method and conducted an independent experiment in which we transferred an approximately equal competition cell density per day in an attempt to more closely replicate the initial season conditions. We found that *C. albicans* was excluded in both experiments, rather than stably co-existing with *C. glabrata.* This shows that negative frequency dependence cannot always predict stable co-existence in *in vitro* competition. It remains to be found whether this would occur for other microbial species in different environments.

Detection of genetic adaptations in *C. glabrata* that allowed it to exploit the niche of *C. albicans* during long-term competition would support previous studies that have described evolutionary changes over ecological timescales (Odling-Smee *et al.,* 2013), due to short generation times of microbes (Feldgarden *et al.,* 2003). Studies of yeast adaptation to limiting glucose identified gene duplication of high affinity hexose transporters HXT6 and HXT7,

which resulted in greater glucose transport, cell yield and relative fitness (Brown *et al.,* 1988).

Long-term exclusion of *C. albicans* at intermediate glucose concentration was robust to different initial competitor frequencies and for a doubling and halving of an initial competition cell density containing *C. albicans* at low initial fraction. In all cases, *C. albicans* was completely excluded after 9 days. These results contrast with the outcome of long-term co-existence of *E. coli* genotypes in seasonal batch cultures, whereby transfers with different competitor starting frequencies all converged on the stable equilibrium fraction (Levin, 1972; Turner *et al.,* 1996). These studies did not test whether differences in initial competition density altered long-term outcomes.

Ten-fold increases in competition cell density over a single season resulted in *C. glabrata* being fitter than *C. albicans* at low (0.05%), intermediate (1%) and high (4%) glucose concentrations, whereas a one-thousand-fold decrease in *C. albicans* at low glucose (0.1%) did not change competitive outcomes. *C. glabrata* is a Crabtree-positive species so produces ethanol (Van Urk *et al.,* 1990) and grows well under anaerobic conditions like its close relative, *S. cerevisiae* (Roetzer *et al.,* 2011; Rozpedowska *et al.,* 2011). In contrast, *C. albicans* is Crabtree-negative and relies on aerobic conditions for growth (Rozpedowska *et al.,* 2011).

We tested for oxygen limitation favouring *C. glabrata* by competing *C. glabrata* and *C. albicans* in a range of different volumes in larger culture tubes. We found that *C. albicans* fitness was negatively correlated with competition volume for single season competition in low glucose SU and SC media, supporting our hypothesis. This indicates that SA/V ratio is important for oxygen uptake, as the smaller ratio for larger tube volumes created oxygen limitation and favoured *C. glabrata.* Ethanol production could be measured in the competition cultures (Verduyn *et al.,* 1984). Previously, ten times increases in inoculum size of *C. glabrata* and *C. albicans* in isolation created additive effects on seasonal biomass and longer exponential growth (Cuenca-Estrella *et al.,* 2001), but the effect on growth in co-culture was not tested. Studying differences in competition density is relevant for better understanding infections, as antifungal

resistance is greater at higher densities in biofilms (Perumal *et al.,* 2007). Quorum sensing may be a relevant mechanism of growth suppression of *C. albicans* through farnesol production (Weber *et al.,* 2010) but this remains to be explored.

In contrast, lowering initial cell densities by one thousand times in low glucose still resulted in *C. albicans* having greater fitness than *C. glabrata,* although larger increases in *C. albicans* frequencies occurred at the lower cell density. This was likely due to the increased number, rather than rate, of doublings over the single season as the populations were further away from carrying capacity. It remains to be tested whether lower cell densities would change *C. albicans* relative fitness at higher glucose concentrations and whether co-existence would still be predicted. Using lower competition densities is relevant for understanding niche establishment and commensal interactions of *Candida* species prior to pathogenic overgrowth.

C. albicans relative fitness significantly varied across one-season competitions when in competition with different *C. glabrata* clinical strains at low glucose concentration. *C. albicans* was most fit in competition with *C. glabrata* strain NCPF 3605, showing that this strain was the poorest competitor in low glucose. This correlates with strain 3605's isolation from a diabetic patient (**Table A.1.2.S1**) and its likely preferential adaptation to higher blood glucose concentrations, as strain 3605 could outcompete *C. albicans* over long-term competition in high glucose. In contrast, we found that clinical strain 3309 isolated from the gastrointestinal tract was more competitive than *C. albicans.* In comparison, *C. albicans* had a greater relative fitness when in competition with strain BG2 that was isolated from the vagina, a higher glucose environment than the gastrointestinal tract (Karabocuoglu *et al.,* 1994; Owen and Katz, 1999). This indicates that the species composition of infections could vary between different body sites and patients. Antifungal resistance is likely to be greater in infections in which *C. glabrata* is a better competitor, due to its intrinsic drug resistance (Fidel *et al.,* 2009). *Candida* species colonise a diversity of host sites (Underhill and Iliev, 2014) and differences in *C. glabrata* clinical isolate genetics (Healey *et al.,* 2016) could influence strain competitive abilities. In a previous study of clonal types of the bacterial opportunistic

pathogen MRSA (methicillin-resistant *Staphylococcus* aureus), it was found that clones with a greater competitive fitness were also more drug-resistant (Knight *et al.,* 2012). By designing treatments that manipulate the metabolic environment (Allison *et al.,* 2011), for example by reducing glucose availability, there is potential to reduce the frequency of *C. glabrata* strains that have adapted as better competitors in infection sites with greater glucose concentrations.

2.6 Conclusions of the Chapter

In conclusion, our results are threefold:

1) The outcome of *in vitro Candida* species competition in clinically relevant environments is dependent on resources.

2) Short-term negative frequency-dependent dynamics cannot always predict long-term competitive outcomes, as shown in mixed *Candida* species competitions.

3) *C. glabrata* competitive abilities differ across clinical strains.

Interactions between *C. albicans* and *C. glabrata* will be explored in a model invertebrate host in Chapter 3, in which we explore the effect of strain virulence on host immunity.

3. Chapter 3: Dual *Candida* Species Interactions in the Host Model *Galleria mellonella*

3.1 Introduction

Dual species fungal infections, particularly those consisting of *Candida* species, compose a significant proportion of all fungal infections and are more difficult to treat than single species infection (Boktour *et al.,* 2004). This has stemmed from the rise of non-*albicans* species in infections, with *C. glabrata* second most commonly isolated after *C. albicans* (Odds *et al.,* 1996). Multi-species infections are responsible for 2-10% of *Candida* species bloodstream infections and the most common combination reported is *C. glabrata* and *C. albicans,* resulting in a high mortality rate (Boktour *et al.,* 2004; Nace *et al.,* 2009). In addition, approximately 15% of biofilms in oral *Candida* infections are dual species, notably *C. albicans* with *C. glabrata* or *C. krusei* (Samaranyake *et al.,* 1987). Multi-species infection (candidemia) can occur in patients with cancer (Boktour *et al.,* 2004) or HIV (Patel *et al.,* 2012) and is more difficult to treat with single antifungal therapy due to the presence of intrinsically drug-resistant species. *Candida* species also interact with *Aspergillus* species in the respiratory tract (Peleg *et al.,* 2010) and with bacteria in one quarter of bloodstream candidemias (Klotz *et al.,* 2007).

Mixed-species interactions in infections lack detailed characterisation and their nature can be highly diverse (Harrison, 2007). Some studies describe one *Candida* species enhancing the invasion of another in epithelial infections (Silva *et al.,* 2011; Alves *et al.,* 2014), whereas others have found that co-infection can lead to out-competition (Kirkpatrick *et al.,* 2000; Henry-Stanley *et al.,* 2005; Thein *et al.,* 2007), resulting from competition for common resources (Harrison, 2007). Species may directly inhibit each other via toxin release or over-stimulation of the immune response (Brown *et al.,* 2009), but often it is difficult to elucidate the mechanism in *in vivo* systems (Henry-Stanley *et al.,* 2005; Tampakakis *et al.,* 2009). Quorum sensing, the cell density-dependent chemical regulation of gene expression (Miller and Bassler, 2001), can also have a role in inter-species interactions. This can cause inhibition of competitor

growth in mixed infections (Peleg *et al.,* 2008) or stimulation of virulence factor production to enhance infection virulence (Asad and Opal, 2008).

Species interactions in dual infections are often described as synergistic (Harrison, 2007). Silva *et al. (*2011) and Alves *et al.* (2014) described synergism between *C. albicans* and *C. glabrata* in *in vitro* epithelium as greater fungal invasion and tissue damage in dual compared to single species infections. Synergism has also been described between *Pseudomonas aeruginosa* and oropharyngeal bacterial species isolates (Sibley *et al.,* 2008) in the *Drosophila melanogaster* invertebrate model, resulting in increased expression of virulence genes in *P. aeruginosa* and altered host immune antimicrobial peptide production. Synergistic interactions were defined by greater host mortality in dual compared with single species *P. aeruginosa* infections, when the bacterial species co-infecting with *P. aeruginosa* was non-pathogenic in single infection. Synergism also occurred between *P. aeruginosa* clinical strains and *Streptococcus* species strains in the *Galleria mellonella* wax moth larval model (Whiley *et al.,* 2014), measured by decreased survival in dual compared with single species infection of either species, when total infection dose was equal in single and dual infections. Synergism is also described in mixed-species biofilms whereby *Streptococcus* species can increase growth of *Candida* species (Pereira-Cenci *et al.,* 2008) or increase invasion of mucosal tissue (Diaz *et al.,* 2012).

Alternatively, microbial species interactions in infections can be described as antagonistic (Harrison, 2007). A dual species infection of the nematode worm *Caenorhabditis elegans* with the bacterium *Acinetobacter baumannii* and *Candida albicans* revealed direct reciprocal antagonistic interactions (Peleg *et al.,* 2008) by production of molecules that inhibited growth. In biofilms, antagonistic interactions occur between *P. aeruginosa* and *C. albicans* through physical interactions, production of quorum sensing molecules and immunomodulatory factors by the host and pathogen (Fourie *et al.,* 2016). Antagonism has also been described as a reduction in host fungal burden (colony forming units) of a *Streptococcus* species strain in co-culture with a *Pseudomonas aeruginosa* clinical strain, compared with monoculture in *in vitro* biofilms (Whiley *et al.,* 2014).

To study host-pathogen interactions in fungal infections, a range of *in vivo* infection models are used to mimic pathological symptoms that occur in human

infection environments (MacCallum, 2012). *In vivo* murine models can be used to study virulence of mucosal, host site-specific and systemic infections, although immunosuppression is sometimes required to establish infection with *C. glabrata* (Fidel *et al.,* 1999). Genetic analysis of host immunity is possible and mice have highly conserved innate and adaptive immune systems with humans, however higher costs and ethical constraints reduce sample sizes and repeatability (Buer and Balling, 2003). Alternatively, the minihost vertebrate zebrafish (*Danio rerio)* and the invertebrate nematode (*Caenorhabditis elegans*) models can be used to study virulence-associated fungal morphological changes non-invasively in transparent larvae (Pukkila-Worley *et al.,* 2009; Brothers and Wheeler, 2012). The zebrafish has both innate and adaptive immunity (MacCallum, 2012) and genetic tools are available in both models (Brothers and Wheeler, 2012; Desalermos *et al.,* 2012). These minihosts are however limited, as they cannot be incubated at 37^{o}C to truly replicate the mammalian infection environment (MacCallum, 2012).

To better understand dose-dependent pathogen virulence, the fruit fly (*Drosophila melanogaster*) has proved a useful host. Precise inoculum doses can be injected into the haemolymph (Glittenberg *et al.,* 2011b), whilst gastrointestinal specific infections have been studied by ingestion from food (Glittenberg *et al.,* 2011a). Genetic tools are available to probe host immunity (Kounatidis and Ligoxygakis, 2012). In contrast, the fruit fly is limited as it has innate but not adaptive immunity and cannot be incubated at human physiological temperature (MacCallum, 2012) and is not widely used as an infection model as specialist equipment (incubators and “fly room” (Desalermos *et al.,* 2012)) are required.

An insect model that has successfully been used to study host-pathogen interactions is *Galleria mellonella,* larvae of the greater wax moth, which can be easily maintained in the laboratory (Cotter *et al.,* 2000; Desalermos *et al.,* 2012). Virulence of *C. albicans* (Cotter *et al.,* 2000; Brennan *et al.,* 2002; Borman *et al.,* 2013), *C. tropicalis* (Mesa-Arango *et al.,* 2013), *C. krusei* (Scorzoni *et al.,* 2013) and *C. glabrata* (Junquiera *et al.,* 2011; Borghi *et al.,* 2014; Santos *et al.,* 2017; Ames *et al.,* 2017) has been described. Larval infection can be studied at both 30^{o}C and 37^{o}C, precise inoculum injections into

the haemolymph are easier as the larvae are larger and large sample sizes are possible due to low costs and fewer ethical constraints (Cotter *et al.,* 2000; MacCallum, 2012).

Strain virulence is correlated between *G. mellonella* and mouse models (Brennan *et al.,* 2002; Amorim-Vaz *et al.,* 2015). This makes it a useful model of mammalian systemic infection. This model does present limitations as differences in larval health can occur between batches and inter-laboratory variation can restrict comparability of results (Cook and McArther, 2013), for example if larvae are fed different diets or differ in genetics or microbiota composition. This has been addressed by development of TruLarv™ (Champion, 2016), research grade *G. mellonella* which have been in-bred from a genome sequenced stock and will allow understanding of host genetics, in addition to transcriptomic tools for analysis of host immunity and stress response (Vogel *et al.,* 2011).

Dual *Candida* species interactions in the host have recently been studied in *G. mellonella* (Rossoni *et al.,* 2015). Interestingly, the authors found that dual infection of *C. albicans (*with *C. glabrata* or *C. krusei)* with a doubled total infection dose (2 x 10^6 CFU/larva) compared with a *C. albicans* single species infection (1 x 10^6 CFU/larva), increased larval survival in dual infection beyond that of single *C. albicans* infection. Whilst larvae infected only with *C. albicans* did not survive beyond 18 hours post-injection, larvae survived up until 72 hours in *C. albicans-C. glabrata* infection and 96 hours in *C. albicans-C. krusei* infection. *C. albicans* fungal burden and hypha formation were also lower in dual infection than in single infection. The authors concluded that competitive (antagonistic) interactions occurred in mixed-*Candida* species infections, whereby *C. glabrata* or *C. krusei* were better competitors than *C. albicans* and increased larval survival in dual infection due to their lower virulence. These experiments only tested a single strain of each species and the interactions between different species clinical strains remain to be explored.

3.2 Aims of the Chapter

In this chapter, we aim to further explore interactions in dual species fungal infections and the interaction with host immunity, after establishing *Galleria* as a model to study dose-dependent *Candida* species virulence as described previously (Brennan *et al.,* 2002; Borghi *et al.,* 2014). We selected *G. mellonella* as the infection model to study mixed-species interactions due to the ability to infect larvae with precise inocula, incubate at 37^{o}C and study large sample sizes (Cotter *et al.,* 2000; MacCallum, 2012). We address three aims:

1) To establish *G. mellonella* as a model for studying host-pathogen interactions by testing single species virulence and temperature-dependent virulence of *C. albicans* and *C. glabrata.*

2) To determine whether dual species interactions in mixed *Candida* species infection of *G. mellonella* described by Rossoni *et al.* (2015) can be replicated using similar species lab strains.

3) To further explore dual *Candida* species interactions across a range of clinical strains to determine whether the type of interaction is strain-dependent.

We extended our work from Chapter One on *in vitro* competition assays between *C. glabrata* and *C. albicans,* to investigate species interactions within the environmental complexity of a host and interaction with the immune system. We studied single species dose-dependent virulence of *C. albicans* and *C. glabrata* in *G. mellonella* at two different temperatures that mimic commensal and pathogenic interactions, to confirm previous findings (Cotter *et al.,* 2000; Brennan *et al.,* 2002; Scorzoni *et al.,* 2013; Borghi *et al.,* 2014; Ames *et al.,* 2017). *Candida* species have shown dose-dependent virulence in *G. mellonella* infection, with *C. albicans* being more virulent than *C. glabrata* (Cotter *et al.,* 2000; Rossoni *et al.,* 2015; Ames *et al.,* 2017). Temperature-dependent virulence with single *Candida* species inoculum doses has previously been described in *Candida* species (Mesa-Arango *et al.,* 2013; Scorzoni *et al.,* 2013).

We replicated the experiments of dual species *Candida* infection of *G. mellonella* described by Rossoni *et al.* (2015) and tested for antagonistic or synergistic interactions or lack of interaction across different clinical strains of *C. albicans* and *C. glabrata*, measuring larval survival. We injected equal doses of *C. albicans* in combination with *C. glabrata* or *C. krusei* in dual infections, with the doses of the non-*albicans* species being non-pathogenic in single species infection. Similar to previous studies (Sibley *et al.,* 2008; Whiley *et al.,* 2014), we define interactions as synergistic or antagonistic if we observe a respective decrease or increase in larval survival in dual compared with single species *C. albicans* infection. We report no species interaction if larval survival is not significantly different between dual and single species *C. albicans* infection. Lack of species interaction has previously been observed as a lack of increase in host mortality (Sibley *et al.,* 2008) or biofilm cell concentration (Whiley *et al.,* 2014) in dual infections with a non-pathogenic bacterial species strain and a virulent strain. We further evaluate differences in species strain interactions by comparing host melanisation, a hallmark of the insect immune response (Scorzoni *et al.,* 2013) in different strains.

3.3 Materials and Methods

3.3.1 *Galleria mellonella* Larvae

G. mellonella larvae were ordered from Live Foods Direct (Sheffield, UK: Waxworms (15-25 mm); Product Code-W1000) and were stored in wood shavings in a 15^{o}C incubator for 7-10 days before use to reduce the possibility of using immune-primed larvae resulting from stress of transportation (Browne *et al.,* 2014; 2015). Larvae were kept for 3-4 weeks from this date. 16 larvae (for dual infections) of uniform colour and size (approximately 0.25-0.35 g) were selected per infection group and were stored in 90 mm petri dishes containing a single 90 mm filter paper disc. Larvae were inoculated with 10 µl of cell suspension using a 50 µl Hamilton Gastight syringe (Hamilton, Bonaduz, Switzerland; Product No: 1705), into the top left proleg for single injections. The second left proleg was used as a second site when two injections were given for dual infections. 20 larvae were used per infection group for single species infection experiments. Larvae were discarded if any leakage of the inoculum or larval haemolymph occurred. In all assays, an extra group of larvae injected only with PBS was used as a control against the stress of injection. In all experiments, PBS controls survived the duration of the experiment, or experiments were discarded when greater than 2 larvae of an infection group died. Larvae were removed from the experiments (censored) when they began to pupate.

3.3.2 Single *Candida* Species Infection in *G. mellonella*

Candida strains used were *C. glabrata* ATCC 2001 and *C. albicans* SBC153 (Milne *et al.,* 2011) (see Chapter 2). Overnights were prepared in YPD media and incubated with shaking at 180 rpm in 30^{o}C. After 24 hours, cultures were removed, washed twice in 1 x PBS solution then re-suspended in PBS. Each species was diluted in PBS and cell concentration was counted with the haemocytometer.

Doses of *C. albicans* used for infection were 1, 2 and 4 x 10^{7} cells/ml for *C. albicans* and 1.25, 2.5 and 5 x 10^{8} cells/ml for *C. glabrata* (Ames *et al.,* 2017).

As 10 µl of each concentration was injected into larvae, the final dosages were 1, 2 and 4 x 10^5 cells/larva for *C. albicans* and 1.25, 2.5 and 5 x 10^6 cells/larva for *C. glabrata.* Larvae were incubated in static, dark conditions at 30ºC or 37ºC and survival was recorded every 24 hours for seven days. Each infection assay was repeated three times independently.

3.3.3 Dual *Candida* Species Infection in *Galleria mellonella*: Replication of Experiments Described by Rossoni *et al.* (2015)

The methods of Rossoni *et al.* (2015) were used with modifications as follows. The *Candida* strains used were *C. albicans* ATCC 18804, *C. krusei* ATCC 6258 (**Table 3.1**), *C. albicans* SBC153 (isogenic to clinical isolate SC5314 with ACT1p-GFP-NAT1 insertion (Milne *et al.,* 2011)) and *C. glabrata* ATCC 2001; the latter two strains were described in Chapter 2. Strains were streaked onto SDA (Sabouraud Dextrose Agar) plates and incubated at 37ºC for 24-48 hours until colonies were visible. Overnight cultures were prepared by inoculation of a single colony into YPD medium and incubating at 37ºC for 18 hours. Cells were washed three times in 1xPBS solution then were re-suspended in PBS and diluted for cell enumeration with a haemocytometer. For preparation of infection inocula, strains were diluted in PBS to cell densities of 1 x 10^8 and 2 x10^8 cells/ml, resulting in final concentrations of 1 x 10^6 and 2 x 10^6 CFU/larva.

Dual infections were performed by single or dual site inoculation. For dual site inoculation, 1 x 10^6 CFU/larva of *C. albicans* was inoculated into one proleg and 1 x 10^6 CFU/larva of *C. glabrata* or *C. albicans* was inoculated into the second proleg (Rossoni *et al.,* 2015). For single site inoculation, 2 x 10^6 CFU/larva of each species were vortex mixed in a 50:50 ratio and 10 µl of the cell suspension was inoculated into the top left proleg. Single species infections were run alongside, by injecting 1 x 10^6 or 2 x 10^6 CFU/larva.

Larvae were incubated at 37ºC in the dark for five days and survival was recorded daily (including at 18 hours) for 5 days, based on reaction to physical stimulation. Each experiment was replicated independently three times.

3.3.4 Dual Species *G. mellonella* Infection with Different Doses and Strains

The methods used were as above with modifications. Strains were streaked on SDA plates and incubated at 37ºC and overnight cultures were incubated at 37ºC for 18-22 hours. Firstly, the total dual species infection dose was maintained at 2 x 10^6 CFU/larva but the ratio of species concentrations (*C. albicans: C. glabrata)* mixed together and inoculated at a single site, was altered from 50:50 (1 x 10^6 CFU/larva each species) to each of 30:70 (6 x 10^5 CFU/larva: 1.4 x 10^6 CFU/larva) and 10:90 (2 x10^5 CFU/larva: 1.8 x 10^6 CFU/larva).

A set of clinical strains of *C. glabrata, C. albicans* and *C. krusei* were tested in different combinations in dual infections and larval survival was measured (**Table 3.1**). The total dual species infection dose was 4 x 10^5 CFU/larva, consisting of 2 x 10^5 CFU/larva of each species. Single species infections with 2 x 10^5 CFU/larva were also tested. Each species strain combination in dual infections was tested in one independent experiment, then independent experiments were repeated for a selection of strains showing contrasting species interactions: *C. glabrata* strains BG2, 1184, NCPF 3605 and 3309, *C. krusei* ATCC 6258 and *C. albicans* strain SBC153 and 18804. We then tested a range of doses of *C. glabrata* BG2 and 1184 in single species infections to find the infective dose of each with equal virulence as a *C. albicans* SBC153 infection with 2 x 10^5 CFU/larva.

Table 3.1. *Candida* strains used in single and dual species infections. See Chapter 2 for description of strains *C. albicans* ACT1-GFP (SBC153 (Milne *et al.,* 2011); lab-derived strain isogenic to clinical isolate SC5314 with GFP insertion) and *C. glabrata* strains ATCC 2001, BG2, BG2Δ*ssk2,* NCPF 3605, NCPF 3309. All strains listed below are clinical isolates of Wild-Type genotype.

Strain	**Reference**
***C. albicans* strains**	
ATCC 18804	Reference strain isolated from human skin infection (American Type Culture

	Collection). Used by Rossoni *et al.* (2015) and received as kind gift from Donna MacCallum, University of Aberdeen
ATCC 90028	Reference strain isolated from blood (American Type Culture Collection). Quality control for antifungal susceptibility testing (NCCLS, 2002).
B311/ ATCC 32354	Lab reference strain (Sokol-Anderson *et al.,* 1988)
NCPF 3302	Isolated from chronic mucocutaneous candidosis and is azole-resistant (UKNCC; Haynes and Westerneng, 1996)
***C. glabrata* strains**	
85/038	Zhou and Thiele, 1991
11088A	Haynes and Westerneng, 1996
1184	Kind gift from Ken Haynes, University of Exeter. Origin unknown.
***C. krusei* strains**	
ATCC 6258	Isolated from bronchomycosis (American Type Culture Collection). Reference strain used in antifungal susceptibility testing (NCCLS, 2002). Used by Rossoni *et al.* (2015).

3.3.5 Host Melanisation Response

The methods used are as described in Ames *et al.* (2017) and Scorzoni *et al.* (2013), with modifications. Larvae in groups of three were injected with PBS, 2 x 10^5 CFU/larva of *C. glabrata* BG2 or *C. glabrata* 1184 in a single experiment. In a separate experiment, the same infectious doses were used but *C. glabrata* BG2 and *C. krusei* ATCC 6258 were compared. At 2 and 6 hours post-injection, three larvae per infection group were put on ice. Haemolymph was collected in

a micro-centrifuge tube by removing the final tip of the body. Haemolymph was diluted in IPS (Insect Physiological Saline: 150 mM sodium chloride, 5 mM potassium chloride, 10 mM Tris-HCl pH6.9) and melanin production was quantified in a plate reader at OD 415 nm. This assay is robust for reporting melanin biosynthesis as a similar absorbance wavelength was used to measure laccase activity (the oxidative enzyme involved in melanin synthesis) via production of an intermediate product of melanin biosynthesis (Williamson, 1994; Alvarado-Ramírez *et al.,* 2008).

3.3.6 Statistical Analyses

Survival data collected from three independent experiments (biological replicates) were analysed for significant between-replicate differences using pairwise log rank tests with OASIS 2 software (Han *et al.* 2016; Ames *et al.,* 2017). If no significant differences occurred, then experiments were pooled. Kaplan-Meier survival curves were plotted using the 'survfit' function in the R-package 'Hmisc' (Harrell *et al.,* 2016) using R version 3.3.2 (R Core Team, 2016). Significant differences between survival curves in the probability of death over the measured time points were deduced from pairwise log-rank tests with Bonferroni correction for multiple comparisons, using OASIS 2 software (Han *et al.,* 2016; Ames *et al.,* 2017). Mean survival times and standard errors were also computed. Larvae that pupated during the experiment and those that were alive at the end of the experiment were censored. One-way ANOVA tests and Tukey *post hoc* tests were used to deduce between-group differences in host melanisation.

3.4 Results

3.4.1 Single *Candida* Species Infection of *G. mellonella*: Dose and Temperature-Dependent Effects

In order to test the dual species interactions described by Rossoni *et al.* (2015), we firstly investigated single *Candida* species virulence and temperature dependency in *G. mellonella,* to establish the model to measure dose-dependent virulence of reference strains in our laboratory. We picked three different infective doses for each of *C. glabrata* ATCC 2001 and *C. albicans* SBC153 (Ames *et al.,* 2017) and measured larval survival over seven days at two different temperatures. *C. glabrata* virulence showed significant dose-dependent effects at both 37ºC and 30ºC (**Figure 3.1a and b**; **Table A.2.1.S1**). For example, at 30ºC mean larval survival was 3.93 +/- 0.36 days for 1.25 x 10^6 CFU/larva compared with 1.75 +/- 0.19 days with 5 x 10^6 CFU/larva. At 37ºC mean survival was 4.90 +/- 0.25 days for 1.25 x 10^6 CFU/larva and 1.95 +/- 0.09 days for 5 x 10^6 CFU/larva. There were no significant differences in larval survival time between the two temperatures for any of the three doses of *C. glabrata*. These results contrast with the temperature effects described in Ames *et al.* (2017), likely due to variation in the health of different larval batches.

C. albicans also showed significant dose-dependence at both temperatures (**Figure 3.1c and d; Table A.2.1.S1**). At 30ºC mean larval survival was 6.54 +/- 0.16 days for 1 x 10^5 CFU/larva compared with 1.26 +/- 0.12 days for 4 x 10^5 CFU/larva. At 37ºC mean larval survival time was 5.59 +/- 0.20 days for 1 x 10^5 CFU/larva compared with 1.06 +/- 0.03 days for 4 x 10^5 CFU/larva. *C. albicans* showed significant temperature-dependent virulence at low and intermediate doses (1 x 10^5 CFU/larva: p = 0.00; 2 x 10^5 CFU/larva: p = 4.20E-6) but not at the highest dose (4 x 10^5 CFU/larva) at which percentage survival was reduced below 10% at both temperatures, on the first day post-injection. Overall, approximately ten times greater infective doses of *C. glabrata,* compared with *C. albicans,* were required for similar virulence (Ames *et al.,* 2017).

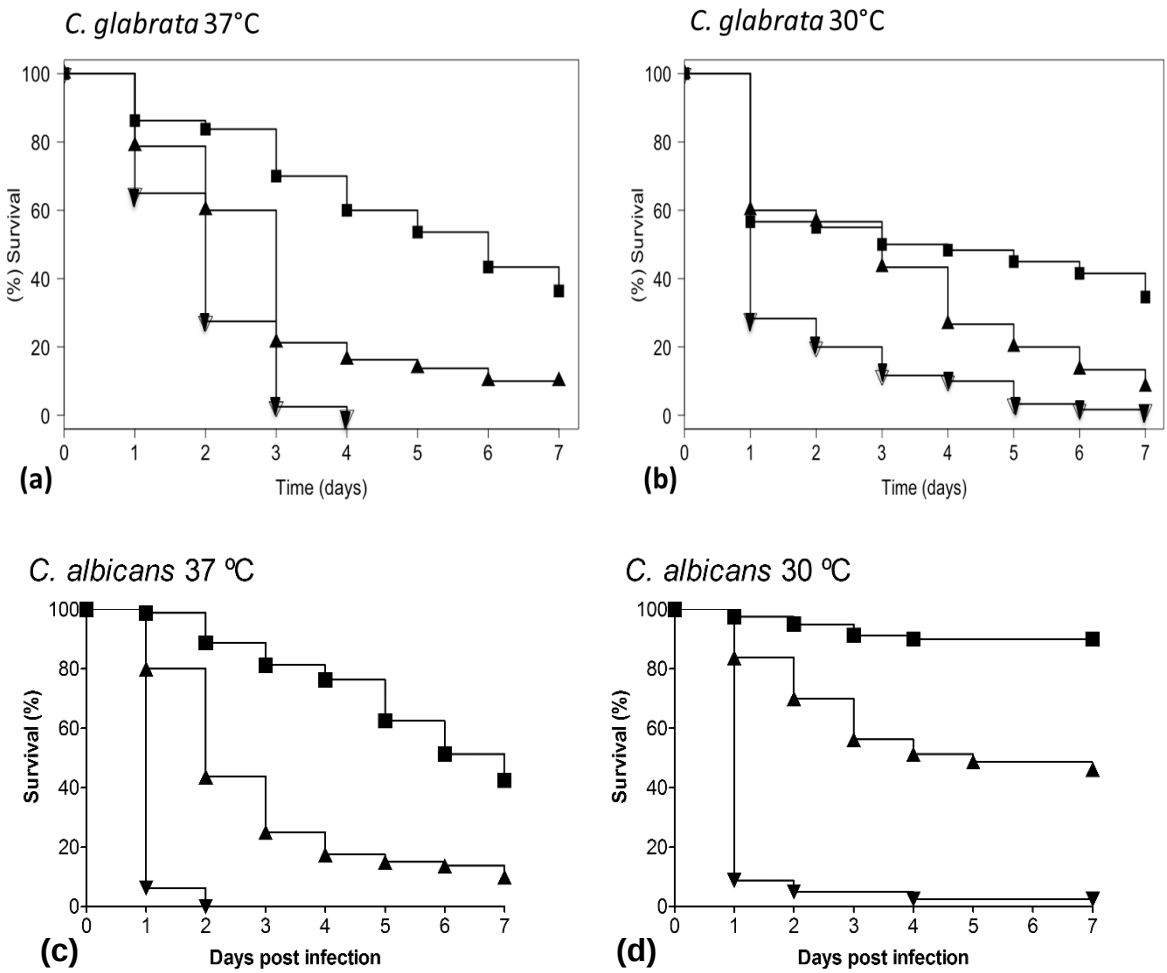

Figure 3.1. Survival of *G. mellonella* infected with *C. glabrata* or *C. albicans* at two different temperatures. Kaplan-Meier survival plots show virulence of *C. glabrata* strain ATCC 2001 at 37ºC **(a)** and 30ºC **(b),** similar to results of Ames *et al.* (2017). Infective doses are 1.25 x 10^6 CFU/larva (squares), 2.5 x 10^6 CFU/larva (triangles) and 5 x 10^6 (upside-down triangles). Data is pooled from 3 biological replicates. Virulence plots of *C. albicans* strain SBC153 (isogenic to NGY152 with ACT1-GFP insertion) at 37ºC **(c)** and 30ºC **(d)** are presented. Infective doses are 1 x 10^5 CFU/larva (squares), 2 x 10^5 CFU/larva (triangles) and 4 x 10^5 CFU/larva (upside-down triangles). Data is pooled from 4 biological replicates. See **Table A.2.1.S1** for statistical results from Log-rank tests.

3.4.2 Dual *Candida* Species Infection in *Galleria mellonella*: Replication of Experiments from Rossoni *et al.* (2015)

We firstly tested repeatability of the antagonistic species interaction from Rossoni *et al.* (2015), whereby an increase in larval survival occurred with dual

Candida species infection at double the total infection inoculum as a single species *C. albicans* infection. Following the same methods with minimal modifications, a dual infection with 1 x 10^6 CFU/larva of each of *C. albicans* strain SBC153 and *C. glabrata* strain ATCC 2001 did not produce a significant increase in larval survival (**Figure 3.2b**), in contrast to Rossoni *et al.* (2015). Larval survival time for infection with 1 x 10^6 and 2 x 10^6 CFU/larva of *C. albicans* SBC153 did match previous results as all larvae had died at 18 hours, but mean survival time in the dual species group was 18.63 +/- 0.63 hours (**Table A.2.1.S2**). For single species infections with 1 x 10^6 CFU/larva, *C. albicans* was significantly more virulent than *C. glabrata* ($P = 0.00$); mean larval survival time was 71.75 +/- 4.48 hours with *C. glabrata* and 18 hours with *C. albicans* (**Figure 3.2a**).

Secondly, we tested whether similar antagonistic interactions between *C. albicans* and *C. krusei* described in Rossoni *et al.* (2015) could be replicated, using the same strains from the paper. Again, no increase in larval survival was observed in dual species infection compared with *C. albicans* infections of 1 and 2 x 10^6 CFU/larva, resulting in death of all larvae in the three infection groups at 18 hours (**Figure 3.2d**). No significant mortality was seen in PBS injection controls, controlling against stress of injection. As seen in Rossoni *et al.* (2015), *C. krusei* had significantly lower virulence than *C. albicans* with 1 x 10^6 CFU/larva infection ($P < 0.001$) (1 biological replicate: **Figure 3.2c**). *C. krusei* had a mean survival time of 46.88 +/- 7.73 hours (**Table A.2.1.S2**).

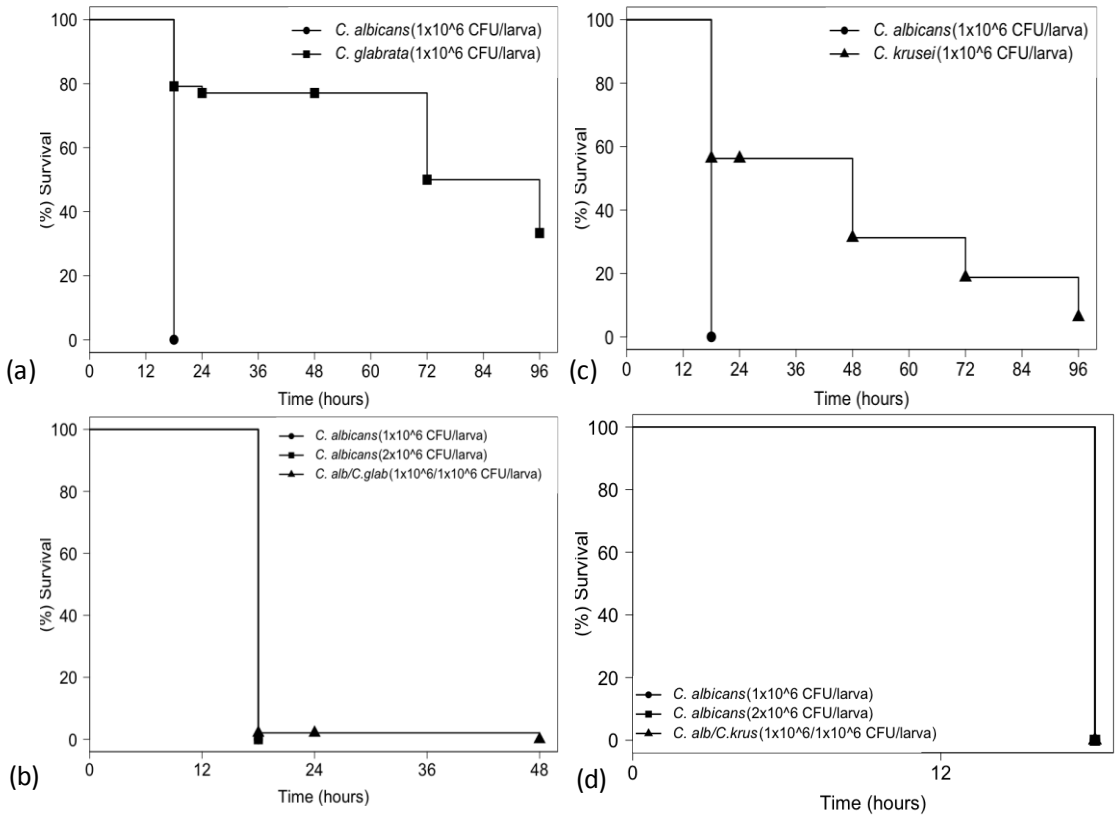

Figure 3.2. Survival curves for single and dual *Candida* species *G. mellonella* infection. Survival of *G. mellonella* infected with single species *C. albicans*, *C. glabrata* and *C. krusei* in comparison with dual *C. albicans*/ non-*albicans* infections. Methods of Rossoni *et al.* (2015) were replicated. (a) and (b): strains used were *C. albicans* ACT1-GFP (SBC153) and *C. glabrata* ATCC 2001. (c) and (d): strains used were *C. albicans* ATCC 18804 and *C. krusei* ATCC 6258 (same strains as Rossoni *et al.* (2015)). Data were pooled from 3 biological replicates in (a) and (b) and from 2 biological replicates in (d). Data in (c) is from 1 biological replicate. Significant differences between survival curves were determined with log-rank tests and mean survival times were calculated and results are presented in **Table A.2.1.S2.**

3.4.3 Dual *Candida* Species Infection of *G. mellonella*: Manipulating Species Ratio, Total Infective Dose and Species Strains

We extended the work of Rossoni *et al.* (2015) to determine whether species interactions in *G. mellonella* were dependent on species inoculum ratio in dual infection. Firstly, maintaining the total dose of 2 x 10^6 CFU/larva, a dual infection with a species ratio of 30:70 (0.6 x 10^6 *C. albicans* SBC153/ 1.4 x 10^6 CFU/larva *C. glabrata* ATCC 2001) showed no significant difference in survival (P = 1.00; 1 biological replicate- data not shown) compared with a single species *C.*

albicans infection (2 x 10^6 CFU/larva). A dual infection with a 10:90 species ratio (0.2 x 10^6 CFU/larva *C. albicans*/ 1.8 x 10^6 CFU/larva *C. glabrata*) showed a small increase in larval survival (mean 25.5 +/- 3.88 hours) compared with 2 x 10^6 *C. albicans* (mean 18.38 +/- 0.36 hours) but this was not significant (Bonferroni-corrected *P* = 0.137; 1 biological replicate- data not shown). This indicates that *C. albicans* showed higher virulence in our work than in the experiments of Rossoni *et al.* (2015), such that antagonistic species interactions were not seen.

As the dose of *C. albicans* used in Rossoni *et al.* (2015) was much higher than doses required for virulence in our experiments (**Figure 3.1c**)*,* for all future single-dual species experiments we used a dose of 2 x 10^5 CFU/larva of *C. albicans,* which showed intermediate virulence (**Figure 3.1c**). In combination with 2 x 10^5 CFU/larva of *C. glabrata (*below virulent dose: **Figure 3.1a**), we found no significant difference in larval survival between dual infection and single 2 x 10^5 CFU/larva *C. albicans* infection *(P* = 0.0799; 1 biological replicate-data not shown). In dual infections, with *C. albicans* dose maintained at 2 x 10^5 CFU/larva and *C. glabrata* dose increased above 2 x 10^5 CFU/larva, larval survival decreased in dual compared with single *C. albicans* infection.

We then built on the work of Rossoni *et al.* (2015) by testing whether species interactions were strain-dependent. We compared larval survival between a single species *C. albicans* infection of 2 x 10^5 CFU/larva and dual infection of *C. albicans* with different strains of *C. glabrata* or *C. krusei* (2 x 10^5 CFU/larva of each species), in one independent experiment. In single species *C. glabrata* and *C. krusei* infections, a dose of 2 x 10^5 CFU/larva was too low to cause infection (**Table 3.2**). In addition, no significant differences in larval survival with 2 x 10^5 CFU/larva of *C. albicans* occurred across four clinical strains tested (*P* = 0.7277; **Table 3.3**). No difference in survival (no interaction) occurred in dual infections of *C. albicans* SBC153 with *C. glabrata* strains ATCC 2001, NCPF 3605, BG2, BG2Δ*ssk2,* 85/038 and 11088A (**Table 3.4**), compared with single species *C. albicans* infection. In contrast, significant decreases in larval survival in dual compared with single species *C. albicans* infections (synergistic interactions) occurred with *C. albicans* SBC153 and *C. glabrata* NCPF 3309, 1184 and *C. krusei* ATCC 6258. No interaction was seen between *C. albicans*

ATCC 90028 and the lab reference *C. glabrata* strain ATCC 2001. In dual infections with *C. krusei* ATCC 6258, synergistic interactions occurred with *C. albicans* strains ATCC 90028 and B311, but there was no interaction in dual infection with *C. albicans* strain NCPF 3302.

In all dual *Candida* species strain infections of *G. mellonella* described above, we did not see an increase in larval survival in dual compared with single species *C. albicans* infections as found in Rossoni *et al. (*2015). Importantly, we did, however, see potential synergistic interactions between some species strains and no interaction between others. We explored these contrasting interactions and influence on larval immunity in further experiments described in the next section.

Table 3.2. Comparison of *G. mellonella* survival between single species *C. glabrata* and *C. krusei* strain infections. Infections had an inoculum dose of 2 x 10^5 CFU (strains described in **Table 3.1**). *G. mellonella* larval survival was measured daily over 96 hours in one experiment for each species strain pairing. N = 16 in infection groups. Data was analysed in R (version 3.3.2; R Core Team, 2016) using the survival package 'Hmisc' to calculate mean survival times and log-rank comparison of larval survival across the strains. Log-rank test chi-squared = 7.11, *P* = 0.5244.

Strain	**Mean survival time +/- SE (hours)**
C. glabrata 11088A	96.00 +/- 0.00
C. glabrata 1184	91.13 +/- 4.88
C. glabrata 85/038	96.00 +/- 0.00
C. glabrata ATCC 2001	96.00 +/- 0.00
C. glabrata BG2	96.00 +/- 0.00
C. glabrata BG2Δ*ssk2*	93.00 +/- 3.00
C. glabrata NCPF 3309	96.00 +/- 0.00
C. glabrata NCPF 3605	96.00 +/- 0.00
C. krusei ATCC 6258	96.00 +/- 0.00

Table 3.3. Comparison of *G. mellonella* survival between single species *C. albicans* strain infections. Infections had an inoculum dose of 2 x 10^5 CFU (strains described in **Table 3.1**). *G. mellonella* larval survival was measured daily over 96 hours in one experiment for each species strain pairing. N = 16 in infection groups. Data was analysed in R (version 3.3.2; R Core Team, 2016) using the survival package 'Hmisc' (Harrell *et al.,* 2016) to calculate mean survival times and log-rank comparison of larval survival across the strains. Log-rank test chi-squared = 1.31, *P* = 0.7277.

***C. albicans* strain**	**Mean survival time +/- SE (hours)**
ATCC 90028	37.88 +/- 7.60
B311	48.75 +/- 6.59
NCPF 3302	38.25 +/- 6.15
SBC153	37.13 +/- 4.46

Table 3.4. Comparison of *G. mellonella* survival between single species strain *C. albicans* infections and dual infection of *C. albicans* with different strains of *C. glabrata* and *C. krusei*. Single species infections of *C. albicans* had an inoculum dose of 2 x 10^5 CFU; dual species infections consisted of 2 x 10^5 CFU/larva *C. albicans* and 2 x 10^5 CFU/larva of a strain of *C. glabrata* or *C. krusei* (described in **Table 3.1**). *G. mellonella* larval survival was measured daily over 96 hours in one experiment for each species strain pairing. N = 16 in dual and single species infection groups. Data was analysed in R (version 3.3.2; R Core Team, 2016) using the survival package 'Hmisc' (Harrell *et al.,* 2016) to calculate mean survival times and log-rank comparison of larval survival between the dual and single *C. albicans* species infection groups.

***C. albicans* strain**	***C. glabrata* or *C. krusei* strain**	**Dual infection: Mean survival time +/- SE (hours)**	**Single infection (2×10^5 CFU/larva *C. albicans):* Mean survival time +/- SE (hours)**	**Log-rank test chi-squared value: dual versus single 2×10^5 CFU/larva *C. albicans* infection**	**p value from log-rank test**
SBC153	*C. krusei* ATCC 6258	18.38 +/- 0.38	27.00 +/- 3.19	7.68	0.00558
SBC153	*C. glabrata* ATCC 2001	21.75 +/- 2.56	30.00 +/- 4.24	3.36	0.06694
SBC153	*C. glabrata* NCPF 3605	26.25 +/- 3.94	27.00 +/- 3.19	0.02	0.8929
SBC153	*C. glabrata* NCPF 3309	38.25 +/- 4.83	54.00 +/- 7.10	4.64	0.03129
SBC153	*C. glabrata* BG2	48.38 +/- 8.75	54.00 +/- 7.10	0.49	0.4829
SBC153	*C. glabrata* BG2Δ*ssk2*	39.38 +/- 5.50	54.00 +/- 7.10	2.68	0.1015
SBC153	*C. glabrata* 1184	20.63 +/- 1.89	37.12 +/- 4.46	14.78	0.0001209
SBC153	*C. glabrata* 85/038	28.13 +/- 3.50	37.13 +/- 4.46	3.32	0.06844
SBC153	*C. glabrata* 11088A	27.75 +/- 4.17	37.13 +/- 4.46	2.7	0.1006
ATCC 90028	*C. krusei* ATCC 6258	19.89 +/- 1.88	37.89 +/- 7.60	7.85	0.005079
ATCC	*C. glabrata*	24.38 +/-	37.89 +/-	1.82	0.1773

90028	ATCC 2001	3.26	7.60		
B311	*C. krusei* ATCC 6258	19.13 +/- 0.60	48.75 +/- 6.59	21.61	3.341e-06
NCPF 3302	*C. krusei* ATCC 6258	36.38 +/- 6.61	38.25 +/- 6.15	0.06	0.799

3.4.4 Strain-Dependent Dual *Candida* Species Interactions in *G. mellonella*

We replicated dual *Candida* species infection of *G. mellonella* with *C. albicans* strain SBC153 in combination with two *C. glabrata* strains that did not appear to interact with *C. albicans* (strains NCPF 3605 and BG2) (**Table 3.4**), and two *C. glabrata* strains with proposed synergistic interactions (NCPF 3309 and 1184). To deduce lack of interaction or synergistic interaction between *C. albicans* and different strains of *C. glabrata* in individual dual-species infections, we compared larval survival between single species infections of 2 x 10^5 and 4 x 10^5 CFU/larva of *C. albicans* and *C. glabrata,* with a dual species infection of 2 x 10^5 CFU/larva of each species. For all four strains of *C. glabrata,* there was no significant decrease in larval survival in the single infections (**Figure 3.3**). As a result, a dual infection with 2 x 10^5 CFU/larva of any *C. glabrata* strain in combination with 2 x 10^5 CFU/larva of *C. albicans* would be expected to show no significant difference in larval survival compared with a single infection of 2 x 10^5 CFU/larva of *C. albicans*. A significant decrease in larval survival in dual species infection compared with 2 x 10^5 CFU/larva of *C. albicans* in single infection would signify a synergistic interaction.

Across three independent experiments, there was no significant difference in larval survival between single (2 x 10^5 CFU/larva) *C. albicans* infection and dual infection with *C. glabrata* NCPF 3605 ($P = 1$; **Figure 3.3(b); Table A.2.1.S3**), supporting a lack of species interaction. Larval survival was significantly greater in dual than single species infection with a total infection dose of 4 x 10^5 CFU/larva *C. albicans* ($P < 0.0001$; **Table A.2.1.S3**).

In contrast, larval survival was significantly lower in dual infection compared with single *C. albicans* infection (2 x 10^5 CFU/larva), for *C. albicans* SBC153 in combination with *C. glabrata* strain BG2 (*P* = 0.0269; mean survival time- dual: 37.5 +/- 3.98 hours, single- 50.75 +/- 3.73 hours) (**Figure 3.3(a); Table A.2.1.S3**) or *C. glabrata* strain NCPF 3309 (**Figure 3.3(d); Table A.2.1.S3**) (*P* = 0.0003; mean survival times: 30.63 +/- 2.65 hours and 48.63 +/- 4.42 hours), suggesting synergistic species strain interactions. Larval survival was greater in dual infections than in single species infections with 4 x 10^5 CFU/larva *C. albicans* ($p < 0.01$; **Figure 3.3(a)** and (**d); Table A.2.1.S3**). In dual infection with *C. glabrata* strain 1184, larval survival was significantly lower compared with 2 x 10^5 CFU/larva *C. albicans* (*P* = 4.80e-07; mean survival times: 21.75 +/- 1.80 hours, 41.88 +/- 3.85 hours) (**Figure 3.3c; Table A.2.1.S3**) and larval survival in dual infection was equal to that of 4 x 10^5 CFU/larva of *C. albicans* in single infection (*P* = 1.00), suggesting a stronger synergistic response with this strain.

We then tested the effects of *C. albicans* and *C. krusei* species strain interactions on larval survival over independent experiments. When single species infections of *C. krusei* were included in the same experiment that tested dual species infection of *C. albicans* SBC153 with *C. krusei,* we found no significant decrease in larval survival with 2 x 10^5 CFU/larva of *C. krusei* compared with the sterile PBS control (**Figure 3.4(a)).** We did, however, see a significant decrease in larval survival with 4 x 10^5 CFU/larva of *C. krusei* (mean survival time = 87.25 +/- 2.90 hours) but survival was still much greater than in single species *C. albicans* infections (**Figure 3.4(a); Table A.2.1.S4**). Dual infection of *C. albicans* SBC153 with *C. krusei* resulted in a significant decrease in larval survival relative to a single *C. albicans* infection of 2 x 10^5 CFU/larva (*P* = 0.0003; mean survival times 22.00 +/- 1.59 hours and 36.25 +/- 3.57 hours) (**Figure 3.4(a); Table A.2.1.S4**). Larval survival in dual infection was equal to that of a single infection of 4 x 10^5 CFU/larva of *C. albicans* (*P* = 1.00). Similarly, dual infection with *C. albicans* strain 18804 and *C. krusei,* the strains used in Rossoni *et al.* (2015), resulted in lower larval survival than a single infection of 2 x 10^5 CFU/larva *C.albicans* strain 18804*,* (*P* = 8.50e-9) and mean survival time for dual infection was 18.75 +/- 0.29 hours (**Figure 3.4(b); Table A.2.1.S4**). This indicated strong synergistic interactions between *C. albicans* and *C. krusei.* It is, however, important to note that both *C. krusei* single species infections that

were run alongside the dual infection with *C. albicans* strain 18804 and *C. krusei* caused significant decreases in larval survival (**Figure 3.4(b)),** so the extent of the dual species synergistic interaction could not be unambiguously determined. Our results suggested a synergistic interaction as larval survival in dual infection was not significantly different from that of single infection with 4 x 10^5 CFU/larva of *C. albicans,* despite the higher larval survival with 2 x 10^5 CFU/larva of *C. krusei* (mean survival time = 55.75 +/- 5.13 hours) than with *C. albicans* (mean survival time = 40.38 +/- 4.05 hours) (**Figure 3.4(b)).**

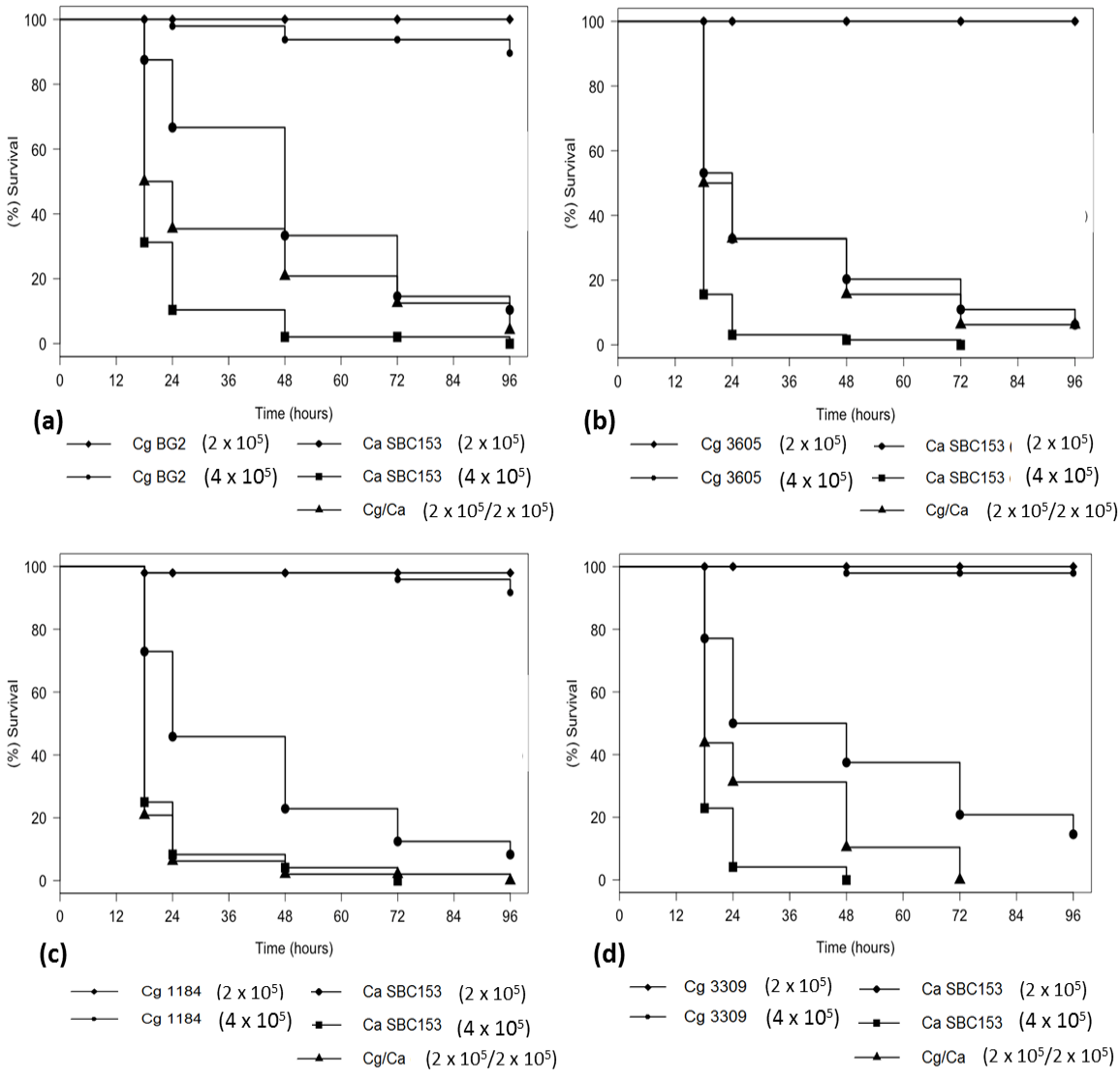

Figure 3.3. Survival curves for single species *C. albicans* and *C. glabrata* infections and dual *C. albicans*-*C. glabrata* infection of *G. mellonella*, with different *C. glabrata* strains. Larval population survival (%) is plotted every 24 hours up until 96 hours. Each plot shows *C. albicans* strain SBC153 infection at 2 x 10^5 (larger circles) and 4 x 10^5 (larger squares) CFU/larva, *C. glabrata* infection at 2 x 10^5 (small diamonds) and 4 x 10^5 (small circles) and the dual species infection (2 x 10^5

CFU/larva of each species; larger triangles). Different *C. glabrata* strains tested in single and dual infections: **(a)** BG2; **(b)** NCPF 3605; **(c)** 1184; **(d)** NCPF 3309. Data was pooled from three biological replicates (N = 16 per infection group per biological replicate) for each plot, apart from **(b)** which was pooled from four biological replicates. Single species *C. glabrata* infections caused no significant decreases in larval survival for any strains compared with PBS control infections (Log-rank tests: $P > 0.800$). See **Table A.2.1.S3** for statistical results from Log-rank tests comparing larval survival in single species *C. albicans* infections with dual species infection.

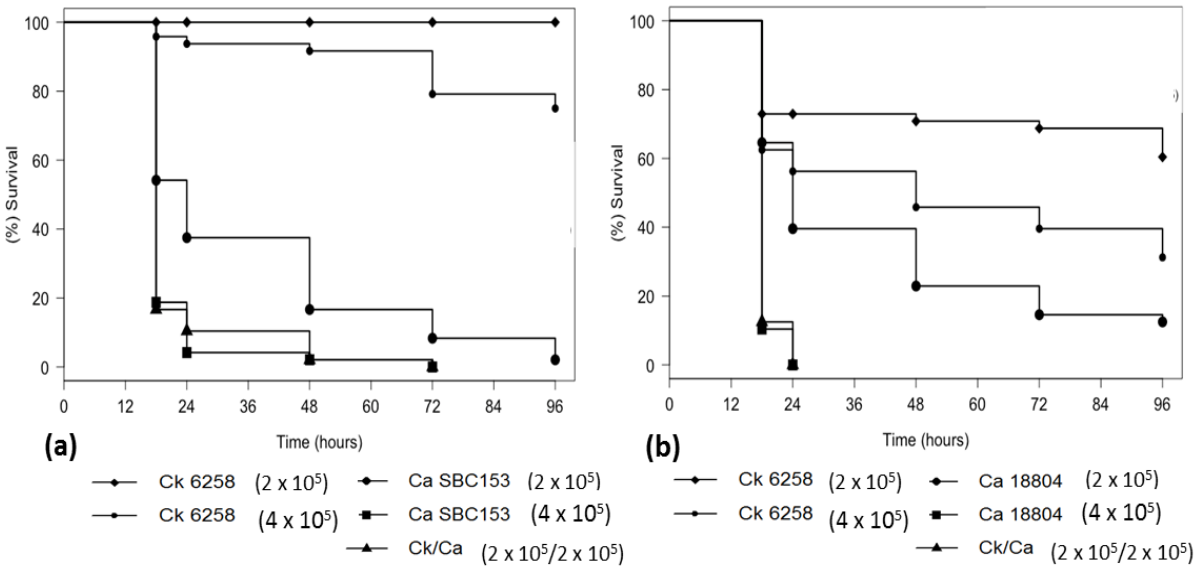

Figure 3.4. Survival curves for single species *C. albicans* and *C. krusei* infections and dual *C. albicans*-*C. krusei* infection of *G. mellonella*. Larval population survival (%) is plotted every 24 hours up until 96 hours. Each plot shows *C. albicans* infection at 2 x 10^5 (larger circles) and 4 x 10^5 (larger squares) CFU/larva, *C. krusei* infection at 2 x 10^5 (small diamonds) and 4 x 10^5 (small circles) and the dual species infection (2 x 10^5 CFU/larva of each species; larger triangles). **(a)** Infections are with *C. albicans* strain SBC153 and *C. krusei* ATCC 6258. *C. krusei* infection of 2 x 10^5 CFU/larva did not significantly affect larval survival (Log-rank test: $P = 1.00$) but 4 x 10^5 CFU/larva significantly decreased survival ($P = 0.0062$; mean survival time = 87.25 +/- 2.90 hours). **(b)** Infections are with *C. albicans* strain ATCC 18804 and *C. krusei* ATCC 6258, the same strains used in Rossoni *et al.* (2015). Unexpectedly, *C. krusei* infections caused significant decreases in survival compared with the PBS control (Log-rank test: $P < 0.001$) and survival was dose-dependent (Log-rank test: $P = 0.0208$; mean survival time = 73.38 +/- 4.99; 55.75 +/- 5.13 hours, for 2 x 10^5 and 4 x 10^5 CFU/larva respectively). Data was pooled from three independent experiments for each plot (N = 16 per infection group per biological replicate). See **Table A.2.1.S4** for

statistical results from Log-rank tests comparing larval survival in single species *C. albicans* infections with dual species infection.

3.4.5 Comparative Virulence and Host Melanisation Response across *C. glabrata* Strains

To investigate potential causes of differences in the strength of the synergistic response between *C. albicans* and *C. glabrata* strains BG2 and 1184, we compared strain virulence and *G. mellonella* immune response as we observed qualitative differences in host melanisation response. After testing a range of doses of the two *C. glabrata* strains we found that, 5 x 10^6 CFU/larva of strain BG2 whereas 1.25 x 10^6 CFU/larva of strain 1184 resulted in comparable larval survival to an infection with 2 x 10^5 CFU/larva of *C. albicans* (**Figure 3.5(a)** and (**b)** respectively**; Table A.2.1.S5**).

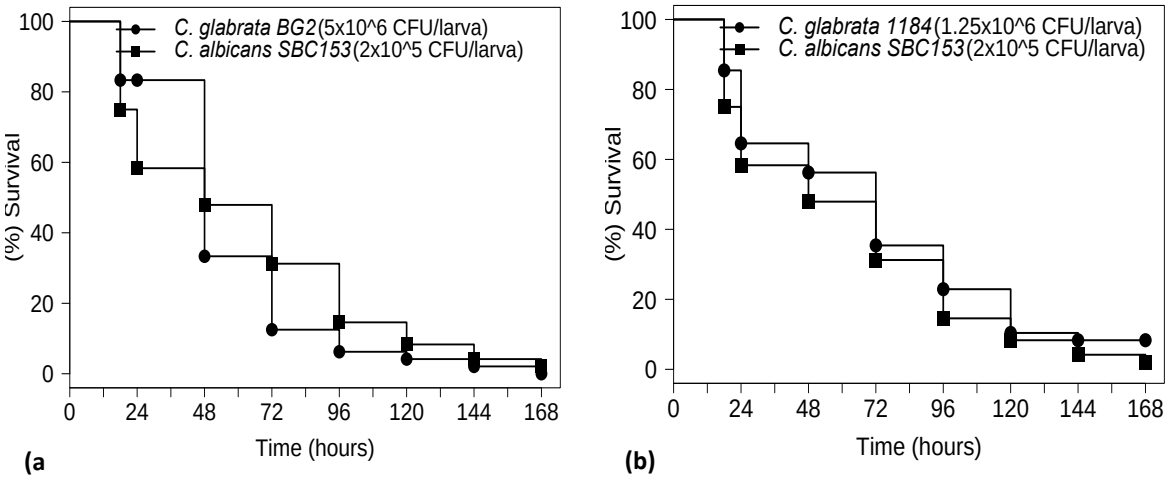

Figure 3.5. Survival curves of *G. mellonella* infection for doses of *C. glabrata* strains BG2 and 1184 with comparative virulence to *C. albicans*. (a) Comparative survival of 5 x 10^6 CFU/larva of *C. glabrata* BG2 (circles) and 2 x 10^5 CFU/larva of *C. albicans* SBC153 (squares) over 168 hours (7 days). **(b)** Comparative survival of 1.25 x 10^6 CFU/larva of *C. glabrata* 1184 (circles) and 2 x 10^5 CFU/larva of *C. albicans* SBC153 (squares). Each plot represents pooled data from three independent experiments and statistical analyses are presented in **Table A.2.1.S5.**

To quantify differences in *G. mellonella* melanisation responses induced by different *C. glabrata* strains, we injected larvae with 2 x 10^5 CFU/larva in single

species infections and measured melanin levels in the larval haemolymph, similarly to the methods of Scorzoni *et al.* (2013) and Ames *et al.* (2017)). We also tested melanisation response with *C. krusei* strain 6258 as this strain showed a similar level of synergism as *C. glabrata* strain 1184 when in dual infection with *C. albicans* SBC153 (**Figures 3.3** and **3.4**). Larval melanisation was significantly greater with C*. glabrata* strain 1184 infection than the PBS control or *C. glabrata* BG2 infection at 2 and 6 hours (**Figure 3.6(b)**). At 2 hours post-inoculation, larval melanisation with *C. krusei* infection was approximately two-fold greater than in PBS-injected control larvae (*P* = 0.04651) (**Figure 3.6(a)**) whereas *C. glabrata* BG2 infection caused equal melanisation to the PBS control (**Figure 3.6(a); (b)).** At 6 hours, melanisation from *C. krusei* infection was significantly greater than with strain BG2 infection (*P* = 0.001650).

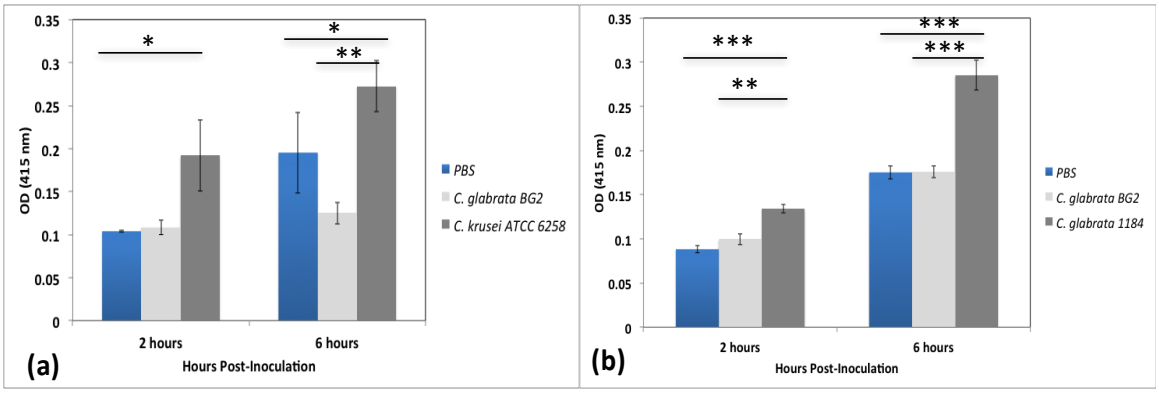

Figure 3.6. Melanisation response in *G. mellonella* with single species *C. glabrata* strain or *C. krusei* infection. *G. mellonella* were infected with 2 x 10^5 CFU/larva of *C. glabrata* BG2 (light grey bars) and *C. krusei* **(a)** or *C. glabrata* BG2 and 1184 **(b)** and melanisation (OD_{415}) was measured at 2 and 6 hours, relative to PBS-injected controls (blue bars). Columns represent means +/- SE bars. Bars labelled with asterisks represent significant differences from Tukey's *post hoc* test following one-way ANOVA: * = *P* < 0.05; ** = *P* < 0.01; *** = *P* < 0.001. **(a)** 2 hours: $F_{2, 6}$ = 6.192; *P* = 0.0348 (PBS-*C. krusei*: *P* = 0.04651; PBS-*C. glabrata* BG2: *P* = 0.9845; *C. glabrata* BG2-*C. krusei: P* = 0.05707). 6 hours: $F_{2, 6}$ = 20.57; *P* = 0.00206 (PBS-*C. krusei: P* = 0.03517; *C. glabrata* BG2-*C. krusei: P* = 0.001650; PBS-*C. glabrata* BG2: *P* = 0.05089). **(b)** 2 hours: $F_{2, 6}$ = 32.93; *P* = 0.0005820 (PBS-*C. glabrata* 1184: *P* = 0.0005782; *C. glabrata* BG2-*C. glabrata* 1184: *P* = 0.002620; PBS- *C. glabrata* BG2: *P* = 0.2137). 6 hours: $F_{2, 6}$ = 47; *P* = 0.0002160 (PBS-*C. glabrata* 1184: *P* = 0.0003750; *C. glabrata* BG2-*C. glabrata* 1184: *P* = 0.0003879; PBS-*C. glabrata* BG2: *P* = 0.9986).

3.5 Discussion

In this chapter, we investigated dual *Candida* species interactions in the *in vivo* model *Galleria mellonella* and the influence of different *C. glabrata* clinical strains on the nature of the interactions. We tested dual species infection of *C. albicans* with *C. glabrata* or *C. krusei* and measured host survival during infection, for different species strain combinations. Importantly, we found that interactions between *Candida* species do not uniformly influence host survival, indicating that the type and strength of the interaction is dependent on the clinical strain. We also found that host immune response quantitatively varied across *C. glabrata* strains. These findings have implications for characterising the virulence of mixed-*Candida* species fungal infections in different host patients.

Firstly, we sought to replicate the experiments of Rossoni *et al.* (2015) that described antagonistic interactions of *Candida* species in *G. mellonella,* but we could not replicate the increase in larval survival in dual species compared with single *C. albicans* infection using lab strains. This suggested that *C. glabrata* or *C. krusei* could not outcompete *C. albicans* or did not trigger an effective host response (I. Gudelj and S.Bates, *pers. comm.,* April 2016). It is unclear why these differences occurred and is likely due to variation in larval batches, supplier or laboratory environmental conditions. We found that both *C. glabrata* and *C. krusei* showed a much greater decrease in larval survival by 96 hours than described by Rossoni *et al.* (2015) (*C. glabrata:* 66% (ours), 19% (Rossoni *et al.,* 2015); *C. krusei:* 94% (ours), 34% (Rossoni *et al.,* 2015)). The infection dose of *C. albicans* (1 x 10^6 CFU/larva) used by Rossoni *et al. (*2015) was highly virulent as all larvae were dead at 18 hours, therefore we could not deduce whether the two species interacted synergistically or no interaction occurred in dual infection. In our experiments, lower doses of 1-4 x 10^5 CFU/larva of *C. albicans* in single infection were sufficient to cause a decrease in larval survival at 37^{o}C.

We extended the experiments of Rossoni *et al.* (2015) by testing dual infections with different clinical *Candida* species strains at lower infective doses and identified synergistic interactions or absence of interaction dependent on strain combination. No species interaction occurred in dual infection of *C. albicans* SBC153 with *C. glabrata* NCPF 3605, but larval survival decreased to varying degrees with three *C. glabrata* strains (BG2, NCPF 3309 and 1184) and *C. krusei* (ATCC 6258), suggesting synergistic interactions. Due to significant decreases in larval survival with single species infections of *C. krusei,* it was difficult to unambiguously determine synergism in the dual infection. Our method for deducing synergistic species interactions could be made more robust by combining doses of two *Candida* species with equal virulence in dual infection and comparing larval survival with single species infections of the same dose of each species that were used in dual infection. Synergism would be deduced if larval survival was lower in dual infection than in either of the single species infections. Our described synergistic species interactions contrast with studies showing competitive interactions in *in vitro* biofilms, whereby *C. glabrata* or *C. krusei* exerts an antagonistic influence on *C. albicans* (El-Azizi *et al.,* 2004; Henry-Stanley *et al.,* 2005; Thein *et al.,* 2007; Rossoni *et al.,* 2015; Santos *et al.,* 2016). Alternatively, competitive interactions may not necessarily occur due to niche differentiation based on morphological or biochemical differences (Silva *et al.,* 2011).

Our results contribute to studies (Silva *et al.,* 2011; Alves *et al.,* 2014; Tati *et al.,* 2016) that have described dual-*Candida* species synergistic interactions and identified strain differences that impact on strength of interaction. In both *Drosophila* (Sibley *et al.,* 2008) and *Galleria* (Whiley *et al.,* 2014), the strength of synergistic interactions between *Pseudomonas aeruginosa* and *Streptococci* depended on the species strain combination and interaction with the immune system. Increased tissue invasion and damage was observed in dual *C. glabrata-C. albicans* infection in *in vitro* oral and vaginal epithelium (Silva *et al.,* 2011; Alves *et al.,* 2014) across strains, potentially caused by increased *C. glabrata* nutrient acquisition via *C. albicans* tissue damage (Brunke and Hube, 2013). In an immunosuppressed murine model of oral candidiasis (Tati *et al.,* 2016), synergism was characterised by increased colonisation and biofilm density in dual infections of *C. glabrata* and *C. albicans,* and *C. glabrata* was

found to adhere to *C. albicans* hyphae. *C. glabrata* strains showed differing degrees of synergism characterised by dual infection burden and our results support these findings by describing differences in host survival across *C. glabrata* strains in *G. mellonella*.

Of particular interest is the strongly synergistic response we find in dual infections of *C. albicans* with *C. glabrata* 1184 or *C. krusei* ATCC 6258*. C. krusei* may form synergistic interactions with *C. albicans* due to hyphal attachment in co-infection, as described for *C. glabrata* (Tati *et al.,* 2016). Understanding the interaction mechanism *in vivo* has medical significance as *C. krusei* is associated with a high mortality rate and intrinsic antifungal azole resistance (Scorzoni *et al.,* 2013) and is often co-isolated with *C. albicans* in HIV patients (Rossoni *et al.,* 2015). In the case of *C. glabrata* 1184, there are no previous studies that describe the origin of this strain or characterise its virulence (apart from Ames *et al.* (2017)) or dual species interactions. This highlights the need for better characterisation of the virulence properties and growth kinetics of fungal strains in dual species clinical infections.

We found no synergistic interaction between the species' strains *C. albicans* SBC153 and *C. glabrata* NCPF 3605 as there was no significant difference in *G. mellonella* survival between single infection with 2 x 10^5 CFU/larva of *C. albicans* and dual infection with 2 x 10^5 CFU/larva of each species. Lack of synergistic interaction between species has been described in *C. glabrata-C. albicans* infection in a type 1 diabetic murine vaginal infection model (Nash *et al.,* 2016). *C. glabrata* BG2 (a vaginal isolate) showed no significant increase in tissue invasion, biofilm formation or immune response in dual compared with single species *C. albicans* infection. Our results showed that absence of synergistic interaction between species (with *C. glabrata* strain 3605) was possible in systemic *G. mellonella* infection. Interestingly, NCPF 3605 was isolated from a diabetic patient (UKNCC, 2000) so the lack of synergistic interaction between species could be linked to *C. glabrata* strain adaptations to a high glucose environment rather than infection site. In our work, *C. glabrata* BG2 showed weak synergism with *C. albicans* and synergism was also described for this strain in murine oral infection (Tati *et al.,* 2016). Alternatively, lack of synergistic interaction between species in our work could be correlated

with strain virulence level, as NCPF 3605 is highly attenuated compared with other *C. glabrata* strains (Ames *et al.* (2017)). Virulence differences across *C. glabrata* strains could explain the gradation in synergistic responses. We showed that a four times greater dose of BG2 than 1184 was required for equal virulence, which supports the greater virulence of strain 1184 described in Ames *et al.* (2017).

We identified differences in the extent of host immune melanisation during early stages of infection across *C. glabrata* strains BG2 and 1184 and *C. krusei,* despite injecting avirulent doses of each strain. Dose-dependent melanisation has occured in *C. glabrata* strain ATCC 2001 (Ames *et al.,* 2017) and in *C. krusei (*Scorzoni *et al.,* 2013). Melanisation across clinical strains was only tested for *C. krusei* and did not quantitatively vary, unlikely the strain differences we observed in *C. glabrata.* Fast melanisation caused by *C. krusei* may be due to the larger rod-shaped cells and clumps of filaments causing greater immune stimulation (Scorzoni *et al.,* 2013). Similarly, *C. glabrata* strain 1184 may cause greater host melanisation than strain BG2 due to greater cell agglutination. Differences in melanisation could explain the differences in strain virulence and interactions in dual infections, as over-activation of the host immune response can be detrimental to the host (Sibley *et al.,* 2008).

Single species infections showed that *C. albicans* had dose- and temperature-dependent virulence at lower infective doses ($1 \times 10^5 – 4 \times 10^5$ CFU/larva), correlating with previous studies (Cotter *et al.,* 2000; Scorzoni *et al.,* 2013). A significant temperature effect was shown for a single dose of *C. albicans* (Scorzoni *et al.,* 2013) and *C. tropicalis* (Mesa-Arango *et al.,* 2013), although no temperature effect occurred for *C. krusei* (Scorzoni *et al.,* 2013). One possible determinant of temperature-dependent virulence is the change in growth kinetics. *C. albicans* has a two-fold greater growth rate at 37^{o}C than 30^{o}C and reaches a higher population density in stationary phase (Scorzoni *et al.,* 2013). In contrast, *C. krusei* has a slightly greater growth rate at 37^{o}C but no difference in final population density.

Temperature-dependent effects may also be due to changes in growth morphology between 30^{o}C and 37^{o}C. *C. albicans* forms hyphae during infection

at 37ºC in *G. mellonella*, which contributes to virulence due to tissue invasion and biofilm formation (Fuchs *et al.,* 2010). Studies have described this morphogenetic switch to occur at 37ºC (Shen *et al.,* 2008), due to regulation by the heat-shock protein Hsp90 (Shapiro and Cowen, 2012). In contrast, *C. krusei* only forms pseudohyphae (elongated cells) rather than true hyphae, which may decrease its invasive capacity (Samaranayake and Samaranayake, 1994). Alternatively, temperature may impact on host immune response through altered expression of invertebrate immune genes (Linder *et al.,* 2008) and lowered phagocytosis (Ratcliffe, 1985; Mesa-Arango *et al.,* 2013) at higher temperatures, or host and pathogen responses could both be altered.

3.6 Conclusions of the Chapter

In conclusion, our results are threefold:

1) Competitive interactions do not always occur in dual-*Candida* species *in vivo* infections; species can interact synergistically or form no interaction and the strength of interaction is strain-dependent.

2) Differences in *C. glabrata* strain virulence and host immune melanisation are correlated with the degree of synergistic interaction with *C. albicans* in dual infection.

3) Virulence is temperature-dependent for low and intermediate doses of *C. albicans.*

These results build on our experiments from Chapter 2 which investigated *in vitro* short and long-term competition dynamics between *C. glabrata* and *C. albicans* and identified differences in competitive interactions between *C. glabrata* strains. Chapter 4 will explore differences in growth kinetics of *C. glabrata* strains in *in vitro* glucose-limited cultures and comparative strain abilities to evolve antifungal resistance.

4. Chapter 4: Growth Kinetics of *C. glabrata* Clinical Strains and the Evolution of Antifungal Resistance

4.1 Introduction

Candida species inhabit many different body sites in which resource levels vary, so they must adapt their metabolism in order to survive and grow in these complex environments (Brown *et al.,* 2014a). Carbon sources, particularly glucose, are important energy sources for growth, although *S. cerevisiae* can also sense and uptake nitrogen, phosphorus and trace nutrients (Gagiano *et al.,* 2002). Host niches are glucose-limited and concentrations vary between sites; glucose levels are normally present at 0.06-0.1% in the bloodstream (Barelle *et al.,* 2006), 0.5% in the vagina (Owen and Katz, 1999) and up to 0.25% in faeces (Karabocuoglu *et al.,* 1994). Glucose is not normally present in the urine but can be detected at concentrations of 11 mmol/l (0.2% w/v) in the urine or blood of diabetics (WHO Committee on Diabetes Mellitus, 1980; Gibson *et al.,* 1990).

Differential regulation of metabolic gene expression in *C. albicans* has been described in environmental adaptation and in the transition between commensal and pathogenic forms (Brown *et al.,* 2014a). This allows efficient nutrient uptake and assimilation. Nutrient sensing and transport have been well characterised in *Saccharomyces cerevisiae,* including the description of low and high affinity glucose sensors and transporters (Ozcan *et al.,* 1996) that are tuned to the environment (Lagunas, 1993) and control expression of respiratory or fermentative genes (Gagiano *et al.,* 2002). A glucose sensor and transporters have also been described in *C. albicans* (Brown *et al.,* 2006). *S. cerevisiae* and *C. albicans* are highly sensitive to a range of glucose concentrations resulting in changes in gene expression (Yin *et al.,* 2003; Rodaki *et al.,* 2009). *C. glabrata* shares a close evolutionary relation to *S. cerevisiae* and can switch from respiration to fermentation in the transition from low to high glucose (Postma *et al.,* 1989b; Van Urk *et al.,* 1990; Roetzer *et al.,* 2011), unlike *C. albicans* which retains respiratory activity at high glucose (Rozpedowska *et al.,* 2011). This raises the question as to whether *C. glabrata* strains that colonise different body sites with contrasting resource levels (Cataldi *et al.,* 2016), show different

growth properties on glucose and adaptations to host-imposed stresses and antifungal treatment.

Growth of microbial populations in the laboratory is typically quantified in seasonal resource environments (batch cultures) in which defined growth phases occur over time, described by a growth curve (Monod, 1949; Cunningham *et al.,* 2010). The lag phase characterises initiation of enzymatic reactions and is followed by an increase in microbial growth rate that remains constant during the exponential phase of growth. Growth rate slows as microbial density approaches the maximum that the environment can sustain, due to nutrient limitation or accumulation of toxic metabolites. Cells enter stationary phase as the population growth rate decreases to zero and the carrying capacity is reached. This pattern of growth has been described in batch cultures of bacteria (Thornton, 1922; Schmidt *et al.,* 1985) and in *Candida* species (Cuenca-Estrella *et al.,* 2001). Thus, density-dependence exerts a control on intrinsic (*per capita*) growth rate such that a logistic model of population growth best describes change in population density over time in resource-limited microbial cultures (Vandermeer, 2010). This is described by the Verhulst equation (**1**) (Verhulst, 1845; Murray, 1990; Vandermeer, 2010) and is shown diagrammatically in **Figure 4.1**. In relation to the logistic equation, the parameters r (growth rate) and K (carrying capacity) can be calculated from microbial data to describe growth properties on limiting resources (Reding-Roman *et al.,* 2017).

$\frac{dN}{dt} = rN\left(\frac{K-N}{K}\right)$; **(1),**

where $\frac{dN}{dt}$ represents population growth rate (change in size over time), r is exponential *per capita* growth rate (h^{-1}), N is population size, K is population size at carrying capacity and $r\left(\frac{K-N}{K}\right)$ represents intrinsic *per capita* growth rate (h^{-1}).

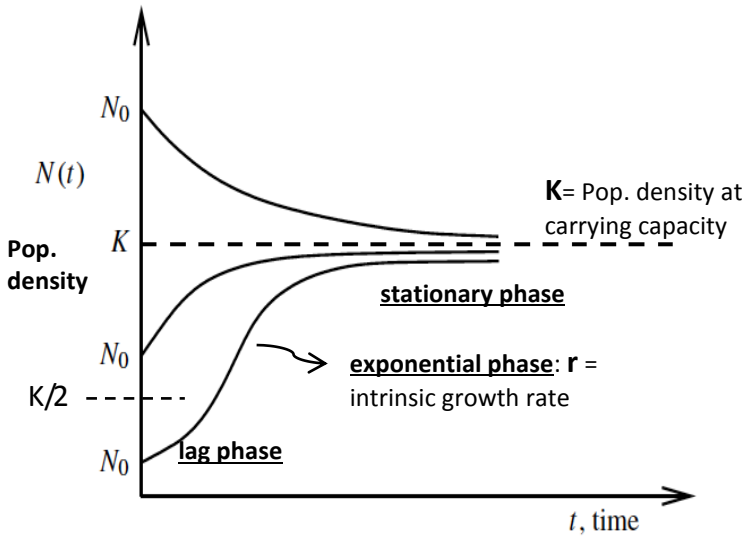

Figure 4.1. Logistic population growth described by the Verhulst equation. This figure is adapted from Figure 1 in Murray (1990) and describes change in population size over time when controlled by density-dependent factors over seasonal growth. Population sizes shown are as follows: N_0 is initial, N_t is size at time, t, K is size at carrying capacity of the environment and K/2 is half carrying capacity. Intrinsic growth rate ($r(\frac{K-N}{K})$) is controlled by how far the population size (N) is away from carrying capacity (K) (term $(\frac{K-N}{K})$ which decreases growth rate as N approaches K). Growth rate is lower when N_0 is below K/2 and population growth takes a sigmoidal form. Populations with different starting densities (N_0 values) will converge on K, the stable population density maintained by environmental controls.

The ability of microbes to take up and assimilate nutrients and to possess metabolic flexibility is important for stress adaptation and virulence (Barelle *et al.,* 2006; Brown *et al.,* 2014a). In *C. albicans,* gene regulatory networks link metabolism with stress resistance, virulence and cell wall remodelling in different host niches (Brown *et al.,* 2014a). When glucose is limiting in host niches, flexibility to switch to metabolism of alternative carbon sources can aid oxidative and osmotic stress adaptation, virulence and antifungal resistance (Ene *et al.,* 2012; Brown *et al.,* 2014a, b; Miramón and Lorenz, 2017). In addition, switching between glycolytic, gluconeogenic and glyoxylate pathways in different host niches is important for virulence in *C. albicans* (Lorenz and Fink, 2001; Barelle *et al.,* 2006; Miramón and Lorenz, 2017).

Variation in glucose levels differentially affects regulation of stress responses across yeast species, indicating adaptation to environments with different levels of nutrient availability (Roetzer *et al.,* 2011). Whilst both *C. albicans* and *S. cerevisiae* are sensitive to low levels of glucose, *C. albicans* up-regulates oxidative and cationic stress genes over a range of glucose concentrations whereas *S. cerevisiae* down-regulates homologous genes (Rodaki *et al.,* 2009). Both *S. cerevisiae* and the closely evolutionarily related pathogenic yeast *C. glabrata* show an environmental stress response whereby conserved stress protective genes are induced in response to a range of stresses (Roetzer *et al.,* 2008; Roetzer *et al.,* 2011). For example, oxidative stress response genes are upregulated in response to glucose starvation. *C. glabrata* shows greater stress resistance due to the stressful environments it encounters in competition with other microbes on mucosal surfaces and from host immune defences during phagocytosis (Roetzer *et al.,* 2011).

Glucose also upregulates antifungal stress resistance genes in *C. albicans* (Rodaki *et al.,* 2009) and in *C. glabrata* (Ng *et al.,* 2016). Antifungal resistance is increasing in *Candida* species, particularly in *C. glabrata* (Pfaller *et al.,* 2012; Sanglard, 2016), but current antifungal susceptibility testing is limited in predicting clinical resistance (Sanglard and Odds, 2002). Intrinsic resistance occurs naturally and is likely to have arisen from frequent toxin exposure within the host microbiota, prior to administration of antifungals (Roetzer *et al.,* 2011). Acquired resistance has evolved with antifungal usage (Fidel *et al.,* 1999) and for *C. glabrata,* this has occurred against all antifungal classes: azoles, echinocandins, polyenes (amphotericin B) and nucleoside analogues (flucytosine) (Pfaller *et al.,* 2012). Standardised antifungal susceptibility testing (Clinical and Laboratory Standards Institute (CLSI), 2008; European Committee on Antimicrobial Susceptibility Testing (EUCAST), (Arendrup *et al.,* 2012)) are commonly used to detect antifungal activity via growth inhibition defined by the MIC (minimum inhibitory concentration) of drug that is required to substantially inhibit growth (Sanglard, 2016). This measure can be a poor predictor of *in vivo* resistance and clinical outcomes, as it does not take into account host immune status, strain virulence and fitness and other environmental parameters such as nutrient concentrations at different host sites (Sanglard and Odds, 2002; Anderson, 2005; Kanafani and Perfect, 2008).

Whilst research into antibiotic adaptation dynamics in bacterial infections is increasing (Palmer and Kishony, 2013), few studies have investigated the evolutionary dynamics of antifungal adaptation (Cowen *et al.,* 2002; Anderson, 2005). Experimental *in vitro* evolution of antifungal resistance allows real-time dynamics of changing pathogen fitness and resistance mechanisms to be studied and replicated under controlled conditions, such that the specific effects of selection pressure and environment on adaptation can be determined (Cowen *et al.,* 2002; Anderson, 2005). Evolutionary dynamics such as rates of adaptation (Hegreness *et al.,* 2008), growth kinetics and mechanisms of resistance in parallel-evolved replicate populations have been studied in bacteria (Toprak *et al.,* 2011; Lindsey *et al.,* 2013; Oz *et al.,* 2014). In fungi, *in vitro* evolution of antifungal resistance has been studied in *C. albicans* with fluconazole and amphotericin B (Cowen *et al.,* 2000; Vincent *et al.,* 2013) and in *S. cerevisiae* with fluconazole (Anderson *et al.,* 2003), but real-time *in vitro* dynamics of *C. glabrata* resistance and fitness adaptations across different clinical strains have not been characterised.

4.2 Aims of the Chapter

In this Chapter, we focus on growth kinetics of *C. glabrata* strains in different glucose level environments and explore the influence on virulence and antifungal resistance adaptation. We address three main aims:

1) To compare growth rate, carrying capacity and yield (efficiency of biomass production per unit of resource (Pfeiffer *et al.,* 2001)) across *C. glabrata* strains in different glucose environments.

2) To investigate whether differences in strain growth kinetics are related to different virulence levels.

3) To determine whether strain growth kinetics are correlated with differential abilities to adapt to antifungal treatment.

We measured logistic growth parameters and yield of *C. glabrata* in single-season (24-hour) batch cultures in minimal medium supplemented with a range of physiologically relevant glucose concentrations. This expanded the work of Ng *et al.* (2016) who found differences in growth rates across three different strains of *C. glabrata* over a small range of glucose concentrations, but did not characterise the relationship with carrying capacity or yield. We then selected strains with the most contrasting growth kinetics and determined whether these traits correlated with differences in virulence in the *G. mellonella* infection model.

Finally, we compared the ability of strains with contrasting growth kinetics to adapt to treatment with the antifungal caspofungin. We selected caspofungin, a cell wall-targeting echinocandin class antifungal that is fungicidal as it destroys cell wall integrity (Kartsonis *et al.,* 2003). Caspofungin is often used as the primary therapy for *C. glabrata* infections due to common resistance to fluconazole, however *C. glabrata* is increasingly becoming caspofungin-resistant and resistance rate more than doubled in a recent 10-year study (Alexander *et al.,* 2013). Although common mechanisms of resistance are well described (Sanglard, 2016), only one study has looked at the evolution of resistance over time in *C. glabrata* (Singh-Babak *et al.,* 2012). The authors studied resistance evolution through serial isolation of patient samples rather than in controlled *in vitro* evolution so the influence of selection environment and dynamics of pathogen fitness could not be measured. We measured evolution of the caspofungin dose response inhibition profile via serial transfers of replicate populations in a range of constant drug concentrations. This allows for dynamic comparison of changing population fitness at different drug concentrations and was described by Peña-Miller *et al.* (2014) for characterising bacterial resistance evolution.

4.3 Materials and Methods

4.3.1 Cell Growth in Synthetic Complete Medium at Different Glucose Concentrations

These methods are as described in Reding-Roman *et al.* (2017), but are provided in more detail below.

4.3.1.1 Media and Stock Solutions

Overnight cultures of each strain were prepared in YPD medium (Yeast Peptone Dextrose with 20 mg ml^{-1} glucose (2% w/v)) in 4 ml volumes in universal tubes, via inoculation of a single colony per tube. Following 18-24 hours incubation at 30^{o}C and 180 rpm, overnights were centrifuged and washed once in PBS solution prior to re-suspension in SC (Synthetic Complete) minimal medium at the appropriate glucose concentration.

SC medium was prepared at 14 different glucose concentrations ranging 0.25-32 mg ml^{-1} by autoclaving media components (excluding glucose and 10% of the final media volume) prior to addition of filter-sterilised glucose solution. D-Glucose was dissolved in distilled, de-ionised water to reach a final concentration of 320 mg ml^{-1} (32% w/v) and sterilised through a 0.22 µm filter unit. Glucose was diluted appropriately in autoclaved SC media and by addition of water to make up the final volume where necessary, to prepare SC medias with 4, 12, 20, 24 and 32 mg ml^{-1} final glucose concentrations. All other SC media were prepared from a 200 mg ml^{-1} (20% w/v) glucose stock solution.

4.3.1.2 *Candida glabrata* Strains

All strains used were the clinical strains and the osmotic stress-signalling mutant of the BG2 strain (BG2 Δ*ssk2)* described in **Table A.1.2.S1** (ATCC 2001, BG2, BG2Δ*ssk2,* NCPF 3605 and NCPF 3309). Strains were preserved in glycerol at -80^{o}C and were streaked on YPD agar and incubated at 30^{o}C for 48 hours then maintained at room temperature prior to preparation of overnight cultures.

4.3.1.3 Single Season Cell Growth Assays

Overnight cultures of each strain were split into separate universal tubes based on the number of glucose concentrations to be tested. Each was centrifuged and re-suspended in equal volume in 1 x PBS. A 1:7 dilution of each was prepared in PBS and one universal of overnight culture per strain was further diluted for cell enumeration with a haemocytometer, to calculate cell concentration in cells/ml. Cultures were centrifuged and re-suspended in equal volumes of the appropriate glucose concentration SC media, per strain. All universals were diluted in their SC media to reach a concentration of 6.49×10^6 cells/ml and cell suspensions were diluted in PBS and plated on YPD to verify viable cell concentration (CFU/ml).

Cell growth per strain, per glucose concentration was measured in 96-well clear flat-bottom, non-adherent polystyrene microtiter plates (Greiner Bio-One; Product code: 655161) via inoculation of wells containing 75 µl of the appropriate glucose concentration SC medium, with 75 µl of diluted cells to reach a final volume of 150 µl per well (final cell concentration within wells approximately 3.25×10^6 cells/ml). Background controls containing 150 µl of media were included for each SC media used in the plate. The outer border wells were filled with 150 µl of distilled, DI water to reduce edge effects of evaporation. Each of the five strains were grown in triplicate cultures within a 96-well plate over the 14 different glucose concentrations and experiments were repeated over three independent biological replicates, resulting in a sample size of 9 replicates per strain and glucose concentration.

96-well plates were sealed with transparent film and 2 holes were punctured in the film over the centre of each well via a sterile needle, for aeration. Plates were incubated at 30^{o}C over 24 hours with orbital shaking at 182.6 rpm (amplitude 4 mm) in a Tecan M200 microtiter plate reader, with OD (Optical Density) readings at 650 nm wavelength taken every 20 minutes. OD is used as a proxy for total biomass (number of cells and cell size), which indicates the total carbon assimilated over time and can easily be tracked during growth (Reding-Roman *et al.,* 2017).

4.3.1.4 Data Analysis and Statistics

Data for each strain and glucose concentration condition was compiled across biological replicates and imported into MATLAB for analysis and fitting of a four-parameter growth model, which is a modified solution of the logistic equation that includes lag phase (equation (9); Reding-Roman *et al.* (2017)). The model-estimated blank OD (optical density) readings of the media-only wells were subtracted from microbial growth data of all culture wells. Yield (efficiency of glucose conversion into biomass) was calculated as K (carrying capacity) divided by glucose concentration (mg ml^{-1}).

In order to achieve mechanistic descriptions of the data, we fitted growth kinetic equations that incorporated yield (efficiency of biomass production) as a variable function of glucose concentration, to growth rate (r), carrying capacity (K) and yield data measured at different glucose concentrations (Meyer *et al.,* 2015; Reding-Roman *et al.,* 2017). Yield was modelled as a variable function due to a proposed switch from respiration to fermentation at higher glucose concentrations that is predicted to decrease efficiency of biomass production through incomplete respiration and production of waste metabolites (Pfeiffer *et al.,* 2001; MacLean and Gudelj, 2006; Meyer *et al.,* 2015; Reding-Roman *et al.,* 2017). Final data plots, statistical analyses of model fits and t-tests to compare growth parameters were produced in MATLAB and were completed by Carlos Reding-Roman, University of Exeter.

Barplots of growth kinetic parameters (r, K and yield) across *C. glabrata* strains were plotted for low (1 mg ml^{-1}) and intermediate (10 mg ml^{-1}) glucose concentrations in Excel. R version 3.4.3 (R Core Team, 2017) was used for two-way ANOVA tests to analyse the effects of *C. glabrata* strain, glucose concentration and their interaction on each of growth rate, carrying capacity and yield. Tukey *post hoc* tests were used to deduce significant pairwise differences. We tested for the asumptions of normality and homoscedasticity for the ANOVA model by visualising the distribution of the standardised residuals and the relationship with model-fitted values.

4.3.2 Comparative Virulence of *C. glabrata* Strains

Galleria mellonella larval survival assays (as described in Chapter 3) were used to compare virulence of *C. glabrata* strains 2001 and 3605 at an intermediate inoculum dose (2.5 x 10^6 CFU/larva). Methods from Ames *et al.* (2017) were used with modifications. 20 larvae per *C. glabrata* strain were injected with the inoculum dose in the top left proleg and experiments were repeated twice independently. Using OASIS 2 software (Han *et al.,* 2016), the log-rank test confirmed that there were no significant differences in larval survival for each *C. glabrata* strain between the two independent experiments so the data was pooled. Data was analysed in R (R Core Team, 2016) using the package 'Hmisc' (Harrell Jr *et al.,* 2006) to plot Kaplan-Meier survival plots, calculate mean survival times and compare survival between strains using the log-rank test. Ames *et al.* (2017) tested larval survival at the mammalian physiological temperature of 37^{o}C, whereas we incubated larvae at 30^{o}C as we measured *in vitro* growth kinetics of *C. glabrata* at this temperature (described above).

4.3.3 *In vitro* Experimental Evolution of Populations of *C. glabrata* Strains 2001 and 3605 on a Gradient of Caspofungin Concentrations

To compare the abilities of *C. glabrata* strains 2001 and 3605 to evolve caspofungin resistance in the laboratory, we tested for growth adaptation in replicate populations of each strain that were grown across a gradient of caspofungin concentrations in 10 mg ml^{-1} glucose Synthetic Complete medium, an intermediate glucose concentration to allow for sufficient growth of *C. glabrata* strains 2001 and 3605 (see **Figure 4.2** for experimental design). A single overnight culture of each strain founded all replicate populations at the eight different caspofungin concentrations and the drug-free growth control. Replicate populations were serially transferred every 24 hours to fresh media and drug conditions, maintaining the same environmental conditions for each population in subsequent seasons. A total of 14 serial transfers of all populations were completed in the evolutionary experiment and the whole experiment was repeated on three separate 14-day periods. We used this as a high-throughput approach to test adaptation of populations at a range of clinically-relevant caspofungin concentrations (Espinel-Ingroff *et al.,* 2013) over

time. The highest caspofungin concentration used was approximately 8 times the MIC50 recorded previously for *C. glabrata* isolates (Espinel-Ingroff *et al.,* 2013) and that found in our pilot experiments. We tracked real-time growth of all populations during each season via OD (optical density) measurement in a Tecan M200 microtiter plate reader. The 96-well plate was sealed with transparent film and 2 holes were punctured over the centre of each well via a sterile needle, for aeration. Plates were incubated at 30ºC over 24 hours with orbital shaking at 182.6 rpm (amplitude 4mm), with OD (Optical Density) readings at 650 nm wavelength taken every 20 minutes. In Experiment 1, day 6 and 13 cells were grown in an orbital shaking incubator with only a single reading taken at 24 hours (after 60 seconds shaking) on the Tecan reader.

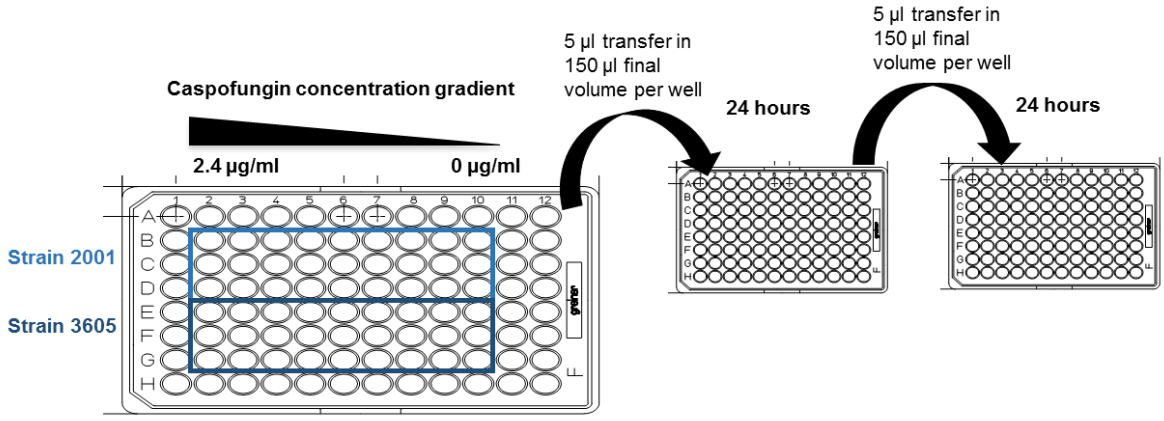

Figure 4.2. Experimental design for populations of *C. glabrata* strains 2001 and 3605 evolving on a gradient of caspofungin concentrations. Experimental populations were evolved in 96-well plates. Eight different caspofungin concentrations representing a 1.75-fold dilution series from 2.4 µg/ml were prepared separately in 10 mg ml^{-1} glucose Synthetic Complete medium. Aliquots of 75 µl of a single drug concentration were added to 6 replicate wells from rows B to G in a single column of the 96-well plate. The prepared plate contained a decreasing gradient of caspofungin concentrations from columns 2 to 9. The 6 replicate wells in column 10 contained 75 µl aliquots of 10 mg/ml SC medium alone and represented growth controls. Column 11 contained 6 replicate wells of 150 µl of 10 mg ml^{-1} SC medium alone as media controls. 75 µl aliquots of diluted cells of strain 2001 were added to all wells in rows B - D in columns 2 - 10 of the plate. Diluted cells of strain 3605 were added to all wells in rows E – G in columns 2 – 10 of the plate. The outer border wells of the plate were filled with 150 µl of distilled, DI water to reduce edge effects of evaporation. On each subsequent day, a new 96-well plate was prepared with the same caspofungin concentration

gradient and identical layout, but 145 µl aliquots of each drug concentration were added to the plate wells. Following 24 hours of incubation and measurement of *C. glabrata* growth in the previous day's 96-well plate, cells in all wells were re-suspended and a 5 µl aliquot from each well was pipette-transferred to the corresponding well in the newly-prepared 96-well plate. Identical daily transfers were completed for a total of 14 days. The entire experiment was repeated over 3 separate 14-day periods with a separate overnight culture of the ancestral stock of strains 2001 and 3605 used for each experiment.

A working caspofungin stock solution was prepared from powder stock (provided by Christopher Thornton, University of Exeter, UK**)** stored at -80^{o}C, which was diluted in sterile distilled, de-ionised water to reach a final concentration of 5 mg ml^{-1} and stored at -20^{o}C. Caspofungin concentrations required for the evolutionary experiment were prepared by appropriate dilutions of the 5 mg ml^{-1} stock solution in SC medium. Eight drug concentrations were separately prepared from the 5 mg ml^{-1} caspofungin stock, diluted in 1% w/v glucose SC and vortex-mixed in Eppendorf tubes. Prepared caspofungin concentrations differed by 1.75-fold, ranging 0.1 – 4.8 µg/ml (final concentrations following 2-fold dilution with cell suspension in the 96-well plate were 0.05- 2.4 µg/ml). The two *C. glabrata* strains were each diluted to a final concentration of 6.49 x 10^{6} cells/ml (2 x final concentration in 96-well plate) in SC medium before adding to the plate.

In subsequent seasons, caspofungin concentrations prepared in Eppendorfs matched the final concentrations (0.05- 2.4 µg/ml) in the plate wells, added in 145 µl aliquots to wells. Serial transfer of 5 µl aliquots to these wells from the previous season's populations did not alter the caspofungin concentration in the final 150 µl per well. Following daily transfers, remaining volumes of all cell populations were frozen at -80^{o}C in a final concentration of 15% v/v glycerol (Fisher Scientific UK, Loughborough, UK; Product Code: G/0650/17) within each plate well by adding appropriate volumes of 50% v/v glycerol stock to each well and pipette mixing.

Data was imported into MATLAB (MATLAB and Statistics Toolbox Release, 2012a) for analysis and model fitting of the four-parameter logistic growth equation to daily growth profile data at each drug concentration. The data was

blank-corrected by subtracting the OD at time 0 predicted from the logistic model fit, from all other time points in each growth curve. This best-fit model was used to compute growth rate (r) and carrying capacity (K). Growth profile data was used to calculate final OD at 24 hours and AUC (area under the growth profile curve) as extra measures of microbial fitness (Roemhild *et al.,* 2015).

We measured the daily dose response profile of each strain via final OD (at 24 hours) measurement across populations at different drug concentrations. As described in Roemhild *et al.* (2015), growth inhibition in daily dose responses was measured as % relative growth, the OD at 24 hours of each drug-treated population as a percentage of the mean OD of the no drug-treated populations. We used IC50 as a measure of drug sensitivity, similar to the IC75 measure used in Roemhild *et al.* (2015) and analogous to the caspofungin MIC described in clinical studies (Espinel-Ingroff *et al.,* 2013). In a large inter-lab comparison of *C. glabrata* isolates, caspofungin MICs ranged between 0.031-0.5 µg/ml (Espinel-Ingroff *et al.,* 2013). A four-parameter logistic dose response model was fitted to the growth data across populations evolving on the gradient of caspofungin concentrations. The model was used to predict IC50 and slope (gradient of inhibition: Hill coefficient) using R package 'drc' and to compare parameters between dose response profiles (Ritz *et al.,* 2015; R Core Team, 2016). Plots show all data points (**Figure 4.9**; **Figure A.3.1.S8-S11**) or the best fit of the model with associated 95% confidence region (**Figure A.3.1.S6**).

We used the *lme4* package (Bates *et al.,* 2015) with R version 3.4.3 (R Core Team, 2017) to conduct a linear mixed effects analysis of the effect of caspofungin concentration on relative growth of *C. glabrata*. We tested the influence of *C. glabrata* strain, day of the evolutionary experiment and caspofungin concentration as fixed effects and also tested for 2-way or 3-way interactions. The individual 14-day evolutionary experiments were treated as a random effect with a random intercept, to account for variation between separate experimental runs. We checked the distribution of the standardised residuals from the fitted model for normality and checked for homoscedasticity in the standardised residuals with the Fligner-Killeen test, which showed lack of significant heteroscedasticity (Fligner-Killeen:med chi-squared = 93.808, df =

161, *P* = 1). We started with a full model including the three main effects and all possible interactions and obtained *P*-values from likelihood ratio tests comparing the full model with alternative models with individually-removed interactions. These tests showed the significance of individual interactions.

4.4 Results

4.4.1 Resource-Dependent Growth Kinetic Relationships across and within *C. glabrata* Strains

We grew five clinical strains of *C. glabrata* in minimal medium at 14 different glucose concentrations over single seasons, measuring optical density and calculating growth rate (r), carrying capacity (K) and yield (efficiency of biomass production) per glucose concentration for each strain (Reding-Roman *et al.,* 2017). Growth rate increased with glucose concentration across all strains of *C. glabrata*, reaching a maximum at intermediate glucose concentrations (**Figure 4.3(a**); **Figure A.3.1.S1**). Further increases in glucose concentration above this level resulted in saturation of growth rate followed by a decrease for all strains. Population size at carrying capacity (K) also increased with glucose concentration across all *C. glabrata* strains (**Figure 4.3(b); Figure A.3.1.S2**), but saturated above intermediate glucose concentrations. Efficiency of biomass conversion (yield) rapidly declined at low glucose concentrations for *C. glabrata* (**Figure 4.3(c); Figure A.3.1.S3**) then saturated at a low level (below 0.05 OD mg ml^{-1}) for further increases in glucose concentration. A model that described a non-linear relationship between yield and glucose concentration for *E. coli* (Meyer *et al.,* 2015) was a good fit to the data for each *C. glabrata* strain (**Figure 4.3(c); Figure A.3.1.S3**).

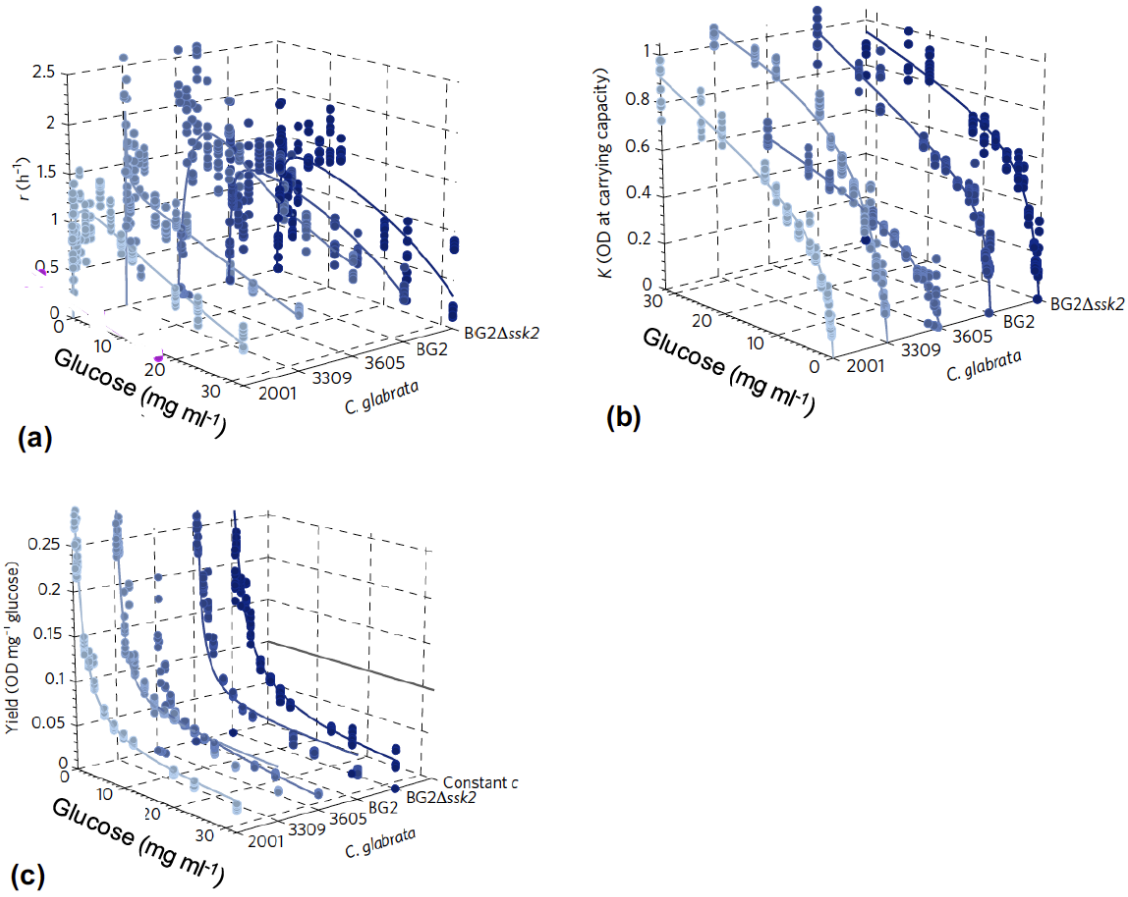

Figure 4.3. Growth kinetics of five *C. glabrata* strains measured over a range of glucose concentrations. These data plots were taken from Figure 1 of Reding-Roman *et al.,* (2017). Growth kinetic data is shown for 5 clinical strains of *C. glabrata* (see Methods) plotted along the z-axis. Growth parameters were measured over 14 glucose concentrations for each *C. glabrata* strain and N = 9 for each concentration. Glucose concentrations are plotted in ascending order along the x-axis in **(a)** and **(c)** and in descending order in **(b).** Growth parameters measured on the y-axis: **(a)** *per capita* growth rate (h^{-1}) (r), **(b)** population size (OD) at carrying capacity (K) and **(c)** yield (OD/ mg ml^{-1} glucose). Separate 2-dimensional plots for each strain were constructed for each of the datasets in **(a) (Figure A.3.1.S1), (b)** (**Figure A3.1.S2** with glucose concentrations plotted in ascending order on the x-axis) and **(c) (Figure A.3.1.S3)**. Growth parameters were estimated from best fit of a logistic equation to growth profile data (Reding-Roman *et al.,* 2017). Dots represent experimental data whereas solid lines are model predictions based on mechanistic equations derived in Meyer *et al.,* (2015) and Reding-Roman *et al.,* (2017), which incorporate yield (efficiency of glucose conversion to biomass) to vary as a function of glucose concentration. The fitted model relationship between yield and glucose concentration **(c)** is a robust fit to the data for all *C. glabrata* strains (adjusted R^2 = 0.995, 0.98, 0.99, 0.95, 0.98) (Reding-Roman *et al.,* 2017). In **(c),** the last solid line fitted on the z-axis

shows the predicted lack of relationship if yield was not glucose concentration-dependent. Data plots and model fitting were completed by Carlos Reding-Roman, University of Exeter.

We investigated whether relationships existed between growth rate (r), carrying capacity (K) and yield within each *C. glabrata* strain. We found that a parabolic profile robustly described the r/K relationship for each strain across all glucose concentrations (**Figure 4.4;** Reding-Roman *et al.,* 2017). A mechanistic model (Reding-Roman *et al.,* 2017), which described growth rate as a product of glucose-dependent yield and uptake, was a robust fit to the data. Growth rate and carrying capacity were positively correlated ("trade-up") between low and intermediate glucose concentrations and negatively correlated ('trade-off") between intermediate and high glucose concentrations. Similarly, growth rate (r) and yield were also described by a parabolic relationship for each strain of *C. glabrata* across glucose concentrations (**Figure 4.5**). As yield is negatively correlated with K (**Figure 4.3**), the glucose concentration-dependent correlations were reversed: rate and yield were positively correlated ("trade-up") at higher glucose and negatively correlated ("trade-off") at lower glucose (**Figure 4.5**). Growth rates were maximised at intermediate glucose concentrations (**Figure 4.4** and **4.5**).

We then compared the rate versus carrying capacity and rate versus yield parabolic profiles across *C. glabrata* strains and found that the shapes differed (**Figure 4.6**; top panels). Strain 3605, isolated from a diabetic patient, showed profiles that were noticeably skewed towards higher growth rate, with lower carrying capacities and yields compared with all other strains. We compared mean growth rate, carrying capacity and yield, measured across all glucose concentrations, between strains 2001 (lab reference strain) and 3605 and found that strain 3605 had a significantly higher growth rate but lower carrying capacity and yield than strain 2001 (**Figure 4.6**; bottom panels).

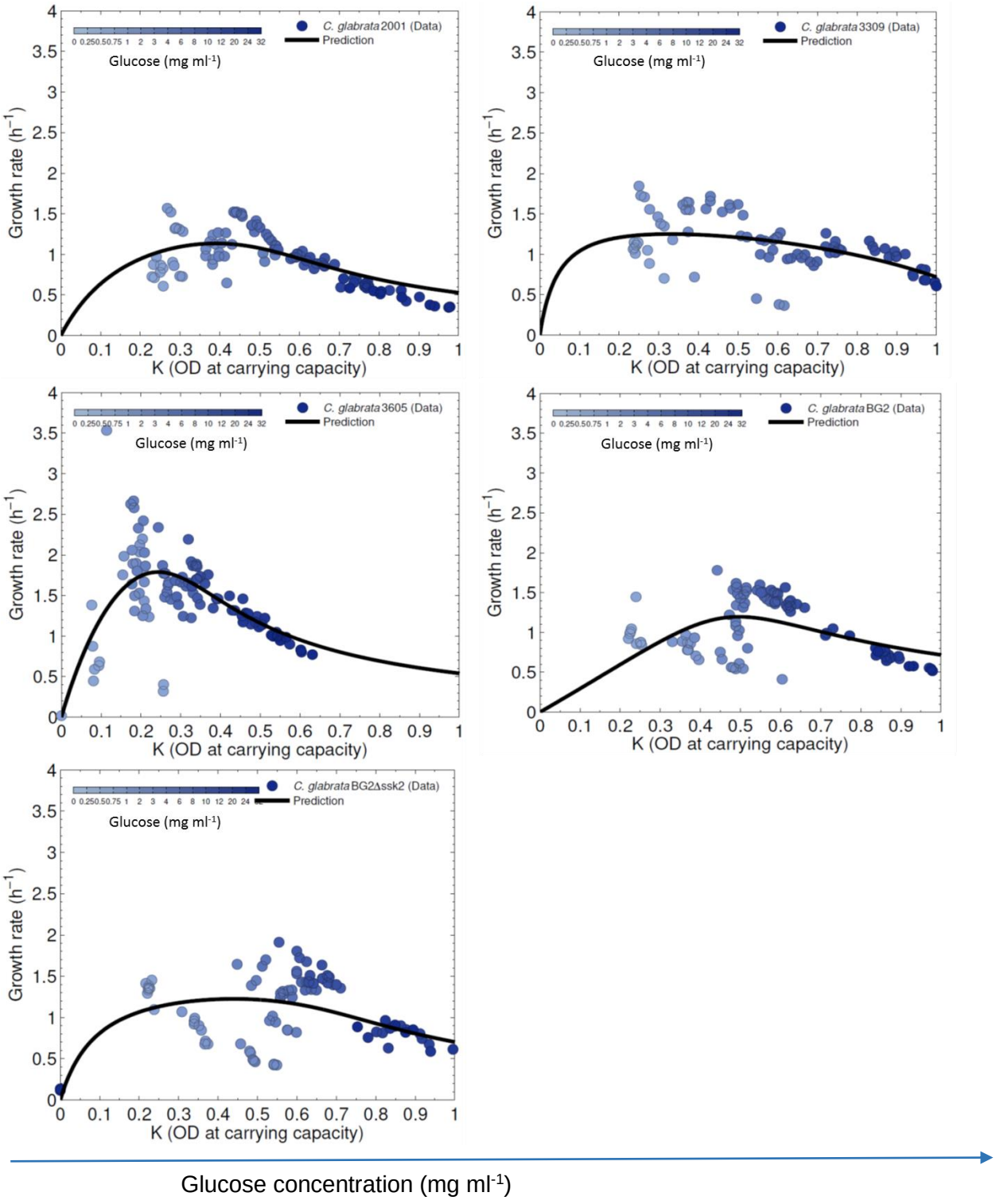

Figure 4.4. Relationship between growth rate (r) and carrying capacity (K) in five *C. glabrata* strains. These plots are taken from Supplementary Figure S5 in Reding-Roman *et al.* (2017). Data points are plotted from all 14 glucose concentrations (N = 9 per glucose) with the colour gradient from light to dark blue indicating increasing glucose concentration. Plots from left to right, top to bottom show strains 2001, 3309, 3605, BG2 and BG2Δ*ssk2.* The black solid lines represent a fit of a model equation that describes growth rate as a product of yield (glucose concentration-dependent) and

glucose uptake rate (Meyer *et al.,* 2015; Reding-Roman *et al.,* 2017). Carrying capacity (K) is equal to yield multiplied by glucose concentration (mg ml^{-1}).

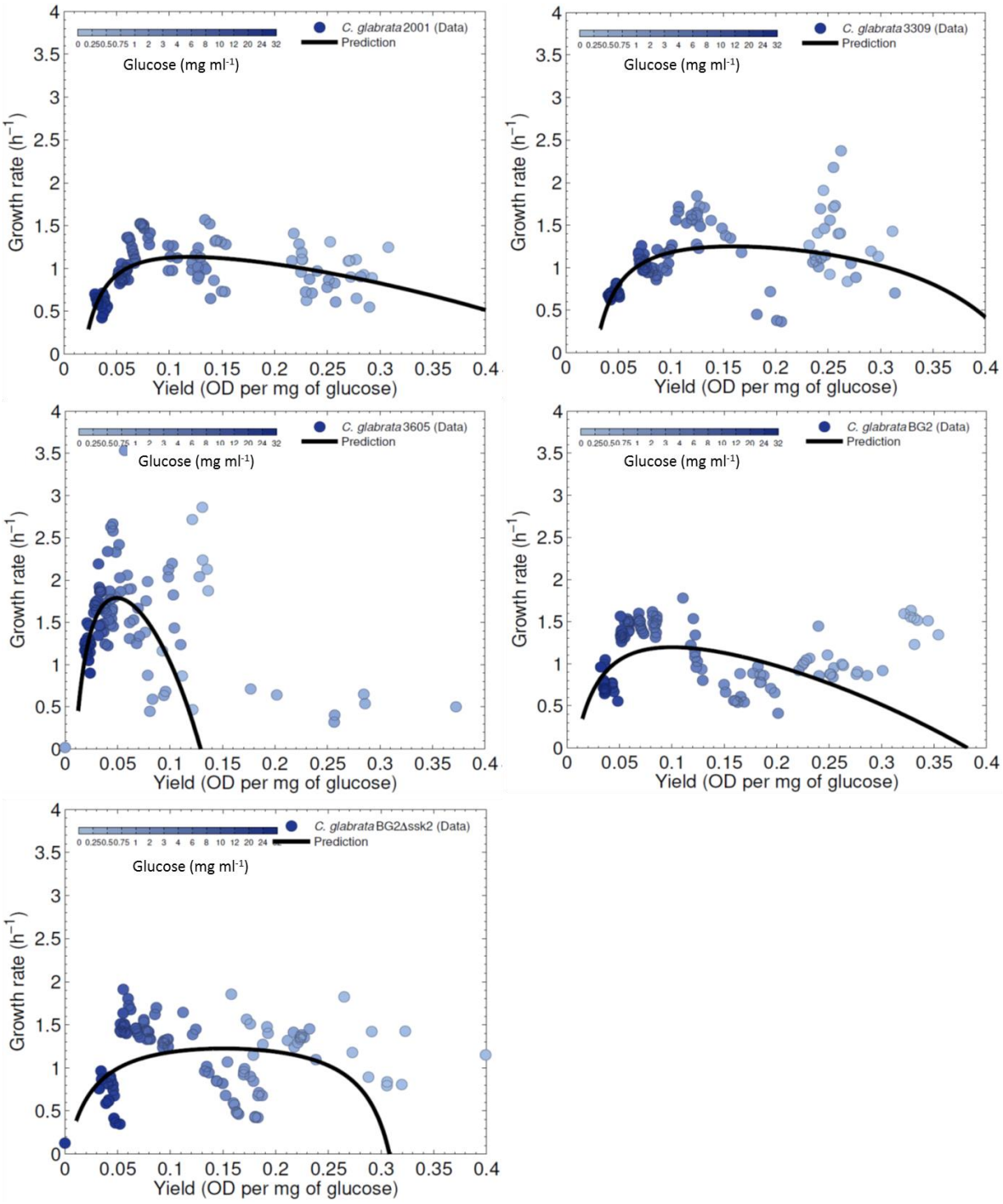

Figure 4.5.

Relationship between growth rate (r) and yield (OD mg ml^{-1} glucose) in five *C. glabrata* strains. These plots were generated by Carlos Reding-Roman, University of Exeter, using data described in Reding-Roman *et al., (*2017). Data points are plotted from all 14 glucose concentrations (N = 9 per glucose) with the colour gradient from dark to light blue indicating decreasing glucose concentration. Plots from left to right,

top to bottom show strains 2001, 3309, 3605, BG2 and BG2Δ*ssk2.* The black solid lines represent a model fit, describing growth rate as a product of yield (glucose concentration-dependent) and glucose uptake rate (Meyer *et al.,* 2015; Reding-Roman *et al.,* 2017).

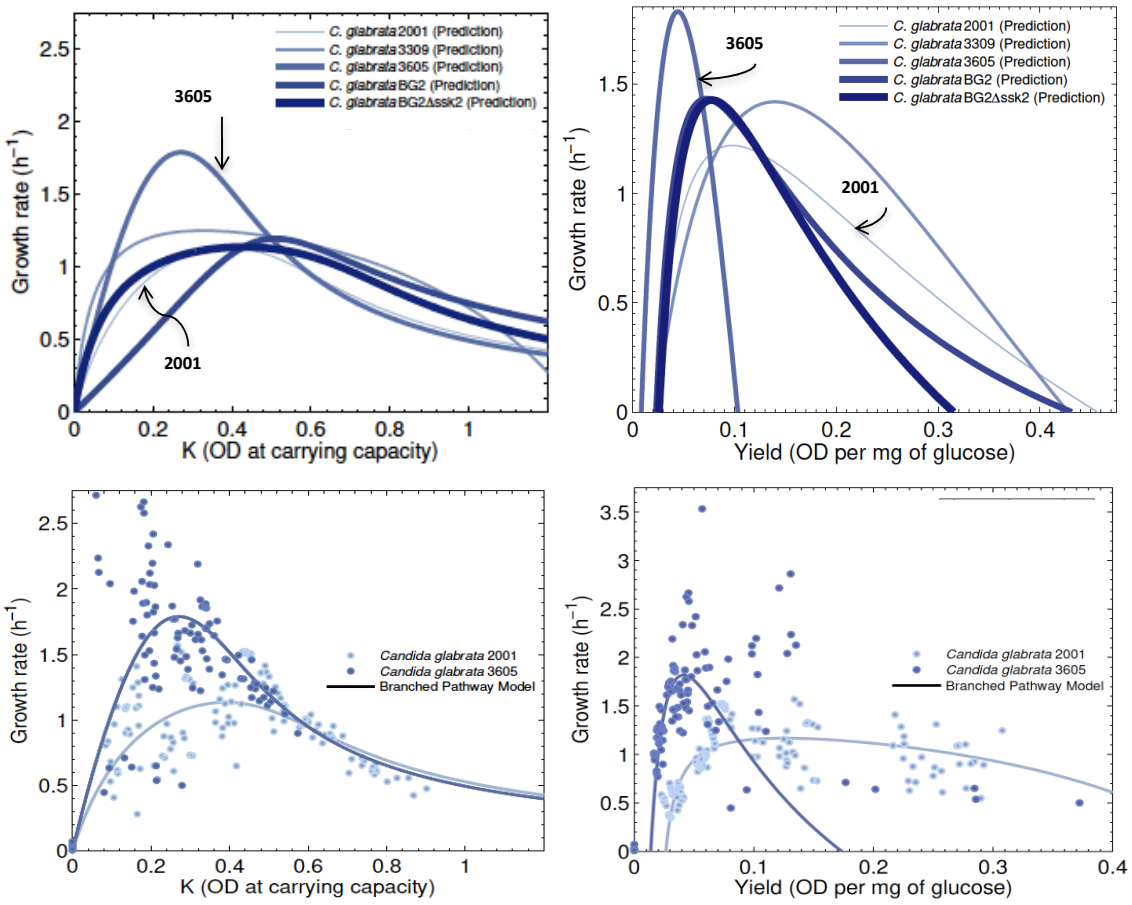

Figure 4.6. Comparison of r/K and r/yield relationships across *C. glabrata* strains. r/K plots (left panels) were taken from Reding-Roman *et al.,* (2017) and r/yield plots (right panels) were created by Carlos Reding-Roman, University of Exeter. The top two panels compare the parabola model fits across all five strains (shown by blue colour gradient) taken from data presented in **Figure 4.4** and **4.5**. Strains 3605 (diabetic patient) and 2001 (lab reference) with contrasting parabola shapes are labelled. The bottom left panel compares *C. glabrata* strain 2001 (light blue) with strain 3605 (dark blue), contrasting in growth rate and carrying capacity (t-test for r: t = -4.52, df = 250, $P < 10^{-5}$; for K: t = 7.72, df = 250, $P < 10^{-12}$). The solid blue lines show the model fits (adjusted R^2 = 0.982, 0.878) (Reding-Roman *et al.,* 2017). The bottom right panel compares *C. glabrata* strain 2001 (light blue) with strain 3605 (dark blue), contrasting in yield (Kruskal-Wallis rank sum test: chi-squared = 78.658, df = 1, $P < 2.2e\text{-}16$). The solid blue lines show the model fits (Reding-Roman *et al.,* 2017).

We then tested for glucose concentration-specific differences in mean growth rate, K and yield across *C. glabrata* strains through further analysis of the strain data collected at intermediate (10 mg ml^{-1}) and low (1 mg ml^{-1}) glucose concentrations. We used two-way ANOVA tests to analyse the effect of *C. glabrata* strain, glucose concentration and their interaction on growth rate, carrying capacity and yield.

Growth rate significantly differed across *C. glabrata* strains (2-way ANOVA: $F_{4, 80} = 37.11$, $P < 2e\text{-}16$) and glucose concentrations (2-way ANOVA: $F_{1, 80} = 246.36$, $P < 2e\text{-}16$), and the magnitude of the strain differences varied with glucose concentration (strain x glucose concentration interaction, 2-way ANOVA: $F_{4, 80} = 76.70$, $P < 2e\text{-}16$) (**Figure 4.7(a)).** Strain 3605 had a significantly greater growth rate than strains BG2, 3309 and 2001 at intermediate glucose concentration (10 mg ml^{-1}) (Tukey HSD *post hoc* test- 3605:BG2, $P < 0.01$; 3605:3309, $P < 0.001$; 3605:2001, $P = 0.000$), but a significantly lower growth rate than each of these strains and BG2Δ*ssk2* at low glucose concentration (1 mg ml^{-1}) (Tukey HSD *post hoc* test- $P = 0.000$). Additionally, strains 2001 and 3309 had significantly lower growth rates than strains BG2 and BG2Δ*ssk2* in intermediate glucose (Tukey HSD *post hoc* test- 2001: BG2, $P < 0.001$; 2001: BG2Δ*ssk2*, $P = 0.000$; 3309: BG2, 3309: BG2Δ*ssk2*, $P < 0.001$). Strains 2001 and 3309 only had significantly lower growth rates than strain BG2Δ*ssk2* in low glucose (Tukey HSD *post hoc* test- 2001: BG2Δssk2, $P = 0.000$; 3309: BG2Δssk2, $P < 0.01$). Growth rate was significantly greater at intermediate (I) than low (L) glucose concentration for strains 3605 and BG2 only (Tukey HSD *post hoc* test- 3605 (I): 3605 (L), $P = 0.000$; BG2 (I): BG2 (L), $P < 0.001$).

Carrying capacity significantly varied across C. glabrata strains (2-way ANOVA: $F_{4, 80} = 441.57$, $P < 2e\text{-}16$) and glucose concentrations (2-way ANOVA: $F_{1, 80} = 5299.65$, $P < 2e\text{-}16$) (**Figure 4.7(b)).** The difference in carrying capacity between strains significantly varied between low and intermediate glucose concentrations (strain x glucose concentration interaction, 2-way ANOVA: $F_{4, 80} = 35.48$, $P < 2e\text{-}16$).

Strain 3605 had a significantly lower carrying capacity than all of the other four strains at intermediate and low glucose concentrations (Tukey HSD *post hoc* test- $P = 0.000$). Additionally, strains 2001 and BG2 had significantly lower carrying capacities than strains 3309 and BG2Δ*ssk2* in intermediate glucose (Tukey HSD *post hoc* test- 2001: 3309, BG2: 3309, $P = 0.000$; 2001: BG2Δ*ssk2*, BG2: BG2Δ*ssk2*, $P < 0.001$). The carrying capacity of strain BG2Δ*ssk2* was significantly lower than that of strain 3309 in intermediate glucose (Tukey HSD *post hoc* test- $P = 0.000$). Carrying capacity was significantly greater at intermediate (I) than low (L) glucose concentration for all five strains (Tukey HSD *post hoc* test- $P = 0.000$).

Yield significantly varied across *C. glabrata* strains (2-way ANOVA: $F_{4, 80} = 218.1$, $P < 2e\text{-}16$) and glucose concentrations (2-way ANOVA: $F_{1, 80} = 1627.5$, $P < 2e\text{-}16$) (**Figure 4.7(c)).** The difference in yield between strains significantly varied between low and intermediate glucose concentrations (strain x glucose concentration interaction, 2-way ANOVA: $F_{4, 80} = 124.9$, $P < 2e\text{-}16$). Strain 3605 had a significantly lower yield than strains 2001, 3309 and BG2Δ*ssk2* at intermediate glucose concentration (Tukey HSD *post hoc* test- 3605: 2001, $P < 0.05$; 3605: 3309, $P < 0.001$; 3605: BG2Δ*ssk2,* $P < 0.01$). Strain 3605 had a lower yield than all four of the other strains at low glucose concentration (Tukey HSD *post hoc* test- $P = 0.000$). Strain BG2Δ*ssk2* had a significantly lower yield than strain 3309 in low glucose (Tukey HSD *post hoc* test- $P < 0.01$). Yield was significantly greater at low than intermediate glucose for all strains except strain 3605 (Tukey HSD *post hoc* test- $P = 0.000$).

We concluded that strains 2001 and 3605 had most contrasting growth strategies as all three growth parameters significantly differed between the strains at both glucose concentrations (**Figure 4.7**). At low glucose, strain 2001 compared with strain 3605 had a 6.3-fold higher growth rate and a 12.8-fold greater carrying capacity and yield. **Figure A.3.1.S4** (left panels) show example growth profile plots and model fits, indicating a flat growth profile for strain 3605. At intermediate glucose, strain 2001 compared with strain 3605 had a 1.8-fold lower growth rate and 1.8-fold greater carrying capacity and yield. **Figure A.3.1.S4** (right panels) show logistic growth profile shapes for each strain and the balance between growth rate (r) and carrying capacity (K). Between glucose

concentrations, strain 3605 had a 13.9-fold greater growth rate at intermediate than low glucose whereas strain 2001 had no difference (**Figure 4.7**). Carrying capacity was 2.3-fold greater for strain 2001 at intermediate glucose and 17.2-fold greater for strain 3605. Yield was 4.3-fold greater for strain 2001 at lower glucose but there was no significant change for strain 3605.

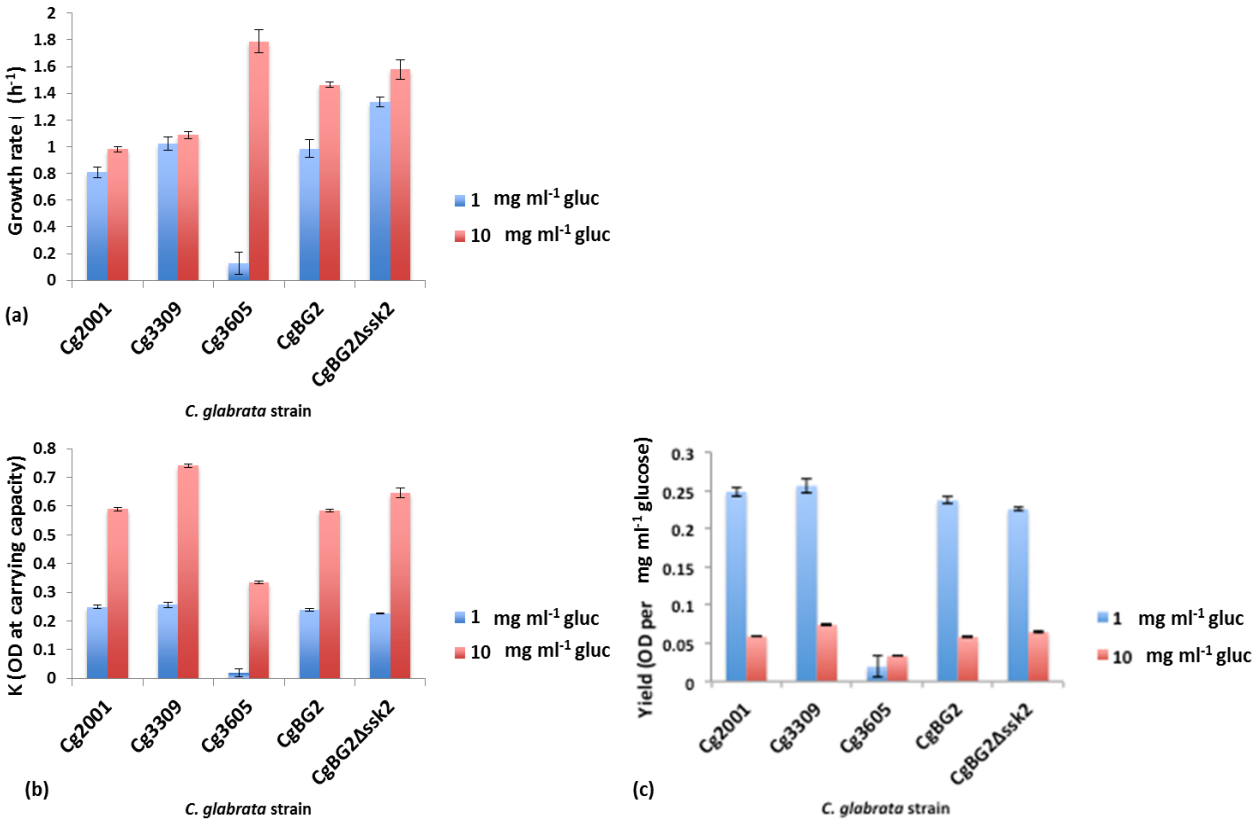

Figure 4.7. Growth rates, carrying capacities (K) and yields across *C. glabrata* strains at low and intermediate glucose concentrations. Figures are plotted from data collected at 1 and 10 mg ml^{-1} presented in earlier plots. Growth parameters were measured across all strains and both glucose concentrations (low and intermediate) **(a)** Growth rate (r) *per capita* (h^{-1}); **(b)** K (OD at carrying capacity); **(c)** Yield (OD per mg ml^{-1} glucose). Bar plots show mean value +/- SE.

4.4.2 Comparative Virulence of *C. glabrata* Strains 2001 and 3605

To determine whether contrasting growth kinetics of *C. glabrata* strains 2001 and 3605 correlated with differences in virulence, we measured survival of *Galleria mellonella* wax moth larvae over single strain infection at 30ºC. Over 10 days, we found that strain 2001 caused a significantly greater decrease in larval survival, with a negligible change in survival of strain 3605 (**Figure 4.8**). Mean survival time (+/- SE) of strain 2001 was 5.65 +/- 0.53 days, compared with 9.63 +/- 0.25 days for strain 3605.

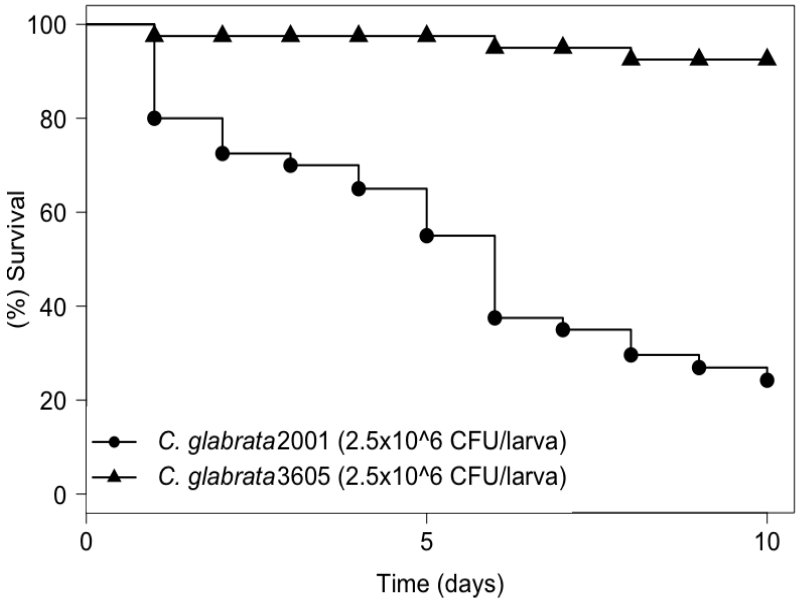

Figure 4.8. Survival of *Galleria mellonella* infected with *C. glabrata* strain 2001 or 3605 at 30ºC. Survival was measured daily for 10 days following infection with a moderate dose of either strain. Data was pooled from two independent experiments that showed no significant differences in survival and N = 40 for each strain. Kaplan-Meier survival curves were plotted: Log rank test = 40.56, df = 1, *P* = 1.907e-10.

4.4.3 Experimental Evolution of Populations of *C. glabrata* Strains 2001 and 3605 Across a Gradient of Caspofungin Concentrations

For each *C. glabrata* strain, we measured the daily growth density relative to the no-drug treated control for triplicate populations evolving at each of eight caspofungin concentrations. The experimental evolution was repeated over three 14-day experiments (E1-3), using a separate overnight culture of each strain per experiment to found all replicate populations. Both strains were

evolved at drug concentrations diluted in SC medium at intermediate glucose concentration (10 mg ml^{-1}) as strains 2001 and 3605 were greatly contrasted in growth rate and carrying capacity at this glucose concentration (**Figures 4.3-4.7**) (Reding-Roman *et al.,* 2017).

By treating variation between independent experiments as a random effect, we found that relative growth of *C. glabrata* over time between the start, mid and end-points of the evolutionary experiment (across days 1, 7 and 14) was significantly influenced by strain (effect of strain x day interaction, likelihood ratio test: $\chi^2(2) = 11.77$, $P = 0.00278$), but this effect was not significantly dependent upon caspofungin concentration (effect of strain x day x caspofungin concentration interaction, likelihood ratio test: $\chi^2(2) = 2.97$, $P = 0.226$). The average relative growth percentage of strain 2001 increased by 19.9 between days 1 and 7 and a by a further 5.4 between days 7 and 14 (**Figure A.3.1.S5 (a)).** In contrast, average relative growth percentage of strain 3605 only increased by 6.7 between days 1 and 7, followed by a decrease of 3.9 between days 7 and 14 (**Figure A.3.1.S5(b)).** The inhibitory influence of higher caspofungin concentrations on relative growth was reduced over time (effect of day x caspofungin concentration interaction, likelihood ratio test: $\chi^2(2) = 10.48$, $P = 0.00530$), signifying *C. glabrata* growth adaptation to caspofungin.

Higher caspofungin concentrations had a greater inhibitory effect on relative growth for strain 3605 than strain 2001, but overall the effect of caspofungin on growth was not influenced by strain (effect of strain x caspofungin concentration interaction, likelihood ratio test: $\chi^2(1) = 3.25$, $P = 0.0716$). Caspofungin had a minimal inhibitory effect on relative growth of both strains between 0 and 0.15 µg/ml and could stimulate growth of strain 3605 above that of the no-drug treated control (**Figure A.3.1.S5(b)**). Independently, caspofungin concentration had an inhibitory effect on growth (effect of caspofungin concentration, likelihood ratio test: $\chi^2(1) = 425.35$, $P < 2.2e\text{-}16$), strain 2001 had greater growth than strain 3605 (effect of strain, likelihood ratio test: $\chi^2(1) = 5.22$, $P = 0.0223$) and *C. glabrata* relative growth increased over time (effect of day, likelihood ratio test: $\chi^2(2) = 21.73$, $P = 1.999e\text{-}05$).

For each strain, we fitted a single four-parameter logistic dose response model to daily growth data across all populations evolving on the gradient of caspofungin concentrations. To test for caspofungin adaptation over time, we compared the dose response model fit across evolving populations on days 1, 7 and 14 of the evolutionary experiments. For strain 2001, we found that the gradient of sensitivity (slope) of the profile significantly decreased over time in Experiments 2 and 3, resulting in flatter dose response profiles as populations evolving at higher caspofungin concentrations increased their relative growth (**Figure 4.9**; left panels; **Table A.3.1.S1**). Interestingly, in populations transferred at the third highest caspofungin concentration (0.78 µg/ml), relative growth was initially very low or non-detectable, but adaptation occurred over serial transfers, with relative growth above 50% at day 14 in all three independent experiments (**Figure 4.9**; left panels).

By tracking real-time growth by automated optical density (OD) measurement, in Experiment 3 that was representative of the three experiments, we identified logistic growth in strain 2001 populations grown at 0 – 0.26 µg/ml on day 1 (**Figure A.3.1.S14**), and at 0.45 µg/ml on days 7 (**Figure A.3.1.S15**) and 14 (**Figure A.3.1.S18**). On day 7, low growth occurred at 0.78 µg/ml with standard error across replicates (**Figure A.3.1.S19**) and a similar profile was observed at 1.37µg/ml by day 14 (**Figure A.3.1.S18**). Detectable growth by day 14 in 2.4 µg/ml caspofungin was not consistently identified across the technical replicates.

Strain 2001 adaptation to caspofungin measured by the IC50 (50% inhibitory concentration) significantly increased between days 1 and 14 in all three experiments (**Figure 4.9**; left panels; **Table A.3.1.S2**), but the fold increase in IC50 varied: experiment 1: 2.1-fold; experiment 2: 6.4-fold; experiment 3: 3.6-fold. Fluctuation in the increasing trend in IC50 value was shown at intermediate time points in the three experiments (**Figures A.3.1.S8, 10, 12**). In Experiments 1 and 3, significant increases in the concentrations of caspofungin inhibiting between 15 and 50% of relative growth (IC15 - IC50 values) occurred between days 1 and 7, shown by non-overlapping 95% confidence intervals of dose response model prediction (**Figure A.3.1.S5** (left panels); **Figure**

A.3.1.S7). In all three experiments, significant increases in caspofungin IC45 - IC60 values of relative growth occurred between days 1 and 14.

For strain 2001, relative growth varied between replicate populations evolving at post-IC50 concentrations (**Figure 4.9**; left panels; **Figures A.3.1.S8, 10, 12),** particularly during the early stages of growth adaptation**.** At 0.78 µg/ml caspofungin, the standard error of relative growth between technical replicate populations was 37% on day 7 in the first and second biological replicates (**Figure 4.9**; left panels). Across all nine replicate populations relative growth ranged from 3-115% and relative growth became greater than 50% in all populations by day 11 (**Figures A.3.1.S8, 10, 12).** At 1.37 µg/ml, adaptation was lower as relative growth was not consistently greater than 50% by day 14 across all replicate populations. Standard error of relative growth was greater than 21% at day 7 and after (**Figures A.3.1.S8, 10, 12).** At 2.4 µg/ml, relative growth was not above 50% by day 14 in any of the replicate populations in Experiments 2 and 3.

Strain 3605 did not show significant evolution of the caspofungin dose response profile across populations evolving across the gradient of caspofungin concentrations in the three independent experiments (**Figure 4.9**; right panels; **Figure A.3.1.S6**, left panels). The slope of the dose response profile did not change over time, apart from a slightly significant decrease in gradient between day 1 and 14 for Experiment 2 (**Table A.3.1.S3**), indicating a lack of consistent adaptation across replicate populations and at higher drug concentrations over time. The change in caspofungin susceptibility over time (IC50) in Experiment 3 was intermediate to the response in the other two experiments (**Figure 4.9**; right panels). In Experiment 3, logistic growth occurred in populations adapted to 0-0.26 µg/ml caspofungin concentration on day 1 (**Figure A.3.1.S15**), growth occurred at 0.45 µg/ml by day 7 (**Figure A.3.1.S17**) and at 0.78 µg/ml by day 14 (**Figure A.3.1.S19**).

At 0.78 µg/ml caspofungin, standard error of relative growth of strain 3605 was greater than 40% by day 14 in Experiments 1 and 3, but relative growth was not consistently above 50% across technical replicate populations (**Figure 4.9**; right panels). Sensitivity to caspofungin (IC50) did not significantly change between

days 1 and 14, apart from an increase in IC50 between days 1 and 7 in Experiment 3 (**Table A.3.1.S5**). IC50 varied across the three independent experiments (**Figure 4.9;** right panels; **Figures A.3.1.S9, 11, 13**) and in Experiment 2, daily IC50 was consistent and no growth occurred in populations transferred at 0.45 µg/ml and above (**Figure A.3.1.S11**). Experiment 2 had highly overlapping dose response profiles on days 1, 7 and 14, whereas a small (non-significant) increase in IC50 between days 1 and 7 occurred in Experiments 1 and 3 (**Figure 4.9**; right panels; **Figure A.3.1.S6**, left panels). Relative growth was not consistently greater than 50% across technical replicates at 1.37 and 2.4 µg/ml in all three experiments.

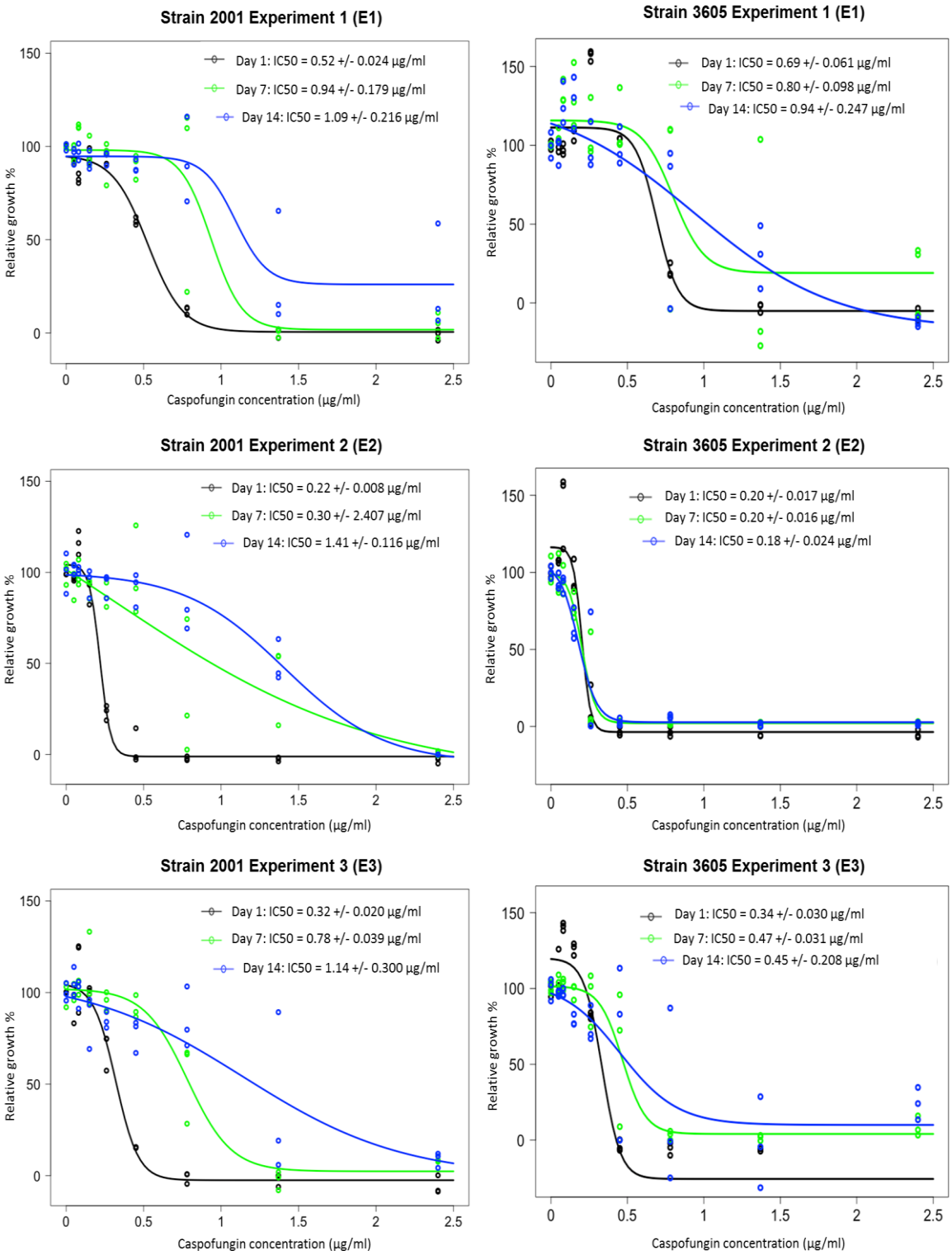

Figure 4.9. Evolution of populations of *C. glabrata* strains 2001 and 3605 on a gradient of caspofungin concentrations in three independent experiments. Left panels show evolution of populations of strain 2001; right panels show evolution of populations of strain 3605. The three separate plots per strain represent independent 14-day evolutionary experiments, each started from a separate overnight culture. In each independent experiment, three replicate populations of each strain were grown at eight different caspofungin concentrations and a drug-free environment, in 10 mg ml^{-1}

Synthetic Complete medium within a 96-well plate (see Methods). The plate was incubated for 24 hours with OD readings taken and all replicate populations were transferred to identical fresh drug conditions every 24 hours, respectively for each set of three replicate populations evolving at each drug concentration (see **Figure 4.2** for experimental design). Relative growth was calculated from OD measurement of all populations at 24 hours, as % growth relative to the no drug control. The plots show changes in the dose response profile shape across populations evolving on the gradient of drug concentrations over time, with all replicate populations plotted as data points. The solid line curves represent 4-parameter logistic model fits (R-package 'drc'; Ritz *et al.*, 2015). Days 1, 7 and 14 dose responses are plotted (black, green, blue respectively) and IC50 estimates with their standard errors predicted from the logistic model are presented for each curve. Comparison of IC50 parameters- 2001 E1: Day 1 compared with Day 7,14, $P < 0.01$; 2001 E2: Day 1 compared with Day 14, $P = 0.00$; 2001 E3: Day 1 compared with Day 7,14, $P < 0.001$; 3605 E1, E2, E3: no significant differences apart from E3: Day 1 and Day 7, $P < 0.05$. Comparison of slopes/ gradients of profiles (Hill coefficient)- 2001 E1: no significant differences; 2001 E2: Day 1 and 7,14, $P < 0.01$; 2001 E3: Day 1 and 14, $P < 0.01$; 3605 E1, E2, E3: no significant differences apart from E2: Day 1 and 14, $P < 0.05$.

4.5 Discussion

Candida species occupy diverse host sites that vary in nutrient concentrations, to which they must adapt in order to grow and resist other environmental stresses (Brown *et al.,* 2014a). Metabolic adaptations to glucose in the yeasts *C. albicans* (Rodaki *et al.,* 2009) and *S. cerevisiae* (Yin *et al.,* 2003) have been described, but growth kinetic adaptations over a range of glucose levels in *C. glabrata* strains, and relationships with virulence and antifungal susceptibility have not been characterised. It is, therefore, important to investigate the influence of environment-dependent growth kinetics on antifungal adaptation to gain a better understanding of susceptibility and evolution of resistance in infections. We measured growth parameters of different strains of *C. glabrata* over a range of glucose concentrations (Reding-Roman *et al.,* 2017) and compared evolution of antifungal adaptation between the strains most contrasting in growth kinetics. We identified conserved relationships between growth parameters across the strains, but found differences in virulence and evolution of the antifungal susceptibility response in two strains that were most contrasting in average growth rates, carrying capacities and yields. Our results contribute to understanding *C. glabrata* metabolic adaptation in different infection environments and identify growth traits associated with antifungal adaptation, which could improve characterisation and susceptibility testing of fungal infections.

During growth of five strains of *C. glabrata* in minimal medium, we found that growth rate (r) and carrying capacity (K) non-linearly increased with glucose concentration and that yield (efficiency of biomass production per mg ml^{-1} of glucose) sharply decreased at higher glucose (Reding-Roman *et al.,* 2017). These trends are similar to those described by Monod (1949) for growth of bacterial cultures over increasing concentrations of a single limiting resource. In contrast to Monod kinetics, we found that K was non-linearly correlated with glucose and saturated at high concentrations, rather than continuously increasing (Reding-Roman *et al.,* 2017). Whilst Monod (1949) described growth rate saturation at high glucose concentrations, we found that *C. glabrata* growth rate decreased at the highest glucose concentrations, a trend also observed in *E. coli* (Reding-Roman *et al.,* 2017).

The growth kinetic trends on glucose that we observe were consistent with prior mechanistic models that rely on glucose metabolism proceeding via a 'branched pathway' (MacLean and Gudelj, 2006; Meyer *et al.,* 2015; Reding-Roman *et al.,* 2017). Glucose can be completely respired via glycolysis and the TCA (tricarboxylic acid cycle) producing a high yield of ATP, or incompletely respired to produce a much lower yield of ATP via glycolysis and excretion of metabolites (a separate metabolic 'branch' resulting in faster ATP production) (MacLean and Gudelj, 2006). Complete respiration occurs at low glucose whereas glycolysis is the dominant form of metabolism at high glucose, resulting in decreasing yield that we observe with increasing glucose (Reding-Roman *et al.,* 2017). As growth rate is the product of yield and glucose uptake rate (Beardmore *et al.,* 2011; Reding-Roman *et al.,* 2017) and K is the product of yield and glucose concentration (Reding-Roman *et al.,* 2017), a large decrease in yield at high glucose concentration is linked to decreasing growth rate and saturation in K.

These observations correlate with changes in metabolic gene expression described in the yeasts *S. cerevisiae* and *C. albicans* during the transition from low to high glucose (Yin *et al.,* 2003; Rodaki *et al.,* 2009) as central metabolic genes (TCA cycle) and glycolytic genes were alternatively up-regulated at very low (0.01%) and high (> 0.1%) glucose respectively. This correlates with the switch from respiration to fermentation in the transition from low to high glucose in *S. cerevisiae,* which shares a close evolutionary relation with *C. glabrata* (Postma *et al.,* 1989b; Van Urk *et al.,* 1990; Roetzer *et al.,* 2011). Our work also fits with a recent study that described the ability of *C. glabrata* to grow on glucose concentrations ranging 0.1-20 mg ml^{-1}, due to upregulation of high or low affinity glucose sensors at low or high glucose respectively, indicating its tuned nutrient adaptations (Ng *et al.,* 2015).

Due to incorporation of variable yield into models predicting growth rate and carrying capacity at different glucose concentrations, we observed parabolic relationships between growth rate and K and between growth rate and yield in all five strains of *C. glabrata* (Reding-Roman *et al.,* 2017). At low glucose concentrations, r and K were positively correlated which matches the trend

described by Monod (1949) at resource-limiting concentrations of substrate and correlates with results in *E. coli* (Meyer *et al.,* 2015). Rate and yield were positively correlated at high glucose and negatively correlated at low glucose concentrations (Reding-Roman *et al.,* 2017). Pfeiffer *et al.* (2001) theoretically described a similar parabolic profile in heterotrophic organisms due to thermodynamic and biochemical constraints on the rate of glucose utilisation and yield of ATP production, resulting in a balance between fermentation and respiration (Pfeiffer *et al.,* 2001; MacLean, 2008).

Rate and yield are theoretically predicted to trade off during microbial growth on limited resources (Beardmore *et al.,* 2011) and a trade-off between rate of glucose metabolism and biomass yield has been found in *S. cerevisiae* in a glucose-limited chemostat (Postma *et al.,* 1989b; MacLean, 2008) and across Crabtree-positive yeast species (Merico *et al.,* 2007; MacLean, 2008). Following experimental evolution of rate and yield of ATP production in *E. coli* populations, these two traits were only negatively correlated within but not between populations (Novak *et al.,* 2006). The rate-yield trade-off in microbial cultures has also evolved with environmental spatial structure that provides an advantage for a high yield strategy, otherwise fast growth rate is preferred as resource uptake is faster (Bachmann *et al.,* 2013). We show that rate and yield can trade off between high and low glucose and that this transition in growth kinetics is predicted to occur in seasonal environments that experience temporal changes in resource availability, as described for *S. cerevisiae* (MacLean and Gudelj, 2006).

Previous work has described a positive correlation between rate and yield as a ‘maintenance’ strategy whereby growth rate and biomass yield concurrently decrease under starvation or stressful conditions and energy is allocated for stress protection (Pirt, 1965; Lele and Watve, 2014; Lipson, 2015). This has been seen in experimental evolution of *E. coli* in oscillating environments in which starvation is experienced and led to poor adaptation to nutrient-rich environments (Ying *et al.,* 2015). We observed decreasing rate and yield in *C. glabrata* under high glucose environments and show that a mechanistic model can capture both positive and negative relationships between rate and yield for

a single organism, dependent on a switch from respiration to fermentation (Meyer *et al.,* 2015; Reding-Roman *et al.,* 2017).

In comparison of the rate-K and rate-yield parabolae across *C. glabrata* strains, strain 3605 had a significantly greater average growth rate but lower K and growth yield than the lab reference strain 2001 (Reding-Roman *et al.,* 2017). These results indicate that *C. glabrata* strains show host patient or host site-specific adaptations, particularly as strain 3605 was isolated from a diabetic patient whereas strain 2001 was from the gastrointestinal tract of another patient (**Table A.1.2.S1**). Exposure to higher glucose concentrations (greater than 0.2% w/v typically in diabetics (WHO Committee on Diabetes Mellitus 1980; Gibson *et al.* 1990)) may cause genetic changes resulting in a higher growth rate, perhaps due to increased fermentation associated with low yield (Pfeiffer *et al.,* 2001) or mutations that increase expression of low affinity glucose sensors (Ng *et al.,* 2015). Recently, a study compared growth rates of three different *C. glabrata* strains including ATCC 2001 used in our work (isolated from faeces with up to 0.25% glucose (Karabocuoglu *et al.,* 1994)) and two strains isolated from very low glucose sites (Ng *et al.,* 2016). Whilst the low glucose-adapted strains had higher growth rates than strain 2001 at very low glucose concentration in lab media, there were no significant differences in growth rates at higher glucose. This indicates that strains from different host sites can have different growth adaptations and highlights the need to better characterise *C. glabrata* strains in infections as growth properties may be linked to stress resistance (Ng *et al.,* 2016).

A lower average growth rate and higher carrying capacity (K) and yield of strain 2001 compared with 3605 (Reding-Roman *et al.,* 2017) correlated with higher virulence of strain 2001 in the *G. mellonella* wax moth model. We tested virulence at 30^{o}C as we measured *in vitro* growth kinetics at this temperature, but results support those comparing virulence of the two strains at 37^{o}C (Ames *et al.,* 2017). Growth rate is traditionally described to positively correlate with pathogen fitness and virulence (Anderson and May, 1982), due to debilitation of the host (Perlman, 2008). Alternatively, growth rate can be negatively correlated with virulence in human pathogens (Leggett *et al.,* 2017), which indicates that other pathogen life-history traits, virulence factors or host immunological

response contribute to virulence (Day *et al.,* 2007; Frank and Schmid-Hempel, 2008; Perlman, 2009; Ames *et al.,* 2017). In our experiments, we show that a higher carrying capacity or yield may be responsible for greater virulence.

C. glabrata strain 2001, but not strain 3605, showed significant adaptation to daily caspofungin dosing in three independent 14-day experiments, evidenced by an increase in its IC50 measured across populations evolving on a gradient of caspofungin concentrations, due to greater relative growth of populations evolving at higher caspofungin concentrations. As evolution was performed at intermediate glucose concentration (10 mg ml^{-1}), a greater carrying capacity and yield but lower growth rate of strain 2001, compared with strain 3605, correlated with caspofungin adaptation. During batch cultures, resource concentrations change from high to low (Levin, 1972; Rainey *et al.,* 2000) and we found that at low glucose (1 mg ml^{-1}), strain 2001 had a higher growth rate and higher carrying capacity and yield than strain 3605. This suggests that a higher carrying capacity and yield of strain 2001 facilitated caspofungin adaptation and that strain growth rate and yield likely engage in a trade-off during the seasonal transition to low glucose. Rate-yield trade-offs have influenced community functions (Lipson, 2015) and adaptation to variable environments in nature (Lele and Watve, 2014).

In *S. cerevisiae,* the rate-yield trade-off has been found in chemostat cultures, in which it is possible to manipulate the nutrient dilution rate to control growth rate (Zakrzewska *et al.,* 2011). At lower growth rates, full respiration occurred leading to a higher biomass / ATP yield that provided energy for increased resistance to oxidative, acid and heat stresses. This may explain adaptation to caspofungin, another stress inflicted on the cell, in *C. glabrata* strain 2001 due to conservation of stress responses between these evolutionarily conserved yeasts (Roetzer *et al.,* 2011). A slower growth rate has also been implicated in increased antibiotic tolerance or resistance in bacteria (Gilbert *et al.,* 1990; Claudi *et al.,* 2014), but it is unclear whether this is due to the rate-yield trade-off or counteraction of the mode of drug action.

C. albicans, a solely respiratory yeast, showed up-regulation of genes related to azole antifungal, oxidative and osmotic stress resistance upon exposure to 1%

glucose (same concentration as our work), due to co-regulation of metabolic and stress response pathways (Rodaki *et al.,* 2009). In addition, high glucose concentrations can induce oxidative stress resistance in *C. glabrata,* whereas low glucose concentrations (0.01-0.2%) could promote biofilm formation and amphotericin B stress resistance (Ng *et al.,* 2016). Overall, this highlights that different nutrient levels in host environments affect pathogen growth kinetics and/or metabolic-stress regulatory networks (Brown *et al.,* 2014a) which in turn influence *in vivo* antifungal susceptibility. *In vitro* standardised susceptibility testing is limited, as it does not test susceptibility under a range of physiological conditions that model host environment, immunity and strain-specific growth and virulence in infections (Kanafani and Perfect, 2008).

Across and within independent evolutionary experiments, differences in relative growth occurred between technical replicate populations that adapted to high caspofungin concentrations, particularly at 0.78 µg/ml. This could indicate differences in adaptive mechanisms or their time of acquisition across populations, although there was a significant increase in IC50 across all replicate populations, which suggests parallel evolution of phenotype across independent evolutions (Bailey *et al.,* 2015). Studies of *in vitro* experimental evolution of antifungal resistance are limited and lack dynamic growth kinetic measurement of replicate populations. In 2000, Cowen *et al.* tested parallelism of evolution across six populations of *C. albicans* evolving in the antifungal drug fluconazole at high inhibitory doses that were tuned to double the MIC (Minimum Inhibitory Concentration) of the adapting populations. Variation in MIC changes over time, overexpression of resistance genes and competitive fitness occurred across the populations, which was not seen in media-adapted replicate populations (Cowen *et al.,* 2001). This variation may have been due to the emergence of different resistant mutations in different populations by chance, as population sizes were small (Cowen *et al.,* 2002).

In contrast, evolution of *S. cerevisiae* with stepwise increases in fluconazole across replicate populations showed very similar increases in competitive fitness adaptations across three replicate populations (Anderson *et al.,* 2003; Anderson *et al.,* 2005). Environmental conditions and selection pressure (Lindsey *et al.,* 2013) are likely to be important in determining the parallelism of

evolution (Bailey *et al.,* 2015). The method of antifungal dosing that we employ is similar to that described by Peña-Miller *et al.* (2014), who tested resistance adaptation in the dose-response profile across *E. coli* populations evolving at different concentrations of the bacteriostatic antibiotic erythromycin. Eight replicate populations were evolved at each drug concentration and after five days of transfers, standard error in growth density was present across replicate populations treated with a high drug dose, supporting our results in *C. glabrata.*

4.6 Conclusions of the Chapter

We draw two main conclusions from our results:

1) Growth kinetic parameters varied across *C. glabrata* strains: strain 3605 isolated from a diabetic patient had a higher average growth rate but lower carrying capacity and yield than the lab reference strain 2001.

2) A lower growth rate but higher carrying capacity of strain 2001 compared with strain 3605 was correlated with greater virulence and caspofungin dose response profile adaptation.

In Chapter 5, we further characterise caspofungin adaptations across replicate populations within and between the independent *in vitro* evolution experiments. We test fitness costs in the absence of caspofungin and seek phenotypic and genotypic differences at population and sub-population levels to further test parallelism in evolution.

5. Chapter 5: Fitness Costs and Adaptations in Experimental Evolution of Caspofungin Resistance in *C. glabrata* Strain 2001

5.1 Introduction

In this Chapter, we extend our work from Chapter 4 that identified significant evolution of the caspofungin dose response profile of *C. glabrata* strain 2001. We characterise adaptations of evolved populations from the three independent 14-day evolutionary experiments.

Antibiotic resistance is often associated with fitness costs in different environments, which limit the rate of resistance evolution and type of mutations that can occur (Andersson *et al.,* 2006; Hall *et al.,* 2015). Pathogen fitness is described in terms of growth, virulence or transmission and costs are usually measured by growth rate (Cohen *et al.,* 2003; Andersson *et al.,* 2006) or competition between resistant and susceptible cells (Andersson and Hughes, 2010) in the absence of antibiotic (MacLean *et al.,* 2010). Costs depend on the physiological effects of resistance mechanisms (Andersson *et al.,* 2006), for example mutations in enzymatic targets of drugs can have pleiotropic effects on normal cell functioning and stress resistance, which can prevent resistance mutations from being maintained (Vincent *et al.,* 2013). Costs of resistance measured by growth rate or population density in stationary phase correlate with costs measured by selective effects inferred from competition assays (Hall *et al.,* 2015). Conversely, fitness costs can be absent due to cost-free mutations (Ramadhan and Hegedus, 2005), co-selection of resistance with other traits, or environmental dependency of costs (Andersson *et al.,* 2006; Hall *et al.,* 2015). Costs could also appear absent due to further evolution and compensatory mutations that maintain resistance (Nagaev *et al.,* 2001; Andersson *et al.,* 2006; Nilsson *et al.,* 2006) and virulence (Cohen *et al.,* 2003).

Typically, evolution of antimicrobial resistance is studied in bacteria and selection has occurred with cidal drugs (Blaser *et al.,* 1987) at drug concentrations above the MIC (Minimum Inhibitory Concentration), the lowest

drug concentration required to cause a significant reduction in microbial growth to a specified level (usually 50 or 90% growth inhibition- CLSI, 2008). In particular, administration of a high drug dose which aims to inhibit all pathogens imposes a strong selective pressure for development of resistance (Read *et al.,* 2011). This selective region has been described as the 'Mutant Selection Window' and defines the antimicrobial concentrations between the MIC of wild-type bacteria and the MIC of the most resistant mutant (Drlica, 2003). At these concentrations, high fitness cost mutations are predicted to develop due to the strong drug selection pressure and the high drug concentration that is necessary to maintain a competitive advantage of resistant cells over susceptible cells (Andersson and Hughes, 2014).

Rapid rather than gradual antibacterial or antifungal dose increases and frequent dosing can cause population extinction and limit mutational capacity (Andes *et al.,* 2006; Lindsey *et al.,* 2013), but antifungal resistance mutations have occurred when drug is administered at a constant high dose (Anderson *et al.,* 2003; Vincent *et al.,* 2013). Drug-resistant mutants of *S. cerevisiae* that evolved on agar containing a high dose of fluconazole showed no fitness costs (Anderson *et al.,* 2003), whereas fitness costs occurred in *C. albicans* populations treated with a high dose of amphotericin B in liquid media (Vincent *et al.,* 2013). Fitness costs of resistance mutations occurred in serial clinical isolates from a patient treated with the fungicidal drug caspofungin (Singh-Babak *et al.,* 2012), but the repeatability of resistance mechanisms and associated fitness costs between replicate populations under controlled environmental conditions were not investigated.

Positive selection and the repeatability of evolutionary adaptations can be determined by parallel evolution (Elena and Lenski, 2003; Palmer and Kishony, 2013). Parallel evolution is defined as the same mutations or mutations in conserved gene targets emerging in independent lineages, which suggests positive selection of adaptive changes rather than chance mutations (Palmer and Kishony, 2013). In experimental evolution, parallelism is identified by comparing adaptation across replicate populations that have been founded from the same ancestral genotype and evolved under the same selective conditions

(Elena and Lenski, 2003). Identification of similar phenotypic changes is predicted to underlie genotypic similarities (Bailey *et al.,* 2015).

Parallelism in adaptation has been found across bacterial and fungal replicate populations, but does not always occur. Parallelism across populations has occurred in metabolic genes during experimental evolution in constant nutrient-limited environments, evidenced by conserved growth kinetic changes in *S. cerevisiae* (Ferea *et al.,* 1999) and conserved non-synonymous mutations in *E. coli* (Lenski *et al.,* 1991; Maddamsetti *et al.,* 2017). In experimental evolution of *E. coli,* transient diversity in fitness did occur early in evolution but this was due to the timing and order of mutational acquisition rather than different adaptive pathways (Lenski *et al.,* 1991). Parallelism can occur in the evolution of antibiotic resistance, whereby sequential increases in drug concentration have led to parallel changes in MIC and resistance mutations in *S. cerevisiae* (Anderson *et al.,* 2003; Anderson, 2005) and in *E. coli* (Toprak *et al.,* 2011). Alternatively, diversity in fitness adaptations and mutations across replicate populations has occurred in the evolution of antifungal resistance in *C. albicans*, due to chance mutations in different drug resistance mechanisms (Cowen *et al.,* 2000; 2001) which may have occurred due to smaller population sizes (Anderson *et al.,* 2003).

Fitness adaptations can also vary within populations, characterised by phenotypic and genotypic heterogeneity between sub-population clones, which can evolve over time within infection of a single patient (Mowat *et al.,* 2011) and independently within replicate populations (Herron and Doebeli, 2013). Sub-population heterogeneity is important to characterise because large differences in antibiotic susceptibility can occur between colonies of a patient sample, decreasing the reliability of standardised susceptibility testing for informing treatment options (Mowat *et al.,* 2011). Heterogeneity could be maintained by clonal interference whereby equally beneficial mutations in different sub-populations are selected, or by frequency-dependent interactions facilitated by niche differentiation through metabolic alterations to the environment created by a sub-population (Herron and Doebeli, 2013).

Evolutionary adaptations are typically quantified both phenotypically and genotypically to characterise changes in the selected trait and associated fitness effects (MacLean *et al.,* 2010). During evolution of antibiotic resistance, a standard quantification of changing susceptibility is the MIC (minimum inhibitory concentration) (MacLean *et al.,* 2010) of drug, or similarly the IC (inhibitory concentration) of drug, which can be used to define fungal growth inhibition at a range of different levels (Elefanti *et al.,* 2013). This has commonly been used to track resistance at regular intervals during batch transfers and has detected resistance associated with mutations in fungi (Cowen *et al.,* 2000; Anderson *et al.,* 2003; Vincent *et al.,* 2013) and in bacteria (Toprak *et al.,* 2011). Fitness of mutants under the evolved selection pressure can be tested relative to the ancestor by measuring growth parameters such as length of lag phase, growth rate, final growth density and cell size (Vasi *et al.,* 1994; Lenski *et al.,* 1998; Cowen *et al.,* 2001). Within-population differences in colony morphology can also be measured to characterise population diversity, which may be associated with heterogeneity in drug resistance or virulence (Mowat *et al.,* 2011). Specific DNA targets associated with selected traits can be sequenced (Kugelberg *et al.,* 2005) or the whole genome can be sequenced to identify mutations in unknown targets and obtain a global view of genetic changes associated with antibiotic resistance (Singh-Babak *et al.,* 2012; Toprak *et al.,* 2011; Vincent *et al.,* 2013; Oz *et al.,* 2014).

The evolutionary dynamics of echinocandin resistance evolution between and within populations and associated fitness costs in *Candida glabrata* are poorly understood. Echinocandins, in particular caspofungin, are fungicidal drugs that target the ß-(1,3)-glucan synthase enzyme and prevent synthesis of carbohydrate cross linkages in the cell wall, causing cell lysis (Kartsonis *et al.,* 2003). Mechanisms of caspofungin resistance resulting in elevated MIC values in clinical isolates have been described by drug target alterations due to non-synonymous mutations in the homologous *FKS1* and *FKS2* genes of *C. glabrata.* Mutations in these genes, which encode catalytic subunits of the glucan synthase enzyme, occur in two conserved hotspot regions (Katiyar *et al.,* 2006; Perlin *et al.,* 2007; Katiyar *et al.,* 2012; Domán *et al.,* 2015; Sanglard, 2016). Mutations are most commonly reported in the hotspot 1 region of these genes in clinical isolates (Garcia-Effron *et al.,* 2009; Perlin, 2011; Katiyar *et al.,*

2012; Pham *et al.,* 2014). Mutations in the *FKS1* gene have conferred fitness and virulence costs in *C. albicans* (Ben-Ami *et al.,* 2012). It is unclear whether fitness costs occur from mutations in *FKS1* and *FKS2* genes of *C. glabrata* as one study described no virulence cost of an *FKS2* mutation (Borghi *et al.,* 2014), which conferred a growth kinetic fitness cost in another study (Singh-Babak *et al.,* 2012).

5.2 Aims of the Chapter

In this Chapter, we aim to extend our work from Chapter 4 which identified significant evolution of the caspofungin dose response across replicate populations of *C. glabrata* strain 2001 in three independent 14-day experimental evolutions. This involved daily serial transfers of cell populations at eight different caspofungin concentrations. We focus on characterising differences in growth characteristics across replicate populations, analysing fitness costs and phenotypic and genotypic adaptations. We address three aims:

1) To test whether fitness costs of caspofungin adaptation differ between replicate populations of *C. glabrata* strain 2001 evolved at post-IC50 caspofungin concentrations.

2) To determine whether caspofungin adaptations differ at a sub-population level by characterising colony morphology, virulence and gene targets associated with resistance.

3) To investigate whether population heterogeneity can be independently evolved in separate 14-day caspofungin dose response evolution experiments.

We studied *in vitro* fitness costs of caspofungin resistance by growth profiling in the absence of drug, revived population colonies pre-evolved in different caspofungin concentrations over 14 days (from dose response experiments described in Chapter 4). We chose post-IC50 concentrations as these posed a high selective pressure for adaptation (Read *et al.,* 2011) and high fitness cost mutations may be expected to develop, as described previously for bacteria

(Andersson and Hughes, 2014). Whilst common mechanisms for caspofungin resistance are well described (Sanglard, 2016), parallelism of evolution and sub-population heterogeneity that may determine the predictability and additional mechanisms of caspofungin resistance at the population level, have not been explored. We compared fitness costs between and within evolved replicate populations from independent 14-day caspofungin dose response evolutions described in Chapter 4. We then tested for phenotypic and genotypic heterogeneity and virulence costs at the sub-population level in the independent evolutionary experiments.

5.3 Materials and Methods

5.3.1 Revival of Experimentally-Evolved Populations of *C. glabrata* Strain 2001 from Caspofungin Dosing

In Chapter 4, a single isogenic clone of *C. glabrata* strain 2001 founded 3 replicate populations (technical replicates) at each of 8 different caspofungin concentrations and a media-only growth control. Daily serial transfers into identical medium (1% w/v glucose Synthetic Complete (SC) medium) and drug conditions were performed over 14 days. This experiment was repeated three times independently (biological replicates) over separate 14-day periods. Each daily growth cycle was run in a separate 96-well plate and cultures were frozen daily (-80^{o}C) with glycerol at a final concentration of 15% v/v. To analyse caspofungin adaptations from the first independent experiment, replicate populations evolved at the three highest (post-IC50) caspofungin concentrations (0.78, 1.37 and 2.40 µg/ml) and media-adapted populations were revived from the final day of evolution (end of day 14). From the second and third independent experiments, replicate populations evolved at 0.78 µg/ml and media-adapted populations were revived from day 14. Frozen cells were scraped from the surface of culture wells and streaked on SC 1% w/v glucose agar plates, prior to incubation for 48 hours at 30^{o}C. Single colonies were used to prepare overnight cultures or plates were stored in the fridge until use.

5.3.2 Growth Profiling of Single Colonies in the Absence of Caspofungin

To test for fitness costs in the absence of caspofungin for day-14 populations that had evolved in 0, 1.37 and 2.4 µg/ml of caspofungin in the first 14-day experiment, 2 colonies were selected per revived population. As variation in colony size morphology occurred in revived populations that were evolved at 0.78 µg/ml of caspofungin, 4 single colonies representing different morphologies were selected from each replicate population. Variation in colony size morphology also occurred in replicate population 1 that evolved in 1.37 µg/ml so 3 colonies were selected from this population. From the second and third 14-day experiments, 2 population colonies were selected from each replicate population at 0 and 0.78 µg/ml. Colony size morphology variation was observed at 0.78 µg/ml so a single colony of the two different variants were selected, for comparison to colonies from Experiment 1 (E1). Overnight cultures were prepared from single colonies by inoculation in universal tubes containing SC 1% w/v glucose liquid medium and incubating at 30^{o}C and 180 rpm for 18-24 hours. The *C. glabrata* 2001 wild-type ancestral strain was also revived and an overnight culture was prepared.

Following overnight incubation, a volume of culture from each colony was frozen in a final concentration of 15% v/v glycerol at -80^{o}C. Remaining culture was centrifuged and washed once in 1 x PBS before re-suspending in an equal volume of SC 1% w/v glucose. A single 150 µl aliquot of each colony's culture was added to a well of a 96-well plate and 150 µl of media was added in a separate well. Optical density at 650 nm was read in a Tecan M200 plate reader and growth density of each culture was calculated by subtraction of the media control reading. Dilutions necessary to reach an OD of 0.05 were prepared in SC 1% w/v glucose media (similarly to the methods of Singh-Babak *et al. (*2012)) in Eppendorf tubes and 4 replicate wells of 150 µl of each colony's culture were added to a fresh 96-well plate, alongside the WT ancestor and media-only blank control wells. Cultures were diluted in 1 x PBS and plated on SC 1% glucose agar plates to calculate initial cell concentration, which was approximately 1.5 x 10^{7} cells/ml. Growth profiling was performed in the Tecan plate reader at 30^{o}C and 182 rpm for 24 hours with OD650nm readings taken every 20 minutes. Growth profiling of population colonies from the first 14-day

experiment was repeated in three independent experiments (N = 12 per colony), but in 1 independent experiment (N = 4) for population colonies from the second and third 14-day evolutions.

5.3.3 Data Analysis and Statistics

Data was imported into MATLAB (Matlab, 2012a) to fit the solution of the standard Verhulst logistic growth equation to the data, so that the exponential growth rate could be approximated from the data, similar to analysis described in Roemhild *et al.* (2015). The logistic growth model **(1)** and solution **(2)** used are as described in Reding-Roman *et al.* (2017) and in Chapter 4, with exclusion of the lag phase parameter *L*.

$\frac{dN}{dt}$ = rN(1- N/K); **(1),**

where $\frac{dN}{dt}$ represents population growth rate, r is exponential *per capita* growth rate (1/h), K is carrying capacity (stable optical density in stationary phase) and N represents population size.

$N(t) = ß + \frac{K}{1+q\ X\ e^{-rt}}$; **(2),**

where ß represents estimated optical density reading of the media blank, q is a parameter incorporating the initial population size N(0) and t is time (hrs).

Following model fitting, optical density values of the wells containing cell suspension were blank-corrected by subtracting optical density of the media-only wells. To calculate fitness costs of caspofungin adaptation, relative exponential growth rate and relative final optical density during the 24-hour growth profiles of colonies were compared within and between populations by dividing through fitness values by mean values of the wild-type ancestor, similarly to the methods of Roemhild *et al.* (2015). Relative growth values were presented in box plots and means with standard error bars were overlain to indicate the data spread, as recommended in Krzywinski and Altman (2014), using the R-package “plotrix” (Lemon, 2006). To deduce significant differences in growth parameters across population colonies and the wild-type ancestor,

statistical tests run were one-way ANOVA, Welch's ANOVA and Kruskall-Wallis (as data from some samples was skewed) using R version 3.3.2 (R Core Team, 2016). When differences in growth parameters across groups were detected, all tests produced highly significant p values ($p < 0.001$), so Tukey's *post hoc* test was used to detect significant pairwise differences between population colonies.

5.3.4 Phenotyping of Caspofungin-Evolved Colony Variants

5.3.4.1 Colony Morphology

Replicate populations were revived from frozen stocks and streaked on CHROMagar plates (BD Biosciences, Oxford, UK) to determine different colony sizes and ensure that all colonies were pink indicating that they were *C. glabrata,* rather than any contaminant that had entered the culture. Colony morphologies were also distinguished by dilution plating of colony cultures on SC 1% glucose agar plates.

5.3.4.2 Growth on Different Carbon Substrates

Colonies from populations that were revived for growth profiling (including the wild-type ancestor) were streaked on YPD (Yeast Peptone Dextrose) and YPG (Yeast Peptone Glycerol) agar plates and incubated at 30^{o}C for up to 48 hours, similar to the methods of Singh-Babak *et al.* (2012). Dextrose (glucose) can be respired and fermented whereas glycerol can only be respired.

5.3.4.3 *Galleria mellonella* Survival Assay

G. mellonella wax moth larvae (Live Foods Direct, Sheffield, UK) were injected in the top left proleg with an inoculum size of 2.5×10^6 CFU/larva of one of the following strains: *C. glabrata* strain 2001 WT, population colony P1C1 or P1C2 (day 14 population colonies evolved in 0.78 µg/ml from the first 14-day biological replicate experiment). Each injection group included 20 larvae and another injection group consisted of PBS-injected larvae to control against stress of injection. Larvae were incubated at 30^{o}C in petri dishes containing a

filter paper disc and mortality was recorded daily for 10 days, by recording response to physical stimulation. Data was analysed in R version 3.3.2 (R Core Team, 2016) using the package 'Hmisc' (Harrell Jr *et al.,* 2006) to plot Kaplan-Meier survival plots, calculate mean survival times and compare survival between infection groups using the log-rank test.

5.3.4.4 Dose Response Profiling

We measured the caspofungin dose response profile over a single season for a single media-adapted colony (M1C1), a colony denoted "LCV" (large colony variant) (P1C1) and a colony denoted "SCV" (small colony variant) (P1C2) from the first and third 14-day experiments that showed significant sub-population heterogeneity in fitness costs. Frozen overnight cultures of each colony variant were revived on SC 1% glucose agar and fresh overnight cultures were prepared in SC 1% glucose liquid medium. Dose responses were measured in 96-well plates over single 24-hour periods using the same medium with caspofungin concentrations ranging 0 - 2.40 µg/ml. For colony variants that were resistant to all concentrations up to 2.40 µg/ml, susceptibility to a two-fold dilution series from a maximum caspofungin concentration of 64 µg/ml was tested. The same methods for dose response measurement as described for the initial season of the *in vitro* evolution of caspofungin resistance experiment in Chapter 4, were followed. Dose responses were repeated three times independently and data was pooled, for population colonies from the first 14-day experiment (N = 9 per caspofungin concentration). Dose responses were run once independently for each population colony from the third 14-day experiment (N = 3 per caspofungin concentration). The best-fit 4-parameter logistic dose response was fitted to dose response data from each population colony using the R-package 'drc' (Ritz *et al.*, 2015), as described by Roemhild *et al.* (2015), which was used to estimate the IC50 and slope (gradient) model parameters.

Pilot dose response assays were used to test susceptibility of the remainder of population colonies evolved at 0.78 µg/ml in the three 14-day evolutionary experiments, for which fitness in the absence of caspofungin was tested. For each revived population colony, a single replicate population was tested at each

of eight drug concentrations (0 – 2.4 µg/ml). OD (655nm) was measured after 24 hours incubation with shaking and percentage growth relative to the no-drug treated control was plotted.

5.3.5 Genotyping of Caspofungin Resistance Targets in Single Colonies

Genomic DNA was extracted from the *C. glabrata* strain 2001 wild-type ancestor. From the first and third independent 14-day evolution experiments, DNA was extracted from the following revived day 14 population colonies: a media-adapted colony (M1C1), the LCV (large colony variant; P1C1) and SCV (small colony variant; P1C2). Five gene target regions previously associated with caspofungin resistance were PCR amplified and Sanger sequenced in each strain.

5.3.5.1 Genomic DNA Extraction

DNA was extracted from an overnight culture of each population colony grown in 1% w/v glucose SC medium for 24 hours. To release the DNA, mechanical cell lysis with glass beads was performed, using the protocol of yeast DNA extraction described by Libuda (2007) (**A.4.1**). Briefly, cells were grown overnight, centrifuged and mixed with Smash and Grab Solution, Phenol-Chloroform and acid-washed glass beads. This ensured that the cells were broken open, proteins were precipitated and DNA was purified for subsequent ethanol precipitation, as described previously for DNA extraction from *Candida* strains (Riggsby *et al.,* 1982; Wahyuningsih *et al.,* 2000). The DNA pellet was re-suspended in 1 x TE and was refrigerated for up to a week before use or frozen at -20^{o}C. DNA concentration was quantified with a nanodrop spectrophotometer and bands were visualized by running on a 0.8% w/v agarose gel containing ethidium bromide. DNA concentration of the revived population colonies from the third 14-day evolution ranged 37.5- 68.1 ng/µl.

5.3.5.2 PCR Amplification of Gene Targets and Gel Electrophoresis

PCR primers were ordered from Eurofins Genomics (Ebersburg, Germany). The HS1 and HS2 regions of the *FKS1* and *FKS2* genes were amplified using

primers previously described for *C. glabrata* by Thompson *et al.,* (2008) and Zimbeck *et al.,* (2010) (**Table A.4.1.S1**). The *CDC6* gene was amplified using primers described for *C. glabrata* by Singh-Babak *et al.,* (2012) (**Table A.4.1.S1**). Primer stock solutions were prepared from lyophilised primers by adding appropriate volumes of autoclaved MilliQ water to prepare 100 µM stocks. 20 µM working stock solutions were prepared by further dilution in MilliQ water and were frozen at -20ºC until use. Genomic DNA from each population colony was diluted 1:10 to prepare template DNA for PCR reactions.

Promega instructions for PCRs were followed for 50 µl reaction volumes (Promega, 2014), using GoTaq ® G2 Green Master Mix (Product code: M728A, Madison, USA). All PCR reactions contained the following volumes of reaction components: 25 µl GoTaq, 2 µl of forward primer, 2 µl of reverse primer, 1ul of DNA template and 20 µl of nuclease-free water (Product code: P119A). 2 replicate reactions were run for each gene region of each population colony. The PCR programme was run as follows: initial DNA denaturation- 95ºC for 2 minutes; 35 cycles: denaturation- 94ºC for 30 seconds, annealing- 55ºC (*FKS2* HS1)/ 59ºC (*FKS1* HS1)/ 53ºC (*CDC6, FKS2* HS2)/ 58ºC (*FKS1* HS2) for 45 seconds, extension- 72ºC for 1 minute; final extension- 72ºC for 5 minutes. PCR products were stored in the fridge for up to 1 week before running on a gel.

To check for correct PCR amplification of the gene target regions, 5 µl volumes of PCR product from each population colony and the strain 2001 WT ancestor were run on an 0.8% w/v agarose gel containing ethidium bromide and bands were visualised under UV light. Separate gels were then run with 30 µl of PCR product from each reaction and DNA bands were excised from the gel using a scalpel whilst visualising the bands on a UV transilluminator. Each DNA band was added to a 2 ml screw-cap tube and tubes were weighed before and after to calculate the weight of the gel slice (mg). Gel slices were stored in the fridge before purification. DNA was purified by centrifugation using a silicone minicolumn and membrane binding solution to extract DNA and membrane wash solution to remove the remaining gel product (Wizard SV Gel and PCR Clean-Up- Promega, 2009) (**A.4.1**). As PCR reactions for each gene target of each population colony were run in duplicate, the two dissolved gel slices for

each were combined in a single silicone minicolumn to increase the DNA concentration. Eluted DNA from each minicolumn was quantified with a nanodrop spectrophotometer and DNA was frozen at -20ºC until use.

5.3.5.3 Sanger Sequencing Sample Preparation and Data Analysis

Samples were prepared for Sanger sequencing using the 'Sample Submission Guide for Value Read Tubes' from Eurofins Genomics (Ebersburg, Germany). Premixed samples were prepared in a 17 µl final volume in a 1.5 ml microcentrifuge tube. Purified DNA was diluted in nuclease-free water to a final concentration of 5 ng/µl in 15 µl volume. The final 2 µl volume consisted of either 10uM of the forward or reverse primer of the PCR-amplified gene target. The same primers were used for sequencing as for the PCR reactions. The *FKS1* and *FKS2* hotspot 1 and 2 gene targets were sequenced in both the forward and reverse directions and the *CDC6* gene was just sequenced in the forward direction.

Samples were sent to Eurofins Genomics (Ebersburg, Germany) for sequencing and DNA sequence data was analysed by nucleotide and amino acid sequence alignment against the *C. glabrata* strain ATCC 2001/ CBS138 reference genome (Gene target GenBank accession numbers: *FKS1*- XM_446406, *FKS2*- XM_448401, *CDC6*- XM_448250; Dujon *et al.,* 2004; Garcia-Effron *et al.,* 2009), using MEGA (Molecular Evolutionary Genetics Analysis) software (MEGA7: Kumar *et al.,* 2016).

5.4 Results

5.4.1 Fitness Costs of Caspofungin Adaptation Between and Within Evolved Replicate Populations of *C. glabrata* Strain 2001 in Experiment 1

We observed a significant shift in the caspofungin IC50 (50% inhibitory concentration) of strain 2001 between days 1 and 14 in Experiment 1 of 14-day evolution of populations on a caspofungin gradient (**Figure 4.8**). As growth increased from negligible to detectable levels across replicate populations at

post-IC50 concentrations (**Figure 4.8),** we tested for fitness costs of resistance by growth profiling in the absence of caspofungin. When reviving day 14 populations, we observed morphological variation within populations (individual colonies), particularly for 0.78 µg/ml-evolved populations. During a single season, we saw no significant difference in relative intrinsic growth rate across colonies from the three replicate populations evolved in media alone or in 2.4 µg/ml of caspofungin, and the wild-type ancestor (**Figure 5.1**; left panels; **Table A.4.2.S1**).

In contrast, highly significant growth rate differences across colonies both within and between populations occurred for 0.78 and 1.37 µg/ml evolved populations (**Figure 5.1**; left panels; **Table A.4.2.S1**). For 0.78 µg/ml, significant sub-population differences only occurred in replicate population 1 and colonies 2- 4 were significantly different from the ancestor (**Table A.4.2.S2**). P1C2 had a significantly lower growth rate than all other colonies from the three populations, so we denoted this colony as a "small colony variant" (SCV) (**Figure 5.1**). We denoted P1C1 evolved at 0.78 µg/ml as a "large colony variant", due to lack of significant deviation in growth rate from the wild-type ancestor. For 1.37 µg/ml, significant sub-population differences were only found in replicate population 2 (**Table A.4.2.S2**). Colony 2 in this population was significantly different from the ancestor. Smaller differences in growth rate occurred between colonies for 1.37 µg/ml than for 0.78 µg/ml evolved populations and no population colonies were significantly different from all others across 1.37 µg/ml evolved populations.

We compared the final growth density reached in stationary phase (OD (24 hours)) across day 14 population colonies previously evolved at 0, 0.78, 1.37 and 2.40 µg/ml caspofungin. We found no significant differences in OD (optical density) at 24 hours between colonies evolved in 0.00 and 2.40 µg/ml caspofungin, but we did find significant differences across replicate populations evolved at 0.78 and 1.37 µg/ml and within population differences at 0.78 µg/ml only (**Figure 5.1**; right panels; **Table A.4.2.S1**; **Table A.4.2.S2**). For 0.78 µg/ml, colony P1C2 had a significantly higher growth density than P1C4 but was not significantly different from all other population colonies and the ancestor.

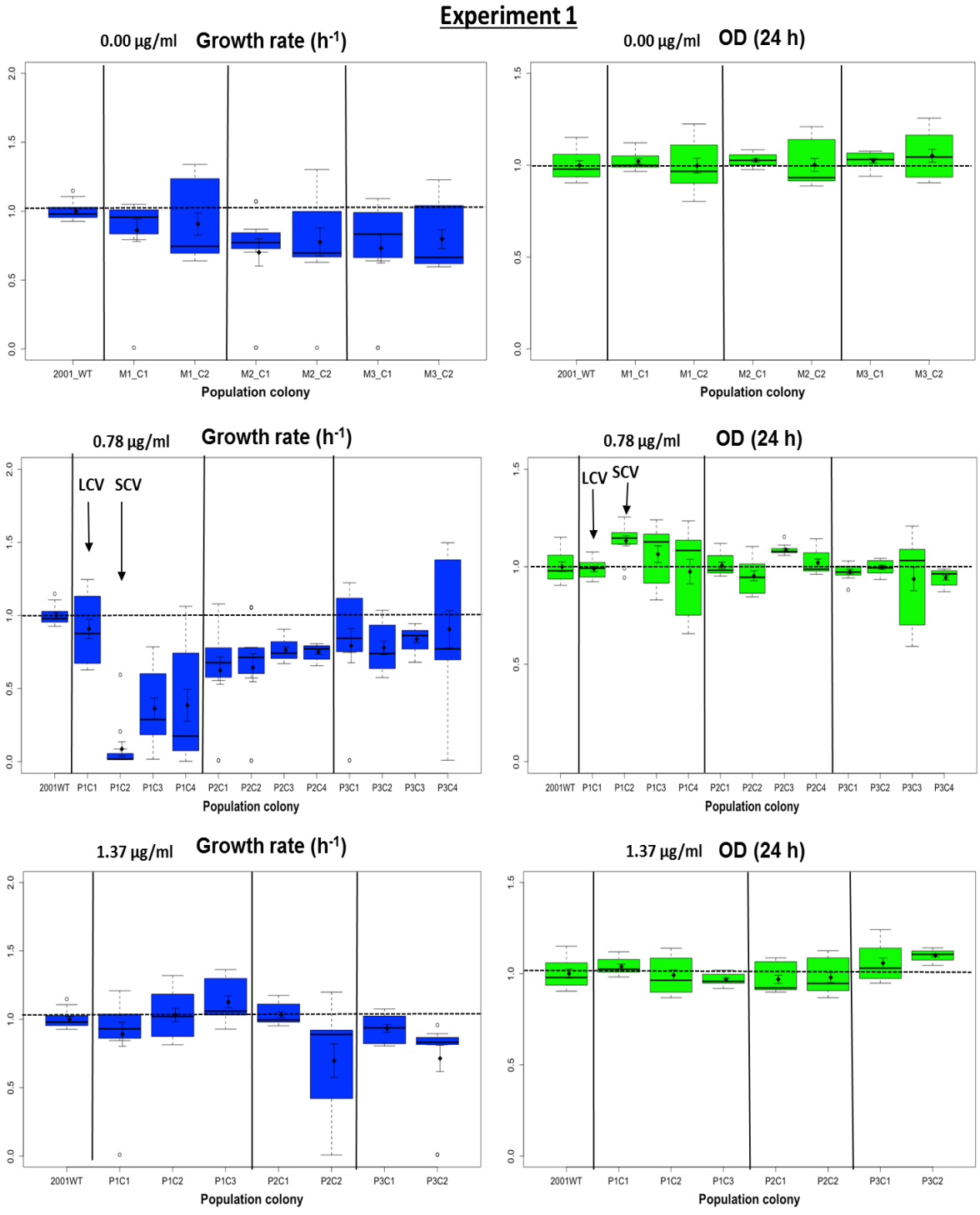

Figure 5.1. Fitness costs of caspofungin adaptation in individual colonies of parallel-evolved populations of *C. glabrata* strain 2001 in Experiment 1 (E1) of the 14-day evolution. Growth kinetic measurements are shown for colonies revived from day 14 from each of three populations (separated by vertical lines) previously evolved in media alone (0.00 µg/ml), 0.78 µg/ml, 1.37 µg/ml or 2.40 µg/ml of caspofungin. Colony growth kinetics were measured in the same medium (SC 1% w/v glucose) in

the absence of caspofungin over 24 hours. Relative growth values presented were calculated by dividing through by average values of the WT ancestor (2001WT), similar to Roemhild *et al.* (2015; Fig. S4). Relative growth values of 1 (shown by dotted line) indicate no change from WT. Growth assays were performed three times independently and data pooled from all experiments is presented (N = 12 per colony measurement). Boxplots show the median value as a horizontal line, 1st and 3rd quartiles as box limits, whiskers marking 1.5 x interquartile range in both directions and empty plotted points as outliers. Black points and error bars overlaying each box represent mean and standard error. Left panels show growth rate (1/h) which is the logistic parameter r (exponential growth rate). Growth rate: $P < 0.0001$ between colonies evolved in 0.78 and 1.37 µg/ml (Kruskal-Wallis/ One-way ANOVA tests); $P > 0.05$ between colonies evolved in 0.00 and 2.40 µg/ml (Kruskal-Wallis test). Right panels show OD (optical density) reached at 24 hours: $P < 0.001$ between colonies evolved in 0.78 and 1.37 µg/ml; $P > 0.05$ between colonies evolved in 0.00 and 2.40 µg/ml. P1C1 in 0.78 µg/ml is denoted as LCV ("large colony variant") and P1C2 in 0.78 µg/ml is denoted as SCV ("small colony variant").

5.4.2 Phenotyping of Sub-Population Colony Diversity in a Single Caspofungin-Evolved Replicate Population in Experiment 1

To further phenotypically characterise sub-population diversity, we selected colonies P1C1 and P1C2 from replicate population 1 evolved at 0.78 µg/ml, as P1C1 had a significantly lower relative growth rate than all other population colonies but growth rate of P1C2 was not significantly different from the ancestor (**Figure 5.1**; left panels). The growth profile of P1C2 was flatter (**Figure 5.2a.2**) and appeared to reach an early plateau followed by further growth such that final density was similar to that of P1C1 (**Figure 5.2a.1**). We denoted colony P1C2 as a "small colony variant" (SCV) as it formed much smaller colonies on agar than P1C1- a "large colony variant" (LCV). This difference in colony morphology was observed for growth on the carbon substrates glucose (YPD plates: **Figure 5.2b.2**) and glycerol (YPG plates: **Figure 5.2b.1**), the latter being a non-fermentable carbon source so colony growth indicated respiratory function. Colony morphology of the large colony variant was similar to that of the wild-type ancestor. Reviving a sample of the

entire replicate population on CHROMagar clearly demonstrated the sub-population diversity in colony size (**Figure 5.2c**). All colonies were pale-dark pink indicating that all colonies were *C. glabrata* rather than bacterial or fungal contaminants. We also identified these differences in colony size in the same population revived from day 7, the mid-point of the evolutionary experiment. To determine the stability of the small colony phenotype, we serially passaged three replicate populations of the day 14 revived SCV in the same medium over 14 days in the absence of caspofungin and found that the phenotype was entirely preserved.

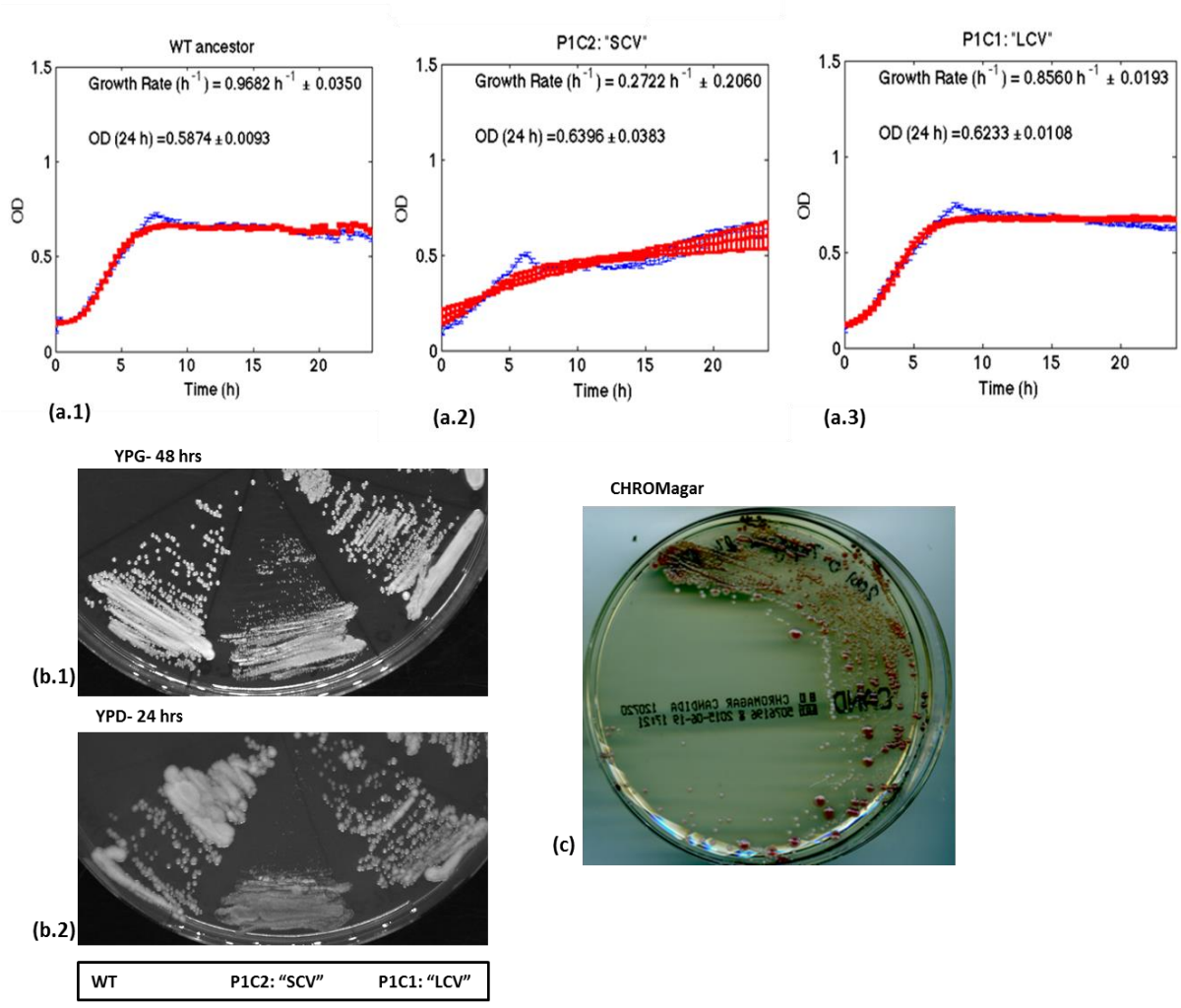

Figure 5.2. Growth profiling, substrate usage and colony morphology of individual colonies revived from a single 0.78 µg/ml caspofungin-adapted population of *C. glabrata* strain 2001. Growth assays and phenotyping are shown for colonies P1C1 and P1C2 revived from population 1 at day 14 that had been evolved in 0.78 µg/ml caspofungin (**Figure 5.1), in comparison to the strain 2001 wild-type (WT) ancestor.** Data are from 1 biological replicate of the revived colony variants. **(a.1-3)** show growth profiles measured by OD (optical density) over 24 hours in the same

media (1% w/v glucose SC) in the absence of caspofungin. Growth was measured across 4 replicate cultures from each colony and the blue profile shows the means and standard error bars. The red profiles show mean predicted OD values from a best fit logistic growth model with standard errors shown. *Per capita* growth rate (1/h) is calculated from the logistic model fit and final growth density (OD) is also reported. **(b.1)** and **(b.2)** show growth on YPG (Yeast Peptone Glycerol) and YPD (Yeast Peptone Dextrose) respectively, for the *C. glabrata* strain 2001 wild-type (WT) ancestor, P1C2 and P1C1 (left to right). Colony growth was slower on YPG than YPD so plates were incubated for 48 hours and 24 hours respectively. Colony size of P1C2 was much smaller than that of P1C1 so the colonies were denoted "SCV" (small colony variant) and "LCV" (large colony variant) respectively. **(c)** Population 1 evolved at 0.78 µg/ml over 14 days (containing P1C1 and P1C2) was revived by streaking on CHROMagar and white/pink colonies indicate *C. glabrata.* Larger, darker pink colonies are the "LCV" and smaller, paler colonies are the "SCV".

We then compared the virulence of an intermediate dose of the wild-type ancestor, small and large colony variant in the wax moth larval model *Galleria mellonella* to determine whether the caspofungin-adapted colonies with different growth rates showed fitness costs. Using an inoculum dose of 2.5×10^6 CFU/larva, we found no significant difference in virulence between the three strains when larvae were incubated at 30^{o}C (**Figure 5.3**), the same temperature to which the colonies were adapted during the 14-day evolution experiment.

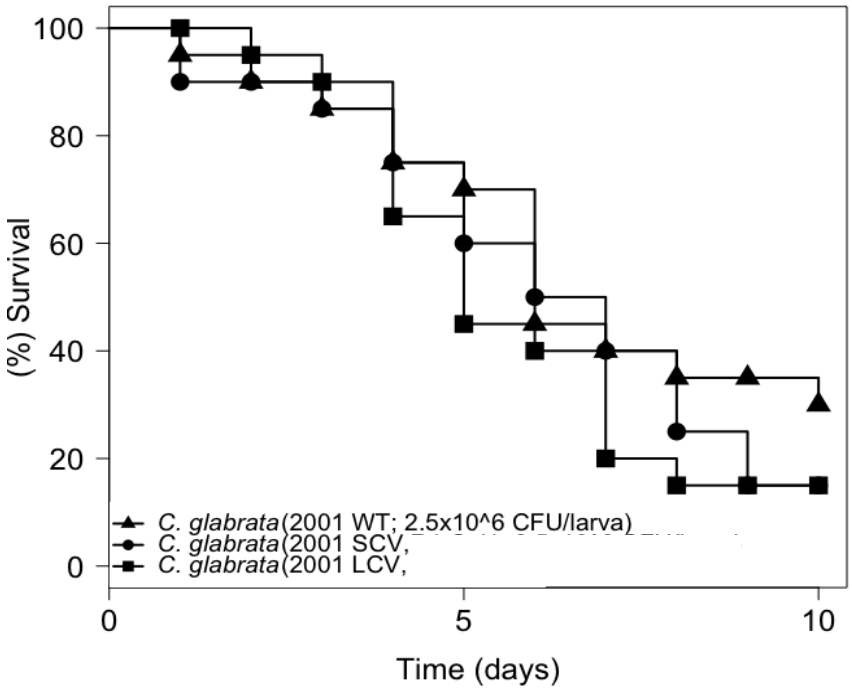

Figure 5.3. Comparative survival of Galleria mellonella with injection of *C. glabrata* strain 2001 WT and 0.78 µg/ml caspofungin-evolved colonies. Groups of 20 *G. mellonella* wax moth larvae were injected with 2.5 x 10^6 CFU/larva of either the WT ancestor of strain 2001, the SCV (P1C2) or the LCV (P1C1) (as denoted in **Figure 5.2**). Data is from 1 biological replicate. Larvae were incubated at 30^{o}C and mortality was recorded daily for 10 days. Log-rank test compared survival across the 3 groups; *P* = 0.4365. Mean survival times (days): 2001 WT = 6.70 +/- 0.66; SCV = 6.30 +/- 0.62; LCV = 5.85 +/- 0.52.

5.4.3 Independent Evolution of Fitness Costs and Adaptations within Populations in Experiments 2 and 3 of the 14-Day Caspofungin Evolution

To identify whether sub-population diversity could be independently-evolved, we measured growth kinetics of day 14 colonies evolved in 0.78 µg/ml caspofungin in Experiment 2 of the 14-day experiment described in Chapter 4, completed over a separate 14-day period. We found significant differences in growth rate (**Figure 5.4**; left panels; **Table A.4.2.S3**) and final optical density (**Figure 5.4**; right panels; **Table A.4.2.S3**) between replicate populations in media-adapted and in 0.78 µg/ml-adapted populations, although no significant sub-population diversity occurred, apart from differences in final optical density

between colonies in the second media-adapted population. We, therefore, did not find small and large colony variants co-isolated in any replicate population.

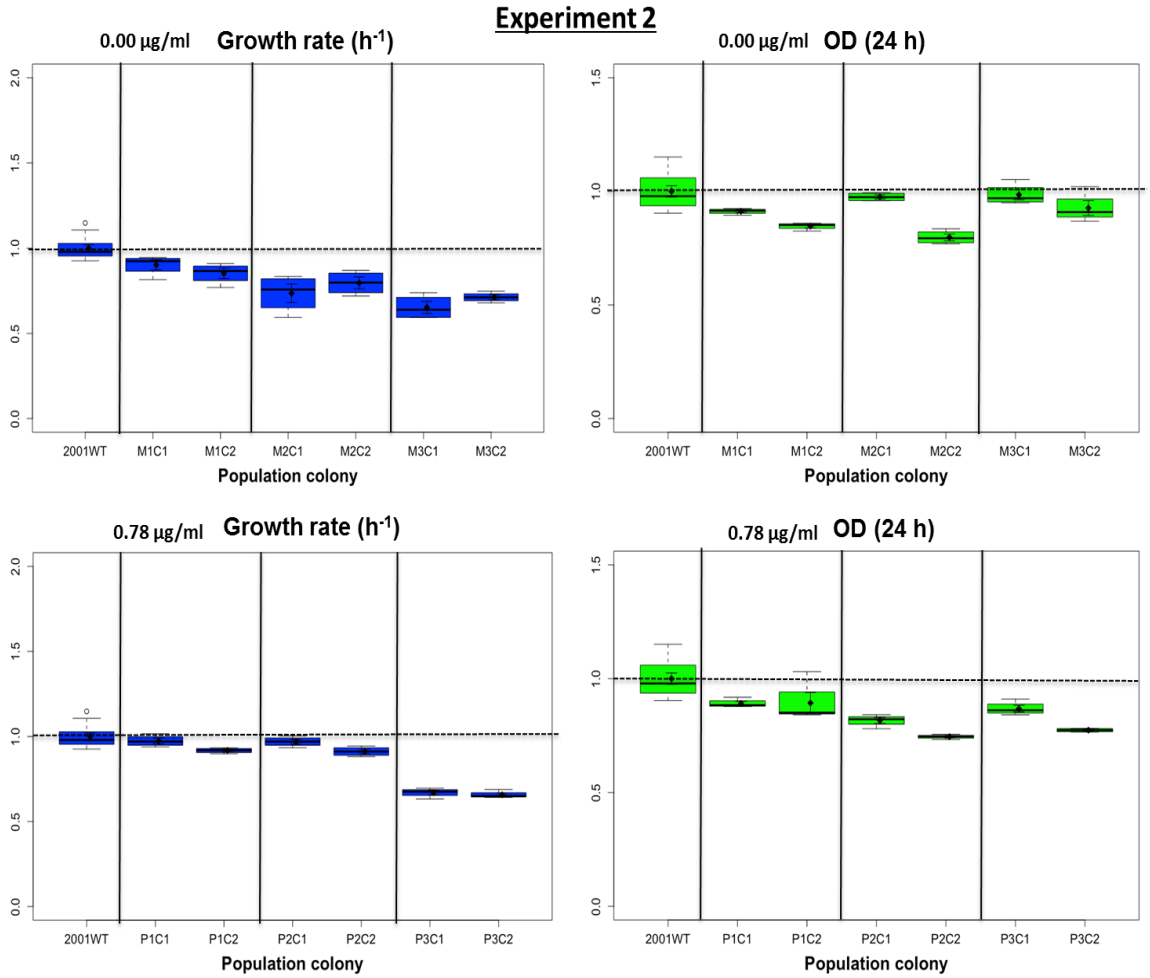

Figure 5.4. Fitness costs of caspofungin adaptation in colonies of day 14 populations of *C. glabrata* strain 2001 from Experiment 2 (E2) of the 14-day evolution. Growth measurements are shown for colonies revived from day 14 from each of three populations (separated by vertical lines) previously evolved in media alone (0.00 µg/ml) or 0.78 µg/ml caspofungin. Growth kinetics were measured in the same medium (SC 1% w/v glucose) in the absence of caspofungin for 24 hours. Relative growth values presented were calculated by dividing through by average values of the WT ancestor (2001WT), similar to data presentation in Roemhild *et al.* (2015; Fig. S4). Relative growth values of 1 (shown by dotted line) indicate no change from WT. Growth assays were performed in one experiment and N = 4 per colony measurement, except for the WT ancestor for which N = 12 (same dataset used for relative fitness calculation as for first evolution experiment). Boxplots show the median value as a horizontal line, 1st and 3rd quartiles as box limits, whiskers marking 1.5 x interquartile range in both directions and empty plotted points as outliers. Black points and error bars overlaying each box represent mean and standard error. Left panels

show intrinsic growth rate (1/h): 0.00 µg/ml- One-way ANOVA ($F_{6, 29}$ = 19.61, *P* = 5.27e-09); 0.78 µg/ml- One-way ANOVA ($F_{6, 29}$ = 45.11, *P* = 2.08e-13). OD (right panels): 0.00 µg/ml- Kruskal-Wallis chi-squared = 23.634, df = 6, *P* = 0.0006098; One-way ANOVA: $F_{6, 29}$ = 8.033, *P* = 3.68e-05; 0.78 ug/ml- Kruskal-Wallis chi-squared = 29.68, df = 6, *P* = 4.521e-05; One-way ANOVA: $F_{6, 29}$ = 13.14, *P* = 3.84e-07. Small and large colonies were not co-isolated in any of the three populations evolved at 0.78 µg/ml.

We then measured growth kinetics of day 14 colonies evolved in 0.78 µg/ml caspofungin from Experiment 3 (E3) of the 14-day evolution. We found highly significant differences in relative growth rate between replicate populations evolved in 0.78 µg/ml and in media-adapted replicate populations (**Figure 5.5(a)**; left panels; **Table A.4.2.S4**). A slightly significant within population difference was seen for the first media-adapted population but not in the other two populations. For 0.78 µg/ml, significant sub-population differences in growth rate were observed in all 3 replicate populations but were most significant in population 1, showing that sub-population heterogeneity similar to that observed in the biological replicate 1 experiment could be evolved in an independent 14-day period. P1C2 had a significantly lower growth rate than all other population colonies, including the ancestor so we denoted it as a “small colony variant” (SCV). P1C1 from the same population did not have a significantly different growth rate from the wild-type ancestor so was denoted as a “large colony variant” (LCV).

Relative OD at 24 hours was not significantly different across media-evolved populations but significant differences were found across 0.78 µg/ml-evolved populations and within the first replicate population (**Figure 5.5(b)**; right panels; **Table A.4.2.S4**). Colony P1C1 had a significantly lower, and colony P1C2 had a significantly greater, relative final OD than the wild-type ancestor. Differences in colony growth rates were supported by the much smaller colony size for P1C2 than P1C1 that we observed on 1% w/v glucose SC agar (**Figure 5.5(b)**). The growth profiles of the two colony variants demonstrated maximisation of either growth rate (P1C1) or total growth density (P1C2) (**Figure 5.5(c)**). We, however, did not find sub-population differences in colony size in the same population revived from days 3, 5 or 7 of the evolution of dose response

experiment. To test the stability of the small colony phenotype, we serially passaged three replicate populations of the day 14 revived SCV in the same medium over 14 days in the absence of caspofungin. We found reversion back to the wild-type colony size for some colonies in one replicate population after six days, with complete reversion in all populations by the end of the experiment (day 14).

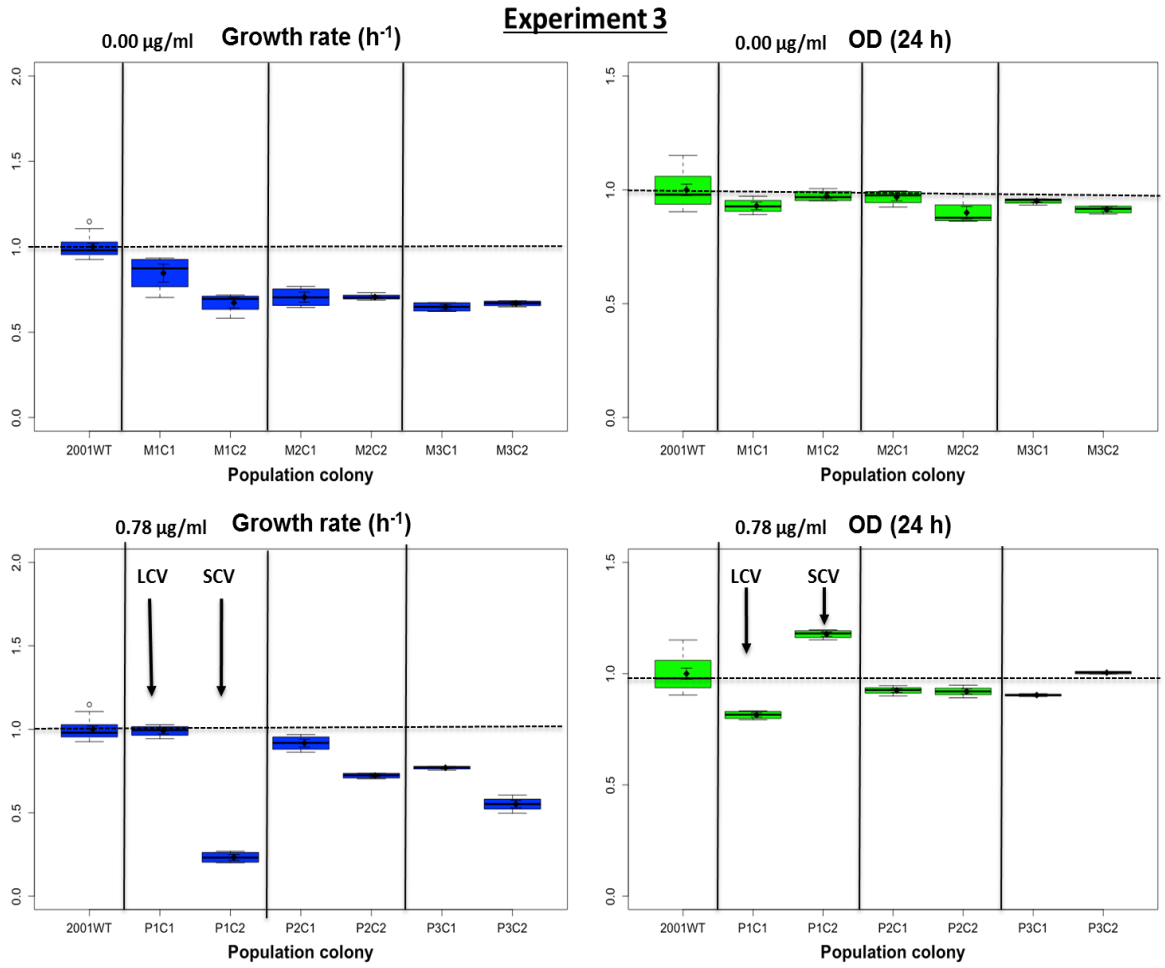

(a)

(b)

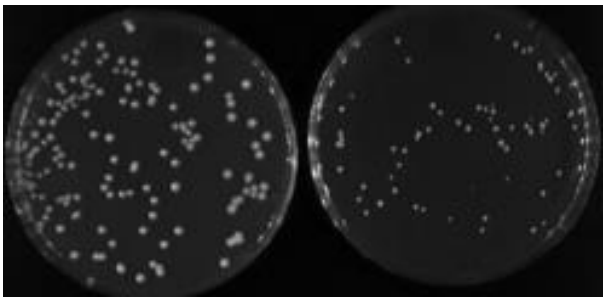

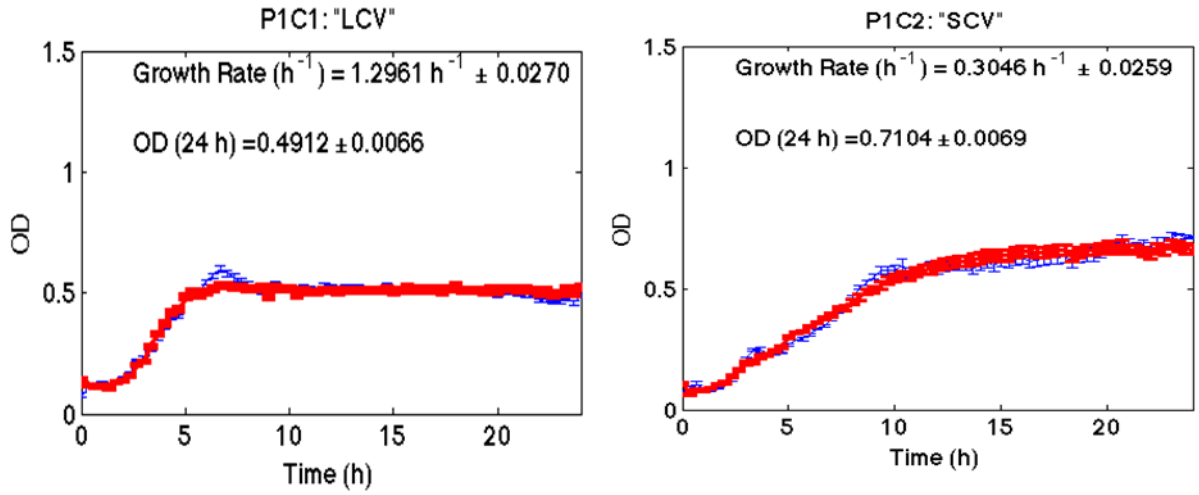

(c)

Figure 5.5. Fitness costs and caspofungin adaptations in colonies of day 14 populations of *C. glabrata* strain 2001 evolved at 0.00 or 0.78 µg/ml from Experiment 3 (E3) of the 14-day evolution. (a) Growth measurements are shown for 2 colonies revived from day 14 from each of three populations (separated by vertical lines) previously evolved in media alone (0.00 µg/ml) or 0.78 µg/ml caspofungin. Growth was measured in the same medium (SC 1% w/v glucose) in the absence of caspofungin for 24 hours. Relative growth values were calculated by dividing through by average values of the WT ancestor (2001WT), similar to data presentation in Roemhild *et al.* (2015; Fig. S4). Relative growth values of 1 (shown by dotted line) indicate no change from WT. Growth assays were performed in one experiment and N = 4 per colony measurement, except for the WT ancestor for which N = 12 (same dataset used as for first evolution experiment). Boxplots show the median value as a horizontal line, 1st and 3rd quartiles as box limits, whiskers marking 1.5 x interquartile range in both directions and empty plotted points as outliers. Black points and error bars overlaying each box represent mean and standard error. Left panels show exponential growth rate (1/h). Right panels show final optical density reached after 24 hours of growth. Growth rate: 0.00 µg/ml- One-way ANOVA ($F_{6, 29}$ = 33.8, P = 8.11e-12); 0.78 µg/ml- One-way ANOVA ($F_{6, 29}$ = 146.3, P < 2e-16). OD: 0.00 µg/ml- Kruskal-Wallis chi-squared = 12.293, df = 6, P = 0.05575; 0.78 µg/ml- Kruskal-Wallis chi-squared = 27.764, df = 6, P = 0.0001041; Welch's ANOVA (unequal variances): $F_{6.00, 10.33}$ = 167.12, P = 1.127e-09; One-way ANOVA: $F_{6, 29}$ = 17.91, P = 1.46e-08. The "small colony variant" (SCV) and "large colony variant" (LCV) identified at 0.78 µg/ml caspofungin are labelled. **(b)** SC 1% w/v glucose agar plates showing colony size of P1C1 (left) and P1C2 (right), two population colonies from day 14 of evolution in 0.78 µg/ml caspofungin. **(c)** Growth profiles for colonies P1C1 (LCV; left) and P1C2 (SCV; right) evolved at 0.78 µg/ml. Growth profile is shown by the blue line representing the

mean of 4 technical replicates with standard error bars. The red line represents the mean predicted optical density values from the logistic growth model fit, with standard errors.

5.4.4 Characterising Caspofungin Susceptibility of Small and Large Colony Variants in Independent 14-Day Caspofungin Evolution Experiments

We identified the presence of a “small colony variant” (SCV) and “large colony variant” (LCV) within a single replicate population evolved for 14 days in 0.78 µg/ml caspofungin in Experiments 1 (**Figures 5.1-3**) and 3 (**Figure 5.5**). We then measured the caspofungin dose response profiles of a single media-adapted population colony, the SCV and LCV from these two independent 14-day experiments.

In Experiment 1, we found that the large colony variant had significantly lower IC50 – IC95 values than the wild-type ancestor (**Figure 5.6(b); Figure A.4.2.S1; S3; Table A.4.2.S5**), although the dose response profiles of the large colony variant and media-adapted strain were highly overlapping (**Figure 5.6(a)**). The large colony variant was more sensitive than the wild-type ancestor to caspofungin concentrations between 0.26 and 0.78 µg/ml. This is despite its isolation from a population that had been evolved in 0.78 µg/ml caspofungin for 14 days. The gradient of inhibition was not significantly different between the large colony variant and wild type and the profiles of the large colony variant and media-adapted colony showed high similarity (**Figure 5.6(a)** and (**b)**).

Importantly, the small colony variant was not inhibited by any caspofungin concentrations used in the dose response for the other colonies (0-2.40 µg/ml) (**Figure 5.6(c)**), with relative growth remaining approximately constant across all caspofungin concentrations, but with variation across technical replicates. To find the inhibitory concentration of caspofungin, we tested a much larger range of caspofungin concentrations up to 64 µg/ml, as described previously (Wiederhold, 2009) and found that the small colony variant had an IC50 of 2.61 +/- 0.136 µg/ml, approximately 10-fold greater than the large colony variant co-

isolated from the same evolved population (**Figure 5.6(d)**). We found that the resistance level was preserved in three replicate populations of the day 14 revived SCV after 14 days of serial propagation in identical medium in the absence of caspofungin, by measuring the sensitivity of a single colony from each population after day 14 (IC50 values: 2.40 +/- 0.146 µg/ml, 2.33 +/- 0.678 µg/ml and 2.70 +/- 0.480 µg/ml).

We conducted pilot dose response assays to test the caspofungin susceptibility of the other colony variants that were revived from populations evolved at 0.78 µg/ml in Experiment 1 (**Figure 5.1**). The IC50 of all revived population colonies apart from E1 P1C4 fell between 0.78 and 1.37 µg/ml (**Figure A.4.2.S5(a)**). This was greater than the IC50s of the wild-type ancestor, media-adapted and LCV strains from Experiment 1 but much lower than the IC50 of the SCV strain in Experiment 1(**Figure 5.6**). The IC50 of colony E1 P1C4 was around 2 µg/ml, which was greater than that of all other strains except the SCV. This was associated with a significantly lower growth rate than the other population colonies apart from the SCV and E1 P1C3 (**Table A.4.2.S2**).

Experiment 1

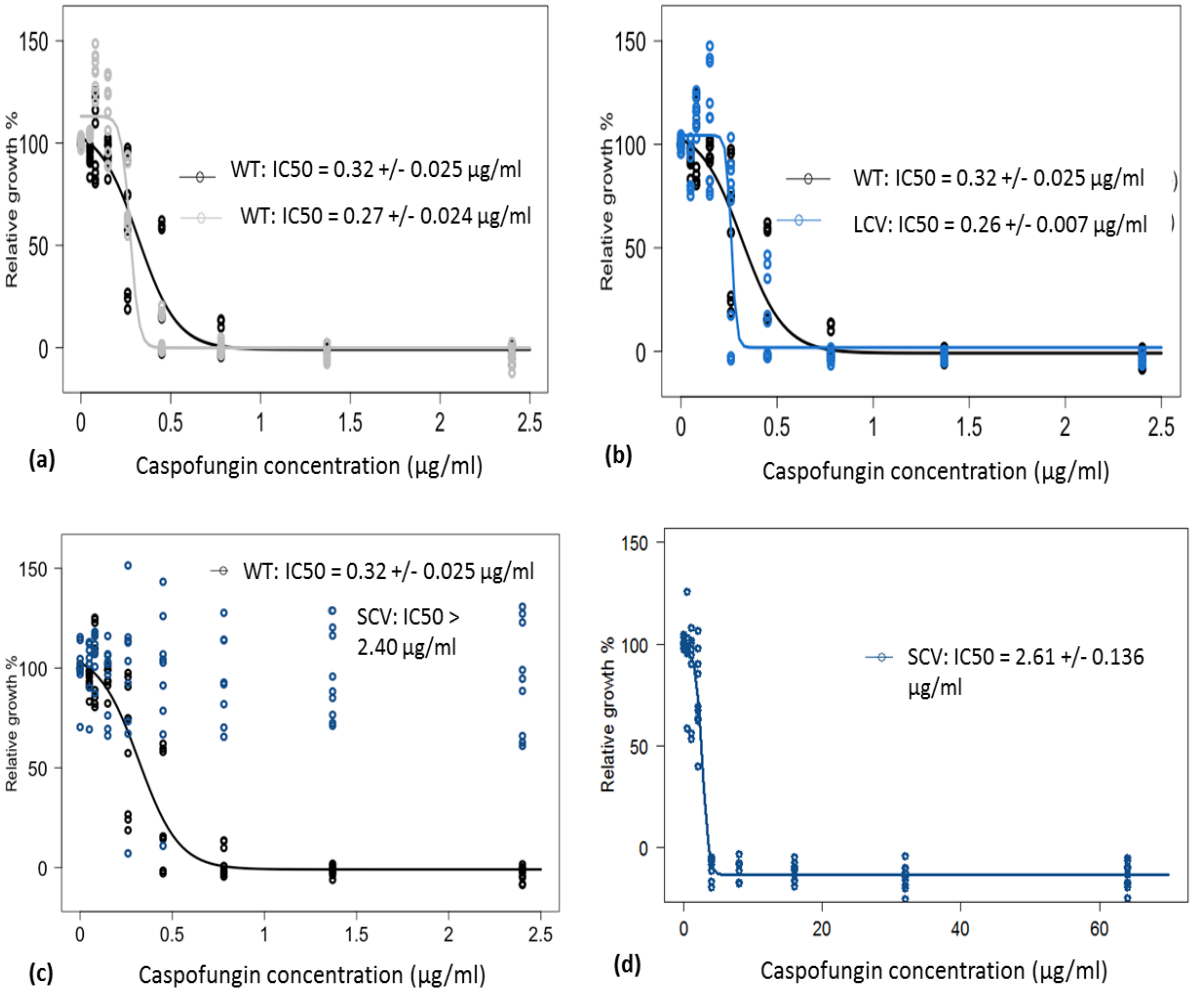

Figure 5.6. Dose response profiles for *C. glabrata* strain 2001 WT ancestor and colony variants from day 14 of Experiment 1 of the 14-day evolution of caspofungin resistance. Dose responses show relative growth % which is measured from final optical density (24 hours) from technical replicates grown at 8 different caspofungin concentrations, divided through by the mean OD of media-alone grown cells. Four parameter logistic dose response curves were fitted to data in each plot using the R package "drc" (Ritz *et al.*, 2015), as described by Roemhild *et al.* (2015) and fits were used to predict the IC50: 50% growth inhibitory concentration of caspofungin presented on the plots (with SE of the estimated value) for each strain. **(a), (b), (c):** WT dose response is plotted from data pooled from day 1 of the three independent 14-day caspofungin evolution experiments described in Chapter 4 (N = 9 for each caspofungin concentration). Data for the other colony variants represents pooled data from three 24-hour dose responses performed on separate days (N = 9 for each caspofungin concentration). **(a)** WT dose response compared with M1C1 (MA)- a single media-adapted colony. **(b)** WT compared with LCV (large colony variant); comparison of IC50: $P = 0.0454$; comparison of slope: $P = 0.6558$. **(c)** WT compared with SCV (small colony variant). No model fit is shown for SCV as none of the

caspofungin concentrations tested were inhibitory. **(d)** Dose response for the SCV at a higher range of caspofungin concentrations: 2-fold dilutions ranging 0 – 64 µg/ml. The 4-parameter logistic dose response model was fitted to estimate IC50.

In pilot dose response assays for revived colonies from populations evolved at 0.78 µg/ml in Experiment 2 (**Figure 5.4**), the IC50s of all colonies were between 0.78 and 1.37 µg/ml, with no population colonies showing high level resistance (**Figure A.4.2.S5(b)**). The IC50 was greater than 1 µg/ml for all colonies apart from E2 P1C1. This lower IC50 of E2 P1C1 was correlated with a significantly higher growth rate in the absence of caspofungin than colonies E2 P3C1 and E2 P3C2 (**Table A.4.2.S3**), although the relationship between IC50 and growth rate would need to be verified over a larger number of population colonies. No population colonies showed as large of a reduction in growth rate as occurred with the highly resistant SCV in Experiment 1.

In Experiment 3, we found no significant difference between the IC50 or slope of the dose response between the wild-type and media-adapted colonies (**Figure 5.7(a); Table A.4.2.S6**), but the media-adapted colony had significantly lower IC65- IC95 values than the wild type and was more sensitive to caspofungin concentrations between 0.26 and 0.78 µg/ml (**Figure A.4.2.S2; S3**). The large colony variant showed a significant increase in its IC50 compared with the wild-type ancestor (**Figure 5.7(b)**) however the gradient of inhibition was not significantly different as relative growth of the large colony variant was still negligible at the highest two concentrations. The estimated IC50 of the large colony variant was 0.83 µg/ml, which was 2.6-fold greater than that of the wild-type ancestor and exceeded the dose of 0.78 µg/ml to which the population was evolved over 14 days. The large colony variant had significantly greater IC5 - IC60 values compared with the wild type and was less sensitive to caspofungin concentrations between 0.05 - 0.78 µg/ml (**Figure A.4.2.S2; S3**). Importantly, the small colony variant was not sensitive to caspofungin concentrations ranging 0- 2.40 µg/ml, and relative growth remained at approximately 100% (**Figure 5.7(c)**). Over a larger range of caspofungin concentrations, we found that the IC50 of the small colony variant was 4.71 +/- 0.236 µg/ml, which was 5.7-fold greater than the large colony variant co-isolated from the same evolved population (**Figure 5.7(d)**).

We conducted pilot dose response assays to test the caspofungin susceptibility of the other colony variants that were revived from populations evolved at 0.78 µg/ml in Experiment 3 (**Figure 5.5(a)**). The IC50s of all population colonies were between 0.78 and 1.37 µg/ml, showing decreased caspofungin susceptibility compared with the wild-type ancestor and media-adapted strain but lower level resistance than the SCV strain in Experiment 3 which had a very low growth rate (**Figure 5.7**). Colony E3 P2C1 had an IC50 below 1 µg/ml which was lower than the IC50s of the other colonies tested in this pilot experiment (**Figure A.4.2.S5(c)**). The IC50 of E3 P2C1 was similar to that of the E3 LCV and these two colonies had significantly greater relative growth rates in the absence of caspofungin than all other colonies (**Table A.4.2.S4**), indicating a link between decreased caspofungin susceptibility and a lower growth rate.

Experiment 3

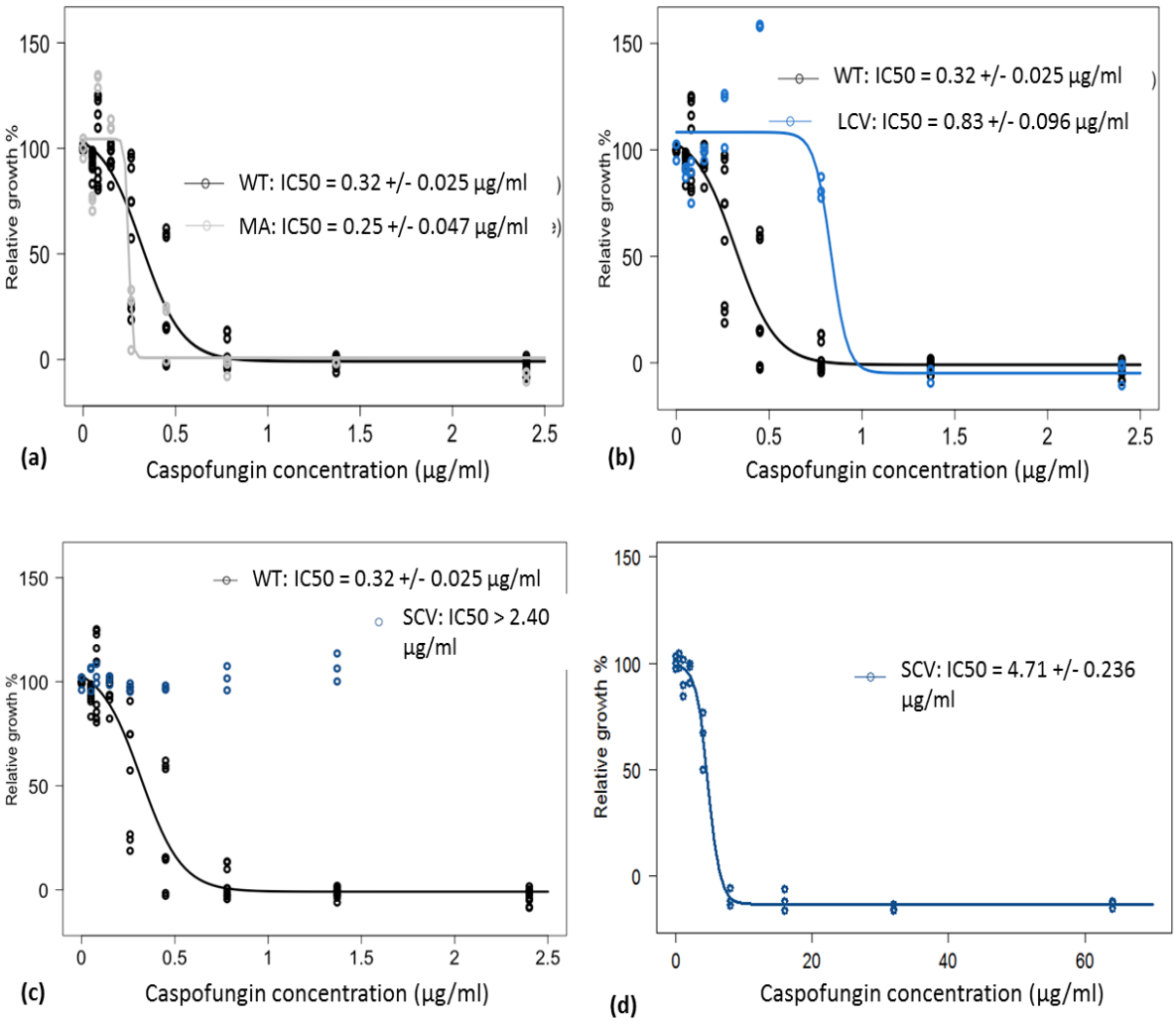

Figure 5.7. Dose response profiles for *C. glabrata* strain 2001 WT ancestor and colony variants from day 14 of Experiment 3 of the 14-day evolution of caspofungin resistance. Dose responses show relative growth % which is measured from final optical density (24 hours) from technical replicates grown at 8 different caspofungin concentrations, divided through by the mean OD of media-alone grown cells. Four parameter logistic dose response curves were fitted to data in each plot using the R package "drc" (Ritz *et al.*, 2015), as described by Roemhild *et al.* (2015) and fits were used to predict the IC50: 50% growth inhibitory concentration of caspofungin presented on the plots (with SE of the estimated value) for each strain. **(a), (b), (c):** WT dose response is plotted from data pooled from day 1 of the three independent 14-day caspofungin evolution experiments described in Chapter 4 (N = 9 for each caspofungin concentration). Data for the other colony variants in all plots represent single 24-hour dose responses performed on separate days (N = 3 for each caspofungin concentration). **(a)** WT dose response compared with M1C1 (MA)- a single media-adapted colony; comparison of IC50: *P* = 0.1940; comparison of slope: 0.7932. **(b)** WT compared with LCV (large colony variant); comparison of IC50: *P* =

0.0011; comparison of slope: *P* = 0.8536. **(c)** WT compared with SCV (small colony variant). No model fit is shown for SCV as none of the caspofungin concentrations tested were inhibitory. **(d)** Dose response for the SCV at a higher range of caspofungin concentrations: 2-fold dilutions ranging 0 – 64 µg/ml. The 4-parameter logistic dose response model was fitted to estimate IC50.

Three replicate populations of the revived SCV from day 14 of Experiment 3 were serially propagated in identical medium but in the absence of caspofungin over 14 days to test the stability of resistance. At the end of the experiment, we found that the highly caspofungin resistant phenotype was lost in all populations **(Figure A.4.2.S4),** consistent with reversion to the wild-type colony size described earlier. By measuring the dose response of a single colony from each population, we found that the IC50 values were significantly greater than the wild-type ancestor in two populations (0.49 +/- 0.023 µg/ml **(Figure A.4.2.S4a)** and 0.44 +/- 0.019 µg/ml **(Figure A.4.2.S4b))** but not in the third population (0.34 +/- 0.055 µg/ml **(Figure A.4.2.S4c)).** The gradient of inhibition (slope) was not significantly different from the wild-type in any of the three populations.

5.4.5 Genetic Characterisation of Common Caspofungin Resistance Targets in Small and Large Colony Variants

To determine genetic mechanisms for differences in caspofungin susceptibility between the small and large colony variants isolated from biological replicates 1 and 3 of the 14-day evolution experiment, we amplified and Sanger-sequenced common gene targets associated with caspofungin resistance (**Figure 5.8**) (Thompson *et al.,* 2008; Singh-Babak *et al.,* 2012). We extracted genomic DNA from the wild-type *C. glabrata* strain 2001 ancestor, media-adapted, small and large colony variants and amplified the desired gene targets, shown by gel electrophoresis of PCR products (**Figure 5.8(a)**). We found no nucleotide or amino acid changes in the hotspot 1 region of the homologous genes *FKS1* and *FKS2* (**Figure 5.8(b),(c)**) in any of the strains from the first and third biological replicate caspofungin dose response experiments, in comparison with the reference genome (Dujon *et al.,* 2004) (**Figure 5.8(d)**). No mutations occurred in hotspot 2 of *FKS1* or *FKS2,* resulting in homologous amino acid sequences

in all strains, consisting of '1340-DWVRRYTL-1348' (Garcia-Effron *et al.,* 2009) for *FKS1* and '1374-DWIRRYTL-1381' (Perlin, 2015) for *FKS2.* We also found no nucleotide changes in *CDC6*, a gene that is involved in DNA replication in which mutation has previously caused a small resistance increase (Singh-Babak *et al.,* 2012).

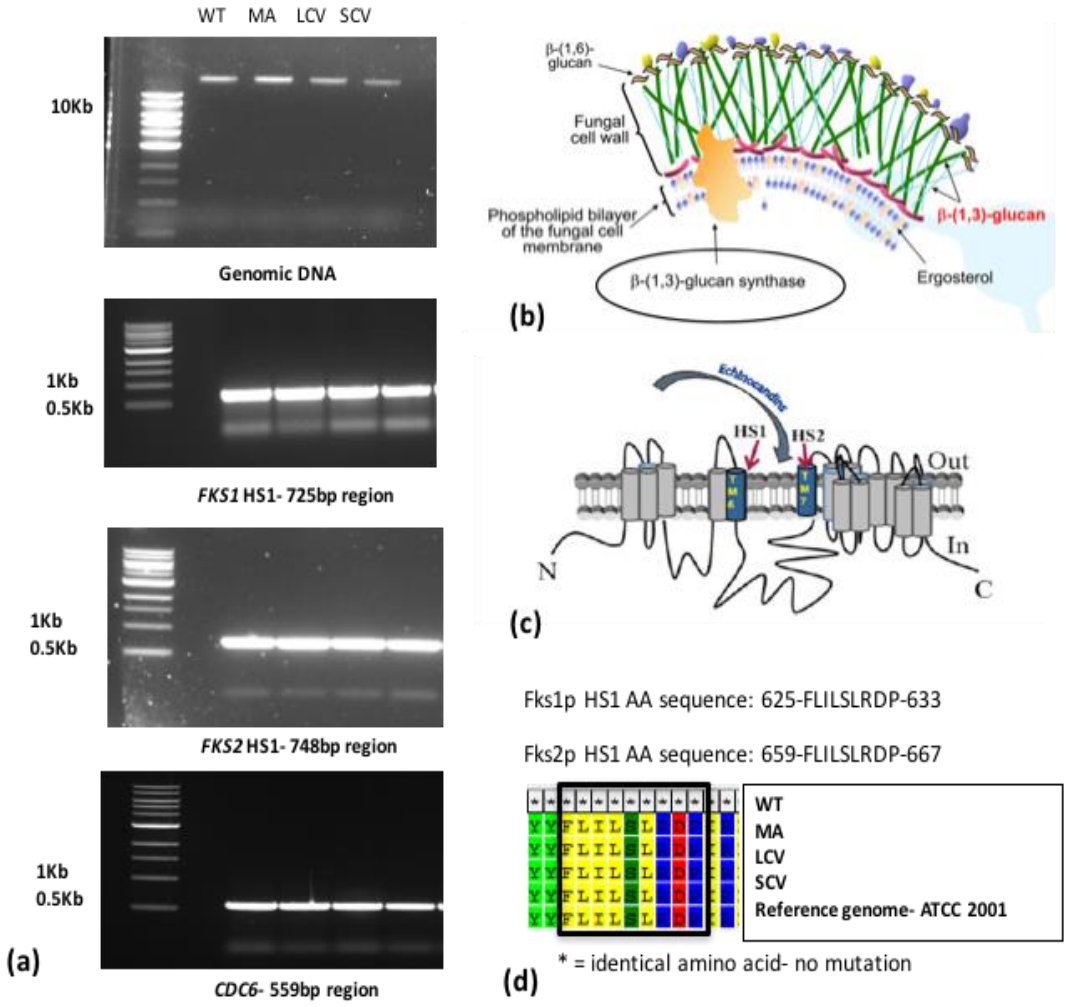

Figure 5.8. Genomic DNA extraction, PCR amplification and Sanger sequencing of caspofungin resistance gene targets in colony variants of *C. glabrata* strain 2001. Qualitative results of gene target amplifications shown for a single media-adapted colony (MA), LCV (large colony variant) and SCV (small colony variant) revived from the 0.78 µg/ml caspofungin-evolved population at day 14 in Experiment 1. Gene target amplifications of the wild-type ancestor (WT) are also shown. Results were identical for single MA, LCV and SCV colonies revived from the 0.78 µg/ml caspofungin-evolved population at day 14 in the third experimental evolution. **(a)** Genomic DNA was extracted from colony variants and amplification of 3 gene target regions are shown: *FKS1* HS1, *FKS2* HS1 and *CDC6,* using primers previously

described for *C. glabrata* (**Table A.4.1.S1**). High intensity bands indicate amplified product. **(b)** Figure adapted from Kartsonis *et al.* (2003). Diagram of fungal cell wall showing caspofungin enzymatic target β-(1,3)-glucan synthase, which is prevented from synthesising β-(1,3)-glucan cross-linkages in the cell wall. **(c)** Figure taken from Perlin (2015). Diagram of transmembrane structure of glucan synthase enzyme in the fungal cell wall and location of channels containing the hotspot target regions (HS1 and HS2) that are commonly mutated with caspofungin resistance. **(d)** Alignment of hotspot 1 (HS1) sequence of amino acids coded from the *FKS1* and *FKS2* genes of the ATCC 2001 reference strain, SCV and LCV, MA (media-adapted) and WT (wild-type) ancestor. The amplified HS1 region of the *FKS* genes contains a homologous sequence of amino acids previously described as a common target for caspofungin resistance mutations (Garcia-Effron *et al.,* 2009). Purified DNA was Sanger sequenced and nucleotide and amino acid sequences were aligned using MEGA software (Kumar *et al.,* 2016). No nucleotide or amino acid changes were detected.

5.5 Discussion

Antibiotic resistance can evolve under different dosing regimens (Palmer and Kishony, 2013) and is quantified both phenotypically and genotypically (MacLean *et al.,* 2010), with mutations often conferring fitness costs (Andersson *et al.,* 2006). The dynamics of resistance evolution across parallel populations are often quantified in bacteria (Toprak *et al.,* 2011; Lindsey *et al.,* 2013; Palmer and Kishony, 2013), but the evolutionary development of mechanisms and phenotypic effects of antifungal resistance across and within parallel fungal populations are not well understood. It is important to investigate the parallelism of antifungal resistance evolution to determine positive selection of resistance determinants (Elena and Lenski, 2003) at the individual and population level. We take the first steps to investigate parallelism of antifungal adaptation, by measuring fitness costs and phenotypic adaptations to the antifungal caspofungin across population colonies of the *C. glabrata* wild-type strain 2001 at post-IC50 caspofungin concentrations. We identified differences in fitness costs across and within parallel populations in independent evolutionary experiments and found sub-population diversity in colony phenotype in the absence of commonly mutated caspofungin resistance targets. Our results contribute to understanding the phenotypic effects and repeatability of caspofungin adaptation under controlled conditions and offer insight into a potentially novel mechanism of population-level antifungal resistance in *C. glabrata.*

We found that growth kinetic fitness costs of caspofungin adaptation varied between replicate populations evolved at the post-IC50 concentration of 0.78 µg/ml, in the three biological replicates of 14-day evolution. In experimental evolution of fluconazole resistance in *C. albicans,* differences in growth rates and stationary cell densities were found across drug-evolved replicate populations due to mutations in different gene targets, highlighting chance selection of different resistance mechanisms (Cowen *et al.,* 2000; 2001; 2002). This may be relevant to caspofungin resistance adaptations as different mutations in the *FKS* genes, encoding the catalytic subunits of the glucan synthase enzyme for cell wall synthesis (Garcia-Effron *et al.,* 2009), result in

different caspofungin susceptibility levels (Arendrup and Perlin, 2014) and may or may not result in fitness costs from reduced catalytic efficiency (Garcia-Effron *et al.,* 2009; Borghi *et al.,* 2014). The fitness costs are likely to be associated with positive selection of resistance mechanisms during caspofungin treatment, rather than genetic drift in small populations (Elena and Lenski, 2003), due to the cidal rather than static mode of drug action (Kartsonis *et al.,* 2003) and lack of fitness cost variation across control media-evolved populations in biological replicate 1 (**Figure 5.1**).

Across independent population colonies of *C. glabrata* strain 2001 that were evolved at 0.78 µg/ml for 14 days, higher resistance levels with IC50 values greater than 2.4 µg/ml were associated with larger significant growth rate fitness costs in the absence of caspofungin. Subsequent serial transfers in media in the absence of caspofungin supported the co-maintenance of high level resistance with a low growth rate. In contrast, smaller increases in IC50 were associated with smaller or negligible growth rate fitness costs. These results are consistent with a negative relationship between resistance level and fitness in the evolution of antibiotic resistance in bacteria. In clinical isolates of *P. aeruginosa,* low level resistance determined by MIC conferred a negligible growth rate cost whereas high level resistance always conferred fitness costs (Kugelberg *et al.,* 2005). A similar relationship was described in a meta-analysis of antibiotic resistance mutations against a range of different antibiotics (Melnyk *et al.,* 2015) and could be explained by trade-offs in energy investment between large-effect resistance mutations and other cellular processes.

Alternatively, larger fitness costs could be caused by higher level resistance resulting from multiple mutations that pleiotropically disrupt normal cell physiology (Kugelberg *et al.,* 2005; Melnyk *et al.,* 2015). Differences in resistance levels between caspofungin-evolved fungal population colonies could be due to different evolved mutations, as described for *FKS* genes for which susceptibility level is dependent on the amino acid substitution (Arendrup and Perlin, 2014). Alternatively, epistatic interactions between multiple mutations (Anderson, 2005) in single evolved colonies could be responsible for between-colony fitness cost differences.

At 2.4 µg/ml, we observed no fitness costs across replicate populations, which contrasts with the theory that fitness costs are greater at higher drug concentrations (Andersson and Hughes, 2014). As we did not collect data on the resistance level of revived population colonies that were evolved at 2.4 µg/ml, we cannot conclude whether the lack of fitness costs signified rapid resistance evolution followed by compensatory adaptation, or phenotypic persistence. Resistance may have evolved faster due to greater selective pressure, as described previously for high fungicide doses (Mikaberidze *et al.,* 2017). This could have allowed more time for compensatory mutations that mitigate fitness costs to have occurred, as described in bacteria (Andersson *et al.,* 2006) and fungi (Singh-Babak *et al.,* 2012). Alternatively, colonies that survived at 2.4 µg/ml could have been phenotypic persisters that were able to tolerate drug treatment but did not have detectable resistance, as described in bacterial (Keren *et al.,* 2004; Lewis, 2007; Day, 2013) and fungal infections (LaFleur *et al.,* 2006).

We found significant sub-population heterogeneity in fitness costs in a single technical replicate population, in two out of three independent 14-day evolutionary experiments in 0.78 µg/ml. This suggests positive selection of heterogeneity as a population-level mechanism of caspofungin resistance. This supports the parallel evolution of metabolic population heterogeneity in experimental populations of *E. coli* (Herron and Doebeli, 2013), whereby populations were dimorphic in colony size and in preferential growth on glucose or acetate (Friesen *et al.,* 2004). Sub-population diversity can be maintained by clonal interference whereby beneficial mutations in different population clones are co-selected (Herron and Doebeli, 2013). Studying sub-population diversity has clinical relevance because dynamic within-strain phenotypic and genotypic heterogeneity occurs in patient samples over time, for example during lung infection with *Pseudomonas aeruginosa* (Mowat *et al.,* 2011). It is necessary to characterise multiple population clones to fully understand antibiotic resistance development and to optimally design treatments.

We found that population heterogeneity in growth rate fitness costs was associated with differences in colony size but similar abilities to utilise different

carbon substrates. The colony with the lowest relative growth rate had a much smaller size (“small colony variant”) compared with another population colony with no significant reduction in growth rate compared with the ancestral strain (“large colony variant”). This supports previous description of spontaneous emergence of the petite phenotype- significantly smaller colonies on agar- in haploid and diploid forms of the yeast *S. cerevisiae* due to deletion of part of the mitochondrial genome that results in respiratory deficiency (Bernardi, 1979). This reduced colony size and impaired oxidative phosphorylation associated with slower growth rate is also found in bacteria and can result in persistent and recurrent infections, in *Staphylococcus aureus* (Proctor *et al.,* 1995; Singh *et al.,* 2009) and a range of other bacterial species (Proctor *et al.,* 2006). As the small colony phenotype leads to increased survival and is caused by a similar physiological mechanism in both prokaryotes and eukaryotes, it is likely that it is an evolutionary adaptation to environmental change (Day, 2013).

Previous studies have described *in vivo* selection of petite mutants in *C. glabrata* isolates from patients undergoing azole (Bouchara *et al.,* 2000) or echinocandin therapy (Singh-Babak *et al.,* 2012). Interestingly, both large and small colonies were found in patient samples and the small colony was unable to grow on the nonfermentable carbon source glycerol, compared with growth on glucose, indicating respiratory deficiency due to deletion of mitochondrial DNA (Bouchara *et al.,* 2000). These findings contrast with our results, as our “small colony variant” was able to grow on both glucose and glycerol, suggesting respiratory function, therefore another potentially growth-related mutation associated with caspofungin adaptation was likely to be causing the fitness cost. We also found no reduction or an increase in relative growth density in our small compared with large colonies, whereas yeast petites have previously been described to have a lower yield due to increased fermentation (Verduyn, 1991).

In bacterial infections, persister cells are important in stressful environments, for example under drug pressure, and are characterised as slower growers which enter a dormant state that allows tolerance of bacteriocidal treatment and population survival (Keren *et al.,* 2004; Lewis, 2007; Day, 2013). Persisters are solely phenotypic variants and are part of naturally existing phenotypic

heterogeneity in an isogenic population (Balaban *et al.,* 2004), so re-growth results in formation of both large and small colonies. Yeast phenotypic persisters have also been described in biofilms treated with fungicidal agents (LaFleur *et al.,* 2006). This contrasts with our findings in *C. glabrata* as the small colony phenotype was maintained in our single season fitness cost growth assays, and over 14 daily serial transfers in the absence of caspofungin for the small colony from the biological replicate 1 experiment.

We compared virulence of our *C. glabrata* small and large colony variants in the wax moth larval infection model *G. mellonella* and found no significant difference in larval survival between the ancestor or either of the colony variants. This contrasts with studies in *S. cerevisiae* (Weger *et al.,* 2002) and *C. glabrata* (Brun *et al.,* 2005) which described significantly reduced virulence of petite mutants in murine models compared with the parental strains, which was attributed to the slower growth rate of petites (Brun *et al.,* 2005). Small colony variants of *S. aureus* have also shown reduced virulence (Musher *et al.,* 1977). Alternatively, recent work has described that pathogen growth rate is not always positively correlated with virulence and a slower growth may be linked with higher virulence due to consideration of other life history factors (Leggett *et al.,* 2017). We propose that it is growth density rather than growth rate that better predicts virulence as we saw highly significant growth rate differences between our small and large colony variants but non-significant differences in growth density.

As our small and large colony variants were isolated from a caspofungin-evolved population that showed significant adaptation (increase in growth density) during 14 days of experimental evolution, we may have expected that resistance mutations occurred with an associated virulence cost, as was previously seen in murine models with caspofungin-resistant mutants of *C. albicans* (Ben-Ami *et al.,* 2012) and *C. glabrata* (Singh-Babak *et al.,* 2012). Our data supports that of Borghi *et al.* (2014) who found no virulence cost of caspofungin-resistant *FKS2* mutants of *C. glabrata* in *G. mellonella,* which highlights differences between the two model systems or in growth or genetic properties of the resistant strains.

We found that our small colony variants had significantly decreased caspofungin susceptibility compared with the large colony variants isolated from the same population. This supports previous discovery of a sub-population of *C. albicans* or *C. tropicalis* biofilm cells that can tolerate high concentrations of chelating agents that are fungicidal (Harrison *et al.,* 2007). This increases overall population tolerance to fungicide. A sub-population of tolerant cells named as persisters also exists when *C. albicans* biofilms, but not planktonic cultures, are treated with the cidal agents amphotericin B and chlorhexidine (LaFleur *et al.,* 2006). These studies indicate that spatial structure within a biofilm was necessary to generate population heterogeneity, but heterogeneity may have occurred in our experiments as a result of temporal variation in resource and drug concentration in batch cultures, rather than spatial variation (Levin, 1972; Rainey *et al.,* 2000).

One study has described co-isolation of a *C. glabrata* petite mutant alongside a regular size isolate during serial evolution of *C. glabrata* within a patient receiving caspofungin therapy (Singh-Babak *et al.,* 2012). This petite mutant had higher caspofungin resistance and cross-resistance to azoles and amphotericin B than the co-isolate. Whilst the heat shock protein Hsp90 and downstream phosphatase calcineurin were required for *FKS* gene-mediated resistance in the regular size isolate, the petite was resistant to calcineurin inhibitors perhaps due to upregulation of other genes. Importantly, the petite phenotype itself was not intrinsically resistant to caspofungin as artificial generation of petites via ethidium bromide treatment did not confer resistance.

Other studies have described generation of *C. glabrata* petite mutants in *in vitro* (Defontaine *et al.,* 1999; Sanglard *et al.,* 2001) and *in vivo* (Bouchara *et al.,* 2000) selection experiments with azoles. These mutants are azole resistant and can be co-isolated with larger colonies with azole sensitivity equal to the wild type (Bouchara *et al.,* 2000). The petite phenotype was due to deletion of mitochondrial DNA (Defontaine *et al.,* 1999; Bouchara *et al.,* 2000; Sanglard *et al.,* 2001) and petites were intrinsically azole resistant when artificially generated with ethidium bromide in the absence of azole exposure (Sanglard *et al.,* 2001). Petites generated with azole or ethidium bromide treatment showed upregulation of ATP-binding cassette (ABC) transporter *CDR* genes. This

suggests that drug efflux (Sanglard, 2016) is a mechanism of antifungal resistance in petites.

Importantly, we found no mutations in the hotspot 1 and 2 regions of the *FKS1* or *FKS2* genes or in the *CDC6* gene in our co-isolated small and large colony variants from two independent evolutionary experiments. This contrasts with numerous studies that exclusively describe caspofungin resistance as a result of mutations in the homologous *FKS* genes encoding different catalytic subunits of the glucan synthase enzyme, which is the cellular target of caspofungin (Kartsonis *et al.,* 2003; Katiyar *et al.,* 2006; Perlin *et al.,* 2007; Katiyar *et al.,* 2012). Non-synonymous mutations are most commonly described in the hotspot 1 region of these genes in clinically resistant isolates (Garcia-Effron *et al.,* 2009; Perlin, 2011; Katiyar *et al.,* 2012; Pham *et al.,* 2014), encoding a transmembrane channel of the glucan synthase (Perlin, 2015). Mutations are most common in the *FKS2* gene (Katiyar *et al.,* 2012) and the most common amino acid change is from serine to proline at amino acid position 663 (S663P) (Zimbeck *et al.,* 2010). Mutations occur less commonly in hotspot 2 of the *FKS* genes (Garcia-Effron *et al.,* 2009; Perlin, 2011) and are absent in some clinical isolates (Pham *et al.,* 2014).

In addition, mutations in the *CDC6* (Cell Division Cycle) gene following *FKS2* mutation can confer a small caspofungin resistance increase in clinical isolates (Singh-Babak *et al.,* 2012). The Cdc6 protein plays an important role in DNA replication initiation in *S. cerevisiae* by forming pre-replicative complexes (Cocker *et al.,* 1996), but has only been considered a target of caspofungin resistance in one study (Singh-Babak *et al.,* 2012). In total, 8 non-synonymous mutations in previously non-characterised targets, in addition to *FKS2* mutation, were found by whole genome sequencing of the final clinical isolate (regular size isolate) of a patient treated with caspofungin (Singh-Babak *et al.,* 2012). It is likely that other genes will have a role in caspofungin resistance in clinical studies, as large-scale gene deletion assays in *C. glabrata* revealed 28 novel genes involved in caspofungin tolerance. These were related to cell integrity pathways, calcineurin signalling and transcriptional regulation (Schwarzmüller *et al.,* 2014).

Population heterogeneity also exists in antibiotic-treated populations and is described as heteroresistance, whereby subpopulations of bacteria exhibit differences in their antibiotic susceptibility levels (El-Halfawy and Valvano, 2015). Most commonly, bacterial cultures predominantly consist of a susceptible population with a small sub-population of highly resistant cells. This poses a clinical challenge and can result in poorer treatment outcomes, as resistance can go undetected in standardised susceptibility testing of single colonies from patient samples rather than a representative analysis of the whole population by characterising several colonies (Mowat *et al.,* 2011). Mechanisms of heteroresistance could be genetic, epigenetic or nongenetic but are not fully understood (El-Halfawy and Valvano, 2015), therefore it is unclear whether heteroresistance can be maintained through serial passages in the absence of antibiotic. One clinical study described selection of resistant cells and replacement of sensitive cells in a heteroresistant bacterial population treated with antibiotic over time (Hernan *et al.,* 2009). Heteroresistance may be seen as an intermediate stage of resistance for a population transitioning from full susceptibility to full resistance (Superti *et al.,* 2009).

We found in one independent evolutionary experiment that the large colony that was co-isolated with the resistant small colony, when in isolation could not grow in the caspofungin concentration to which it was evolved. This suggests that presence of the small colony variant during the evolutionary experiment maintained the large colony in the population over 14 days. Our data supports previous co-isolation of sensitive and resistant mutants in a bactericidal-evolved population of *E. coli*, whereby sensitive cells could survive at drug concentrations above their MIC and resistant cells were resistant to higher drug concentrations than those to which they were evolved (Lee *et al.,* 2010). The mechanism of population-level resistance was due to chemical communication between resistant and sensitive cells and separate drug resistance mutations in resistant cells that increased overall population survival in antibiotic conditions. Alternatively, heteroresistance in bacterial populations can be maintained by within-population division of labour between optimising growth rate or stress resistance (Wang *et al.,* 2014) or by antibiotic degradation (Medaney *et al.,* 2016). Heteroresistance in *C. glabrata* has occurred *in vivo* during fluconazole treatment and may be responsible for persistent infections, but was not

described for echinocandins (Ben-Ami *et al.,* 2016). Metabolic exchange and cooperation between cells has been described in yeast communities (Campbell *et al.,* 2015; 2016) but studies into the population mechanisms of drug resistance in fungal pathogens have not been completed and require future research.

5.6 Conclusions of the Chapter

We draw three main conclusions from our results:

1) Fitness costs of caspofungin adaptation vary across and within parallel populations of *C. glabrata* evolved at caspofungin post-IC50 concentration, measured by differences in growth rate and final growth density in the absence of caspofungin.

2) Sub-population diversity in fitness costs is associated with differences in colony sizes and caspofungin susceptibility levels, but growth on non-fermentable carbon source and virulence is unaffected.

3) Sub-population heterogeneity can be independently evolved in a separate evolutionary experiment and could be a positively selected population-level mechanism of antifungal resistance.

6. Chapter 6: Discussion

6.1 Thesis Overview

Fungal human pathogens pose a severe threat to human health due to the rise of invasive fungal disease with high mortality in immunocompromised patients and the emergence of drug-resistant species (Brown *et al.,* 2012). Research into the interactions between *Candida* species at different resource levels, the effect of species interactions on host survival with different clinical strains and the influence of pathogen growth strategies on antifungal adaptation have not been studied in detail. This thesis addressed these key topics and the main research findings in each of these areas are presented below. The approach for experimental work involved *in vitro* and *in vivo* studies in microbial ecology and evolution using clinical pathogenic *Candida* species. We used simple, controlled short and long-term batch culture experiments and manipulated the culture medium by using artificial media, varying glucose concentration or applying antifungal treatment through time. Using experimental evolution, we were able to test larger sample sizes to increase replicability of the results, sample evolving populations during the experiment and revive evolved populations for further phenotypic analysis. This expands the applicability of these research tools, commonly used in model bacterial and yeast species (Buckling *et al.,* 2009) to study evolution of mixed-species interactions in clinical infections and evolution of antifungal resistance in *C. glabrata.* This discussion will end with thesis conclusions and perspectives on future research questions raised by the results.

6.2 Competition for Resources in Dual Species *in vitro* and *in vivo* Environments

Mixed fungal species communities commonly exist as commensals in different host body sites and lead to mixed-species infections (Jenkinson and Douglas, 2002). Species of the *Candida* genus are the fourth most common cause of bloodstream infections (Wisplinghoff *et al.,* 2004) and *C. albicans* and *C. glabrata* are often co-isolated (Coco *et al.,* 2008). Competition for resources occurs within microbial communities in the human body (Dethlefsen *et al.,* 2006)

but the influence on ecological dynamics and species interactions in mixed-fungal species infections in clinically-relevant and model host environments remain to be characterised. We aimed to investigate whether resource level influenced the outcome of *in vitro* species competition during short and long-term experiments. We then aimed to characterise species interactions in the invertebrate host model *Galleria mellonella,* which could be incubated at physiological temperatures and injected with precise pathogen inoculum doses (Desalermos *et al.,* 2012).

In Chapter 2, we co-cultured *C. albicans* and *C. glabrata* in a range of different glucose concentrations in batch cultures in clinically-relevant synthetic urine media to mimic urinary tract infections. Similar to previous studies (Nilsson, 2012; Beardmore *et al.* (in prep)), we found that competition outcomes were dependent on resource level. *C. albicans* was fitter at lower resource concentrations and *C. glabrata* was fitter at higher resources, resulting in long-term domination of the respective species, depending on resource concentration. Other *in vitro* dual-*Candida* species competition experiments have found either *C. albicans* domination (Kirkpatrick *et al.,* 2000) or exclusion (Thein *et al.,* 2007; Rossoni *et al.,* 2015) but the effect of different resource concentrations on outcomes was not tested. Similar resource-dependent competition outcomes have been described between *S. cerevisiae* and *Candida utilis* (Postma *et al.,* 1989a). These results may be explained by differing species glucose transporter affinities, or fermentation by *C. glabrata* (Van Urk *et al.,* 1990) resulting in less efficient glucose utilisation (Pfeiffer *et al.,* 2001) at low concentrations. Increased fitness of *C. glabrata* in high glucose is consistent with its frequent isolation from diabetic patients (Fidel *et al.,* 1996).

In Chapter 2, we found that *C. albicans* fitness was negative frequency-dependent. Previous studies in bacteria and fungi have calculated negative frequency dependence in competitor fitness due to genotype selection when rare but disadvantage when common (Haldane and Jayakar, 1963; Turner *et al.,* 1996; Feldgarden *et al.,* 2003; MacLean *et al.,* 2006). When fitness of two competitors is equal, stable co-existence is predicted long-term (Antonovics and Kareiva 1988; Ayala and Campbell, 1974; Rainey *et al.,* 2000; Feldgarden *et al.,* 2003; Vellend, 2010) and has been confirmed experimentally (Turner *et al.,*

1996). We predicted that *C. glabrata* and *C. albicans* would show long-term co-existence at intermediate glucose concentrations for species frequencies at which relative fitness of the two species was equal. Instead, we saw exclusion of *C. albicans* over time. Our results may be due to mutational change, which could have improved glucose utilisation of *C. glabrata* (Brown *et al.,* 1998). We provide one example where negative frequency-dependence cannot be used to predict long-term competition outcomes but we do not claim that this result would be seen for other microbial species or under different environmental conditions. *Candida* species are parts of communities of other microbial species in different host sites, which may modify *Candida* species interactions (Jenkinson and Douglas, 2002; de Muinck *et al.,* 2013).

In Chapter 3, we injected *G. mellonella* larvae with dual *Candida* species inocula of different clinical strains of *C. albicans, C. glabrata* and *C. krusei* and compared larval survival between dual and single species strain infections. This allowed us to deduce species interactions in the context of virulence in a model host. We found species synergism evidenced by increased larval mortality in dual compared with single species infection. Our results were consistent with synergistic pathogenesis and infection burden in dual *Candida* species infection of *in vitro* epithelia (Silva *et al.,* 2011; Alves *et al.,* 2014) and a murine model (Tati *et al.,* 2016), but the effects on host survival were not tested with different clinical strain combinations in previous studies.

Our results from Chapter 3 contrast with antagonistic interactions described in recent dual *Candida* species infection of *G. mellonella,* tested just with lab strains of each species (Rossoni *et al.,* 2015). This may be due to differences in larval source or other lab conditions (Cook and McArther, 2013), resulting in higher virulence of *Candida* species lab strains or decreased larval immunity in our experiments.

Our results from Chapters 2 and 3 show that *C. glabrata* and *C. albicans* form ecological interactions in physiologically-relevant environments and that competition for resources influences species domination or virulence. Our results contribute to understanding mixed-fungal species interactions in

commensal and pathogenic environments, which may help to better predict infection outcomes.

It would be interesting to investigate the population dynamics of dual *Candida* species infection in *G. mellonella* to determine the changes in species fitness underlying the synergistic interactions that we found, for comparison to *in vitro* species fitness described in Chapter 2. We hypothesise that the burden of either *C. albicans, C. glabrata* or both species would be greater during dual than single species infections. It would be interesting to investigate the metabolic or molecular mechanisms determining antagonistic or synergistic responses and whether a mixture of the two types of interactions could occur in infections.

6.3 *C. glabrata* Clinical Strain Variation in Competitive Abilities, Species Interactions and Growth Kinetics

Candida species colonise a range of body sites and host patients which vary in resource levels (Brown *et al.,* 2014). Glucose is the main carbon source needed for growth (Gagiano *et al.,* 2002) and yeast species have developed metabolic adaptations to utilise glucose at different concentrations (Ozcan *et al.,* 1996; Yin *et al.,* 2003). It is unknown how *C. glabrata* clinical strains vary in competitive abilities and growth properties in different resource environments. We aimed to investigate whether *in vitro* competitive abilities and *in vivo* interactions between *C. albicans* and *C. glabrata* varied with *C. glabrata* strain. We also aimed to investigate differences in *C. glabrata* strain growth properties when grown in isolation on glucose.

In Chapter 2, we compared *in vitro* competitive abilities of *C. glabrata* clinical strains by competing them with *C. albicans* over a single season and found that relative fitness quantitatively varied across the strains. This may be caused by genetic differences between strains due to their adaptations to different host environmental niches.

In Chapter 3, we tested different *C. glabrata* clinical strains in dual infection with *C. albicans* in the *G. mellonella* model and found that the strength of synergistic

species interaction was dependent on *C. glabrata* strain. A greater synergistic response was correlated with higher *C. glabrata* strain virulence and a greater host immune response. Our results are consistent with prior literature that described differences in infection burden and tissue colonisation in dual *Candida* species infection of a murine infection model with different strains of *C. glabrata* (Tati *et al.,* 2016). Differences in *C. glabrata* strain virulence have been described in a recent study of *G. mellonella* infection (Ames *et al.,* 2017), but our results show the first experimental test and evidence for variation in host immune response triggered by different *C. glabrata* strains, with greater melanisation of a single strain previously associated with higher pathogen dose and larval mortality (Ames *et al.,* 2017).

In Chapter 4, we compared the growth profiles of *C. glabrata* clinical strains over a range of physiologically-relevant glucose concentrations in simple nutrient media during single-season experiments. We found that growth rate and carrying capacity were positively correlated at low glucose concentrations and negatively correlated at high glucose concentrations (Reding-Roman *et al.,* 2017). Growth rate was maximised at intermediate glucose. Yield (efficiency of biomass production) was a decreasing function of glucose concentration. These trends are consistent with those described in strains of *E. coli* due to a switch from respiration to fermentation at higher glucose concentrations (Reding-Roman *et al.,* 2017). The rate-yield trade-off has also been described in *S. cerevisiae* (Zakrzewska *et al.,* 2011). We found within strain variation in the shape of the growth rate/carrying capacity and growth rate/yield profiles (Reding-Roman *et al.,* 2017). Of the strains we tested, a *C. glabrata* strain isolated from a diabetic patient had the highest average growth rate and lowest carrying capacity and yield, compared with a wild-type lab strain. Our results provide proof of principle that *C. glabrata* strains from different host patient environments exhibit different growth traits, but we do not claim that the diabetic strain that we characterised is representative of all strains isolated from diabetic patients.

Our results from Chapters 2, 3 and 4 highlight the need to consider different species strains when studying mixed-fungal species interactions. Adaptations to different resource levels in host environments can influence strain growth

properties and virulence. Studying strain growth at a range of physiologically-relevant glucose concentrations is important for understanding differences in pathogenesis at different body sites and in diabetic patients with elevated glucose levels (Fidel *et al.,* 1996; Brown *et al.,* 2014a). This could contribute to better characterisation of the virulence of single and dual species fungal infections and to better predict infection outcomes in different environments. It would be interesting to investigate genetic mechanisms underlying the growth and virulence differences of *C. glabrata* strains.

6.4 Influence of Pathogen Growth Strategies on Virulence and Antifungal Adaptation

C. glabrata has shown an epidemiological increase, which is of concern due to its greater than 50% death rate, high resistance to the antifungal fluconazole (Fidel *et al.,* 1999; Gudlaugsson *et al.,* 2003; Pfaller *et al.,* 2012) and multidrug resistance to the major drug classes. We have shown that clinical *C. glabrata* strains vary in their growth properties but it is unknown how differing growth strategies (higher growth rate or carrying capacity) influence virulence and antifungal susceptibility. Antifungal susceptibility testing is often performed under standardised conditions *in vitro,* which do not consider the influence of different host environmental conditions and strain virulence on susceptibility, resulting in clinical treatment failures (Sanglard and Odds, 2002; Anderson, 2005; Kanafani and Perfect, 2008). We aimed to investigate the influence of different strain growth properties on host survival and evolutionary adaptation to the antifungal caspofungin, a first-line therapy drug to which clinical resistance is increasing (Alexander *et al.,* 2013). We aimed to test for growth kinetic fitness costs of caspofungin adaptation and sub-population diversity in phenotypic adaptations.

In Chapter 4, we compared virulence of two strains of *C. glabrata* in the invertebrate model *G. mellonella* and used *in vitro* experimental evolution in simple nutrient media to compare caspofungin adaptation of the two strains across replicate populations. We found that a lower growth rate but higher carrying capacity was correlated with greater virulence and decreased susceptibility to caspofungin over time. Our data supports a study in *S.*

cerevisiae in which lower growth rates were correlated with higher resistance to host-imposed stresses due to greater energy investment in stress protection than growth (Zakrzewska *et al.,* 2011). Our data also supports recent evidence that pathogen growth rate is not necessarily positively correlated with virulence, due to conflicting factors such as other pathogen strategies that aid evasion of host immunity or maximise pathogen fitness (Leggett *et al.,* 2017). It also supports the principle that a slower growth rate renders pathogens more resistant to drug treatment (Gilbert *et al.,* 1990; Claudi *et al.,* 2014).

In contrast, our data is inconsistent with studies that describe pathogen growth rate as a fitness measure determining virulence (Anderson and May, 1982; Perlman, 2009). We do not claim that a lower growth rate is necessarily linked to greater virulence, rather that the balance between growth rate and carrying capacity is associated with virulence. We found that a higher carrying capacity is correlated with greater virulence but we do not claim direct causation.

In Chapter 5, we tested for fitness costs and adaptations to caspofungin treatment by growth profiling and plating revived, evolved populations of the wild-type strain of *C. glabrata,* the strain with a lower average growth rate and higher carrying capacity. We found within and between population variation in fitness costs and sub-population diversity in growth rate, colony size and antifungal susceptibility. In independently-evolved populations, we co-isolated small, highly caspofungin-resistant colonies and larger, more sensitive colonies. The small colony had a significantly lower growth rate but comparable carrying capacity (final growth density) to the large colony. The between-population variation in fitness costs supports previous fitness divergence across populations of *C. albicans* that were experimentally evolved with fluconazole (Cowen *et al.,* 2000; 2001). A small colony phenotype has previously been described in both fungal and bacterial populations exposed to environmental stress (Day, 2013). Heteroresistance, the presence of resistant and sensitive colonies in a population, has evolved in bacterial drug-treated populations (Lee *et al.,* 2010; El-Halfawy and Valvano, 2015). It is possible that metabolite exchange can increase stress resistance in fungal communities (Campbell *et al.,* 2015; 2016) but this has not been explored in *C. glabrata.*

Our caspofungin-resistant *C. glabrata* small colony grew on a non-fermentable carbon source and we saw no virulence difference between the small and large colony variants. This suggests that our small colony was not a yeast petite mutant that is deficient in respiratory function and virulence capacity (Singh-Babak *et al.,* 2012). We were able to re-grow our small colony suggesting that it was a genotypic variant, rather than a phenotypic variant as described previously for bacteria and fungi (Balaban *et al.,* 2004; LaFleur *et al.,* 2006). We found that large differences in growth rate did not alter virulence, suggesting that carrying capacity (growth density) is a more reliable predictor of virulence. Interestingly, we saw a high level of caspofungin resistance in our small colony in the absence of mutations in commonly described caspofungin resistance target genes (Garcia-Effron *et al.,* 2009). This suggests that mutation in another gene target not commonly associated with caspofungin resistance occurred, for example in other cell integrity genes or transcriptional regulators (Schwarzmüller *et al.,* 2014).

Our results show that different pathogen growth properties of *C. glabrata* strains can be correlated with virulence and that experimental evolution of echinocandin resistance can be studied in the lab and compared between strains. Our work provides evidence of phenotypic effects and repeatability of caspofungin adaptation. We described a potentially novel mechanism of antifungal resistance in *C. glabrata,* demonstrating the importance of population-level heterogeneity in resistance (El-Halfawy and Valvano, 2015). These results could improve understanding of pathogen evolution of antifungal resistance in infections and may lead to better characterisation of fungal strains in different patients. This may lead to consideration of additional host environmental parameters when using *in vitro* susceptibility testing to inform clinical susceptibility prediction. Within-patient strain diversity in drug adaptation or virulence could also be characterised (Mowat *et al.,* 2011).

We hypothesise that a greater final pathogen growth density is correlated with greater virulence and antifungal resistance. It would be interesting to test this hypothesis over a larger range of *C. glabrata* clinical strains and we could further test evolution of growth strategies associated with virulence by growth profiling *C. glabrata* strains that have been serially-passaged through the *G.*

mellonella model, as tested for *C. albicans* adaptation to a murine host (Lüttich *et al.,* 2013) and *Aspergillus flavus* adaptation to *G. mellonella* (Scully and Bidochka, 2005). Following caspofungin treatment, we hypothesise that co-isolation of small and large colony variants in some populations is a stable resistance mechanism as the sensitive large colony was maintained in the population at inhibitory drug concentrations. We could further test this by investigating population dynamics of the two colony variants over serial transfers and characterising genetic mechanisms of resistance in the small colony.

Our results demonstrate the importance of species interactions and clinical strain variation in better understanding the drug susceptibility and virulence of *Candida* infections. Our finding that higher glucose levels in clinically-relevant environments can increase the prevalence of intrinsically drug-resistant *C. glabrata*, could inform optimal treatment design for infections in different patients and body sites that vary in glucose levels, particularly in diabetic patients. It is therefore important to consider the metabolic dimension when designing antimicrobial treatments (Allison *et al.,* 2011). As substantial variation in growth parameters can occur between species strains isolated from different patient infections, this highlights the need for improved diagnostics, given our finding that two initially susceptible *C. glabrata* strains showed contrasting abilities to adapt to high caspofungin concentrations over time. Measuring the key growth characteristics of clinical strains, such as carrying capacity, under different environmental conditions of relevance to infections could allow better prediction of strain adaptability to antifungals.

As well as consideration of strain-specific growth properties and virulence, our results highlight the importance of detecting the presence and measuring the repeatability of evolved within-population diversity in phenotypic properties and antifungal resistance. In the clinical context, a population could relate to a site-specific patient isolate that shows significant variation in phenotype between individual population clones, as described in bacterial cystic fibrosis infections (Mowat *et al.,* 2011). In addition, the presence of high-level echinocandin resistance in the absence of mutation in commonly-described *FKS* gene hotspot targets (Katiyar *et al.,* 2006) could mean that using *FKS* gene sequencing to

detect clinical resistance (Shields *et al.,* 2012) is ineffective in some cases. Standardised clinical antimicrobial susceptibility testing is limited, as sampling only a few clones from a patient isolate could mean that highly-resistant sub-population clones are undetected, reducing treatment efficacy and leading to further drug resistance evolution. Overall, our results add insight for improved characterisation of fungal infections and consideration of the role of host environment on pathogen growth strategies.

6.5 Conclusions

We draw four main conclusions from the research outcomes of this thesis:

1) Competition for resources occurs between fungal pathogens in nutrient media and in an invertebrate model host. Interactions result in long-term species exclusion or increased host mortality in dual compared with single species infection.

2) *C. glabrata* clinical strains form different strength interactions with *C. albicans* in dual infections. *C. glabrata* strains also quantitatively vary in growth properties on glucose in single species cultures.

3) A lower average growth rate and higher carrying capacity in *C. glabrata* can be associated with higher virulence and greater antifungal adaptation.

4) Caspofungin resistance in *C. glabrata* could be maintained by co-existence of resistant and sensitive colony variants.

6.6 Future Perspectives

Current and future challenges in tackling invasive fungal infections, particularly those caused by species of the *Candida* genus, lie in improving diagnostics and therapeutics to address increasing drug resistance and the threat of new emerging pathogens (Kullberg and Arendrup, 2015). As the number of immunosuppressed patients in hospitals increases, *Candida* species infections

will become more prevalent in those with serious pathologies such as cancer (Farmakiotis *et al.,* 2014) and HIV (Diamond, 1991). A major risk factor for increasing infection prevalence is the overuse of broad spectrum antibiotics, which eliminate commensal bacteria that have an important role in preventing fungal overgrowth (Saiman and Ludington, 2001; Kumar and Singhi, 2013). The increasing prevalence of diabetes among the human population (WHO, 2016) will also contribute to increased infection, particularly by *C. glabrata* (Goswami *et al.,* 2006). Drug-resistant fungal infections will pose a major future challenge, particularly due to difficulty in developing novel drugs that will target a larger range of pathogen sites without affecting human cells (Baldauf *et al.,* 2000; Anderson, 2005). The emergence of new pathogenic species with global epidemiology, multi-drug resistance and broad-spectrum invasive disease, is a real threat as evidenced by the recent and rapid appearance of *Candida auris* (Chowdhary *et al.,* 2017).

In this thesis, we have described resource competition in mixed-*Candida* species infections, differing growth properties and adaptations of *C. glabrata* clinical strains and the influence of pathogen growth traits on virulence and antifungal adaptation. This research provides a basis for future investigation of evolutionary trade-offs between resource competition, virulence and antifungal resistance in single and mixed-*Candida* species infections. This thesis has shown that these types of questions can be addressed for clinical fungal pathogens using controlled *in vitro* experiments and manipulation of different environmental parameters to better understand infection in different host sites or patients. The relevance of *in vitro* experiments to *in vivo* infection environments can be tested by the use of a simple host model.

Previous studies have shown that it is possible to investigate trade-offs between resource competition and antimicrobial resistance in pathogenic species. Smith and Holt (1996) highlighted that resource concentrations could be manipulated to influence the balance between resistant and sensitive species, whilst Allison *et al.* (2011) described increased antibiotic activity by combining drug treatment with metabolite administration. Manipulation of resource concentration can change the balance between resistant and sensitive species if sensitive species are better competitors, leading to elimination of drug-resistant competitors

(Goldhaber, 1994). Models have been developed to study the best strategies to eliminate resistant strains in bacterial infections, by increasing the cost of resistance and encouraging faster growth of sensitive strains (Gomes *et al.,* 2013). Recently, a combination of different resource levels and antifungal fluconazole treatment concentrations have been used *in vitro* to find conditions that will select for sensitive *C. albicans* and eliminate resistant *C. glabrata* (Nilsson, 2012; Beardmore *et al.,* (in prep)). The influence of different *C. glabrata* strains, antifungals and interaction with virulence in a host model remains to be investigated.

Appendices

A.1. Chapter 2 Appendix

A.1.1 Supplementary Materials and Methods

YPD (Yeast Peptone Dextrose) Media

20 g/l Bacteriological peptone (Product code: LP0037; Oxoid Ltd, Basingstoke, Hampshire, England)

20 g/l D-glucose anhydrous (Product code: G/0500/61; Fisher Scientific UK, Bishop Meadow Road, Loughborough, UK)

10 g/l Yeast extract (Product code: LP0021; Oxoid Ltd)

18 g/l Bacteriological agar (if making YPD agar) (Product Code: MC006; Lab M Limited, 1 Quest Park, Moss Hall Road, Heywood, Lancashire, UK)

Dissolve in distilled, DI (de-ionised) water

SC (Synthetic Complete) Media

6.9 g/l Yeast Nitrogen Base (YNB) without amino acids, with ammonium sulphate (Product ref. no: CYN0410; Formedium Ltd, Hunstanton, England)

0.79 g/l Complete drop-out mix (all amino acids) (Product ref. no: DCS0019; Formedium Ltd)

D-glucose anhydrous concentration was varied from 20g/l standard

Dissolve in distilled, DI water

A.1.2 Supplementary Figures and Tables

Figure A.1.2.S1: *C. glabrata* (left) and *C. albicans* (right) monocultures on CHROMagar plates. *C. glabrata* forms pink/purple colonies and *C. albicans* forms blue/green colonies.

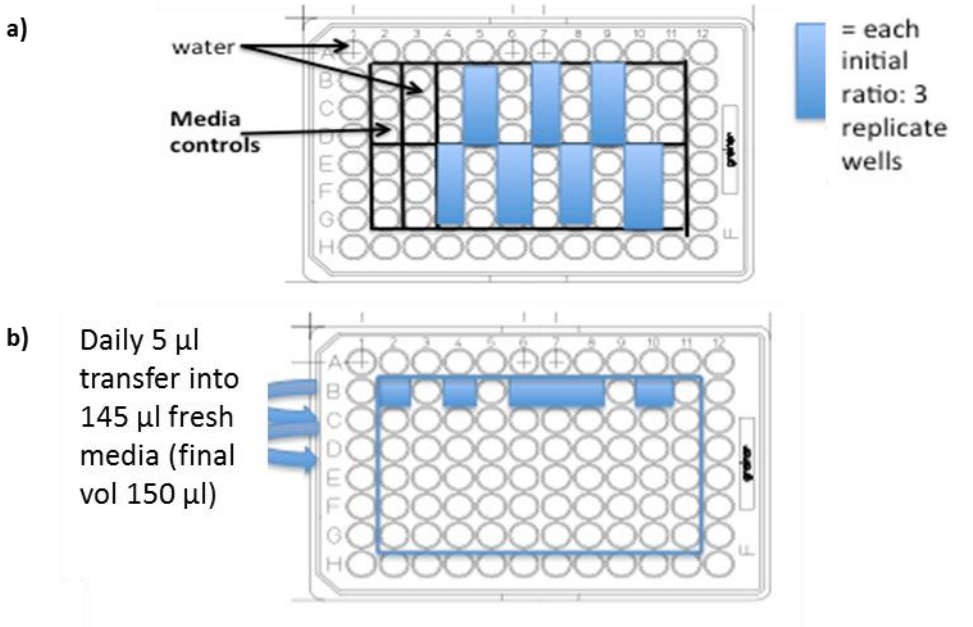

Figure A.1.2.S2: Layout of 96-well plate for one-season and serial transfer competitions for a range of initial species ratios. Experimental layout is similar to that of Nilsson (2012) and Beardmore *et al.* (in prep). **a)** One-season competitions: final volume of each well is 150 µl; those containing cell suspensions used 75 µl of media/ 75 µl of cells, so final cell concentration of each well was half of that estimated via haemocytometer counts. Synthetic Urine media was added to triplicate wells in columns 5, 7 and 9 as well as 4, 6, 8 and 10. Column 2 contained 6 replicate media controls, each of 150 µl volume. Triplicate volumes of *C. glabrata* were added to column 5 as monoculture controls; as for *C. albicans* in column 10. The five remaining columns contained triplicates of the five species ratios (90:10, 70:30, 50:50, 30:70, 10:90) respectively (*C. glabrata: C. albicans*). All remaining wells contained 150 µl of

distilled, de-ionised water. The plate was incubated for 24 hours at 30ºC and 180 rpm. **b)** Competitions over serial transfers: Row B is set up as Day 1 and 75ul of media is added to each of the wells shown in the blue-shaded areas, apart from B2 which is filled with 150 µl SU media as the control. 75 µl of cells are then added to the media wells as follows: monoculture controls- Well 4 is *C. glabrata;* Well 10 is *C. albicans.* Wells in columns 6-8 are the 3 replicates of the co-culture. All intervening wells in the row and the outer border of the plate are filled with 150 µl water. Each day, wells of the subsequent row are prepared with 145 µl of fresh media/water as per the layout of the row above and 5 µl of each of the previous day suspensions are simultaneously transferred into this row. The transparent plate seal is removed and replaced with a fresh seal daily. (Transfer method from Emily Cook, Haynes group, June 2014).

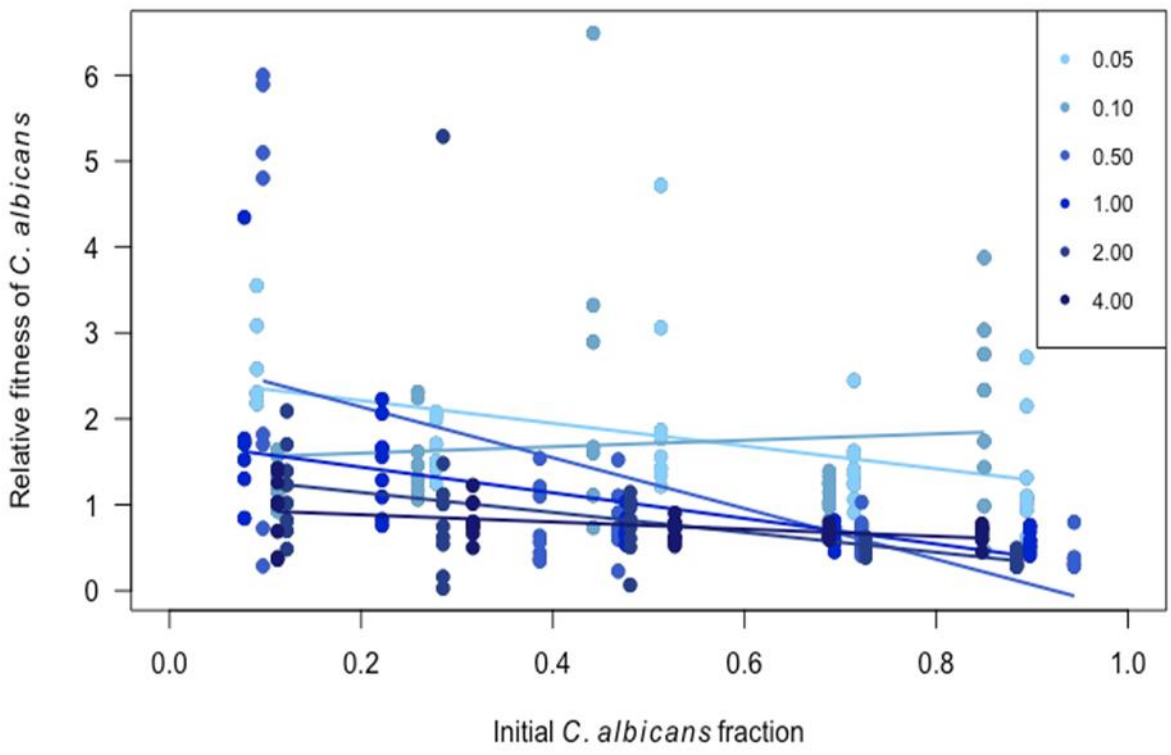

Figure A.1.2.S3. One-season competitions between *C. glabrata* and *C. albicans* for five initial fractions of *C. albicans* and each of six different glucose concentrations in SU media. The data shown in this plot is a combination of all data from Figure 2.3. Relative fitness of C. albicans is calculated as the Malthusian growth parameter and data for each glucose concentration (% w/v) is plotted in a different shade of blue, with darker blue indicating higher glucose. N = 9 for each initial fraction at each glucose concentration. The best fit linear trendline is plotted for each glucose concentration.

Table A.1.2.S1. *C. glabrata* Strains.

Strain	Genotype/ Host Origin	Reference/ Source
ATCC 2001	Sequenced Wild-Type reference strain, isolated from human faeces (pathogenic)	American Type Culture Collection (Kitada *et al.* 1995) (Koszul *et al.* 2003)
BG2	Wild-Type strain derived from parental B strain; clinical isolate from human vaginitis	(Cormack and Falkow 1999)
BG2 Δ*ssk2*	Derived from BG2 strain; mutational inactivation of MAPKKK gene *SSK2*: defective Sln1 branch of osmotic stress signalling	(Gregori *et al.* 2007)
NCPF 3605	Wild-Type clinical isolate from a human with diabetes in the UK in 1989	UKNCC: National Collection of Pathogenic Fungi, Bristol, 2001.
NCPF 3309	Wild-Type clinical isolate from human faeces	UKNCC: National Collection of Pathogenic Fungi, Bristol, 2001.

Table A.1.2.S2. Statistical results from Wilcoxon signed-rank tests to determine significant deviation of *C. albicans* relative fitness from 1 in one-season competition in 0.1% w/v glucose SC media. Significance of *C. albicans* relative fitness from a value of 1 was calculated for five initial *C. albicans* fractions using the two-tailed, one-sample Wilcoxon non-parametric test as populations were non-normally

distributed. The mean initial *C. albicans* fraction is shown and is an average of three plated replicates. Relative fitness was calculated in 9 replicate populations following one-season competition. Negative relative fitness values and highly skewed values (relative fitness > 10) were excluded in the figures and statistical analyses. See **Figure 2.2** for plot.

Initial *C. albicans* fraction	**V-statistic**	***P*-value**
0.03	44	0.007812
0.10	45	0.003906
0.23	45	0.003906
0.38	45	0.003906
0.66	45	0.003906

Table A.1.2.S3. Statistical results from Wilcoxon signed-rank tests or one-sample t-tests to determine significant deviation of *C. albicans* relative fitness from 1 in one-season competition for glucose concentrations in SU media. Statistical results are shown for glucose concentrations in which species co-existence was not predicted from the linear regression. See **Figure 2.3** for plot.

SU 0.05% glucose: Initial *C. albicans* fraction	**V-statistic**	***P*-value**
0.09	28	0.01563
0.28	45	0.003906
0.51	45	0.003906
0.71	43	0.01172
0.89	35	0.1641

SU 0.1% glucose: Initial *C. albicans* fraction	**t-value**	**df**	***P*-value**
0.11	4.42	8	0.002226

0.26	3.7511	8	0.005615
0.44	2.0762	6	0.08317
0.69	2.1806	8	0.06081
0.85	2.6921	7	0.03099

SU 4% glucose: Initial *C. albicans* fraction	**t-value**	**df**	***P*-value**
0.11	-0.37086	8	0.7204
0.32	-2.2941	8	0.05094
0.53	-7.3705	8	7.838e-05
0.69	-15.128	8	3.607e-07
0.85	-10.393	8	6.359e-06

Table A.1.2.S3 continued- different initial competition densities. See **Figure 2.7a** for plots.

SU 1% glucose: 10^7 cells/ml: Initial *C. albicans* fraction	**t-value**	**df**	***P*-value**
0.10	-2.2947	8	0.05089
0.30	-9.7	7	2.614e-05
0.50	-11.875	8	2.321e-06
0.70	-12.447	8	1.621e-06
0.89	-8.5016	8	2.811e-05

SU 4% glucose: 10^7 cells/ml: Initial *C. albicans* fraction	**V-statistic**	***P*-value**
0.10	1	0.01563
0.33	0	0.003906
0.54	0	0.003906

0.70	0	0.003906
0.91	0	0.003906

SU 0.1% glucose: 10^3 cells/ml: Initial *C. albicans* fraction	**t-value**	**df**	***P*-value**
0.088525531	31.413	8	1.147e-09
0.39497314	19.877	8	4.277e-08
0.511993024	14.24	8	5.761e-07
0.706162137	7.011	8	0.0001114
0.920388091	4.539	5	0.006174

Table A.1.2.S4. Statistical results from t-tests for significance of the slope of the negative frequency-dependent relationship for one-season competitions between *C. albicans* and *C. glabrata* at different glucose concentrations and competition cell densities. Statistical results are presented from analysis of the best-fit least-squares linear regression line in Excel, plotted for *C. albicans* relative fitness in replicate populations at five initial *C. albicans* fractions. Negative relative fitness values and highly skewed values (relative fitness > 10) were excluded in the figures and statistical analyses. See **Figures 2.3 and 2.7** for plotted regression lines with R-squared correlation coefficients.

~ 10^6 cells/ml: Glucose concentration (% w/v)	**Slope**	**t-value**	**df**	***P*-value**
0.05	-4.52	-2.58	43	0.01343
0.10	0.38	0.63	40	0.5333
0.50	-2.96	-4.69	41	3.005E-05
1.00	-1.49	-5.54	43	1.696E-06
2.00	-1.16	-2.92	43	0.005566
4.00	-0.42	-3.48	43	0.001166

Glucose concentration (% w/v); cell density (cells/ml)	**Slope**	**t-value**	**df**	***P*-value**
1.00; **10^7**	-0.15	-1.22	42	0.2294
4.00; **10^7**	-0.19	-2.47	42	0.01760
0.10; **10^3**	-0.012	-0.17	40	0.8606

Table A.1.2.S5: Statistical results of significant pairwise comparisons from Tukey *post hoc* tests following one-way ANOVA tests on daily *C. albicans* fractions during long-term competition in 1% w/v glucose SU media. Significant pairings are described for daily differences in *C. albicans* fraction for three different initial fractions and three different initial competitor densities (see text). HF = high frequency; IF = intermediate frequency; LF = low frequency; ID = intermediate density; HD = high density; LD = low density. See **Figure 2.6** for plots**.**

Frequency/ density dependent competition	**Significant daily *C. albicans* fraction pairings**
HF	days 0, 1 and 2 different from each other and all other days; $P = 0.00$ ***
	day 3 from days 7 and 9; $P < 0.01$ **
	day 4 and day 9; $P < 0.05$ *
IF	day 0 different from all days except day 1 and day 1 different from all days except day 0; $P = 0.00$ ***
	day 2 different from all other days: $P < 0.01$ **
	day 3 from days 7 and 9: $P < 0.01$ **
LF, ID	day 0 different from all days except day 1; $P < 0.05$ *
	day 1 different from all days except day 0; $P < 0.001$ ***
	day 2 different from all days except day 3; $P < 0.01$ **
HD	day 0 different from all days except day 1; $P < 0.001$ ***
	day 1 different from all days except day 0; $P < 0.001$ ***
	day 2 different from all days except day 3; $P < 0.001$ ***
	day 3 different from all days except day 2; $P < 0.01$ **
LD	day 0 and day 1 different from all days except each other; $P < 0.001$ ***
	day 2 different from all days; $P < 0.01$ **

A.2 Chapter 3 Appendix

A.2.1 Supplementary Tables

Table A.2.1.S1. Statistical results from log-rank tests for survival curve comparisons between infective doses and temperatures for single species *C. albicans* and *C. glabrata* infections of *G. mellonella*. Statistical analyses represent comparisons between survival curves from **Figure 3.1.** Pairwise comparisons are presented from OASIS 2 software and compare survival between three doses and two temperatures for each species. P-values are corrected (Bonferroni) to account for multiple comparisons.

***C. glabrata:* temperature (ºC); dose (CFU/larva)**	**Chi-squared**	***P*-value**	**corrected _*P*-value**	**Mean survival time (days) +/- SE**
30; 1.25 x 10^6 v.s. 30; 2.5 x 10^6	8.96	0.0028	0.0138	3.93 +/- 0.36 v.s. 3.20 +/- 0.28
30; 1.25 x 10^6 v.s. 30; 5 x 10^6	23.29	0.0000014	0.000007	3.93 +/- 0.36 v.s. 1.75 +/- 0.19
30; 2.5 x 10^6 v.s. 30; 5 x 10^6	8.38	0.0038	0.0189	3.20 +/- 0.28 v.s. 1.75 +/- 0.19
37; 1.25 x 10^6 v.s. 37; 2.5x10^6	28.93	7.50e-08	3.70e-07	4.90 +/- 0.25 v.s. 3.00 +/- 0.20
37; 1.25 x 10^6 v.s. 37; 5 x 10^6	86.66	0	0	4.90 +/- 0.25 v.s. 1.95 +/- 0.09
37; 2.5 x 10^6 v.s. 37; 5 x 10^6	22.8	0.0000018	0.000009	3.00 +/- 0.20 v.s. 1.95 +/- 0.09
30; 1.25 x 10^6 v.s. 37; 1.25x10^6	0.91	0.3405	1	3.93 +/- 0.36 v.s. 4.90 +/- 0.25 v.s.
30; 2.5 x 10^6 v.s. 37; 2.5 x 10^6	0.16	0.6856	1	3.20 +/- 0.28 v.s. 3.00 +/- 0.20 v.s.
30; 5 x 10^6 v.s. 37; 5 x 10^6	0.15	0.7024	1	1.75 +/- 0.19 v.s. 1.95 +/- 0.09

***C. albicans:* temperature (ºC); dose (CFU/larva)**	**Chi-squared**	***P*-value**	**corrected_ *P*-value**	**Mean survival time (days) +/- SE**
30; 1 x 10^5 v.s. 30; 2 x 10^5	35.51	2.60e-09	1.30e-08	6.54 +/- 0.16 v.s. 4.59 +/- 0.28
30; 1 x 10^5 v.s. 30; 4 x 10^5	148.38	0	0	6.54 +/- 0.16 v.s. 1.26 +/- 0.12
30; 2 x 10^5 v.s. 30; 4 x 10^5	85.73	0	0	4.59 +/- 0.28 v.s. 1.26 +/- 0.12
37; 1 x 10^5 v.s. 37; 2 x 10^5	47.7	0	0	5.59 +/- 0.20 v.s. 2.95 +/- 0.21
37; 1 x 10^5 v.s. 37; 4 x 10^5	159.43	0	0	5.59 +/- 0.20 v.s. 1.06 +/- 0.03
37; 2 x 10^5 v.s. 37; 4 x 10^5	92.89	0	0	2.95 +/- 0.21 v.s. 1.06 +/- 0.03
30; 1 x 10^5 v.s. 37; 1 x 10^5	36.9	0	0	6.54 +/- 0.16 v.s. 5.59 +/- 0.20
30; 2 x 10^5 v.s. 37; 2 x 10^5	24.25	8.50e-07	4.20e-06	4.59 +/- 0.28 v.s. 2.95 +/- 0.21
30; 4 x 10^5 v.s. 37; 4 x 10^5	2.03	0.154	0.7701	1.26 +/- 0.12 v.s. 1.06 +/- 0.03

Table A.2.1.S2. Results from survival analyses of single and dual species *Candida* infections of *G. mellonella*, using infective doses from Rossoni *et al.* (2015). Statistical results are from log-rank tests (Cox PH in R) used to compare survival curves presented in **Figure 3.2.** Letters in brackets in column 1 denote plots from **Figure 3.2**, to which the statistical results relate. Mean survival times with standard errors are presented for a descriptive comparison of survival between infection groups.

Survival curve comparison	**Chi-squared value**	***P*-value**	**Mean survival time (hours) +/- SE**

(a) *C. albicans* SBC153/ 1 x 10^6 CFU/larva; *C. glabrata* ATCC 2001/ 1 x 10^6 CFU/larva	70.94	0.0000	18.00 +/- 0.00; 71.75 +/- 4.48
(b) *C. albicans* SBC153/ 1 x 10^6 CFU/larva; *C. albicans* SBC153/ 2 x 10^6 CFU/larva; *C. albicans* SBC153/ 1 x 10^6 CFU/larva, *C. glabrata* ATCC 2001 1 x10^6 CFU/larva	0.29	0.8655	18.00 +/- 0.00 18.00 +/- 0.00 18.63 +/- 0.63
(c) *C. albicans* SBC153/ 1 x 10^6 CFU/larva; *C. krusei* ATCC 6258/ 1 x 10^6 CFU/larva- bio rep 2	11.93	0.0005512	18.00 +/- 0.00; 46.88 +/- 7.73
(d) *C. albicans* SBC153/ 1 x 10^6 CFU/larva; *C. albicans* SBC153/ 2 x 10^6 CFU/larva; *C. albicans* SBC153/ 1 x 10^6 CFU/larva, *C. krusei* ATCC 6258 x10^6 CFU/larva	0.00	1.0000	18.00 +/- 0.00; 18.00 +/- 0.00; 18.00 +/- 0.00;

Table A.2.1.S3. Statistical results from log-rank tests for survival curves of single species *C. albicans* infection and dual species *C. albicans*-*C. glabrata* strain infections of *G. mellonella*. Statistical analyses show comparisons between survival curves in **Figure 3.3.** Separate single species infections for two doses of *C. albicans*

were run alongside each dual species infection and pairwise comparisons with each dual species infection are presented.

Single/ dual species infection pairwise comparison (CFU/larva)	**Chi-squared**	***P*-value**	**corrected _*P*-value**	**Mean survival time (hours) +/- SE**
Figure 3.3(a) (*C. glabrata* strain BG2)				
Ca 2 x 10^5 v.s. Ca 4 x 10^5	38.53	0	0	50.75 +/- 3.73 v.s. 23.38 +/- 1.94
Ca 2 x 10^5 v.s. Cg/Ca 2 x 10^5/ 2 x 10^5	6.11	0.0135	0.0269	50.75 +/- 3.73 v.s. 37.5 +/- 3.98
Ca 4 x 10^5 v.s. Cg/Ca 2 x 10^5/ 2 x 10^5	9.15	0.0025	0.005	23.38 +/- 1.94 v.s. 37.5 +/- 3.98
Figure 3.3(b) (*C. glabrata* strain 3605)				
Ca 2 x 10^5 v.s. Ca 4 x 10^5	25.54	4.30e-07	8.70e-07	36.56 +/- 3.34 v.s. 20.06 +/- 0.97
Ca 2 x 10^5 v.s. Cg/Ca 2 x 10^5/ 2 x 10^5	0.15	0.7028	1	36.56 +/- 3.34 v.s. 34.13 +/- 2.94
Ca 4 x 10^5 v.s. Cg/Ca 2 x 10^5/ 2 x 10^5	22.45	0.0000022	0.0000043	20.06 +/- 0.97 v.s. 34.13 +/- 2.94
Figure 3.3(c) (*C. glabrata* strain 1184)				
Ca 2 x 10^5 v.s. Ca 4 x 10^5	23.5	0.0000012	0.0000025	41.88 +/- 3.85 v.s. 22.5 +/- 1.74
Ca 2 x 10^5 v.s. Cg/Ca 2 x 10^5/ 2 x 10^5	26.69	2.40e-07	4.80e-07	41.88 +/- 3.85 v.s. 21.75 +/- 1.80
Ca 4 x 10^5 v.s. Cg/Ca 2 x 10^5/ 2 x 10^5	0.1	0.7484	1	22.5 +/- 1.74 v.s. 21.75 +/-

				1.80
Figure 3.3(d) (*C. glabrata* strain 3309)				
Ca 2 x 10^5 v.s. Ca 4 x 10^5	39.02	0	0	48.63 +/- 4.42 v.s. 20.38 +/- 0.90
Ca 2 x 10^5 v.s. Cg/Ca 2 x 10^5/ 2 x 10^5	14.27	0.0002	0.0003	48.63 +/- 4.42 v.s. 30.63 +/- 2.65
Ca 4 x 10^5 v.s. Cg/Ca 2 x 10^5/ 2 x 10^5	11.65	0.0006	0.0013	20.38 +/- 0.90 v.s. 30.63 +/- 2.65

Table A.2.1.S4. Statistical results from log-rank tests for single species *C. albicans* infection and dual species *C. albicans-C. krusei* strain infections of *G. mellonella.* Statistical analyses show comparisons between survival curves in **Figure 3.4.** Pairwise comparisons between single species *C. albicans* infections and between single and dual species infections are reported.

Single/ dual species infection pairwise comparison (CFU/larva)	**Chi-squared**	***P*-value**	**corrected _*P*-value**	**Mean survival time (hours) +/- SE**
Figure 3.4(a)				
Ca SBC153 2 x 10^5 v.s. Ca SBC153 4 x 10^5	17.92	0.000023	0.000046	36.25 +/- 3.57 v.s. 20.63 +/- 1.27
Ca SBC153 2 x 10^5 v.s. Ck/Ca 2 x 10^5/ 2 x 10^5	14.35	0.0002	0.0003	36.25 +/- 3.57 v.s. 22.00 +/- 1.59
Ca SBC153 4 x 10^5 v.s. Ck/Ca 2 x 10^5/ 2 x 10^5	0.12	0.7272	1	20.63 +/- 1.27 v.s. 22.00 +/- 1.59
Figure 3.4(b)				
Ca 18804 2 x 10^5 v.s. Ca 18804 4 x 10^5	36.03	0	0	40.38 +/- 4.05 v.s. 18.63 +/-

				0.26
Ca 18804 2 x 10^5 v.s. Ck/Ca 2 x 10^5/ 2 x 10^5	34.51	4.30e-09	8.50e-09	40.38 +/- 4.05 v.s. 18.75 +/- 0.29
Ca 18804 4 x 10^5 v.s. Ck/Ca 2 x 10^5/ 2 x 10^5	0.1	0.7499	1	18.63 +/- 0.26 v.s. 18.75 +/- 0.29

Table A.2.1.S5. Statistical results from log-rank tests for single species *C. albicans* and *C. glabrata* strain infections of *G. mellonella* at equally virulent doses. Statistical analyses show comparisons between survival curves in **Figure 3.5.** All pairwise comparisons are reported.

Single species infection dose (CFU/larva)	**Chi-squared**	***P*-value**	**corrected_*P*-value**	**Mean survival time (hours) +/- SE**
C.albicans 2 x 10^5 v.s. *C. glabrata* BG2 5 x 10^6	0.76	0.3827	0.7654	62 +/- 6.31 v.s. 57 +/- 4.41
C.albicans 2 x 10^5 v.s. *C.glabrata* 1184 1.25 x 10^6	1.43	0.2315	0.4629	62 +/- 6.31 v.s. 70.63 +/- 6.75
C. glabrata BG2 5 x 10^6 v.s. *C.glabrata* 1184 1.25 x 10^6	4.13	0.0421	0.0841	57 +/- 4.41 v.s. 70.63 +/- 6.75

A.3. Chapter 4 Appendix

A.3.1 Supplementary Figures and Tables

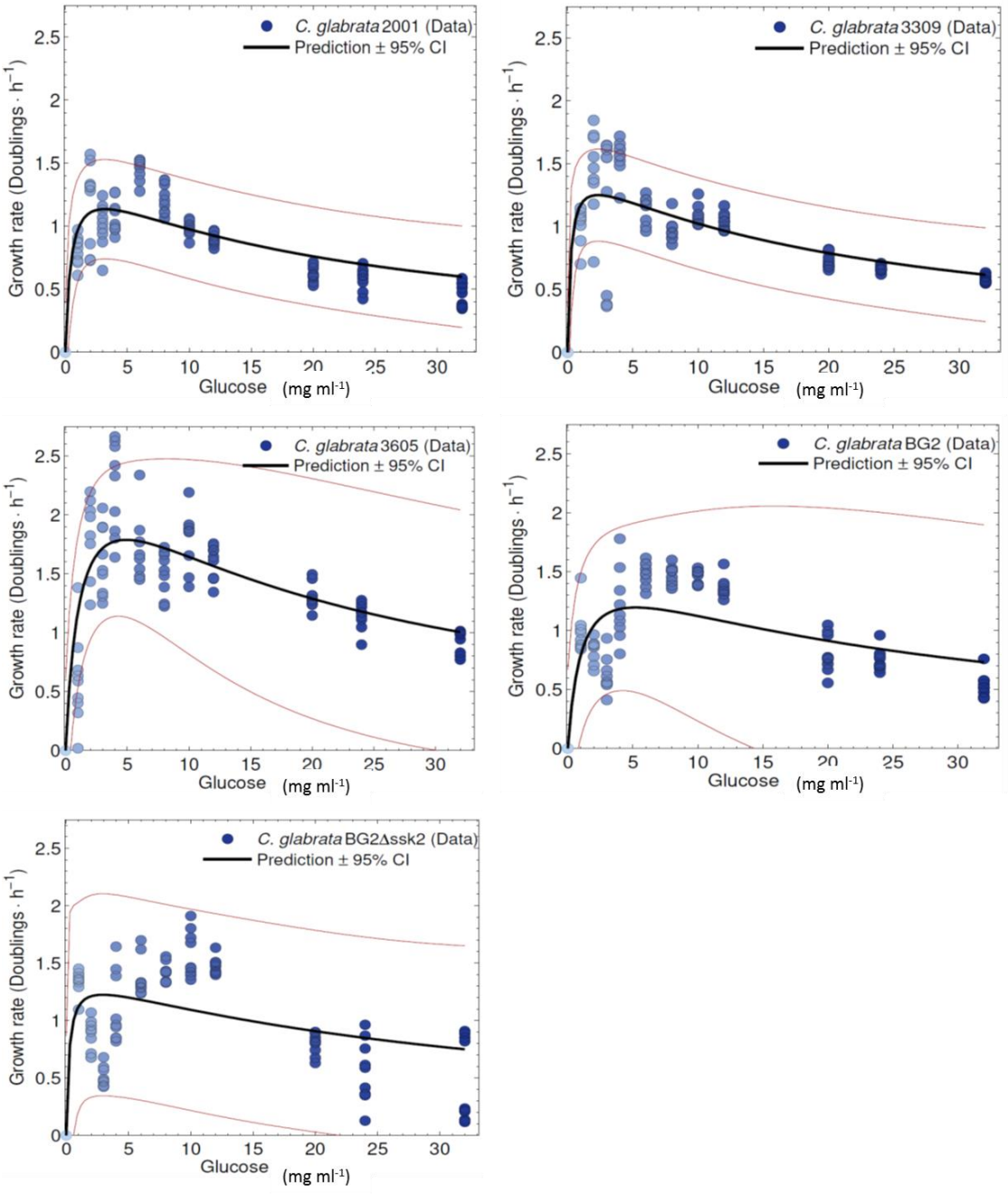

Figure A.3.1.S1. Growth rate (r) for five *C. glabrata* strains measured over a range of glucose concentrations in Synthetic Complete medium. Data is replotted from **Figure 4.3(a)** to show separate two-dimensional representations of each strain's data and fitted model prediction. Each model prediction with 95% CIs was obtained by fitting an equation to the data that assumed growth rate (r) to vary as a Monod function multiplied by yield (biomass produced per mg ml^{-1} of glucose) (Meyer *et al.,* 2015;

Equation (2)- Reding-Roman *et al.,* 2017). N = 9 per glucose concentration per strain and the colour gradient for the plotted points indicates increasing glucose concentration. The model prediction is a robust fit to the data for all strains (adjusted R^2 values = strain 2001: 0.7854; strain 3309: 0.7233; strain 3605: 0.8121; strain BG2: 0.6326; strain BG2Δ*ssk2:* 0.5516). Data plots and model fitting were completed by Carlos Reding-Roman, University of Exeter.

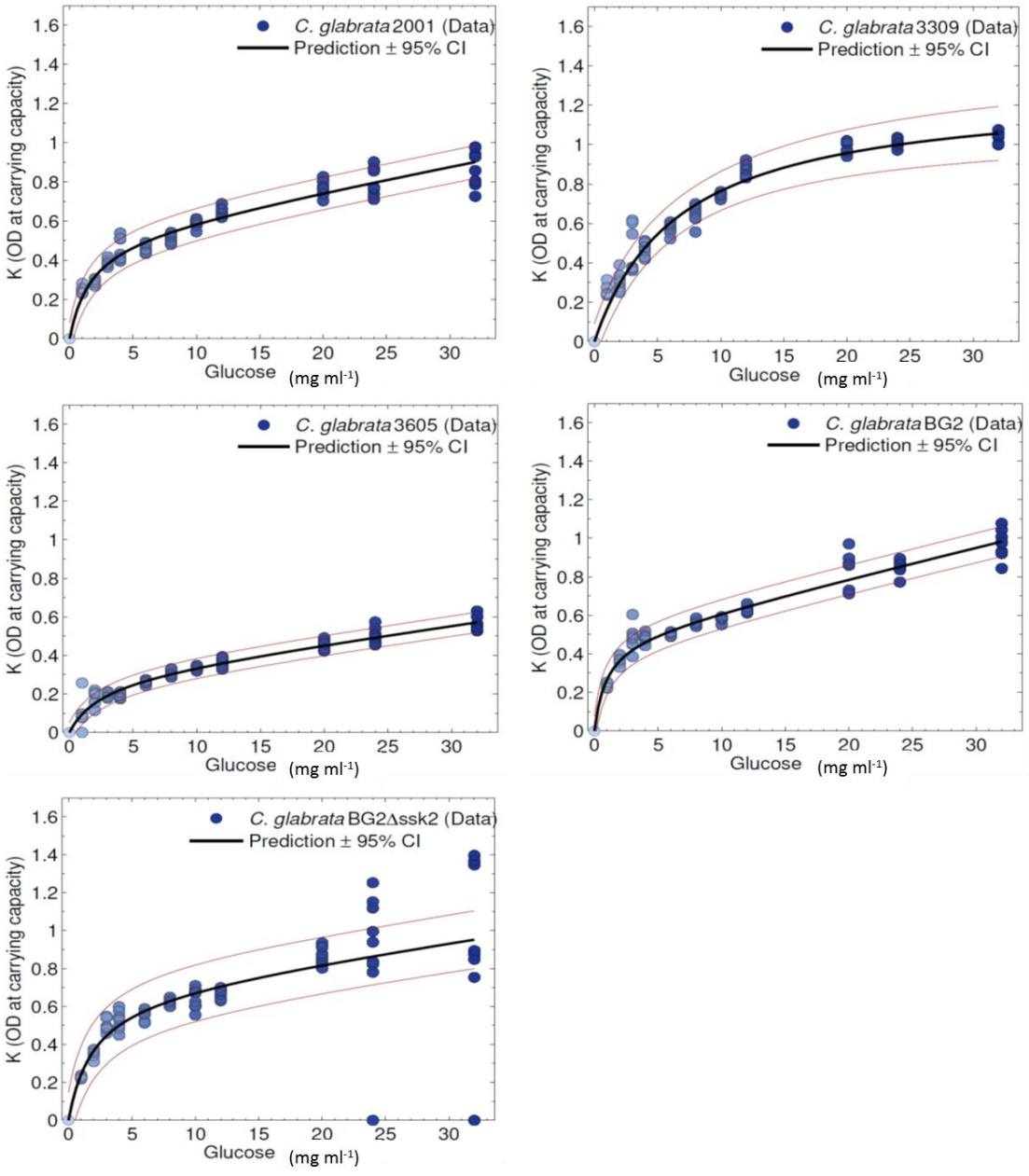

Figure A.3.1.S2. OD at carrying capacity (K) for five *C. glabrata* strains measured over a range of glucose concentrations in Synthetic Complete medium. Data is replotted from **Figure 4.3(b)** to show separate two-dimensional representations of each strain's data and fitted model prediction. Glucose concentration is plotted as an increasing function on the x-axis and is also indicated by the light-dark colour gradient

of plotted points. Each model prediction with 95% CIs was obtained by fitting an equation to the data that assumed K to be a product of yield and glucose concentration (Equation (4)- Reding-Roman *et al.,* 2017). N = 9 per glucose concentration per strain. The model prediction is a robust fit to the data for all strains (adjusted R^2 values = strain 2001: 0.9788; strain 3309: 0.9854; strain 3605: 0.9792; strain BG2: 0.9840; strain BG2Δ*ssk2:* 0.9278). Data plots and model fitting were completed by Carlos Reding-Roman, University of Exeter.

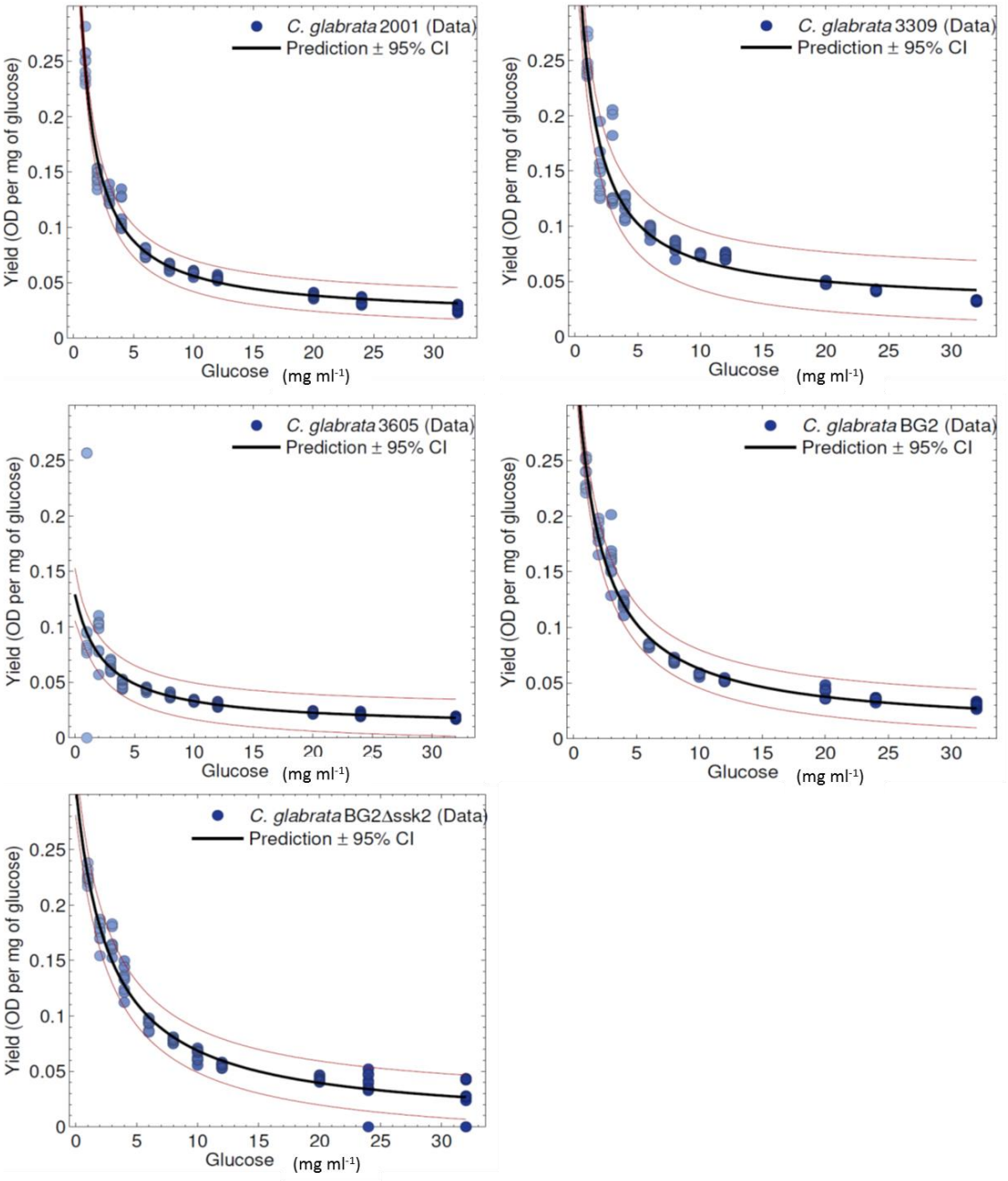

Figure A.3.1.S3. Yield for five *C. glabrata* strains measured over a range of glucose concentrations in Synthetic Urine medium. Data is replotted from **Figure 4.3(c)** to show separate two-dimensional representations of each strain's data and

fitted model prediction. Yield was calculated as K divided by glucose concentration (mg ml^{-1}) and represents the efficiency of biomass production. Each model prediction with 95% CIs was obtained by fitting an equation to the data that assumed yield to depend on environmental glucose concentration rather than being a fixed constant (Meyer *et al.,* 2015; Equation (5)- Reding-Roman *et al.,* 2017). N = 9 per glucose concentration per strain and the colour gradient for the plotted points indicates increasing glucose concentration. The model prediction is a robust fit to the data for all strains (adjusted R^2 values = strain 2001: 0.995; strain 3309: 0.98; strain 3605: 0.99; strain BG2: 0.95; strain BG2Δ*ssk2:* 0.98). Data plots and model fitting were completed by Carlos Reding-Roman, University of Exeter.

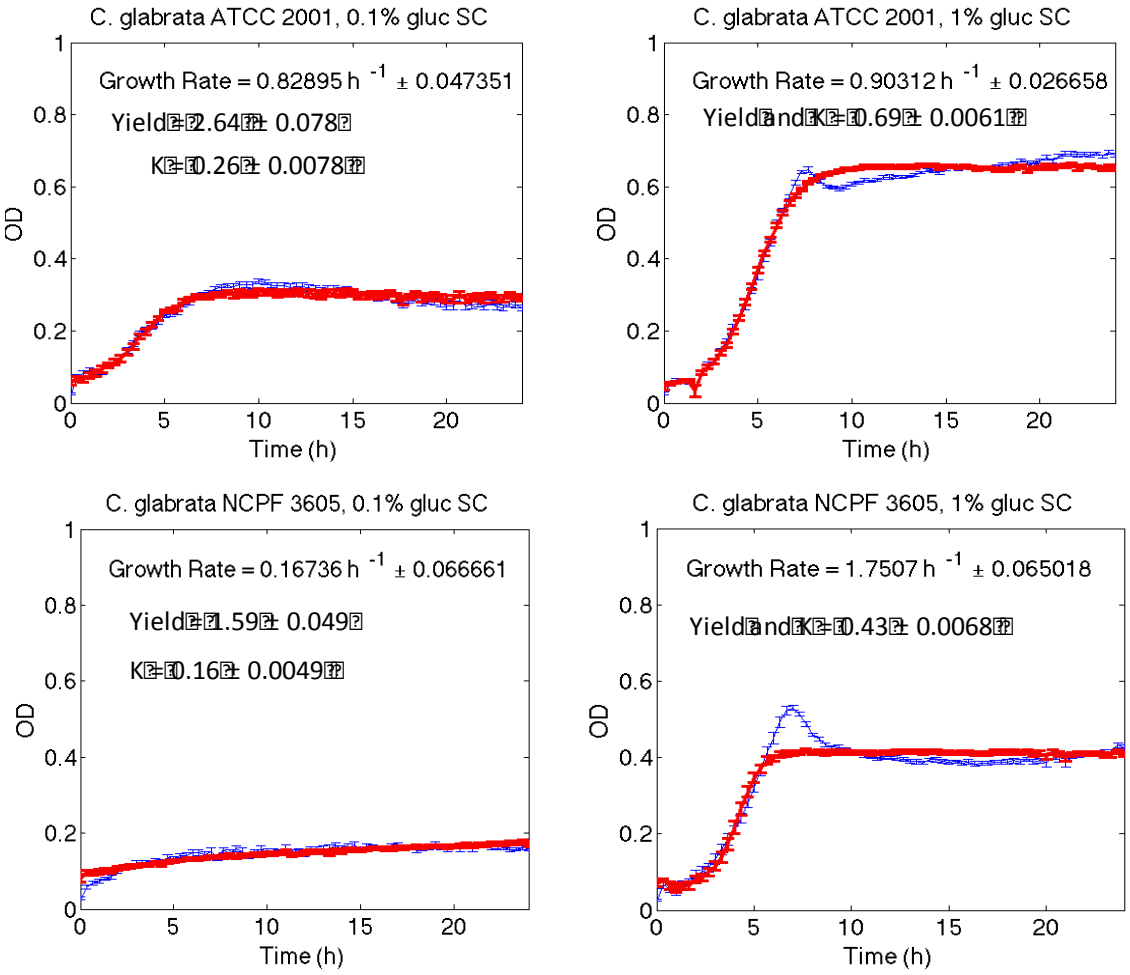

Figure A.3.1.S4. Growth curves of *C. glabrata* strains 2001 and 3605 at low and intermediate glucose concentrations, with fitted logistic models and calculated growth parameters. Plots for 2001 (top) and 3605 (bottom) show change in OD over 24 hours (blue line fitted to means and SE bars shown per time point). The red line on each plot is the best fit of the logistic model and shows predicted means and standard error bars for each time point. Growth parameter values (growth rate and K (carrying capacity)) were estimated from the logistic fit and are shown with their standard errors.

Yield was calculated as K/ % (w/v) glucose, so K and yield are equal at 1% w/v glucose. N = 15 (technical replicates) for each strain and glucose concentration. 0.1% glucose = 1 mg ml^{-1} glucose (“low glucose”); 1% glucose = 10 mg ml^{-1} glucose (“intermediate glucose”). The peaks in OD around 7 hours for each strain grown in 1% glucose could represent transient cell clumping, and they are excluded by the logistic fits to calculate the best fit growth parameters.

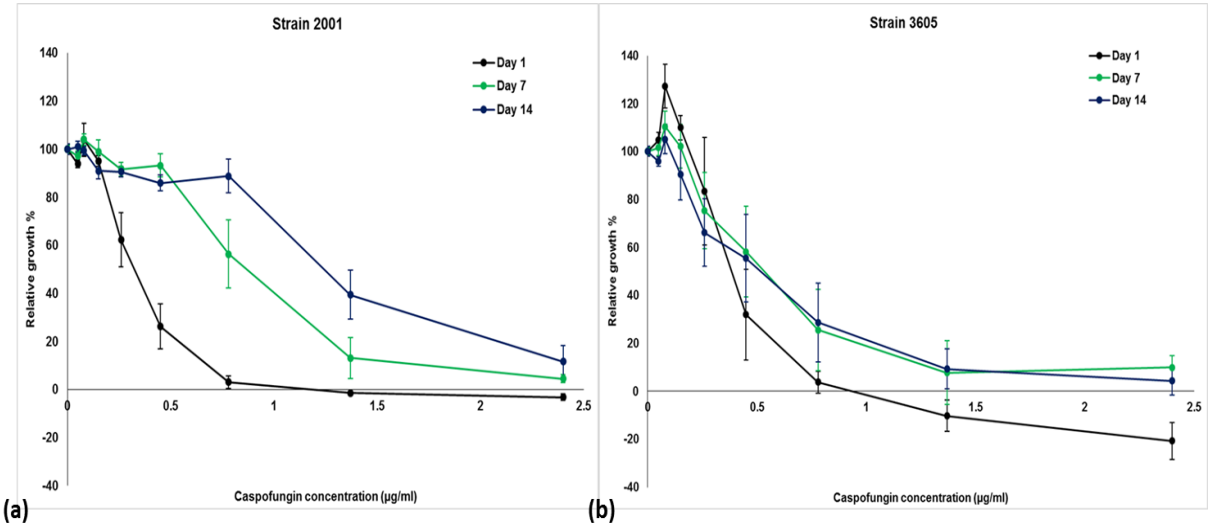

Figure A.3.1.S5 Relative growth of populations of *C. glabrata* strains 2001 and 3605 evolving on a gradient of caspofungin concentrations over 14 days. Populations of each strain were grown across eight different caspofungin concentrations and a no-drug condition and were serially transferred at the end of each 24-hour period. Relative growth % is calculated as the final optical density of a drug-treated population at the end of a 24-hour period as a percentage of the average final optical density of the no-drug treated populations. Data is shown for days 1, 7 and 14 and is combined from the three independent 14-day experiments (3 populations per drug treatment), such that N = 9 per drug concentration per day. Plotted points represent mean relative growth with standard error bars shown. (a) Strain 2001; (b) Strain 3605.

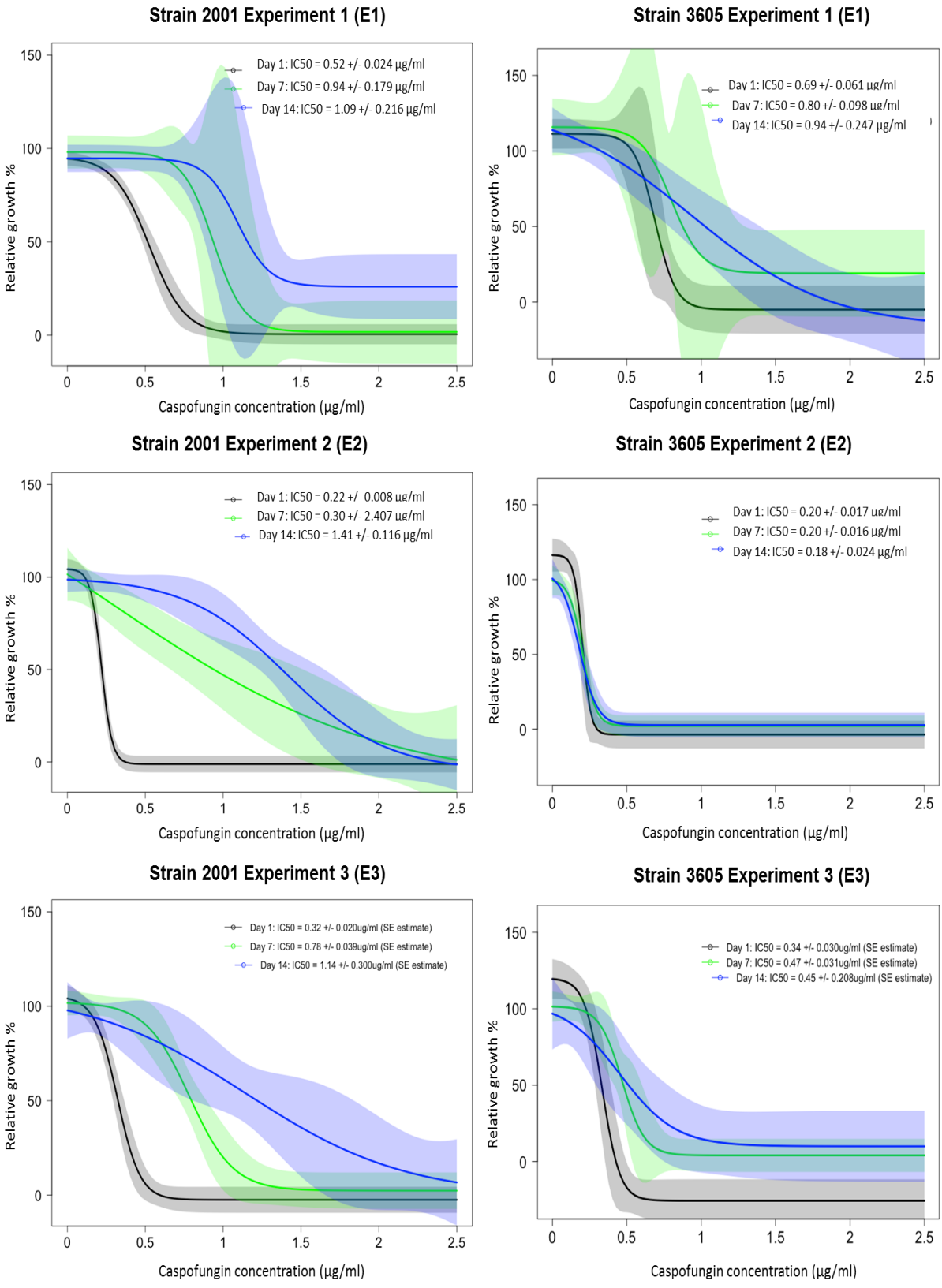

Figure A.3.1.S6. Evolution of caspofungin dose response profile of *C. glabrata* strains 2001 and 3605 in three independent experiments. Left panels show evolution of strain 2001; right panels show evolution of strain 3605. Plots represent model fits (4-parameter logistic dose response) to the data presented in **Figure 4.9** and

95% confidence intervals for the predictions shown by coloured shaded regions. Days 1, 7 and 14 dose responses are plotted (black, green, blue respectively) and IC50 estimates with their standard errors predicted from the logistic model are presented for each curve. Comparison of IC50 parameters- 2001 E1: Day 1 compared with Day 7,14, $P < 0.01$; 2001 E2: Day 1 compared with Day 14, $P = 0.00$; 2001 E3: Day 1 compared with Day 7,14, $P < 0.001$; 3605 E1, E2, E3: no significant differences apart from E3: Day 1 and Day 7, $P < 0.05$. Comparison of slopes- 2001 E1: no significant differences; 2001 E2: Day 1 and 7,14, $P < 0.01$; 2001 E3: Day 1 and 14, $P < 0.01$; 3605 E1, E2, E3: no significant differences apart from E2: Day 1 and 14, $P < 0.05$.

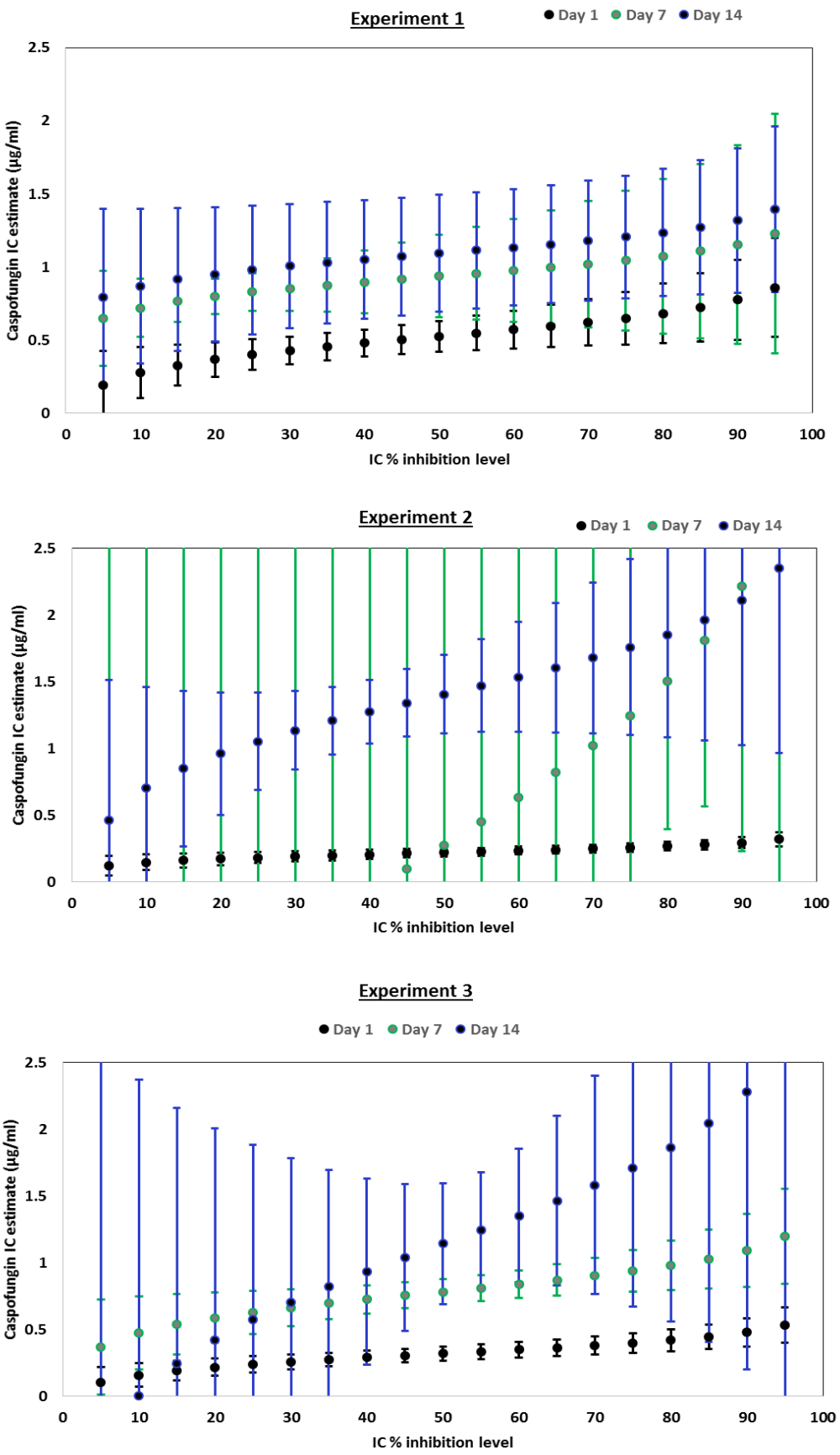

Figure A.3.1.S7. Caspofungin IC estimates from dose-response fits across populations of *C. glabrata* strain 2001 evolving on a gradient of caspofungin

concentrations in three 14-day experiments. Following fitting of 4-parameter logistic dose response profiles to data from days 1, 7 and 14 (**Figure A.3.1.S6;** left panels), the R-package 'drc' (Ritz *et al.*, 2015) was used to calculate IC (inhibitory Concentration) estimates for growth inhibitory levels ranging 5 - 95%, with 5% increments. The estimated inhibitory caspofungin concentrations (μg/ml) are plotted with 95% confidence intervals from the model predictions. The data from Days 1 (black), 7 (green) and 14 (blue) are plotted and significant differences between IC estimates between days at each inhibitory level are deduced from non-overlapping 95% confidence intervals, indicating statistical significance at $P < 0.05$ (Greenland *et al.,* 2016). The three separate plots represent each of the 14-day evolutionary experiments.

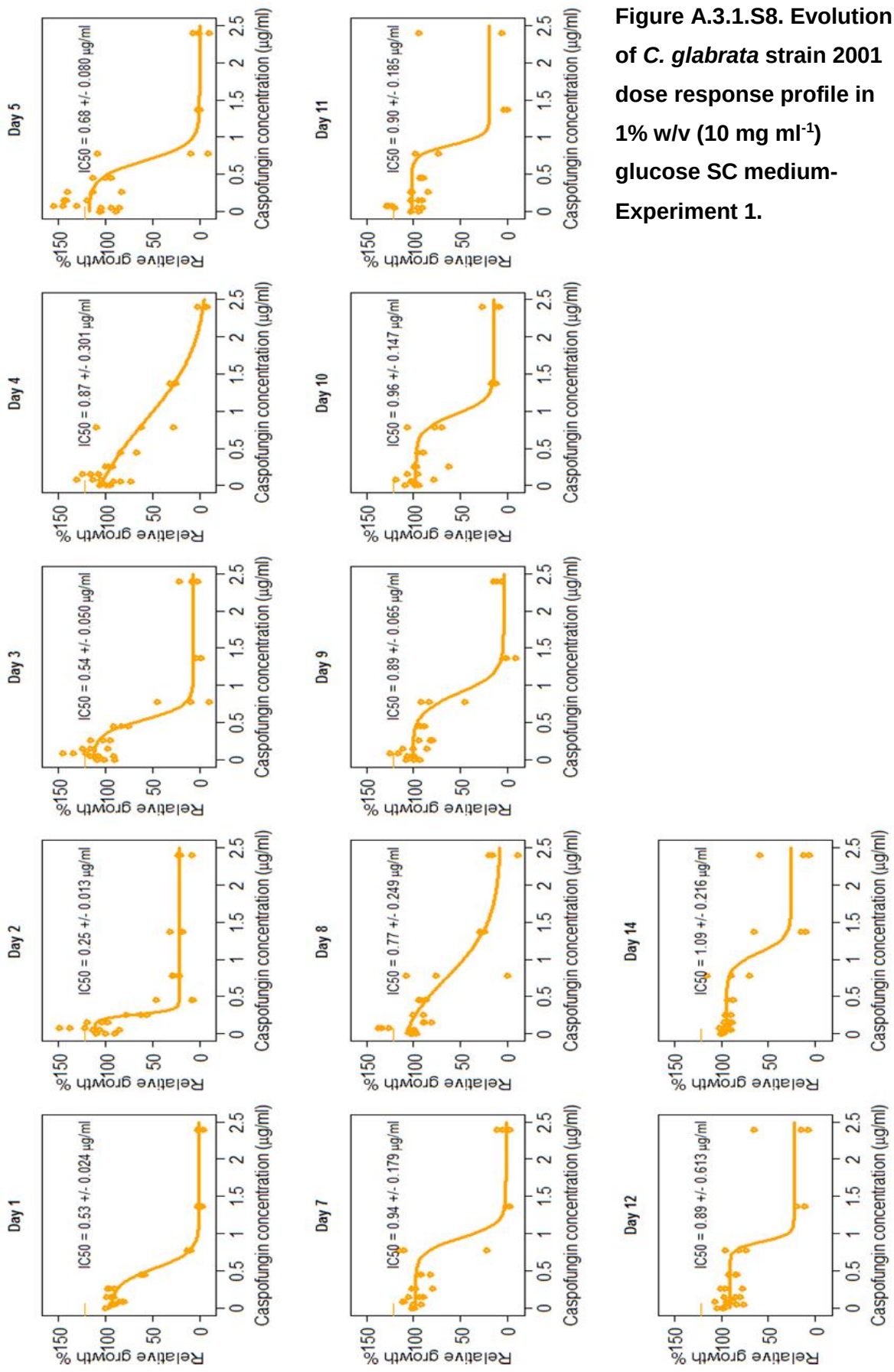

Figure A.3.1.S8. Evolution of *C. glabrata* strain 2001 dose response profile in 1% w/v (10 mg ml^{-1}) glucose SC medium- Experiment 1.

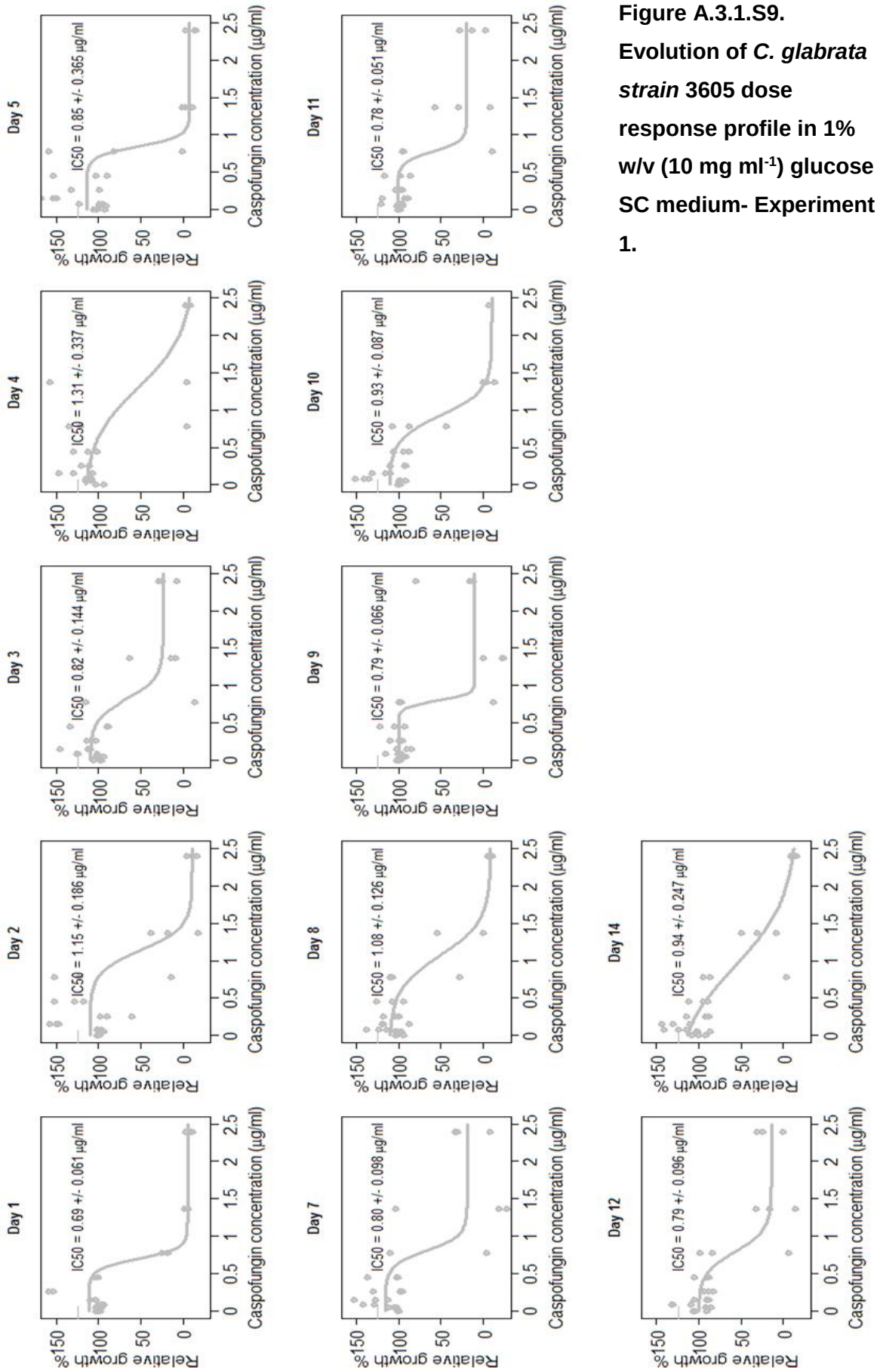

Figure A.3.1.S9. Evolution of *C. glabrata strain* 3605 dose response profile in 1% w/v (10 mg ml^{-1}) glucose SC medium- Experiment 1.

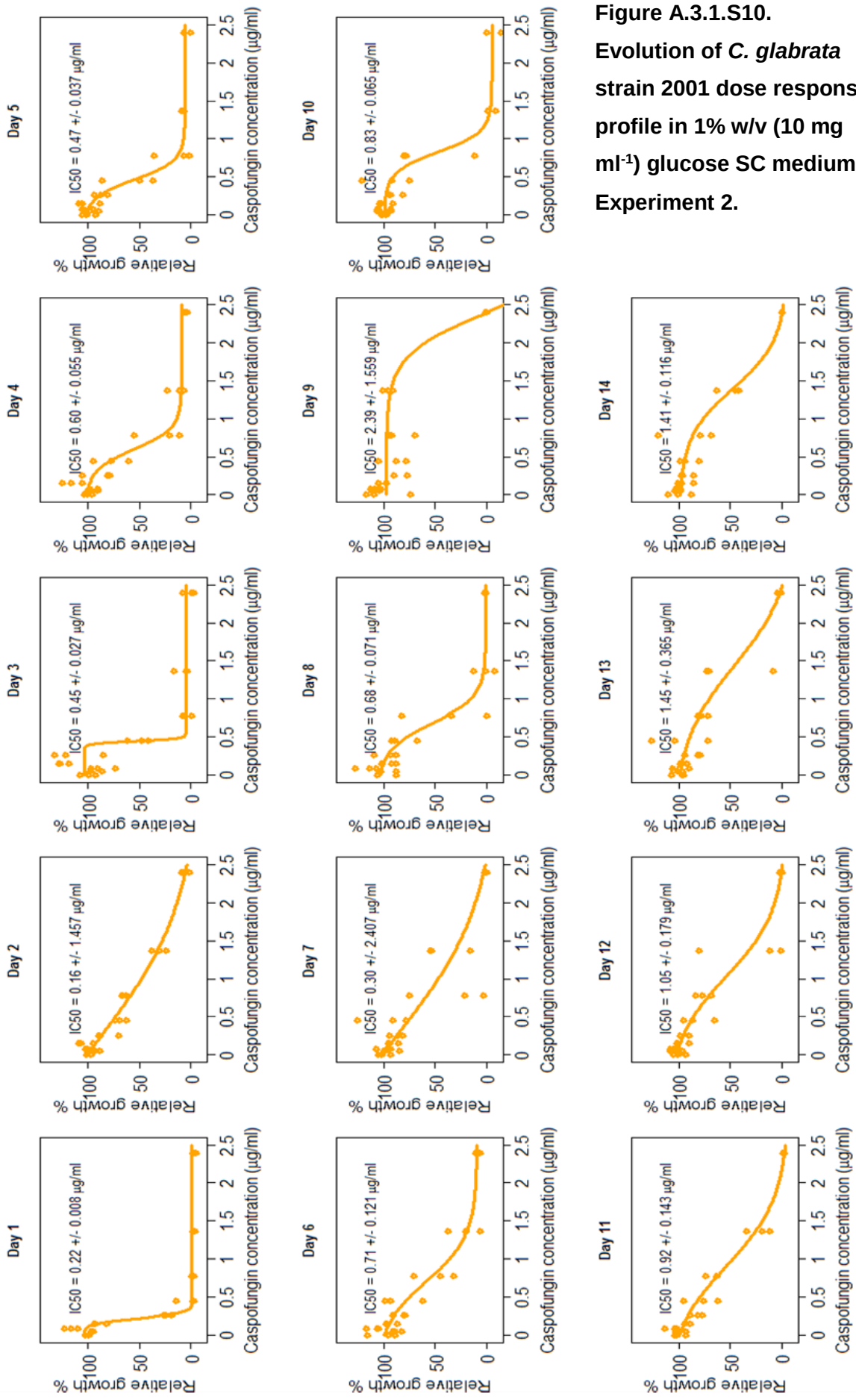

Figure A.3.1.S10. Evolution of *C. glabrata* strain 2001 dose response profile in 1% w/v (10 mg ml^{-1}) glucose SC medium- Experiment 2.

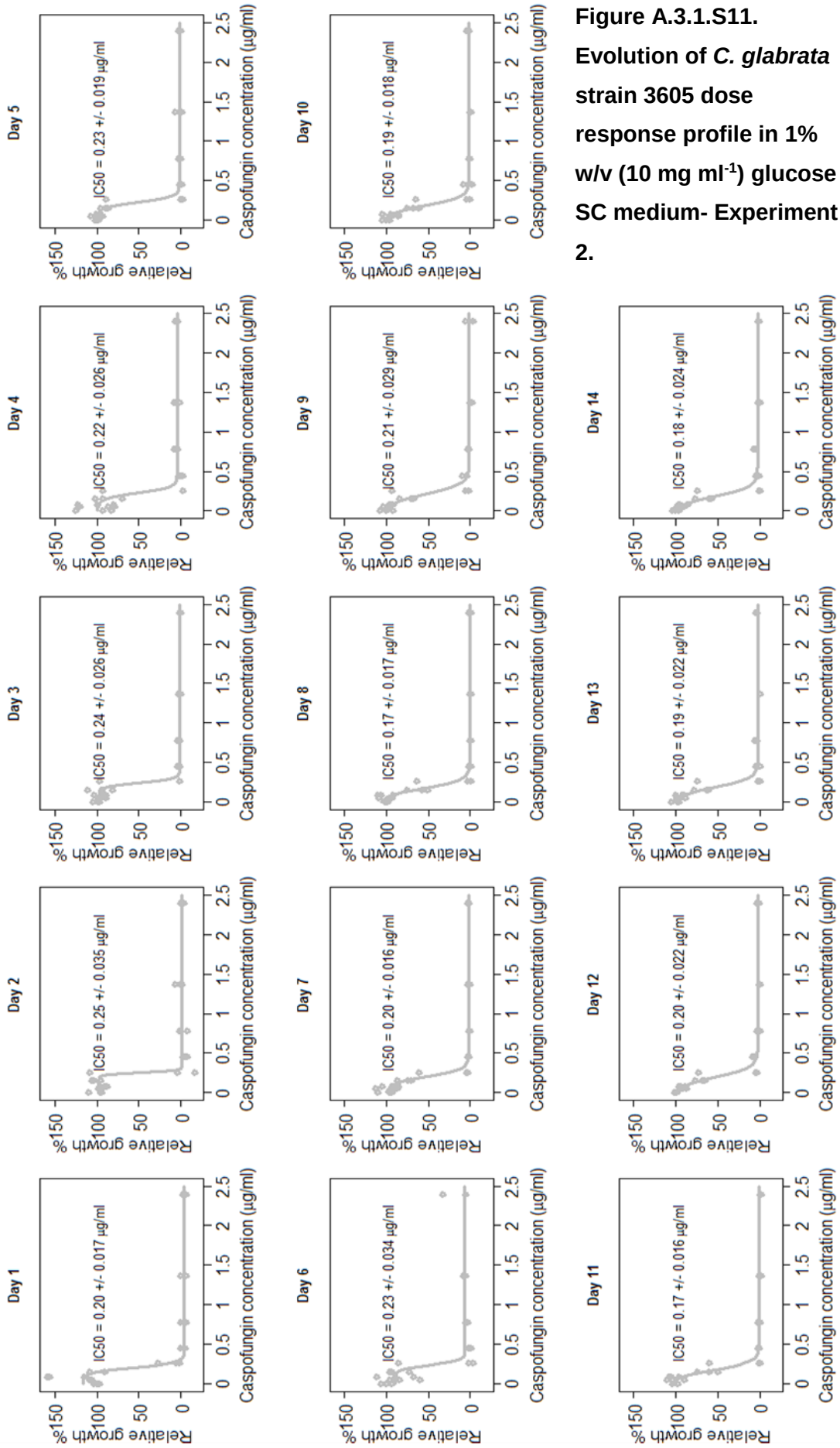

Figure A.3.1.S11. Evolution of *C. glabrata* strain 3605 dose response profile in 1% w/v (10 mg ml^{-1}) glucose SC medium- Experiment 2.

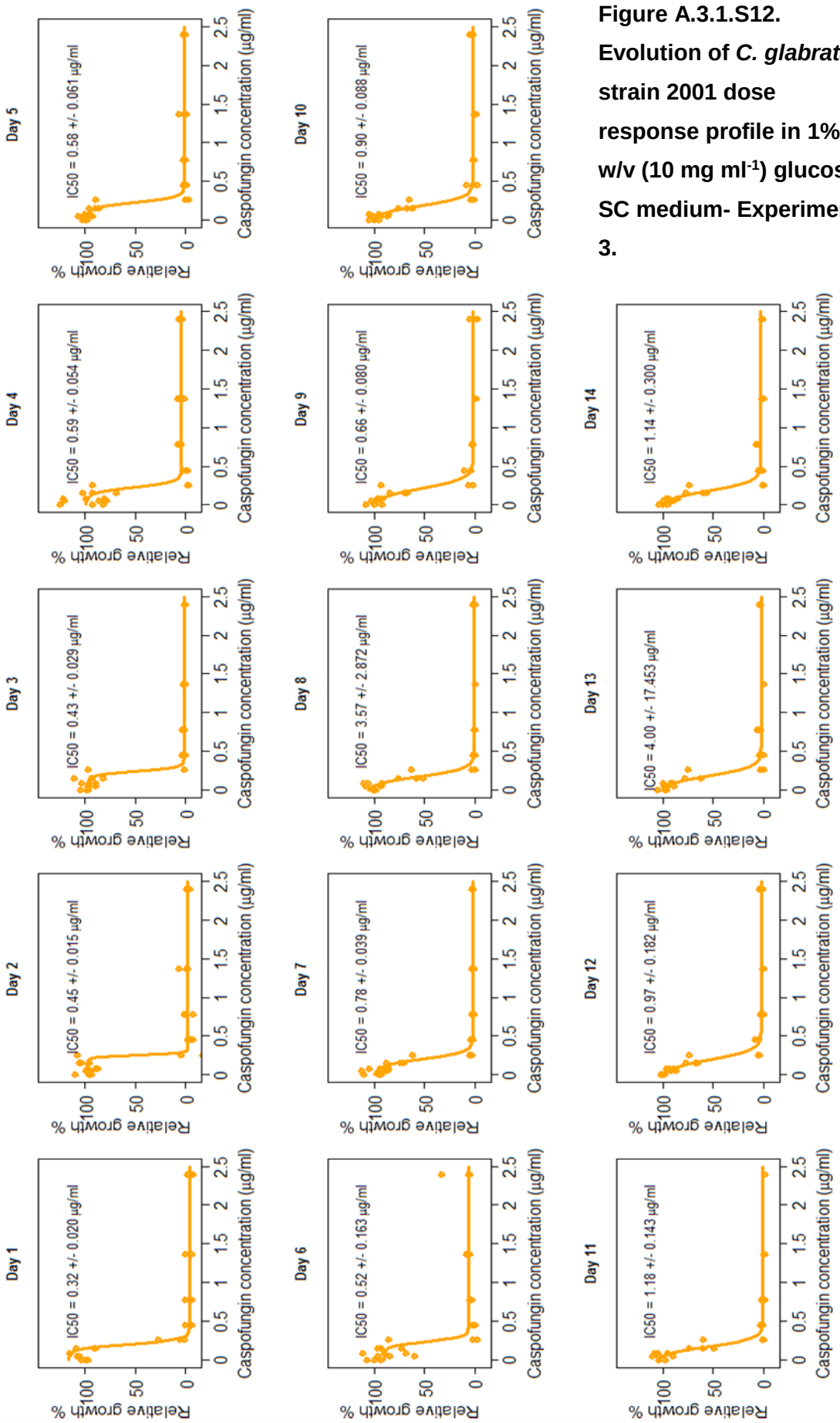

Figure A.3.1.S12. Evolution of *C. glabrata* strain 2001 dose response profile in 1% w/v (10 mg ml^{-1}) glucose SC medium- Experiment 3.

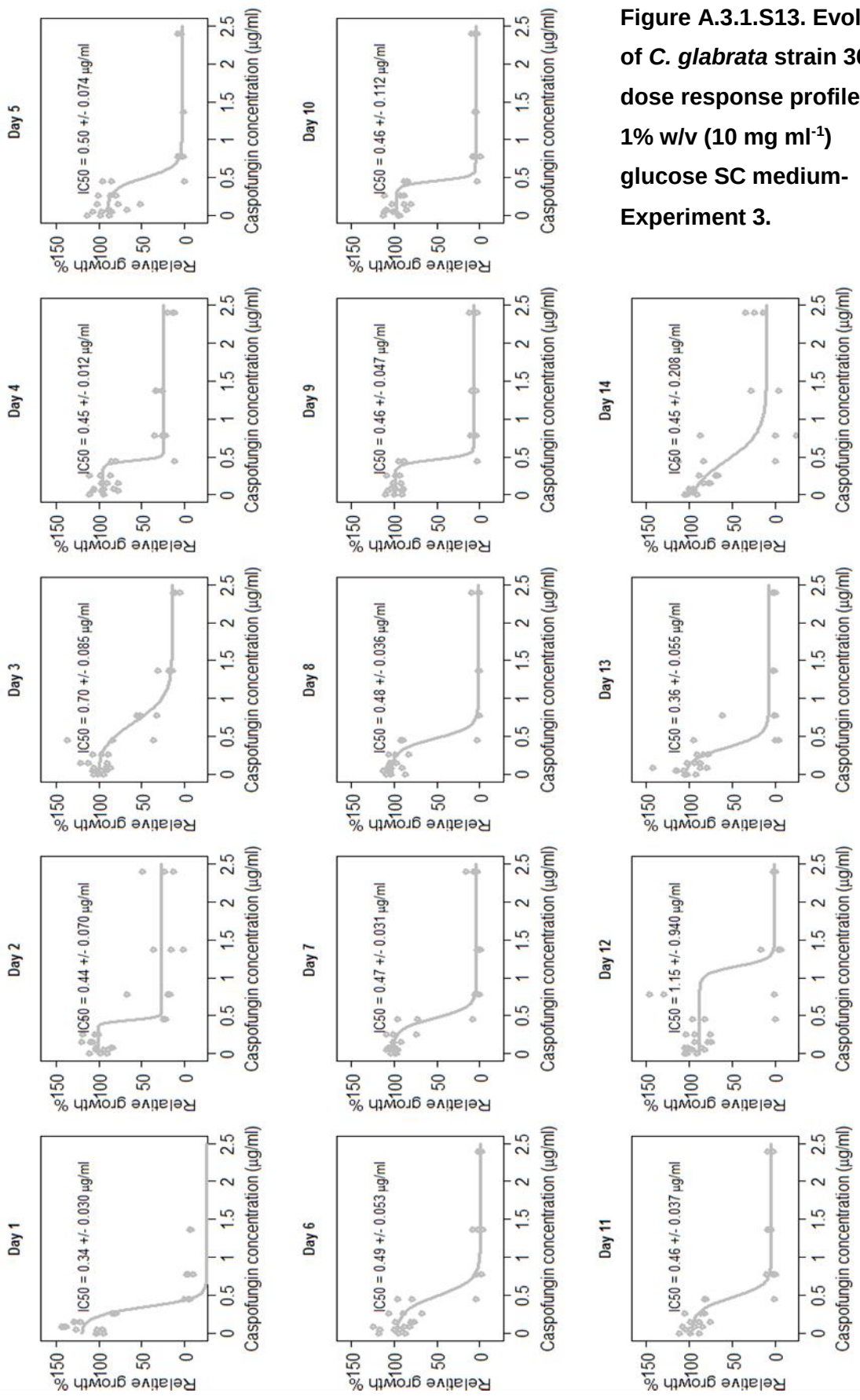

Figure A.3.1.S13. Evolution of *C. glabrata* strain 3605 dose response profile in 1% w/v (10 mg ml^{-1}) glucose SC medium- Experiment 3.

Figure A.3.1.S8-13. Evolution of populations of *C. glabrata* strains 2001 and 3605 on a gradient of caspofungin concentrations in 1% w/v (10 mg ml-1) glucose SC medium over 3 separate 14-day experiments. Each dose response profile plotted across evolving populations, shows growth of three replicate populations at eight caspofungin concentrations and a no drug control. Relative growth is the % growth of each replicate population relative to the no drug control, measured as optical density (OD) after 24 hours of growth of each replicate population divided by the mean OD of the no drug-treated population. All data points are shown and the solid line on each plot is the best-fit 4-parameter logistic model (R package 'drc'; Ritz *et al.*, 2015). Each plot shows estimated IC50 +/- SE. Note that dose responses were not measured on days 6 and 13 in Experiment 1.

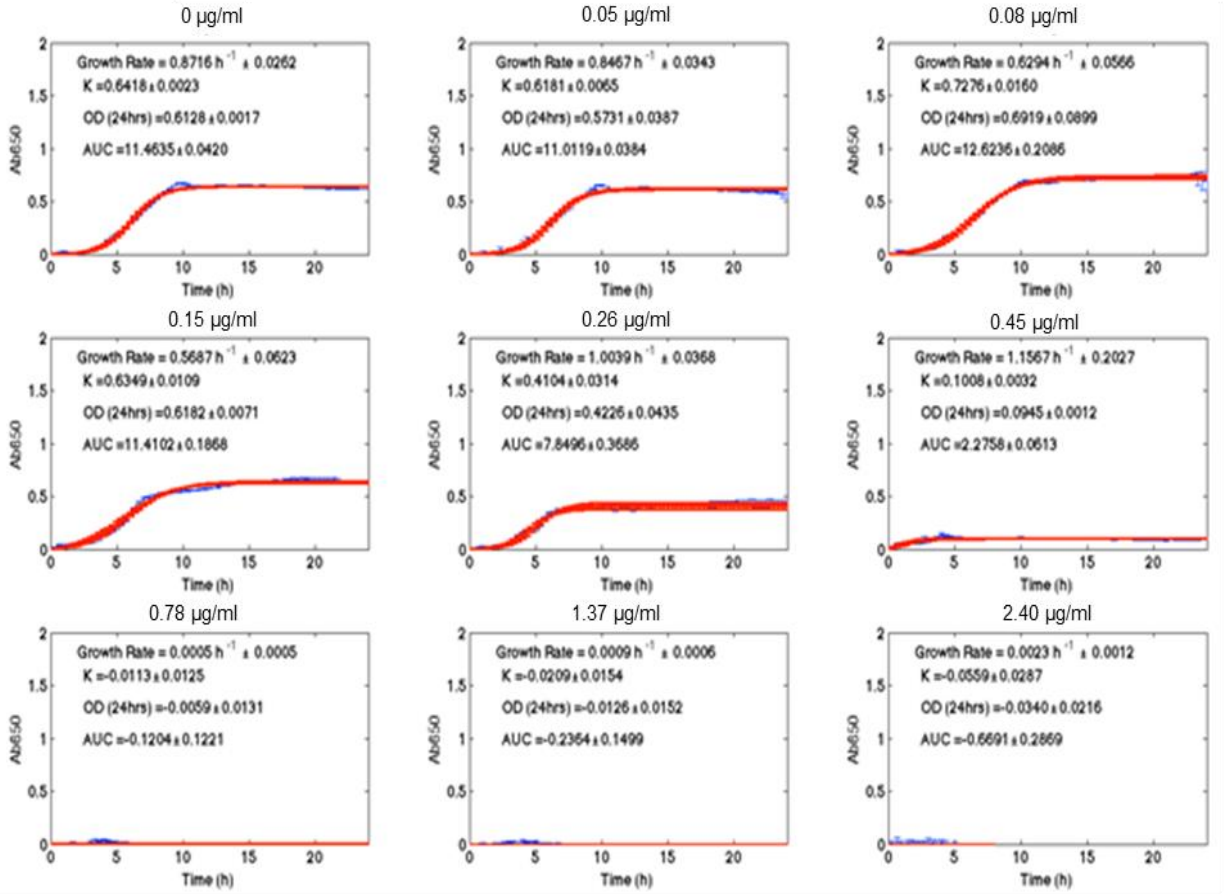

Figure A.3.1.S14. Strain 2001 growth kinetics- Experiment 3, day 1.

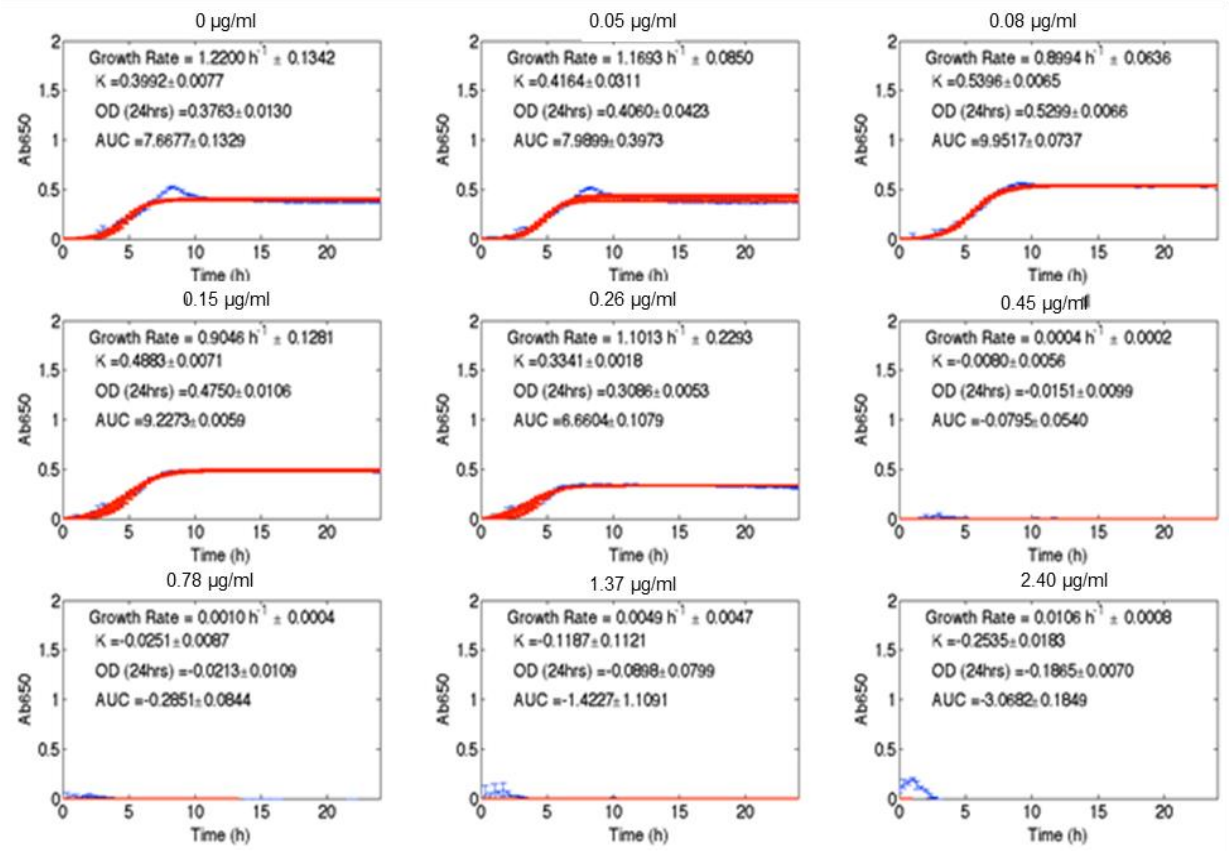

Figure A.3.1.S15. Strain 3605 growth kinetics- Experiment 3, day 1.

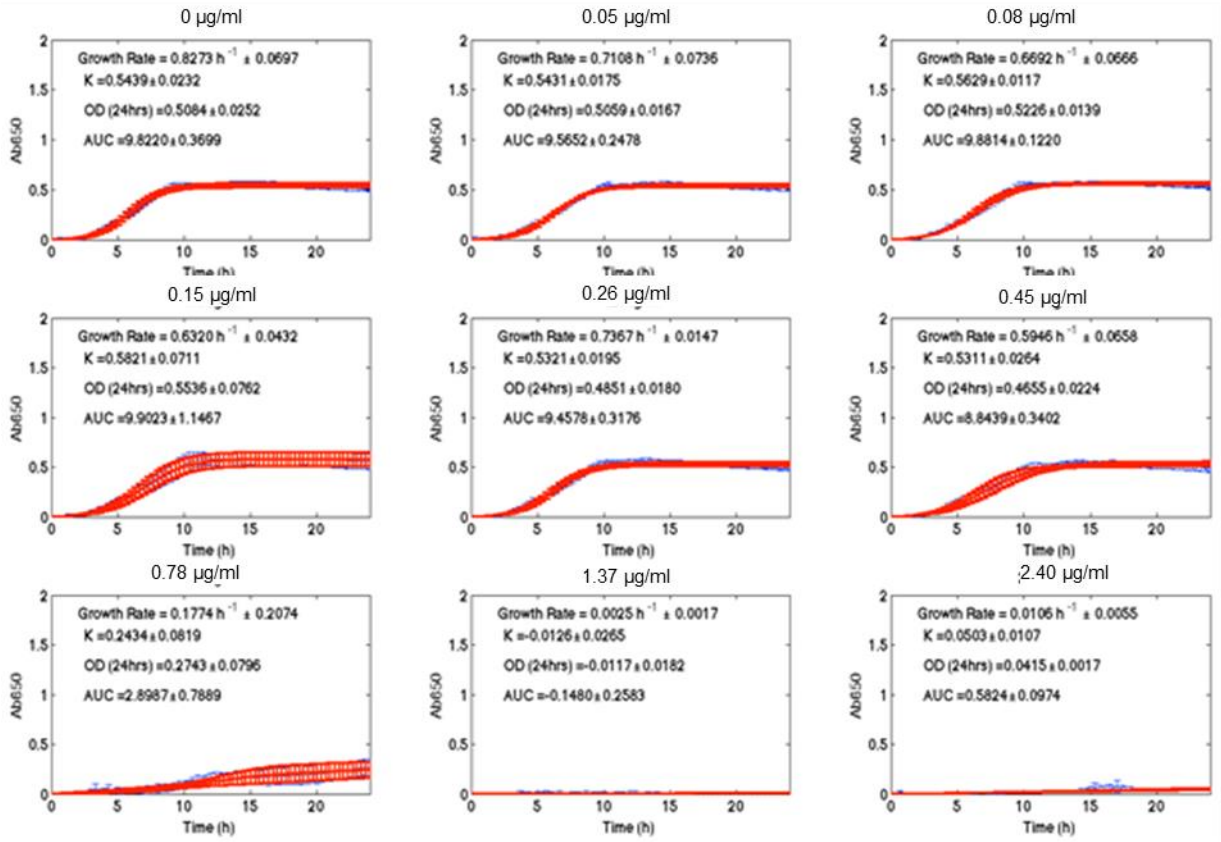

Figure A.3.1.S16. Strain 2001 growth kinetics- Experiment 3, day 7.

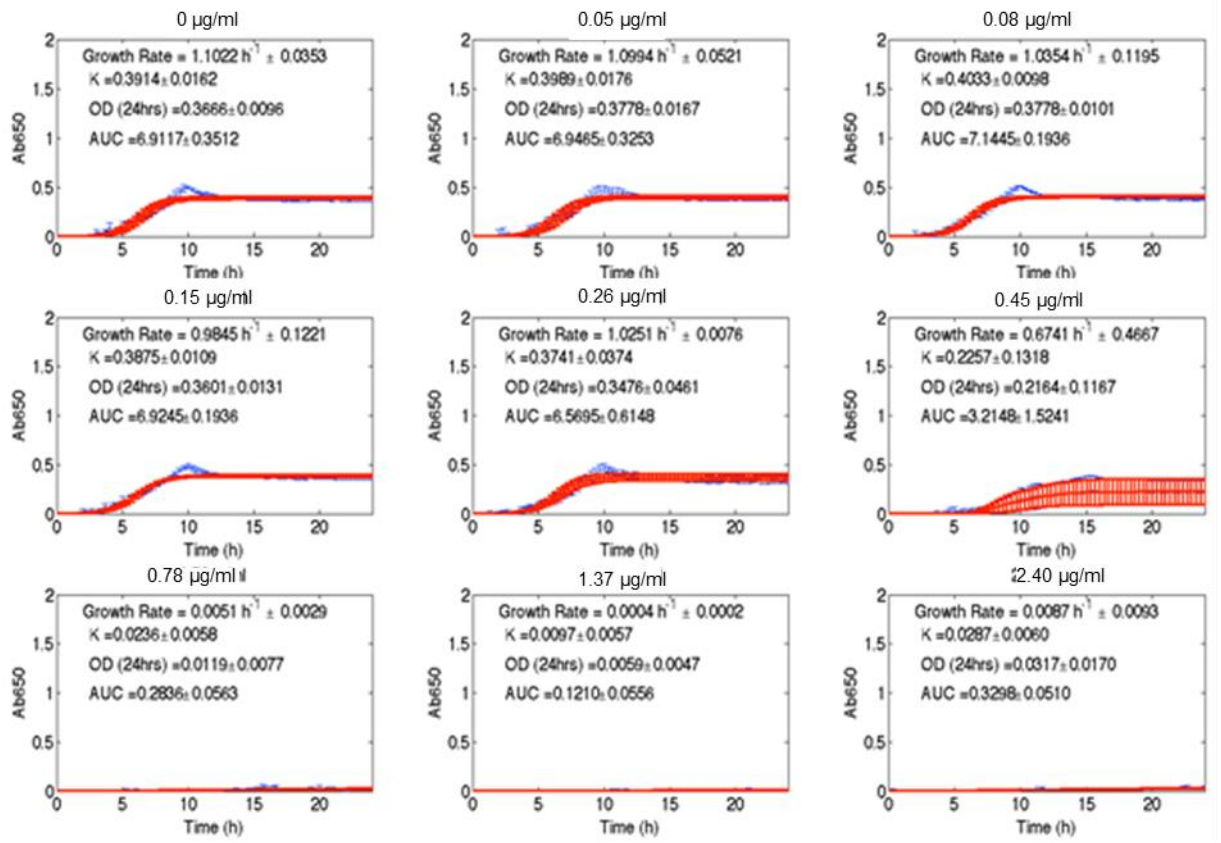

Figure A.3.1.S17. Strain 3605 growth kinetics- Experiment 3, day 7.

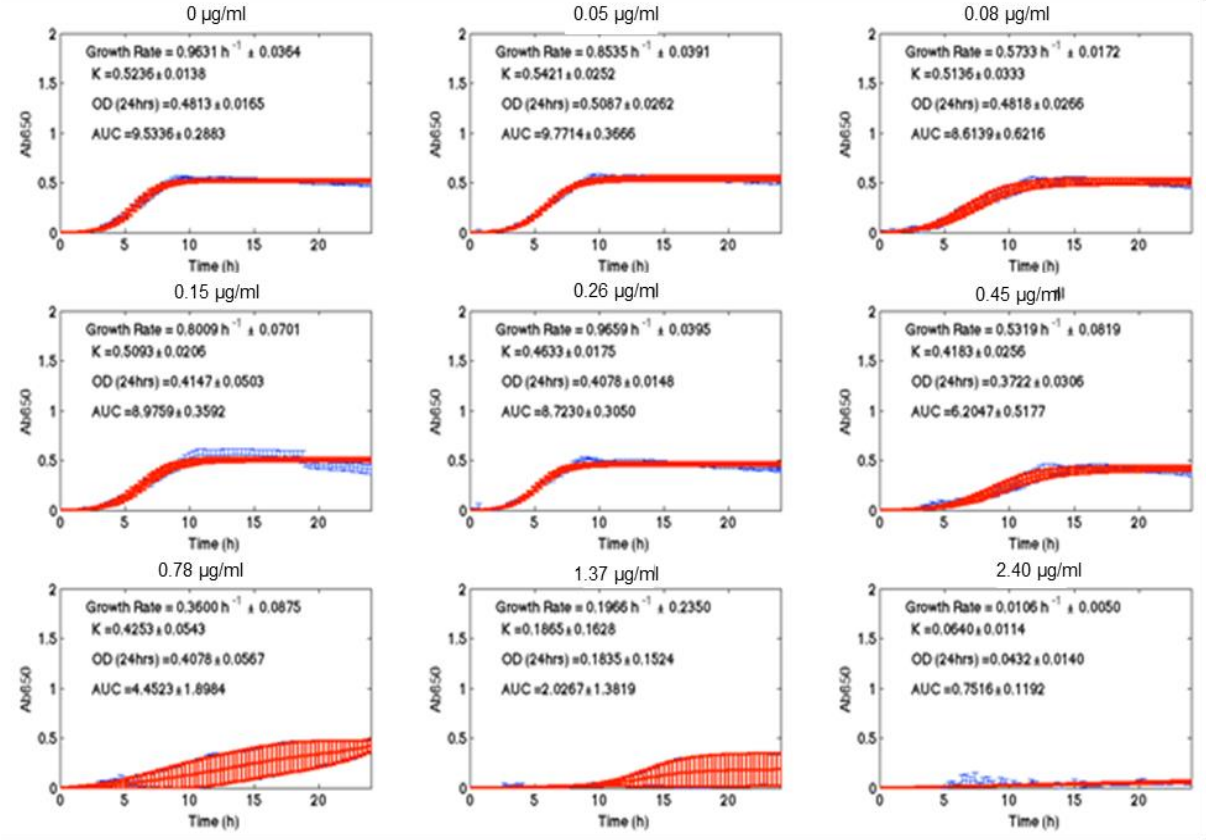

Figure A.3.1.S18. Strain 2001 growth kinetics- Experiment 3, day 14.

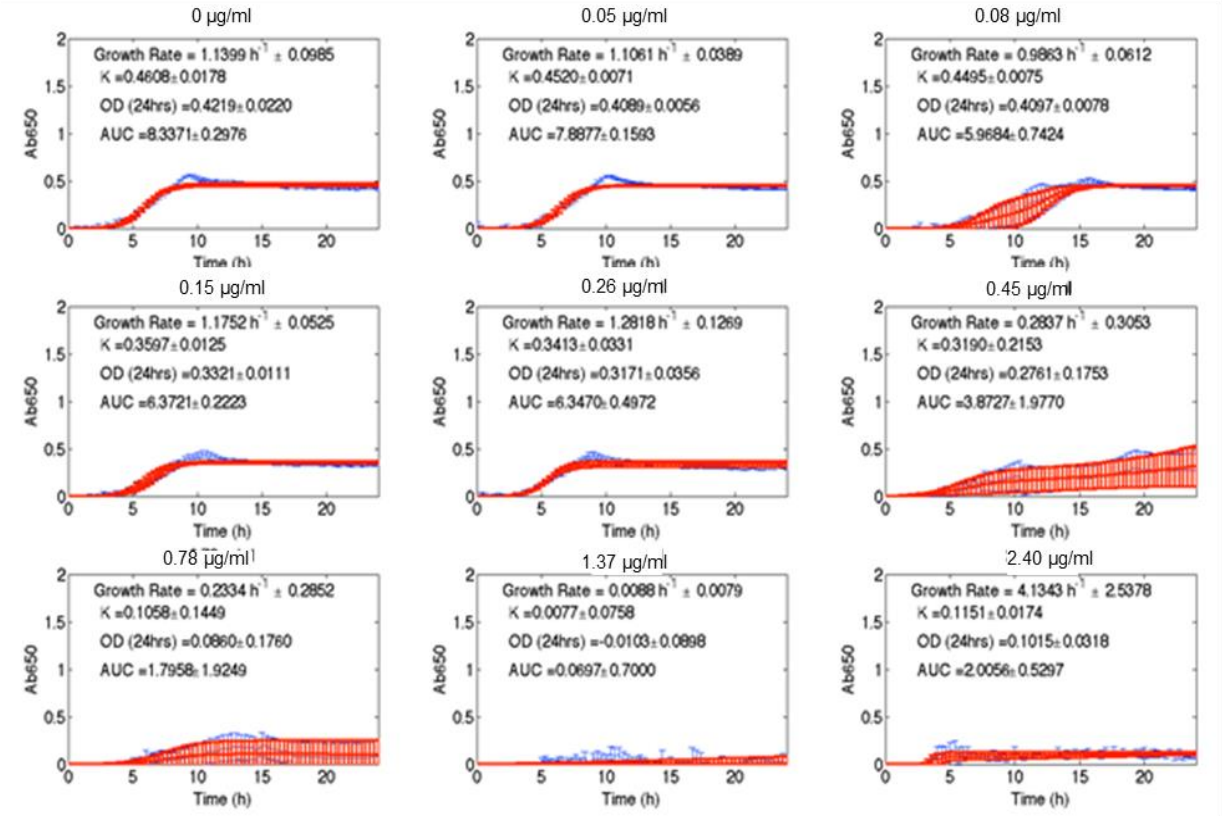

Figure A.3.1.S19. Strain 3605 growth kinetics- Experiment 3, day 14.

Figures A.3.1.S14-19. Growth kinetics of populations of *C. glabrata* strains 2001 and 3605 during evolution on a gradient of caspofungin concentrations in Experiment 3. Growth profile data is shown for the three replicate populations of each strain evolving at each of 8 caspofungin concentrations (0.05- 2.40 μg/ml) and no drug control at day 1 (initial season), day 7 (evolution midpoint) and day 14 (final season) for Experiment 3, as representative of the three 14-day evolution experiments. The blue line on each sub-plot labelled with a specific caspofungin concentration (μg/ml) shows change in mean OD (Ab650) of the three replicate populations with standard error bars, that were serially-transferred at that concentration over 14 days. The red line with error bars represents means and standard errors from the best-fit model prediction of logistic growth. Growth rate (r) and K (carrying capacity) were estimated from the model fit and final OD at 24hrs and AUC (Area Under Curve) were calculated from growth profile data. In all plots, yield and K are directly proportional as all populations were grown at the same glucose concentration (10 mg ml^{-1}).

Table A.3.1.S1. Statistical results for Strain 2001 dose response slope comparisons during caspofungin evolution. Data is presented for pairwise comparisons of the slope (gradient of the dose response: Hill coefficient) of the dose response model fit, comparing days 1, 7 and 14 from each of the three independent evolutionary experiments. See **Figure 4.9** (left panels) for plots of dose responses for days 1, 7 and 14. 'Estimate' represents the difference in the estimated slopes from the two dose response model fits, along with the standard error of the predicted difference. The *P*-value is presented for the null hypothesis that the difference between the two slope estimates is 0 (Ritz *et al.,* 2015).

Experiment/ Day comparison	**Estimate**	**Standard error**	**t-value**	***P*-value**
E1				
Day 1,7	-1.336828	10.378007	-0.128814	0.8979
Day 1,14	-0.950887	7.849947	-0.121133	0.9039
Day 7,14	0.385942	11.981738	0.032211	0.9744
E2				
Day 1,7	28.44084	8.33619	3.41173	0.0011
Day 1,14	26.45505	8.43861	3.13500	0.0025
Day 7,14	-1.98580	2.46053	-0.80706	0.4224
E3				

Day 1,7	6.6328	4.6184	1.4362	0.1555
Day 1,14	11.8122	4.0066	2.9482	0.0044
Day 7,14	5.1794	3.4872	1.4853	0.1420

Table A.3.1.S2. Statistical results for Strain 2001 IC50 comparisons during caspofungin evolution. Data is presented for pairwise comparisons of IC50 (50% inhibition of relative growth) between days 1, 7 and 14 from the three independent evolutionary experiments. See **Figure 4.9** (left panels) for plots of dose responses and IC50 values for days 1, 7 and 14. 'Estimate' represents the difference in the estimated IC50s from the two dose response model fits, along with the standard error of the predicted difference. The *P*-value is presented for the null hypothesis that the difference between the two IC50 estimates is 0 (Ritz *et al.,* 2015).

Experiment/ Day comparison	**Estimate**	**Standard error**	**t-value**	***P*-value**
E1				
Day 1,7	-0.41140	0.15098	-2.72486	0.0081
Day 1,14	-0.56714	0.20706	-2.73902	0.0078
Day 7,14	-0.15575	0.24488	-0.63603	0.5269
E2				
Day 1,7	-0.055059	1.786510	-0.030819	0.9755
Day 1,14	-1.187030	0.147994	-8.020780	0.0000
Day 7,14	-1.131971	1.792495	-0.631506	0.5298
E3				
Day 1,7	-0.462929	0.053968	-8.577904	0.0000
Day 1,14	-0.822344	0.228445	-3.599747	0.0006
Day 7,14	-0.359415	0.231780	-1.550677	0.1256

Table A.3.1.S3. Statistical results for Strain 3605 dose response slope comparisons during caspofungin evolution. Data is presented for pairwise comparisons of the slope (gradient of the dose response: Hill coefficient) of the dose response model fit, comparing days 1, 7 and 14 from each of the three independent evolutionary experiments. See **Figure 4.9** (right panels) for plots of dose responses for days 1, 7 and 14. 'Estimate' represents the difference in the estimated slopes from the two dose response model fits, along with the standard error of the predicted difference. The *P*-value is presented for the null hypothesis that the difference between the two slope estimates is 0 (Ritz *et al.,* 2015).

Experiment/ Day comparison	Estimate	Standard error	t-value	*P*-value
E1				
Day 1,7	4.53329	19.62506	0.23099	0.8180
Day 1,14	12.22120	10.68275	1.14401	0.2566
Day 7,14	7.68791	16.58974	0.46341	0.6445
E2				
Day 1,7	13.36121	10.32088	1.29458	0.1998
Day 1,14	19.30953	9.42642	2.04845	0.0443
Day 7,14	5.94832	8.70717	0.68315	0.4968
E3				
Day 1,7	3.59080	13.31957	0.26959	0.7883
Day 1,14	11.48590	5.87053	1.95653	0.0545
Day 7,14	7.89510	12.71709	0.62083	0.5368

Table A.3.1.S4. Statistical results for Strain 3605 IC50 comparisons during caspofungin evolution. Data is presented for pairwise comparisons of IC50 (50% inhibition of relative growth) between days 1, 7 and 14 from the three independent evolutionary experiments. See **Figure 4.9** (right panels) for plots of dose responses and IC50 values for days 1, 7 and 14. 'Estimate' represents the difference in the estimated IC50s from the two dose response model fits, along with the standard error of the predicted difference. The *P*-value is presented for the null hypothesis that the difference between the two IC50 estimates is 0 (Ritz *et al.,* 2015).

Experiment/ Day comparison	Estimate	Standard error	t-value	*P*-value
E1				
Day 1,7	-0.10788	0.11359	-0.94976	0.3456
Day 1,14	-0.24857	0.28774	-0.86386	0.3907
Day 7,14	-0.14068	0.28536	-0.49300	0.6236
E2				
Day 1,7	0.00014077	0.02355323	0.00597649	0.9952
Day 1,14	0.02222307	0.02810450	0.79072992	0.4318
Day 7,14	0.02208230	0.03001192	0.73578440	0.4644
E3				
Day 1,7	-0.132946	0.055470	-2.396710	0.0193

Day 1,14	-0.118399	0.163250	-0.725259	0.4707
Day 7,14	0.014547	0.166048	0.087609	0.9304

A.4 Chapter 5 Appendix

A.4.1 Supplementary Materials and Methods

Genomic DNA Extraction S. cerevisiae and S. pombe (method taken from Libuda (2007)

Protocol:

1. Grow a 10 ml overnight culture, spot onto YPD to check markers 2. Pellet cells, decant supernatant and resuspend in 0.5 ml water
3. Transfer to a 1.7 ml micro-centrifuge tube
4. Pellet 5 seconds and decant supernatant

5. Briefly vortex pellet to resuspend in remaining medium

6. Add: 0.2 ml Smash and Grab Solution 0.2 ml Phenol-Chloroform

0.3 grams Acid-washed glass beads

7. Vortex for 2-5 minutes using the multi-tube holder or 10 minutes on multi-tube vortexer in the cold room

8. Add 0.2 ml of TE to each tube
9. Spin 5 minutes in centrifuge
10. Transfer aqeous phase to new tube
11. Add 1.0 ml EtOH and mix to ethanol precipitate
12. Spin down 5 minutes, decant supernatant
13. Resuspend pellet in 0.4 ml TE
14. Add 30 µg RNase and incubate for 5 minutes at 370 15. Add 10 µl 4M ammonium acetate and 1.0 ml EtOH 16. Ethanol precipitate on ice for 5 minutes
17. Spin down 10 minutes
18. Optional wash with 0.5 ml 70% EtOH
19. Air dry pellet and resuspend in 100 µl TE

Smash and Grab Solution (100mL)

10 mL 10% SDS *(1%)*
2 mL 100x Triton-X100 *(2%)* 2 mL 5 M NaCL *(100mM)*
1 mL 1 M Tris pH 8.0 *(10 mM)*

(1 mM)

Mix in beaker, adding the detergents while the solution is mixing. Filter sterilise.

Wizard® SV Gel and PCR Clean-Up System

INSTRUCTIONS FOR USE OF PRODUCTS A9280, A9281, A9282, AND A9285.

Quick PROTOCOL

DNA Purification by Centrifugation

Gel Slice and PCR Product Preparation

A. Dissolving the Gel Slice

1. Following electrophoresis, excise DNA band from gel and place gel slice in a 1.5ml microcentrifuge tube.
2. Add 10µl Membrane Binding Solution per 10mg of gel slice. Vortex and incubate at 50–65°C until gel slice is completely dissolved.

B. Processing PCR Amplifications

1. Add an equal volume of Membrane Binding Solution to the PCR amplification.

Binding of DNA

1. Insert SV Minicolumn into Collection Tube.
2. Transfer dissolved gel mixture or prepared PCR product to the Minicolumn assembly. Incubate at room temperature for 1 minute.
3. Centrifuge at 16,000 × *g* for 1 minute. Discard flowthrough and reinsert Minicolumn into Collection Tube.

Washing

4. Add 700µl Membrane Wash Solution (ethanol added). Centrifuge at 16,000 × *g* for 1 minute. Discard flowthrough and reinsert Minicolumn into Collection Tube.
5. Repeat Step 4 with 500µl Membrane Wash Solution. Centrifuge at 16,000 × *g* for 5 minutes.
6. Empty the Collection Tube and recentrifuge the column assembly for 1 minute with the microcentrifuge lid open (or off) to allow evaporation of any residual ethanol.

Elution

7. Carefully transfer Minicolumn to a clean 1.5ml microcentrifuge tube.
8. Add 50µl of Nuclease-Free Water to the Minicolumn. Incubate at room temperature for 1 minute. Centrifuge at 16,000 × *g* for 1 minute.
9. Discard Minicolumn and store DNA at 4°C or –20°C.

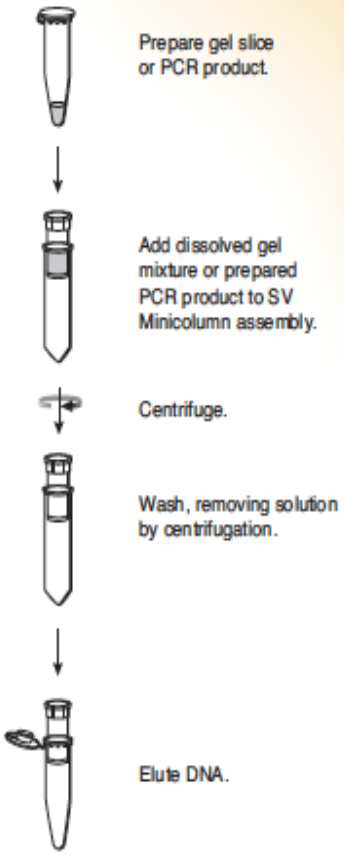

3760MA07_2A

Additional protocol information is available in Technical Bulletin #TB308, available online at:
www.promega.com

ORDERING/TECHNICAL INFORMATION:
www.promega.com • Phone 608-274-4330 or 800-356-9526 • Fax 608-277-2601

Printed in USA. Revised 11/09
Part #9FB072

Table A.4.1.S1. Primers for PCR amplification and Sanger sequencing of caspofungin resistance gene targets. Five gene target regions of *C. glabrata* were amplified using forward and reverse primers described previously (Thompson *et al.,* 2008; Zimbeck *et al.,* 2010; Singh-Babak *et al.,* 2012). The *FKS1* and *FKS2* genes are homologous.

Gene target	Primer	Primer sequence (5'- 3')
FKS1 HS1	FKS1HS1F FKS1HS1R	CCATTGGGTGGTCTGTTCACG GATTGGGCAAAGAAAGAAATACGAC
FKS2 HS1	FKS2HS1F FKS2HS1R	GCTTCTCAGACTTTCACCG CAGAATAGTGTGGAGTCAAGACG
FKS1 HS2	FKS1HS2F FKS1HS2R	GGTATTTCAAAGGCTCAAAAGGG ATGGAGAGAACAGCAGGGCG
FKS2 HS2	FKS2HS2F FKS2HS2R	TCTTGACTTTCTACTATGCG CTTGCCAATGTGCCACTG
CDC6	CDC6F CDC6R	TCGCTGTACATAACAGGTCC CAGTATATGGTTGAAAGACC

A.4.2 Supplementary Figures and Tables

Table A.4.2.S1. Comparison of growth rate (1/h) and final OD (24 hours) across population colonies at different caspofungin concentrations, revived from day 14 of the first experimental 14-day caspofungin evolution. Populations were revived from the 3 highest caspofungin concentrations and the no-drug control. Growth rates relative to the strain 2001 WT ancestor were calculated for 12 replicates of each population colony at each drug concentration. Growth rates were statistically compared across population colonies for each drug concentration and the WT ancestor (N = number of population colonies compared): 0.00 µg/ml: N = 7; 0.78 µg/ml: N = 13; 1.37 µg/ml: N = 8; 2.40 µg/ml N = 7. The Kruskal-Wallis test was used to identify between-colony differences as colony sample data was non-normally distributed.

Caspofungin concentration (μg/ml)	**Kruskal-Wallis chi-squared**	**df**	***P*-value**
Growth rate (h^{-1})			
0.00	10.741	6	0.09672
0.78	67.902	12	7.891e-10
1.37	39.806	7	1.371e-06
2.40	6.0784	6	0.4145
OD (24 hours)			
0.00	6.772	6	0.3424
0.78	41.448	12	4.123e-05
1.37	27.214	7	0.000305
2.40	12.393	6	0.05376

Table A.4.2.S2. Significant pairwise differences in growth rate (h^{-1}) and final OD (24 hours) between population colonies revived from day 14 following evolution at 0.78 μg/ml or 1.37 μg/ml in the first caspofungin dose response evolution. Growth rate, 0.78 μg/ml: Kruskal-Wallis test- *P* = 7.891e-10; Welch's ANOVA for unequal variances- $F_{12.00,\ 54.95}$ = 28.425, *P* < 2.2e-16; One-way ANOVA- $F_{12,143}$ = 11.58; *P* = 4.94e-16. Growth rate, 1.37 μg/ml: Kruskal-Wallis test (*P* = 1.371e-06); One-way ANOVA: $F_{7,88}$ = 5.07, *P* = 7.27e-05. OD (24 hours), 0.78 μg/ml: Kruskal-Wallis test (*P* = 4.123e-05); Welch's ANOVA for unequal variances ($F_{12.00,\ 55.17}$ = 12.859, *P* = 5.331e-12); One-way ANOVA: $F_{12,143}$ = 3.424; *P* = 0.000196. OD (24 hours), 1.37 μg/ml: Kruskal-Wallis test (*P* = 0.000305); Welch's ANOVA: $F_{7.00,\ 36.99}$ = 16.551, *P* = 1.161e-09; One-way ANOVA: $F_{7,88}$ = 4.856; *P* = 0.000116. Due to test results concordance, we used Tukey's *post hoc* test to deduce pairwise significant between-colony differences in growth rate. The colonies shown in bold are significantly different from the others listed in the respective row.

Pairwise comparisons between population colonies	**Adjusted *P*-value**
Growth rate (h^{-1}): 0.78 μg/ml	
2001WT- P1C2; P1C3; P1C4	0.0000
2001WT- P2C1	0.0348
P1C1- P1C2; P1C3; P1C4	< 0.001

P1C2- P2C1; P2C2; P2C3; P2C4; P3C1; P3C2; P3C3; P3C4	< 0.001
P1C3- P2C3; P2C4; P3C2	< 0.05
P1C3- P3C1; P3C3	< 0.01
P1C3- P3C4	0.0001
P1C4- P2C3; P2C4; P3C1; P3C2	< 0.05
P1C4- P3C3	0.0032
P1C4- P3C4	0.0003
Growth rate (h^{-1}): 1.37 μg/ml	
P2C2- 2001WT	0.0482
P1C2- P2C2; P3C2	< 0.05
P1C3- P2C2	0.0007
P1C3- P3C2	0.0013
P2C1- P2C2; P3C2	< 0.05
OD (24 hours): 0.78 μg/ml	
P1C2- P1C4; P3C1	< 0.05
P1C2- P2C2; P3C3; P3C4	< 0.01
P2C3- P3C3	0.0469
OD (24 hours): 1.37 μg/ml	
P3C2- 2001WT; P1C2	< 0.05
P3C2- P1C3; P2C1; P2C2	< 0.01

Table A.4.2.S3. Significant pairwise differences in relative growth rate (h^{-1}) and relative OD (24 hours) between population colonies revived from day 14 in Experiment 2 of 14-day caspofungin evolution. Growth rate, 0.00 μg/ml: One-way ANOVA- (*P* = 5.27e-09). Growth rate, 0.78 μg/ml: One-way ANOVA (*P* = 2.08e-13). OD (24 hours): 0.00 μg/ml: Kruskal-Wallis test (*P* = 0.0006098); One-way ANOVA: *P* = 3.68e-05. OD (24 hours), 0.78 μg/ml: Kruskal-Wallis test (*P* = 4.521e-05); One-way ANOVA: *P* = 3.84e-07. We used Tukey's *post hoc* test to deduce significant pairwise colony differences in growth rate. The colonies shown in bold are significantly different from the others listed in the respective row.

Pairwise comparisons between population colonies	**Adjusted *P*-value**
Growth rate (h^{-1}): 0.00 μg/ml	
2001WT- M1C2	0.0159
2001WT- M2C1; M2C2; M3C1; M3C2	< 0.001
M1C1- M2C1; M3C2	< 0.05
M1C1- M3C1	0.0004
M3C1- M1C2	0.0059
Growth rate (h^{-1}): 0.78 μg/ml	
2001WT- P2C2	0.0442
P3C1- 2001WT; P1C1; P1C2; P2C1; P2C2	0.0000
P3C2- 2001WT; P1C1; P1C2; P2C1; P2C2	0.0000
OD (24 hours): 0.00 μg/ml	
2001WT- M1C2	0.0024
2001WT- M2C2	0.0001
M1C2- M3C1	0.0426
M2C2- M2C1; M3C1	< 0.01
OD (24 hours): 0.78 μg/ml	
2001WT- P2C1; P2C2; P3C2	< 0.001
2001WT- P3C1	0.0156
P2C2- P1C1; P1C2	< 0.05

Table A.4.2.S4. Significant pairwise differences in growth rate (h^{-1}) and OD (24 hours) between population colonies revived from day 14 from Experiment 3 of caspofungin evolution. Growth rate, 0.00 μg/ml: One-way ANOVA (*P* = 8.11e-12). Growth rate, 0.78 μg/ml: One-way ANOVA (*P* < 2e-16). OD (24 hours), 0.78 μg/ml: Kruskal-Wallis test (*P* = 0.0001041); Welch's ANOVA for unequal variances: *P* = 1.127e-09; One-way ANOVA: *P* = 1.46e-08. We used Tukey's *post hoc* test to deduce pairwise significant between-colony differences in growth rate. The colonies shown in bold are significantly different from the others listed in the respective row.

Pairwise comparisons between population colonies	**Adjusted *P*-value**
Growth rate (h^{-1}): 0.00 μg/ml	
2001WT- M1C1	0.0031
2001WT- M1C2; M2C1; M2C2; M3C1; M3C2	< 0.0001
M1C1- M1C2; M2C1; M2C2; M3C1; M3C2	< 0.05
Growth rate (h^{-1}): 0.78 μg/ml	
2001WT- P1C2; P2C2; P3C1; P3C2	0.0000
P1C1- P1C2; P2C2; P3C1; P3C2	0.0000
P1C2- P2C1; P2C2; P3C1; P3C2	0.0000
P2C1- P2C2; P3C1; P3C2	< 0.01
P3C2- P2C2; P3C1	< 0.001
OD (24 hours): 0.78 μg/ml	
2001WT- P1C1; P1C2	< 0.0001
P1C1- P1C2; P3C2	< 0.001
P1C2- P2C1; P2C2; P3C1	0.0000
P1C2- P3C2	0.0019

Table A.4.2.S5. Comparison of IC50 and slope (gradient) parameters for the 4-parameter logistic dose response model fit for colony variants from Experiment 1. See **Figure 5.6** for dose response profiles. R-package 'drc' was used for dose response fitting and parameter comparison (Ritz *et al.,* 2015; Roemhild *et al.,* 2015). Note that WT-MA and MA-LCV comparisons could not be reported as 'NA' was returned in statistical results.

Colony comparison	**Estimate**	**SE**	**t-value**	***P*-value**
IC50				
WT-LCV	0.0555414	0.0276071	2.0119	0.0454
Slope				
WT-LCV	-70.684	158.385	-0.4463	0.6558

Table A.4.2.S6. Comparison of IC50 and slope (gradient) parameters for the 4-parameter logistic dose response model fit for colony variants from Experiment 3. See **Figure 5.7** for dose response profiles. R-package 'drc' was used for dose response fitting and parameter comparison (Ritz *et al.*, 2015; Roemhild *et al.,* 2015).

Colony comparison	**Estimate**	**SE**	**t-value**	***P*-value**
IC50				
WT-MA	0.071381	0.054660	1.3059	0.1940227
WT-LCV	-0.500325	0.149573	-3.3450	0.0010912
MA-LCV	-0.571706	0.154138	-3.7091	0.0003134
Slope				
WT-MA	-93.183	354.686	-0.2627	0.7932
WT-LCV	-21.797	117.900	-0.1849	0.8536
MA-LCV	71.386	373.758	0.1910	0.8488

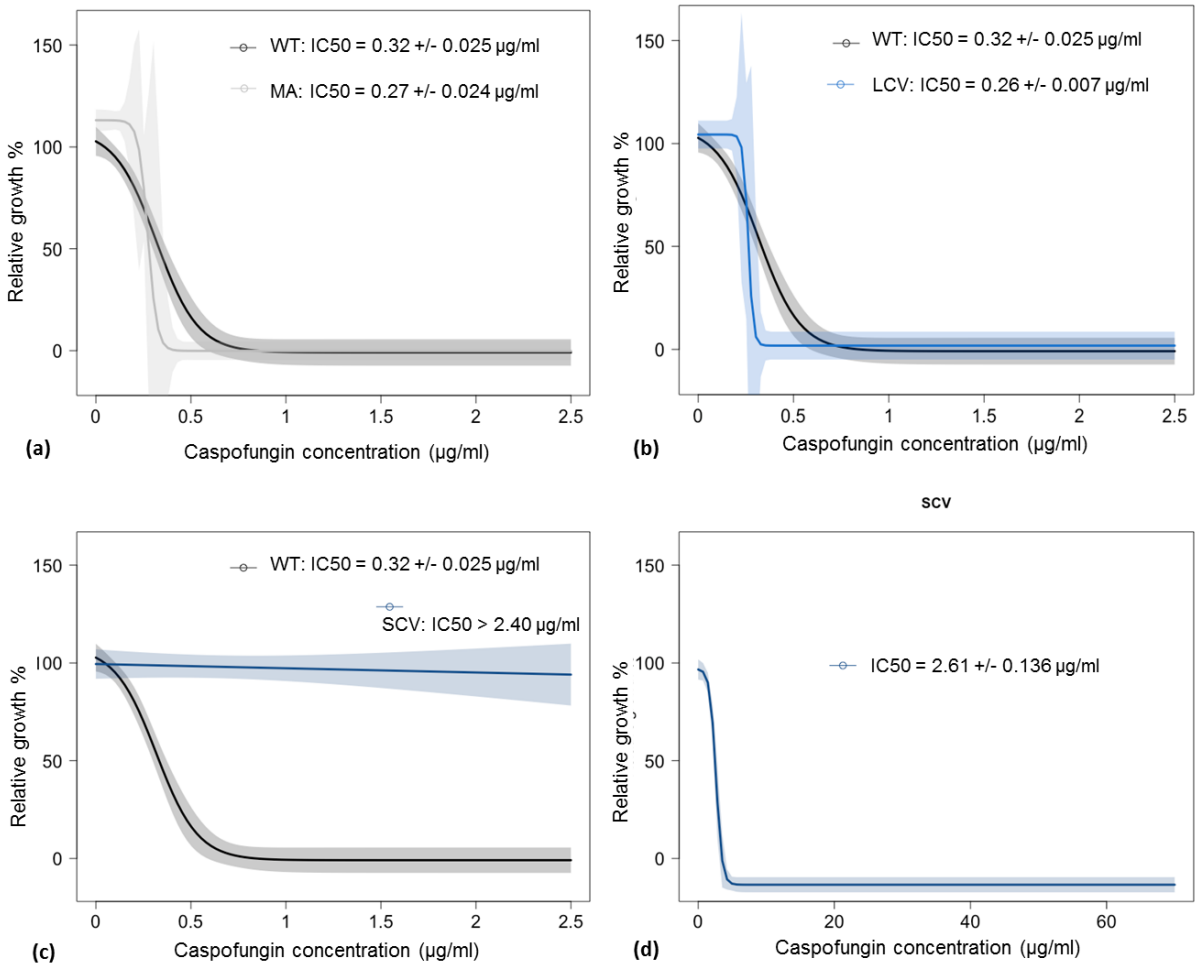

Figure A.4.2.S1. Dose response model predictions with confidence regions for *C. glabrata* strain 2001 WT ancestor and colony variants from day 14 of Experiment 1 of caspofungin evolution. Dose responses show predicted relative growth % which is measured as final optical density (24 hours) of caspofungin-grown cells as a percentage of mean final OD of media-alone grown cells. Four parameter logistic dose response curves with 95% confidence interval shaded regions were fitted using the R package "drc" (Ritz *et al.*, 2015), as described by Roemhild *et al.* (2015) and were used to predict the IC50: 50% growth inhibitory concentration of caspofungin presented on the plots (with SE of the estimated value) for each strain. **(a), (b), (c):** WT dose response is estimated from combined data from day 1 of the three independent 14-day caspofungin evolution experiments described in Chapter 4 (N = 9 for each caspofungin concentration). Dose responses for the other colony variants in all plots are fitted to pooled data from three 24-hour dose responses performed on separate days (N = 9 for each caspofungin concentration). **(a)** WT dose response compared with M1C1 (MA)- a single media-adapted colony. **(b)** WT compared with LCV (large colony variant); comparison of IC50: $P = 0.0454$; comparison of slope: $P = 0.6558$. **(c)** WT compared with SCV (small colony variant). **(d)** Dose response for the SCV at a higher range of

caspofungin concentrations: 2-fold dilutions ranging 0 – 64 µg/ml. The 4-parameter logistic dose response model was fitted to estimate IC50.

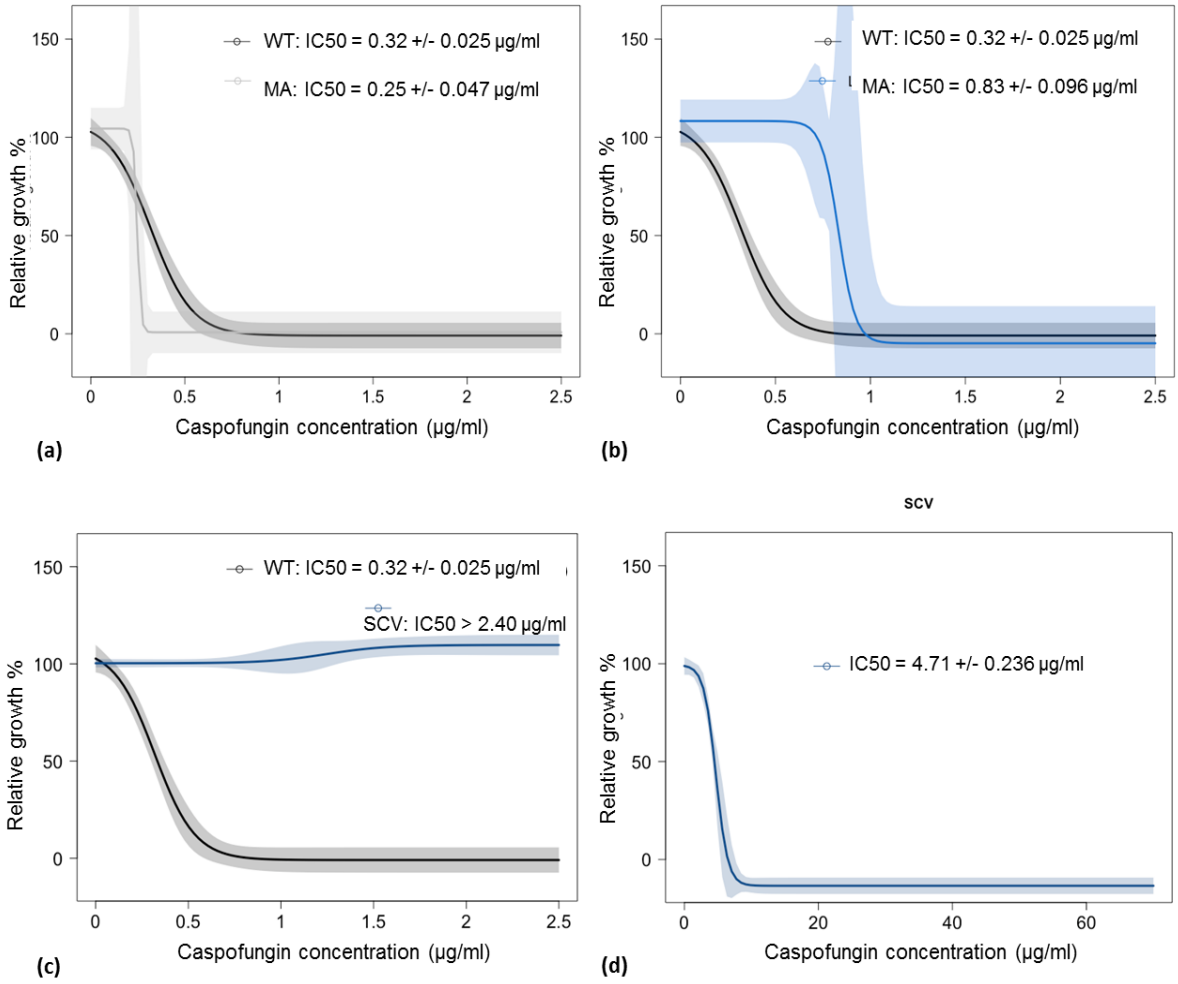

Figure A.4.2.S2. Dose response profile predictions with confidence regions for *C. glabrata* strain 2001 WT ancestor and colony variants from day 14 of Experiment 3 of caspofungin evolution. Dose responses show predicted relative growth % which is measured as final optical density (24 hours) of caspofungin-grown cells as a percentage of mean final OD of media-alone grown cells. Four parameter logistic dose response curves with 95% confidence interval shaded regions were fitted using the R package "drc" (Ritz *et al.*, 2015), as described by Roemhild *et al.* (2015) and fits were used to predict the IC50: 50% growth inhibitory concentration of caspofungin presented on the plots (with SE of the estimated value) for each strain. **(a), (b), (c):** WT dose response is estimated from combined data from day 1 of the three independent 14-day caspofungin evolution experiments described in Chapter 4 (N = 9 for each caspofungin concentration). Dose responses for the other colony variants in all plots were fitted to single 24-hour dose responses performed on separate days (N = 3 for each caspofungin concentration). **(a)** WT dose response compared with M1C1 (MA)- a

single media-adapted colony; comparison of IC50: *P* = 0.1940; comparison of slope: 0.7932. **(b)** WT compared with LCV (large colony variant); comparison of IC50: *P* = 0.0011; comparison of slope: *P* = 0.8536. **(c)** WT compared with SCV (small colony variant). Note that no model fit is shown for SCV as the data do not fit a sigmoidal shape as none of the caspofungin concentrations tested were inhibitory. **(d)** Dose response for the SCV at a higher range of caspofungin concentrations: 2-fold dilutions ranging 0 – 64 µg/ml. The 4-parameter logistic dose response model was fitted to estimate IC50.

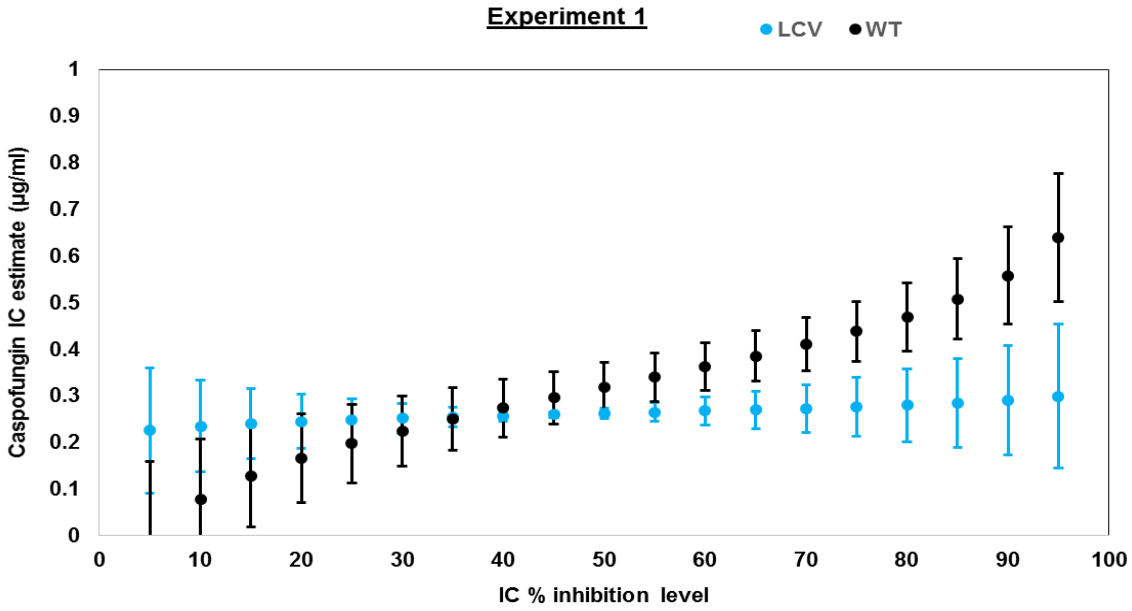

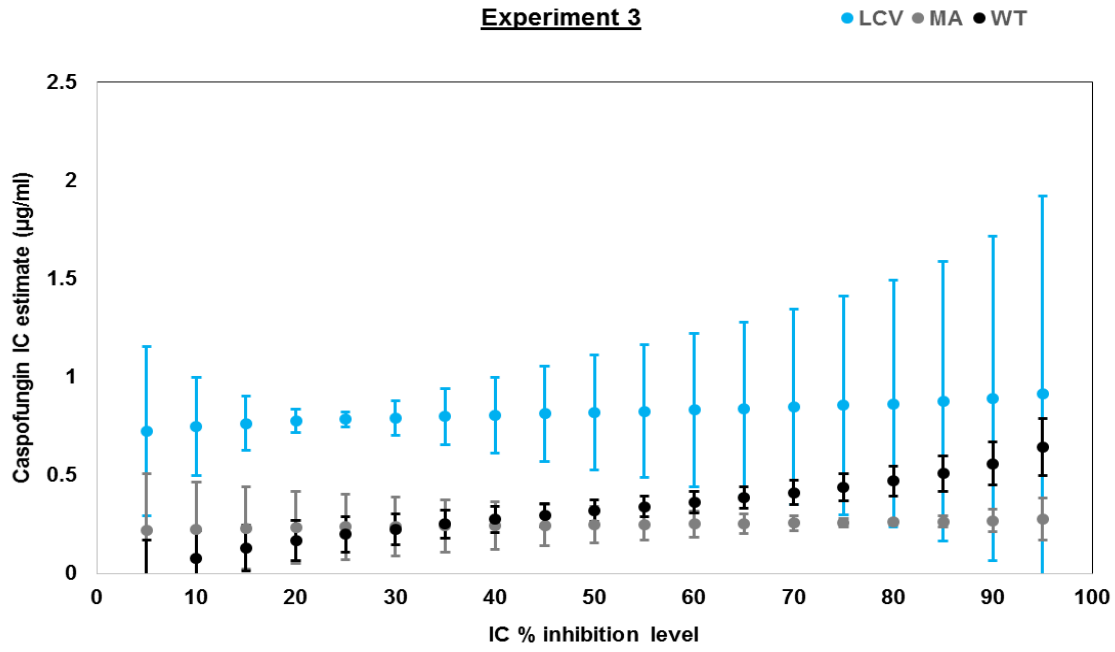

Figure A.4.2.S3. Caspofungin IC estimates over a range of inhibitory levels from dose-response fits to sensitivity tests of the wild-type ancestral strain of *C. glabrata* 2001, media-adapted and large colony variants. Following fitting of 4-parameter logistic dose response profiles to strain data from Experiments 1 (**Figure A.4.2.S1**) and 3 (**Figure A.4.2.S2**), the R-package 'drc' (Ritz *et al.*, 2015) was used to calculate IC (inhibitory Concentration) estimates for growth inhibitory levels ranging 5 - 95%, with 5% increments. The estimated inhibitory caspofungin concentrations (µg/ml) are plotted with 95% confidence intervals from the model predictions. Data from the WT ancestor (black), media-adapted (grey) and LCV (large colony variant) (blue) are plotted and significant differences between IC estimates between strains at each inhibitory level are deduced from non-overlapping 95% confidence intervals, indicating statistical significance at $P < 0.05$ (Greenland *et al.,* 2016). Note that the caspofungin IC estimates are plotted on different scales in the two plots, due to higher caspofungin sensitivity of the large colony variant in biological replicate 1 than 3. Data for media-adapted strains from the two independent experiments is highly similar (**Figure A.4.2.S1; S2**) and is only presented on one plot.

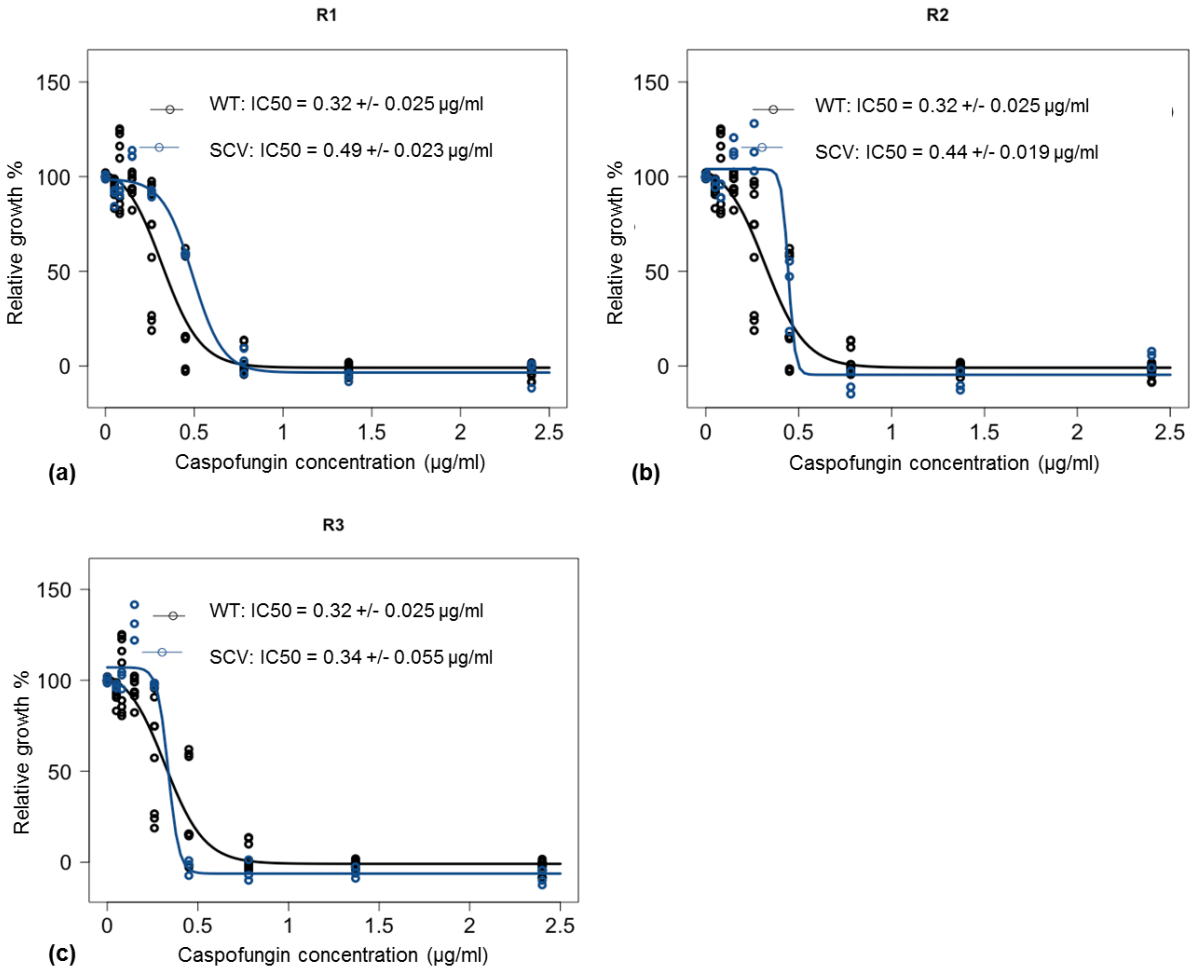

Figure A.4.2.S4. Dose response profiles for the *C. glabrata* ATCC 2001 WT ancestor and a single colony from each of three replicate populations founded from the SCV from Experiment 3 after 14 days propagation without caspofungin. Similar to **Figure 5.7**, dose responses show relative growth % with four parameter logistic model fits to the data using the R package "drc" (Ritz *et al.*, 2015), as described by Roemhild *et al.* (2015). Each plot shows the dose response from a separate replicate population (N = 3 for each caspofungin concentration), in comparison to the wild-type ancestor (N = 9 per caspofungin concentration). Comparison of IC50 values to WT: **(a)** $P = 0.0003355$, **(b)** $P = 0.004628$, **(c)** $P = 0.7972$. Comparison of gradient (slope) values to WT: **(a)** $P = 0.7081$, **(b)** $P = 0.9064$, **(c)** $P = 0.2990$.

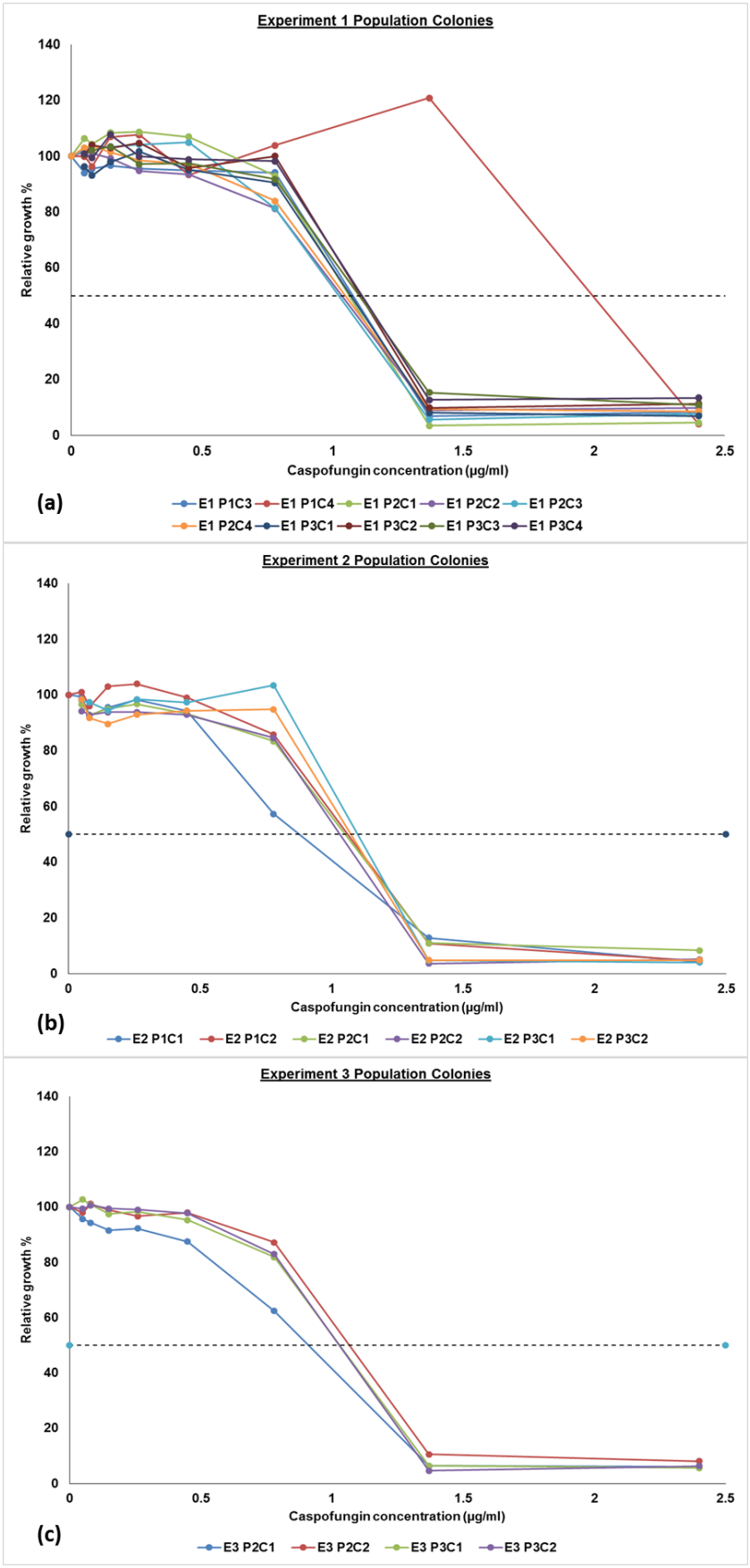

Figure A.4.2.S5. Pilot dose response assays for the revived population colonies of *C. glabrata* strain 2001 evolved at 0.78 µg/ml for 14 days in three independent

experiments. Dose response assays are presented for colonies that were revived from populations evolved at 0.78 µg/ml in the three independent 14-day experiments for which fitness costs in the absence of caspofungin were tested, apart from the SCV and LCV colonies from Experiments 1 and 3. Relative growth was calculated as the final OD at 24 hours of a drug-treated population as a percentage of the final OD of the no-drug treated population. Relative growth was measured for a single replicate of each drug concentration per population colony. The dotted line on each plot represents 50% relative growth inhibition and the IC50 for each population colony is approximated from the intersect of the dotted line with the dose response profile. Population colonies: (a) Experiment 1; (b) Experiment 2; (c) Experiment 3.

Bibliography

Alexander, B.D., Johnson, M.D., Pfeiffer, C.D., Jimenez-Ortigosa, C., Catania, J., Booker, R., Castanheira, M., Messer, S.A., Perlin, D.S. & Pfaller, M.A. (2013). Increasing echinocandin resistance in *Candida glabrata*: clinical failure correlates with presence of FKS mutations and elevated minimum inhibitory concentrations. *Clinical Infectious Disease,* 56(12), 1724-1732.

Allison, K. R., Brynildsen, M. P., & Collins, J. J. (2011). Metabolite-enabled eradication of bacterial persisters by aminoglycosides. *Nature*, 473(7346), 216.

Alvarado-Ramirez E, Torres-Rodriguez JM, Sellart M, Vidotto V (2008). Laccase activity in *Cryptococcus gattii* strains isolated from goats. *Revista Iberoamericana Micología,* 25(3), 150–153.

Alves, C.T., Wei, X.Q., Silva, S., Azeredo, J., Henriques, M. & Williams, D.W. (2014). *Candida albicans* promotes invasion and colonisation of *Candida glabrata* in a reconstituted human vaginal epithelium. *Journal of Infection,* 69(4), 396-407.

Ames, L., Duxbury, S., Pawlowska, B., Ho, H. L., Haynes, K., & Bates, S. (2017). *Galleria mellonella* as a host model to study *Candida glabrata* virulence and antifungal efficacy. *Virulence*, 8(8), 1909-1917.

Amorim-Vaz, S., Delarze, E., Ischer, F., Sanglard, D. & Coste, A.T. (2015). Examining the virulence of *Candida albicans* transcription factor mutants using *Galleria mellonella* and mouse infection models. *Frontiers in Microbiolgy,* 6(367), 1-14.

Anderson, J.B. (2005). Evolution of antifungal-drug resistance: mechanisms and pathogen fitness. *Nature Reviews Microbiology,* 3(7), 547-556.

Anderson, J.B., Sirjusingh, C., Parsons, A.B., Boone, C., Wickens, C., Cowen, L.E. & Kohn, L.M. (2003). Mode of selection and experimental evolution of antifungal drug resistance in *Saccharomyces cerevisiae*. *Genetics,* 163(4), 1287-1298.

Anderson, R.M. & May, R. (1982). Coevolution of hosts and parasites. *Parasitology,* 85(02), 411-426.

Andersson, D.I. (2006). The biological cost of mutational antibiotic resistance: any practical conclusions? *Current Opinion in Microbiology,* 9(5), 461-465.

Andersson, D.I. & Hughes, D. (2010). Antibiotic resistance and its cost: is it possible to reverse resistance? *Nature Reviews Microbiology,* 8(4), 260-271.

Andersson, D.I. & Hughes, D. (2014). Microbiological effects of sublethal levels of antibiotics. *Nature Reviews Microbiology,* 12(7), 465-478.

Andes, D., Forrest, A., Lepak, A., Nett, J., Marchillo, K. & Lincoln, L. (2006). Impact of antimicrobial dosing regimen on evolution of drug resistance *in vivo*: fluconazole and *Candida albicans*. *Antimicrobial Agents and Chemotherapy,* 50(7), 2374-2383.

Antonovics, J. and Kareiva, P. (1988). Frequency-dependent selection and competition: empirical approaches. *Philosophical Transactions of the Royal Society of London B: Biological Sciences*, 319(1196), 601-613.

Arendrup MC, Cuenca-Estrella M, Lass-Flörl C, Hope WW, EUCASTAFST., (2012). EUCAST technical note on the EUCAST definitive document EDef 7.2: method for the determination of broth dilution minimum inhibitory concentrations of antifungal agents for yeasts EDef 7.2 (EUCAST-AFST). *Clinical Microbiology and Infect*ion, 18(7), E246–E247.

Arendrup, M.C. & Perlin, D.S. (2014). Echinocandin resistance: an emerging clinical problem? *Current Opinion in Infectious Diseases,* 27(6), 484-492.

Asad, S. & Opal, S.M. (2008). Bench-to-bedside review: Quorum sensing and the role of cell-to-cell communication during invasive bacterial infection. *Critical Care,* 12(6), 1-11.

Ayala, F. J., & Campbell, C. A. (1974). Frequency-dependent selection. *Annual Review of Ecology and Systematics*, 5(1), 115-138.

Bachmann, H., Fischlechner, M., Rabbers, I., Barfa, N., Dos Santos, F.B., Molenaar, D. & Teusink, B. (2013). Availability of public goods shapes the evolution of competing metabolic strategies. *Proceedings of the National Academy of Sciences,* 110(35), 14302-14307.

Bailey, S.F., Rodrigue, N. & Kassen, R. (2015). The effect of selection environment on the probability of parallel evolution. *Molecular Biology and Evolution,* 32(6), 1436-1448.

Balaban, N.Q., Merrin, J., Chait, R., Kowalik, L. & Leibler, S. (2004). Bacterial persistence as a phenotypic switch. *Science,* 305(5690), 1622-1625.

Baldauf, S.L., Roger, A., Wenk-Siefert, I. & Doolittle, W.F. (2000). A kingdom-level phylogeny of eukaryotes based on combined protein data. *Science,* 290(5493), 972-977.

Barelle, C.J., Priest, C.L., Maccallum, D.M., Gow, N.A., Odds, F.C. & Brown, A.J. (2006). Niche-specific regulation of central metabolic pathways in a fungal pathogen. *Cellular Microbiology,* 8(6), 961-971.

Barnes, R.A., Gow, N.a.R., Denning, D.W., May, R.C. & Haynes, K. (2014). Antifungal resistance: more research needed. *The Lancet,* 384(9952), 1427.

Barns, S., Lane, D., Sogin, M., Bibeau, C. & Weisburg, W. (1991). Evolutionary relationships among pathogenic *Candida* species and relatives. *Journal of Bacteriology,* 173(7), 2250-2255.

Basson, N. (2000). Competition for glucose between *Candida albicans* and oral bacteria grown in mixed culture in a chemostat. *Journal of Medical Microbiology,* 49(11), 969-975.

Bates, D., Maechler, M., Bolker, B. & Walker, S. (2015). Fitting linear mixed-effects models using lme4. *Journal of Statistical Software*, 67(1), 1-48.

Beardmore, R.E., Gudelj, I., Lipson, D.A. & Hurst, L.D. (2011). Metabolic trade-offs and the maintenance of the fittest and the flattest. *Nature,* 472(7343), 342-346.

Ben-Ami, R. & Kontoyiannis, D.P. (2012). Resistance to echinocandins comes at a cost: the impact of *FKS1* hotspot mutations on *Candida albicans* fitness and virulence. *Virulence,* 3(1), 95-97.

Ben-Ami, R., Zimmerman, O., Finn, T., Amit, S., Novikov, A., Wertheimer, N., Lurie-Weinberger, M. & Berman, J. (2016). Heteroresistance to fluconazole is a continuously distributed phenotype among *Candida glabrata* clinical strains associated with *in vivo* persistence. *MBio,* 7(4), e00655-00616.

Bernardi, G. (1979). The petite mutation in yeast. *Trends in Biochemical Sciences,* 4(9), 197-201.

Blaser, J., Stone, B.B., Groner, M.C. & Zinner, S.H. (1987). Comparative study with enoxacin and netilmicin in a pharmacodynamic model to determine importance of ratio of antibiotic peak concentration to MIC for bactericidal activity and emergence of resistance. *Antimicrobial Agents and Chemotherapy,* 31(7), 1054-1060.

Boktour, M.R., Kontoyiannis, D.P., Hanna, H.A., Hachem, R.Y., Girgawy, E., Bodey, G.P. & Raad, Ii (2004). Multiple-species candidemia in patients with cancer. *Cancer,* 101(8), 1860-1865.

Borghi, E., Andreoni, S., Cirasola, D., Ricucci, V., Sciota, R. & Morace, G. (2014). Antifungal resistance does not necessarily affect *Candida glabrata* fitness. *Journal of Chemotherapy,* 26(1), 32-36.

Borman, A.M., Szekely, A., Linton, C.J., Palmer, M.D., Brown, P. & Johnson, E.M. (2013). Epidemiology, antifungal susceptibility, and pathogenicity of *Candida africana* isolates from the United Kingdom. *Journal of Clinical Microbiology,* 51(3), 967-972.

Bouchara, J.-P., Zouhair, R., Le Boudouil, S., Renier, G., Filmon, R., Chabasse, D., Hallet, J.-N. & Defontaine, A. (2000). *In-vivo* selection of an azole-resistant petite mutant of *Candida glabrata*. *Journal of Medical Microbiology,* 49(11), 977-984.

Brennan, M., Thomas, D.Y., Whiteway, M. & Kavanagh, K. (2002). Correlation between virulence of *Candida albicans* mutants in mice and *Galleria mellonella* larvae. *FEMS Immunology and Medical Microbiology,* 34(2), 153-157.

Brothers, K.M. & Wheeler, R.T. (2012). Non-invasive imaging of disseminated candidiasis in zebrafish larvae. *Journal of Visualised Experiments,* 65, e4051.

Brown, A.J., Brown, G.D., Netea, M.G. & Gow, N.A. (2014a). Metabolism impacts upon *Candida* immunogenicity and pathogenicity at multiple levels. *Trends in Microbiology,* 22(11), 614-622.

Brown, A.J., Budge, S., Kaloriti, D., Tillmann, A., Jacobsen, M.D., Yin, Z., Ene, I.V., Bohovych, I., Sandai, D. & Kastora, S. (2014b). Stress adaptation in a pathogenic fungus. *Journal of Experimental Biology,* 217(1), 144-155.

Brown, G.D., Denning, D.W., Gow, N.A., Levitz, S.M., Netea, M.G. & White, T.C. (2012). Hidden killers: human fungal infections. *Science Translational Medicine,* 4(165), 4(165), 1-9.

Brown, S.P., Fredrik Inglis, R. & Taddei, F. (2009). Evolutionary ecology of microbial wars: within-host competition and (incidental) virulence. *Evolutionary Applications,* 2(1), 32-39.

Brown, V., Sexton, J.A. & Johnston, M. (2006). A glucose sensor in *Candida albicans. Eukaryotic Cell,* 5(10), 1726-1737.

Brown, C.J., Todd, K.M. & Rosenzweig, R.F., 1998. Multiple duplications of yeast hexose transport genes in response to selection in a glucose-limited environment. *Molecular Biology and Evolution*, 15(8), 931-942.

Browne, N., Surlis, C. & Kavanagh, K. (2014). Thermal and physical stresses induce a short-term immune priming effect in *Galleria mellonella* larvae. *Journal of Insect Physiology,* 63(1), 21-26.

Browne, N., Surlis, C., Maher, A., Gallagher, C., Carolan, J.C., Clynes, M. & Kavanagh, K. (2015). Prolonged pre-incubation increases the susceptibility

of *Galleria mellonella* larvae to bacterial and fungal infection. *Virulence,* 6(5), 458-465.

Brun, S., Dalle, F., Saulnier, P., Renier, G., Bonnin, A., Chabasse, D. & Bouchara, J.-P. (2005). Biological consequences of petite mutations in *Candida glabrata*. *Journal of Antimicrobial Chemotherapy,* 56(2), 307-314.

Brunke, S. & Hube, B. (2013). Two unlike cousins: *Candida albicans* and *C. glabrata* infection strategies. *Cellular Microbiology,* 15(5), 701-708.

Buckling, A., Maclean, R.C., Brockhurst, M.A. & Colegrave, N. (2009). The Beagle in a bottle. *Nature,* 457(7231), 824-829.

Buer, J. & Balling, R. (2003). Mice, microbes and models of infection. *Nature Reviews Genetics,* 4(3), 195-205.

Campbell, K., Vowinckel, J., Muelleder, M., Malmsheimer, S., Lawrence, N., Calvani, E., Miller-Fleming, L., Alam, M.T., Christen, S. & Keller, M.A. (2015). Self-establishing communities enable cooperative metabolite exchange in a eukaryote. *Elife,* 4, e09943.

Campbell, K., Vowinckel, J. & Ralser, M. (2016). Cell-to-cell heterogeneity emerges as consequence of metabolic cooperation in a synthetic yeast community. *Biotechnology Journal,* 11(9), 1169-1178.

Cataldi, V., Di Campli, E., Fazii, P., Traini, T., Cellini, L., & Di Giulio, M. (2016). *Candida* species isolated from different body sites and their antifungal susceptibility pattern: Cross-analysis of *Candida albicans* and *Candida glabrata* biofilms. *Medical Mycology,* 55(6), 624-634.

Chakrabarti, A. (2011). Drug resistance in fungi - an emerging problem. *Regional Health Forum*, 15(1), 97-103.

Champion, O., (2016). TruLarv™ Research Grade *Galleria mellonella*. Available from: https://www.biosystemstechnology.com [Accessed 24th April 2017].

Chowdhary, A., Sharma, C. & Meis, J.F. (2017). *Candida auris*: A rapidly emerging cause of hospital-acquired multidrug-resistant fungal infections globally. *PLoS Pathogens,* 13(5), e1006290.

Claudi, B., Spröte, P., Chirkova, A., Personnic, N., Zankl, J., Schürmann, N., Schmidt, A. & Bumann, D. (2014). Phenotypic variation of *Salmonella* in host tissues delays eradication by antimicrobial chemotherapy. *Cell,* 158(4), 722-733.

Cleveland, A.A., Farley, M.M., Harrison, L.H., Stein, B., Hollick, R., Lockhart, S.R., Magill, S.S., Derado, G., Park, B.J. & Chiller, T.M. (2012). Changes in incidence and antifungal drug resistance in candidemia: results from population-based laboratory surveillance in Atlanta and Baltimore, 2008–2011. *Clinical Infectious Diseases,* 55(10), 1352-1361.

Clinical and Laboratory Standards Institute. 2008. Reference method for broth dilution antifungal susceptibility testing of yeasts, 3rd ed. Approved standard M27-A3. Clinical and Laboratory Standards Institute, Wayne, PA.

Cocker, J.H., Piatti, S., Santocanale, C., Nasmyth, K. & Diffley, J.F. (1996). An essential role for the Cdc6 protein in forming the pre-replicative complexes of budding yeast. *Nature,* 379(6561), 180-182.

Coco, B., Bagg, J., Cross, L., Jose, A., Cross, J. & Ramage, G. (2008). Mixed *Candida albicans* and *Candida glabrata* populations associated with the pathogenesis of denture stomatitis. *Molecular Oral Microbiology,* 23(5), 377-383.

Cohen, T., Sommers, B. & Murray, M. (2003). The effect of drug resistance on the fitness of *Mycobacterium tuberculosis*. *The Lancet Infectious Diseases,* 3(1), 13-21.

Cook, S.M. & Mcarthur, J.D. (2013). Developing *Galleria mellonella* as a model host for human pathogens. *Virulence,* 4(5), 350-353.

Cormack, B.P. and Falkow, S. (1999). Efficient homologous and illegitimate recombination in the opportunistic yeast pathogen *Candida glabrata*. *Genetics*, 151(3), 979–987.

Cotter, G., Doyle, S. & Kavanagh, K. (2000). Development of an insect model for the *in vivo* pathogenicity testing of yeasts. *FEMS Immunology and Medical Microbiology,* 27(2), 163-169.

Cowen, L.E., Anderson, J.B. & Kohn, L.M. (2002). Evolution of drug resistance in *Candida albicans*. *Annual Reviews in Microbiology,* 56(1), 139-165.

Cowen, L.E., Kohn, L.M. & Anderson, J.B. (2001). Divergence in fitness and evolution of drug resistance in experimental populations of *Candida albicans*. *Journal of Bacteriology,* 183(10), 2971-2978.

Cowen, L.E., Nantel, A., Whiteway, M.S., Thomas, D.Y., Tessier, D.C., Kohn, L.M. & Anderson, J.B. (2002). Population genomics of drug resistance in *Candida albicans*. *Proceedings of the National Academy of Sciences,* 99(14), 9284-9289.

Cowen, L.E., Sanglard, D., Calabrese, D., Sirjusingh, C., Anderson, J.B. & Kohn, L.M. (2000). Evolution of drug resistance in experimental populations of *Candida albicans*. *Journal of Bacteriology,* 182(6), 1515-1522.

Crawley, M., 2007. The R book. John Wiley & Sons Ltd: Chicester.

Cuenca-Estrella, M., Diaz-Guerra, T.M., Mellado, E. & Rodriguez-Tudela, J.L. (2001). Influence of glucose supplementation and inoculum size on growth kinetics and antifungal susceptibility testing of *Candida* spp. *Journal of Clinical Microbiology,* 39(2), 525-532.

Cunningham, A.B., Lennox, J.E. & Ross, R.J. (2010). BIOFILMS: The Hypertextbook. [online]. Available at: https://www.cs.montana.edu/webworks/projects/stevesbook/contents/chapters/chapter002/section002/black/page001.html [Accessed 10 May 2017].

David, L.A., Maurice, C.F., Carmody, R.N., Gootenberg, D.B., Button, J.E., Wolfe, B.E., Ling, A.V., Devlin, A.S., Varma, Y., Fischbach, M.A., Biddinger, S.B., Dutton, R.J. & Turnbaugh, P.J. (2014). Diet rapidly and reproducibly alters the human gut microbiome. *Nature,* 505(7484), 559-563.

Day, M. (2013). Chapter one - yeast petites and small colony variants: for everything there is a season. *Advances in Applied Microbiology,* 85(1), 1-41.

Day, T., Graham, A. L., & Read, A. F. (2007). Evolution of parasite virulence when host responses cause disease. *Proceedings of the Royal Society of London B: Biological Sciences*, 274(1626), 2685-2692.

de Muinck, E.J., Stenseth, N.C., Sachse, D., Vander Roost, J., Ronningen, K.S., Rudi, K. & Trosvik, P. (2013). Context-dependent competition in a model gut bacterial community. *PloS One,* 8(6), e67210.

Defontaine, A., Bouchara, J.-P., Declerk, P., Planchenault, C., Chabasse, D. & Hallet, J.-N. (1999). *In-vitro* resistance to azoles associated with mitochondrial DNA deficiency in *Candida glabrata*. *Journal of Medical Microbiology,* 48(7), 663-670.

Desalermos, A., Fuchs, B.B. & Mylonakis, E. (2012). Selecting an invertebrate model host for the study of fungal pathogenesis. *PLoS Pathogens,* 8(2), e1002451.

Dethlefsen, L., Eckburg, P.B., Bik, E.M. & Relman, D.A. (2006). Assembly of the human intestinal microbiota. *Trends in Ecology and Evolution,* 21(9), 517-523.

Dhar, R., Sägesser, R., Weikert, C. & Wagner, A. (2012). Yeast adapts to a changing stressful environment by evolving cross-protection and anticipatory gene regulation. *Molecular Biology and Evolution,* 30(3), 573-588.

Diamond, R.D. (1991). The growing problem of mycoses in patients infected with the human immunodeficiency virus. *Reviews of Infectious Diseases,* 13(3), 480-486.

Diaz, P. I., Xie, Z., Sobue, T., Thompson, A., Biyikoglu, B., Ricker, A., ... & Dongari-Bagtzoglou, A. (2012). Synergistic interaction between *Candida albicans* and commensal oral streptococci in a novel *in vitro* mucosal model. *Infection and Immunity*, 80(2), 620-632.

Diekema, D., Arbefeville, S., Boyken, L., Kroeger, J. & Pfaller, M. (2012). The changing epidemiology of healthcare-associated candidemia over three decades. *Diagnostic Microbiology and Infectious Disease,* 73(1), 45-48.

Diezmann, S., Cox, C.J., Schonian, G., Vilgalys, R.J. & Mitchell, T.G. (2004). Phylogeny and evolution of medical species of *Candida* and related taxa: a multigenic analysis. *Journal of Clinical Microbiology,* 42(12), 5624-5635.

Doman, M., Kovacs, R., Perlin, D.S., Kardos, G., Gesztelyi, R., Juhasz, B., Bozo, A. & Majoros, L. (2015). Dose escalation studies with caspofungin against *Candida glabrata*. *Journal of Medical Microbiology,* 64(9), 998-1007.

Domergue, R., Castano, I., De Las Penas, A., Zupancic, M., Lockatell, V., Hebel, J.R., Johnson, D. & Cormack, B.P. (2005). Nicotinic acid limitation regulates silencing of *Candida* adhesins during UTI. *Science,* 308(5723), 866-870.

Drlica, K. (2003). The mutant selection window and antimicrobial resistance. *Journal of Antimicrobial Chemotherapy,* 52(1), 11-17.

Dujon, B., Sherman, D., Fischer, G., Durrens, P., Casaregola, S., Lafontaine, I., De Montigny, J., Marck, C., Neuvéglise, C. & Talla, E. (2004). Genome evolution in yeasts. *Nature,* 430(6995), 35-44.

El-Azizi, M.A., Starks, S.E. & Khardori, N. (2004). Interactions of Candida albicans with other *Candida* spp. and bacteria in the biofilms. *Journal of Applied Microbiology,* 96(5), 1067-1073.

El-Halfawy, O.M. & Valvano, M.A. (2015). Antimicrobial heteroresistance: an emerging field in need of clarity. *Clinical Microbiology Reviews,* 28(1), 191-207.

Elefanti, A., Mouton, J. W., Krompa, K., Al-Saigh, R., Verweij, P. E., Zerva, L., & Meletiadis, J. (2013). Inhibitory and fungicidal effects of antifungal drugs against *Aspergillus* species in the presence of serum. *Antimicrobial Agents and Chemotherapy*, 57(4), 1625-1631.

Elena, S. F., & Lenski, R. E. (1997). Long-term experimental evolution in *Escherichia coli.* VII. Mechanisms maintaining genetic variability within populations. *Evolution*, 51(4), 1058-1067.

Elena, S.F. & Lenski, R.E. (2003). Evolution experiments with microorganisms: the dynamics and genetic bases of adaptation. *Nature Reviews Genetics,* 4(6), 457-469.

Ene, I.V., Adya, A.K., Wehmeier, S., Brand, A.C., Maccallum, D.M., Gow, N.A. & Brown, A.J. (2012). Host carbon sources modulate cell wall architecture, drug resistance and virulence in a fungal pathogen. *Cellular Microbiology,* 14(9), 1319-1335.

Espinel-Ingroff, A., Arendrup, M.C., Pfaller, M.A., Bonfietti, L.X., Bustamante, B., Canton, E., Chryssanthou, E., Cuenca-Estrella, M., Dannaoui, E., Fothergill, A., Fuller, J., Gaustad, P., Gonzalez, G.M., Guarro, J., Lass-Florl, C., Lockhart, S.R., Meis, J.F., Moore, C.B., Ostrosky-Zeichner, L., Pelaez, T., Pukinskas, S.R., St-Germain, G., Szeszs, M.W. & Turnidge, J. (2013). Interlaboratory variability of Caspofungin MICs for *Candida* spp. Using CLSI and EUCAST methods: should the clinical laboratory be testing this agent? *Antimicrobial Agents and Chemotherapy,* 57(12), 5836-5842.

Farmakiotis, D., Tarrand, J.J. & Kontoyiannis, D.P. (2014). Drug-resistant *Candida glabrata* infection in cancer patients. *Emerging Infectious Diseases,* 20(11), 1833.

Feldgarden, M., Stoebel, D.M., Brisson, D., Dykhuizen, D.E., 2003. Size doesn't matter: Microbial selection experiments address ecological phenomena. *Ecology*, 84(7), 1679–1687.

Ferea, T.L., Botstein, D., Brown, P.O. & Rosenzweig, R.F. (1999). Systematic changes in gene expression patterns following adaptive evolution in yeast. *Proceedings of the National Academy of Sciences,* 96(17), 9721-9726.

Ferrari, S., Ischer, F., Calabrese, D., Posteraro, B., Sanguinetti, M., Fadda, G., Rohde, B., Bauser, C., Bader, O. & Sanglard, D. (2009). Gain of function mutations in *CgPDR1* of *Candida glabrata* not only mediate antifungal resistance but also enhance virulence. *PLoS Pathogens,* 5(1), e1000268.

Fidel Jr, P.L., Cutright, J.L., Tait, L. & Sobel, J.D. (1996). A murine model of *Candida glabrata* vaginitis. *Journal of Infectious Diseases,* 173(2), 425-431.

Fidel, P.L., Vazquez, J.A. & Sobel, J.D. (1999). *Candida glabrata*: review of epidemiology, pathogenesis, and clinical disease with comparison to *C. albicans*. *Clinical Microbiology Reviews,* 12(1), 80-96.

Fisher, M.C., Gow, N.A. & Gurr, S.J. (2016). Tackling emerging fungal threats to animal health, food security and ecosystem resilience. *Philosophical Transactions of the Royal Society B-Biological Sciences*, 371(1709), 1-6.

Fourie, R., Ells, R., Swart, C. W., Sebolai, O. M., Albertyn, J., & Pohl, C. H. (2016). *Candida albicans* and *Pseudomonas aeruginosa* Interaction, with focus on the role of eicosanoids. *Frontiers in Physiology*, 7(1), 1-15.

Frank, S. A., & Schmid-Hempel, P. (2008). Mechanisms of pathogenesis and the evolution of parasite virulence. *Journal of Evolutionary Biology*, 21(2), 396-404.

Freter, R., Brickner, H., Botney, M., Cleven, D. & Aranki, A. (1983). Mechanisms that control bacterial populations in continuous-flow culture models of mouse large intestinal flora. *Infection and Immunity,* 39(2), 676-685.

Friesen, M.L., Saxer, G., Travisano, M., Doebeli, M. & Elena, S. (2004). Experimental evidence for sympatric ecological diversification due to frequency-dependent competition in *Escherichia coli*. *Evolution,* 58(2), 245-260.

Fuchs, B.B., O'brien, E., El Khoury, J.B. & Mylonakis, E. (2010). Methods for using *Galleria mellonella* as a model host to study fungal pathogenesis. *Virulence,* 1(6), 475-482.

Gagiano, M., Bauer, F.F. & Pretorius, I.S. (2002). The sensing of nutritional status and the relationship to filamentous growth in *Saccharomyces cerevisiae*. *FEMS Yeast Research,* 2(4), 433-470.

Gagneux, S., Long, C.D., Small, P.M., Van, T., Schoolnik, G.K. & Bohannan, B.J. (2006). The competitive cost of antibiotic resistance in *Mycobacterium tuberculosis*. *Science,* 312(5782), 1944-1946.

Garcia-Effron, G., Lee, S., Park, S., Cleary, J.D. & Perlin, D.S. (2009). Effect of *Candida glabrata FKS1* and *FKS2* mutations on echinocandin sensitivity and kinetics of 1,3-beta-D-glucan synthase: implication for the existing susceptibility breakpoint. *Antimicrobial Agents and Chemotherapy,* 53(9), 3690-3699.

Gibson, J., Lamey, P.J., Lewis, M. & Frier, B. (1990). Oral manifestations of previously undiagnosed non-insulin dependent diabetes mellitus. *Journal of Oral Pathology and Medicine,* 19(6), 284-287.

Gibson, J., Lamey, P.J., Lewis, M. & Frier, B. (1990). Oral manifestations of previously undiagnosed non-insulin dependent diabetes mellitus. *Journal of Oral Pathology and Medicine,* 19(6), 284-287.

Gilbert, P., Collier, P. J., & Brown, M. R. (1990). Influence of growth rate on susceptibility to antimicrobial agents: biofilms, cell cycle, dormancy, and stringent response. *Antimicrobial Agents and Chemotherapy*, 34(10), 1865.

Gillum, A.M., Tsay, E.Y. & Kirsch, D.R. (1984). Isolation of the *Candida albicans* gene for orotidine-5'-phosphate decarboxylase by complementation of S. cerevisiae *ura3* and *E. coli pyrF* mutations. *Molecular Genetics and Genomics,* 198(2), 179-182.

Glittenberg, M.T., Kounatidis, I., Christensen, D., Kostov, M., Kimber, S., Roberts, I. & Ligoxygakis, P. (2011a). Pathogen and host factors are needed to provoke a systemic host response to gastrointestinal infection of *Drosophila* larvae by *Candida albicans*. *Disease Models and Mechanisms,* 4(4), 515-525.

Glittenberg, M.T., Silas, S., Maccallum, D.M., Gow, N.A. & Ligoxygakis, P. (2011b). Wild-type *Drosophila melanogaster* as an alternative model system for investigating the pathogenicity of *Candida albicans*. *Disease Models and Mechanisms,* 4(4), 504-514.

Goldhaber, M. (1994). Fighting antibiotic resistance. *Science*, 266(5190), 1462.

Gomes, A. L., Galagan, J. E., & Segrè, D. (2013). Resource competition may lead to effective treatment of antibiotic resistant infections. *PloS One*, 8(12), e80775.

Goswami, D., Goswami, R., Banerjee, U., Dadhwal, V., Miglani, S., Lattif, A.A. & Kochupillai, N. (2006). Pattern of *Candida* species isolated from patients with diabetes mellitus and vulvovaginal candidiasis and their response to single dose oral fluconazole therapy. *Journal of Infection,* 52(2), 111-117.

Gow, N.A. & Netea, M.G. (2016). Medical mycology and fungal immunology: new research perspectives addressing a major world health challenge. *Philosophical Transactions of the Royal Society B-Biological Sciences,* 371(1709), 20150462.

Greenland, S., Senn, S. J., Rothman, K. J., Carlin, J. B., Poole, C., Goodman, S. N., & Altman, D. G. (2016). Statistical tests, P values, confidence intervals, and power: a guide to misinterpretations. *European Journal of Epidemiology*, 31(4), 337-350.

Gregori, C., Schüller, C., Roetzer, A., Schwarzmüller, T., Ammerer, G., Kuchler, K., (2007). The high-osmolarity glycerol response pathway in the human fungal pathogen *Candida glabrata* strain ATCC 2001 lacks a signaling branch that operates in baker's yeast. *Eukaryotic Cell*, 6(9), 1635-1645.

Gudlaugsson, O., Gillespie, S., Lee, K., Berg, J.V., Hu, J., Messer, S., Herwaldt, L., Pfaller, M. & Diekema, D. (2003). Attributable mortality of nosocomial candidemia, revisited. *Clinical Infectious Diseases,* 37(9), 1172-1177.

Guinea, J. (2014). Global trends in the distribution of *Candida* species causing candidemia. *Clinical Microbiology and Infection,* 20(Supplement 6), 5-10.

Haldane, J.B.S. & Jayakar, S.D. (1963). Polymorphism due to selection of varying direction. *Journal of Genetics*, 58(2), 237-242.

Hall, A.R., Angst, D.C., Schiessl, K.T. & Ackermann, M. (2015). Costs of antibiotic resistance - separating trait effects and selective effects. *Evolutionary Appications,* 8(3), 261-272.

Hall, A.R. & Corno, G. (2014). Tetracycline modifies competitive interactions in experimental microcosms containing bacteria isolated from freshwater. *FEMS Microbiology Ecology,* 90(1), 168-174.

Han, S.K., Lee, D., Lee, H., Kim, D., Son, H.G., Yang, J.S., Lee, S.V. & Kim, S. (2016). OASIS 2: online application for survival analysis 2 with features for the analysis of maximal lifespan and healthspan in aging research. *Oncotarget,* 7(35), 56147-56152.

Hardin, G. (1960). Competitive exclusion principle. *Science,* 131(3409), 1292-1297.

Harrell Jr, F.E., with contributions from Charles Dupont and many others. (2016). Hmisc: Harrell Miscellaneous. R package version 3.17-4. https://CRAN.R-project.org/package=Hmisc

Harrison, F. (2007). Microbial ecology of the cystic fibrosis lung. *Microbiology,* 153(4), 917-923.

Harrison, J.J., Turner, R.J. & Ceri, H. (2007). A subpopulation of *Candida albicans* and *Candida tropicalis* biofilm cells are highly tolerant to chelating agents. *FEMS Microbiology Letters,* 272(2), 172-181.

Haynes, K., Westerneng, T., Fell, J. & Moens, W. (1995). Rapid detection and identification of pathogenic fungi by polymerase chain reaction amplification of large subunit ribosomal DNA. *Journal of Medical and Veterinary Mycology,* 33(5), 319-325.

Haynes, K.A. & Westerneng, T.J. (1996). Rapid identification of *Candida albicans, C. glabrata, C. parapsilosis* and *C. krusei* by species-specific PCR of large subunit ribosomal DNA. *Journal of Medical Microbiology,* 44(5), 390-396.

Head, M.G., Fitchett, J.R., Atun, R. & May, R.C. (2014). Systematic analysis of funding awarded for mycology research to institutions in the UK, 1997–2010. *BMJ Open,* 4(1), e004129.

Healey, K.R., Jimenez Ortigosa, C., Shor, E. & Perlin, D.S. (2016). Genetic drivers of multidrug resistance in *Candida glabrata*. *Frontiers in Microbiology,* 7(1), 1-9.

Hegreness, M., Shoresh, N., Damian, D., Hartl, D. & Kishony, R. (2008). Accelerated evolution of resistance in multidrug environments. *Proceedings of the National Academy of Sciences,* 105(37), 13977-13981.

Hendriks, L., Goris, A., Neefs, J.-M., Van De Peer, Y., Hennebert, G. & De Wachter, R. (1989). The nucleotide sequence of the small ribosomal subunit RNA of the yeast *Candida albicans* and the evolutionary position of the fungi among the eukaryotes. *Systematic and Applied Microbiology,* 12(3), 223-229.

Henry-Stanley, M.J., Garni, R.M., Alice Johnson, M., Bendel, C.M. & Wells, C.L. (2005). Comparative abilities of *Candida glabrata* and *Candida albicans* to colonize and translocate from the intestinal tract of antibiotic-treated mice. *Microbial Ecology in Health and Disease,* 17(3), 129-137.

Hernan, R.C., Karina, B., Gabriela, G., Marcela, N., Carlos, V. & Angela, F. (2009). Selection of colistin-resistant *Acinetobacter baumannii* isolates in postneurosurgical meningitis in an intensive care unit with high presence of heteroresistance to colistin. *Diagnostic Microbiology and Infectious Disease,* 65(2), 188-191.

Herron, M.D. & Doebeli, M. (2013). Parallel evolutionary dynamics of adaptive diversification in *Escherichia coli*. *PLoS Biology,* 11(2), e1001490.

Hibbing, M.E., Fuqua, C., Parsek, M.R. & Peterson, S.B. (2010). Bacterial competition: surviving and thriving in the microbial jungle. *Nature Reviews Microbiology,* 8(1), 15-25.

Ito-Kuwa, S., Nakamura, Y., Aoki, S., Nakamura, K., Vidotto, V. & Sinicco, A. (1997). Oral yeasts isolated from normal subjects in three successive trials. *Japanese Journal of Oral Biology,* 39(2), 100-106.

Jenkinson, H.F., Douglas, L.J., 2002. Interactions between *Candida* species and bacteria in mixed infections. In: Brogden, K.A., Guthmiller, J.M., eds.

Polymicrobial Diseases. Washington (DC): ASM Press, Chapter 18. Available from: http://www.ncbi.nlm.nih.gov/books/NBK2486/ [Accessed 31 March 2014]

Jeon, J., Choi, J., Lee, G.-W., Dean, R.A. & Lee, Y.-H. (2013). Experimental evolution reveals genome-wide spectrum and dynamics of mutations in the rice blast fungus, *Magnaporthe oryzae*. *PloS One,* 8(5), e65416.

Junqueira, J.C., Fuchs, B.B., Muhammed, M., Coleman, J.J., Suleiman, J.M., Vilela, S.F., Costa, A.C., Rasteiro, V.M., Jorge, A.O. & Mylonakis, E. (2011). Oral *Candida albicans* isolates from HIV-positive individuals have similar in vitro biofilm-forming ability and pathogenicity as invasive *Candida* isolates. *BMC Microbiology,* 11(1), 247.

Kanafani, Z.A. & Perfect, J.R. (2008). Antimicrobial resistance: resistance to antifungal agents: mechanisms and clinical impact. *Clinical Infectious Disease,* 46(1), 120-128.

Karaböcüoglu, M., Sökücü, S., Gökçay, G., Ucsel, R. & Neyzi, O. (1994). Carbohydrate malabsorption in acute diarrhea. *Indian Pediatrics,* 31(9), 1071-1074.

Kartsonis, N.A., Nielsen, J. & Douglas, C.M. (2003). Caspofungin: the first in a new class of antifungal agents. *Drug Resistance Updates,* 6(4), 197-218.

Katiyar, S., Pfaller, M. & Edlind, T. (2006). *Candida albicans* and *Candida glabrata* clinical isolates exhibiting reduced echinocandin susceptibility. *Antimicrobial agents and chemotherapy,* 50(8), 2892-2894.

Katiyar, S.K., Alastruey-Izquierdo, A., Healey, K.R., Johnson, M.E., Perlin, D.S. & Edlind, T.D. (2012). Fks1 and Fks2 are functionally redundant but differentially regulated in *Candida glabrata*: implications for echinocandin resistance. *Antimicrobial agents and chemotherapy,* 56(12), 6304-6309.

Keren, I., Kaldalu, N., Spoering, A., Wang, Y. & Lewis, K. (2004). Persister cells and tolerance to antimicrobials. *FEMS Microbiology Letters,* 230(1), 13-18.

Kirkpatrick, W.R., Lopez-Ribot, J.L., Mcatee, R.K. & Patterson, T.F. (2000). Growth competition between *Candida dubliniensis* and *Candida albicans*

under broth and biofilm growing conditions. *Journal of Clinical Microbiology,* 38(2), 902-904.

Kitada, K., Yamaguchi, E., Arisawa, M., 1995. Cloning of the *Candida glabrata TRP1* and *HIS3* genes, and construction of their disruptant strains by sequential integrative transformation. *Gene*, 165(2), 203-206.

Klotz, S.A., Chasin, B.S., Powell, B., Gaur, N.K. and Lipke, P.N., (2007). Polymicrobial bloodstream infections involving *Candida* species: analysis of patients and review of the literature. *Diagnostic Microbiology and Infectious Disease*, 59(4), 401-406.

Knight, G. M., Budd, E. L., Whitney, L., Thornley, A., Al-Ghusein, H., Planche, T., & Lindsay, J. A. (2012). Shift in dominant hospital-associated methicillin-resistant *Staphylococcus aureus* (HA-MRSA) clones over time. *Journal of Antimicrobial Chemotherapy*, 67(10), 2514-2522.

Koszul R, Malpertuy A, Frangeul L, Bouchier C, Wincker P, Thierry A, Duthoy S, Ferris S, Hennequin C, Dujon B., (2003). The complete mitochondrial genome sequence of the pathogenic yeast *Candida (Torulopsis) glabrata*. *Federation of European Biochemical Societies Letters*, 534(1-3), 39-48.

Kounatidis, I. & Ligoxygakis, P. (2012). *Drosophila* as a model system to unravel the layers of innate immunity to infection. *Open Biology,* 2(5), 1-14.

Krom, B.P., Kidwai, S. & Ten Cate, J.M. (2014). *Candida* and other fungal species: forgotten players of healthy oral microbiota. *Journal of Dental Research,* 93(5), 445-451.

Krzywinski, M. & Altman, N. (2014). Points of Significance: Visualizing samples with box plots. *Nature Methods,* 11(2), 119-120.

Küçükgöze, G., Alkım, C., Yılmaz, Ü., Kısakesen, H.I., Gündüz, S., Akman, S. & Çakar, Z.P. (2013). Evolutionary engineering and transcriptomic analysis of nickel-resistant *Saccharomyces cerevisiae*. *FEMS Yeast Research,* 13(8), 731-746.

Kugelberg, E., Lofmark, S., Wretlind, B. & Andersson, D.I. (2005). Reduction of the fitness burden of quinolone resistance in *Pseudomonas aeruginosa*. *Journal of Antimicrobial Chemotherapy,* 55(1), 22-30.

Kullberg, B.J. & Arendrup, M.C. (2015). Invasive candidiasis. *The New England Journal of Medicine,* 373(15), 1445-1456.

Kumar, S. & Singhi, S. (2013). Role of probiotics in prevention of *Candida* infection in critically ill children. *Mycoses,* 56(3), 204-211.

Kumar, S., Stecher, G. & Tamura, K. (2016). MEGA7: Molecular Evolutionary Genetics Analysis version 7.0 for bigger datasets. *Molecular Biology and Evolution,* 33(7), 1870-1874.

Lafleur, M.D., Kumamoto, C.A. & Lewis, K. (2006). *Candida albicans* biofilms produce antifungal-tolerant persister cells. *Antimicrobial Agents and Chemotherapy,* 50(11), 3839-3846.

Lagunas, R. (1993). Sugar transport in *Saccharomyces cerevisiae*. *FEMS Microbiology Reviews,* 10(3-4), 229-242.

Lee, H.H., Molla, M.N., Cantor, C.R. & Collins, J.J. (2010). Bacterial charity work leads to population-wide resistance. *Nature,* 467(7311), 82-85.

Leggett, H.C., Cornwallis, C.K., Buckling, A. & West, S.A. (2017). Growth rate, transmission mode and virulence in human pathogens. *Philosophical Transactions of the Royal Society of London B: Biological Sciences,* 372(1719), 1-8.

Lele, U.N. & Watve, M.G. (2014). Bacterial growth rate and growth yield: is there a relationship? *Proceedings of the Indian National Science Academy,* 80(3), 537-546.

Lello, J., Boag, B., Fenton, A., Stevenson, I.R. & Hudson, P.J. (2004). Competition and mutualism among the gut helminths of a mammalian host. *Nature,* 428(6985), 840-844.

Lemon, J. (2006) Plotrix: a package in the red light district of R. R-News, 6(4), 8-12.

Lenski, R.E., Mongold, J.A., Sniegowski, P.D., Travisano, M., Vasi, F., Gerrish, P.J. & Schmidt, T.M. (1998). Evolution of competitive fitness in experimental populations of *E. coli*: what makes one genotype a better competitor than another? *Antonie van Leeuwenhoek,* 73(1), 35-47.

Lenski, R.E., Rose, M.R., Simpson, S.C. & Tadler, S.C. (1991). Long-term experimental evolution in *Escherichia coli*. I. Adaptation and divergence during 2,000 generations. *The American Naturalist,* 138(6), 1315-1341.

Levin, B.R. (1972). Coexistence of two asexual strains on a single resource. *Science,* 175(4027), 1272-1274.

Lewis, K. (2007). Persister cells, dormancy and infectious disease. *Nature Reviews Microbiology,* 5(1), 48-56.

Li, L., Redding, S. & Dongari-Bagtzoglou, A. (2007). *Candida glabrata*, an emerging oral opportunistic pathogen. *Journal of Dental Research,* 86(3), 204-215.

Libuda, D. (2007). Genomic DNA Extraction *S. cerevisiae* and *S. pombe*. [pdf]. Princeton: Princeton University. Available at: https://www.princeton.edu/genomics/botstein/protocols/yeast_DNA.pdf [Accessed 20 Jun. 17].

Linder, J. E., Owers, K. A., & Promislow, D. E. (2008). The effects of temperature on host–pathogen interactions in *D. melanogaster*: Who benefits? *Journal of Insect Physiology*, 54(1), 297-308.

Lindsey, H.A., Gallie, J., Taylor, S. & Kerr, B. (2013). Evolutionary rescue from extinction is contingent on a lower rate of environmental change. *Nature,* 494(7438), 463-467.

Lipson, D.A. (2015). The complex relationship between microbial growth rate and yield and its implications for ecosystem processes. *Frontiers in Microbiology,* 6(1), 1-5.

Lockhart, S., Joly, S., Vargas, K., Swails-Wenger, J., Enger, L. & Soll, D. (1999). Natural defenses against *Candida* colonization breakdown in the oral cavities of the elderly. *Journal of Dental Research,* 78(4), 857-868.

Lorenz, M.C. & Fink, G.R. (2001). The glyoxylate cycle is required for fungal virulence. *Nature,* 412(6842), 83-86.

Lunzer, M., Natarajan, A., Dykhuizen, D.E. & Dean, A.M. (2002). Enzyme kinetics, substitutable resources and competition: from biochemistry to frequency-dependent selection in lac. *Genetics,* 162(1), 485-499.

Lüttich, A., Brunke, S., Hube, B., & Jacobsen, I. D. (2013). Serial passaging of *Candida albicans* in systemic murine infection suggests that the wild-type strain SC5314 is well adapted to the murine kidney. *PloS One*, 8(5), e64482.

MacCallum, D.M. (2012). Hosting infection: experimental models to assay *Candida* virulence. *International Journal of Microbiology,* 2012(1), 1-12.

MacLean, R. (2008). The tragedy of the commons in microbial populations: insights from theoretical, comparative and experimental studies. *Heredity,* 100(5), 471-477.

MacLean, R.C., Fuentes-Hernandez, A., Greig, D., Hurst, L.D. & Gudelj, I. (2010). A mixture of "cheats" and "co-operators" can enable maximal group benefit. *PLoS Biology,* 8(9), 1-11.

MacLean, R.C. & Gudelj, I. (2006). Resource competition and social conflict in experimental populations of yeast. *Nature,* 441(7092), 498-501.

MacLean, R.C., Hall, A.R., Perron, G.G. & Buckling, A. (2010). The population genetics of antibiotic resistance: integrating molecular mechanisms and treatment contexts. *Nature Reviews Genetics,* 11(6), 405-414.

Maddamsetti, R., Hatcher, P. J., Green, A. G., Williams, B. L., Marks, D. S., & Lenski, R. E. (2017). Core genes evolve rapidly in the long-term evolution experiment with *Escherichia coli*. *Genome Biology and Evolution*, 9(4), 1072–1083.

Malani, A.N., Psarros, G., Malani, P.N. & Kauffman, C.A. (2011). Is age a risk factor for *Candida glabrata* colonisation? *Mycoses,* 54(6), 531-537.

Marcet-Houben, M. & Gabaldón, T. (2009). The tree versus the forest: the fungal tree of life and the topological diversity within the yeast phylome. *PloS one,* 4(2), e4357.

Marchesi, J.R., Adams, D.H., Fava, F., Hermes, G.D., Hirschfield, G.M., Hold, G., Quraishi, M.N., Kinross, J., Smidt, H., Tuohy, K.M., Thomas, L.V., Zoetendal, E.G. & Hart, A. (2016). The gut microbiota and host health: a new clinical frontier. *Gut,* 65(2), 330-339.

Martino, P.D., Fursy, R., Bret, L., Sundararaju, B. & Phillips, R.S. (2003). Indole can act as an extracellular signal to regulate biofilm formation of *Escherichia coli* and other indole-producing bacteria. *Canadian Journal of Microbiology,* 49(7), 443-449.

MATLAB and Statistics Toolbox Release 2012a, The MathWorks, Inc., Natick, Massachusetts, United States.

McDonald, J.H. (2014). Handbook of Biological Statistics (3rd ed.). Sparky House Publishing, Baltimore, Maryland.

Medaney, F., Dimitriu, T., Ellis, R.J. & Raymond, B. (2016). Live to cheat another day: bacterial dormancy facilitates the social exploitation of beta-lactamases. *ISME J,* 10(3), 778-787.

Melnyk, A. H., Wong, A., & Kassen, R. (2015). The fitness costs of antibiotic resistance mutations. *Evolutionary Applications*, 8(3), 273-283.

Merico, A., Sulo, P., Piškur, J. & Compagno, C. (2007). Fermentative lifestyle in yeasts belonging to the *Saccharomyces* complex. *FEBS Journal,* 274(4), 976-989.

Mesa-Arango, A.C., Forastiero, A., Bernal-Martinez, L., Cuenca-Estrella, M., Mellado, E. & Zaragoza, O. (2013). The non-mammalian host *Galleria mellonella* can be used to study the virulence of the fungal pathogen *Candida tropicalis* and the efficacy of antifungal drugs during infection by this pathogenic yeast. *Medical Mycology,* 51(5), 461-472.

Meyer, J.R., Gudelj, I. & Beardmore, R. (2015). Biophysical mechanisms that maintain biodiversity through trade-offs. *Nature Communications,* 6(1), 1-7.

Mikaberidze, A., Paveley, N., Bonhoeffer, S. & Van Den Bosch, F. (2017). Emergence of resistance to fungicides: the role of fungicide dose. *Phytopathology,* 107(5), 545-560.

Mikulska, M., Del Bono, V., Ratto, S. & Viscoli, C. (2012). Occurrence, presentation and treatment of candidemia. *Expert Review of Clinical Immunology,* 8(8), 755-765.

Miller, M. B., & Bassler, B. L. (2001). Quorum sensing in bacteria. *Annual Reviews in Microbiology*, 55(1), 165-199.

Milne, S.W., Cheetham, J., Lloyd, D., Aves, S. & Bates, S. (2011). Cassettes for PCR-mediated gene tagging in *Candida albicans* utilizing nourseothricin resistance. *Yeast,* 28(12), 833-841.

Miramón, P. & Lorenz, M.C. (2017). A feast for *Candida*: Metabolic plasticity confers an edge for virulence. *PLoS Pathogens,* 13(2), e1006144.

Monod, J. (1949). The growth of bacterial cultures. *Annual Reviews in Microbiology,* 3(1), 371-394.

Mowat, E., Paterson, S., Fothergill, J.L., Wright, E.A., Ledson, M.J., Walshaw, M.J., Brockhurst, M.A. & Winstanley, C. (2011). *Pseudomonas aeruginosa* population diversity and turnover in cystic fibrosis chronic infections. *American Journal of Respiratory Critical Care Medicine,* 183(12), 1674-1679.

Murray, J.D. (1990). Mathematical Biology. 2nd ed. Berlin: Springer-Verlag.

Musher, D.M. & Mckenzie, S.O. (1977). Infections due to *Staphylococcus aureus*. *Medicine,* 56(5), 383-410.

Nace, H.L., Horn, D. & Neofytos, D. (2009). Epidemiology and outcome of multiple-species candidemia at a tertiary care center between 2004 and 2007. *Diagnostic Microbiology and Infectious Disease,* 64(3), 289-294.

Nagaev, I., Björkman, J., Andersson, D.I. & Hughes, D. (2001). Biological cost and compensatory evolution in fusidic acid-resistant *Staphylococcus aureus*. *Molecular Microbiology,* 40(2), 433-439.

Nash, E.E., Peters, B.M., Lilly, E.A., Noverr, M.C. & Fidel, P.L., Jr. (2016). A murine model of *Candida glabrata* vaginitis shows no evidence of an inflammatory immunopathogenic response. *PloS One,* 11(1), e0147969.

National Committee for Clinical Laboratory Standards. (2002). Reference Method for Broth Dilution Antifungal Susceptibility Testing of Yeasts; Approved Standard—Second Edition. NCCLS document M27-A2 [ISBN 1-56238-469-4]. NCCLS, 940 West Valley Road, Suite 1400, Wayne, Pennsylvania 19087-1898 USA.

Ng, T.S., Desa, M.N.M., Sandai, D., Chong, P.P. & Than, L.T. (2015). Phylogenetic and transcripts profiling of glucose sensing related genes in *Candida glabrata*. *Jundishapur Journal of Microbiology,* 8(11), 1-9.

Ng, T.S., Desa, M.N.M., Sandai, D., Chong, P.P. & Than, L.T.L. (2016). Growth, biofilm formation, antifungal susceptibility and oxidative stress resistance of *Candida glabrata* are affected by different glucose concentrations. *Infection, Genetics and Evolution,* 40(1), 331-338.

Nilsson, S., (2012). Modelling the Evolutionary Ecology of Stress Responses in Microbes. Thesis (PhD). Imperial College, London.

Nilsson, A.I., Zorzet, A., Kanth, A., Dahlström, S., Berg, O.G. & Andersson, D.I. (2006). Reducing the fitness cost of antibiotic resistance by amplification of initiator tRNA genes. *Proceedings of the National Academy of Sciences,* 103(18), 6976-6981.

Novak, M., Pfeiffer, T., Lenski, R.E., Sauer, U. & Bonhoeffer, S. (2006). Experimental tests for an evolutionary trade-off between growth rate and yield in *E. coli*. *The American Naturalist,* 168(2), 242-251.

Odds, F.C. (1996). Epidemiological shifts in opportunistic and nosocomial *Candida* infections: mycological aspects. *International Journal of Antimicrobial Agents,* 6(3), 141-144.

Odds, F.C. and Bernaerts, R.I.A., (1994). CHROMagar *Candida*, a new differential isolation medium for presumptive identification of clinically

important *Candida* species. *Journal of Clinical Microbiology*, 32(8), 1923-1929.

Odds, F.C., Brown, A.J. & Gow, N.A. (2003). Antifungal agents: mechanisms of action. *Trends in Microbiology,* 11(6), 272-279.

Odling-Smee, J., Erwin, D.H., Palkovacs, E.P., Feldman, M.W. & Laland, K.N., (2013). Niche construction theory: a practical guide for ecologists. *The Quarterly Review of Biology*, 88(1), 3-28.

Ott, S. J., Kühbacher, T., Musfeldt, M., Rosenstiel, P., Hellmig, S., Rehman, A., ... & Schreiber, S. (2008). Fungi and inflammatory bowel diseases: alterations of composition and diversity. *Scandinavian Journal of Gastroenterology*, 43(7), 831-841.

Owen, D.H. & Katz, D.F. (1999). A vaginal fluid simulant. *Contraception,* 59(2), 91-95.

Oz, T., Guvenek, A., Yildiz, S., Karaboga, E., Tamer, Y.T., Mumcuyan, N., Ozan, V.B., Senturk, G.H., Cokol, M., Yeh, P. & Toprak, E. (2014). Strength of selection pressure is an important parameter contributing to the complexity of antibiotic resistance evolution. *Molecular Biology and Evolution,* 31(9), 2387-2401.

Ozcan, S., Dover, J., Rosenwald, A.G., Wölfl, S. & Johnston, M. (1996). Two glucose transporters in *Saccharomyces cerevisiae* are glucose sensors that generate a signal for induction of gene expression. *Proceedings of the National Academy of Sciences,* 93(22), 12428-12432.

Palmer, A.C. & Kishony, R. (2013). Understanding, predicting and manipulating the genotypic evolution of antibiotic resistance. *Nature Reviews Genetics,* 14(4), 243-248.

Patel, P.K., Erlandsen, J.E., Kirkpatrick, W.R., Berg, D.K., Westbrook, S.D., Louden, C., Cornell, J.E., Thompson, G.R., Vallor, A.C., Wickes, B.L., Wiederhold, N.P., Redding, S.W. & Patterson, T.F. (2012). The changing epidemiology of oropharyngeal candidiasis in patients with HIV/AIDS in the era of antiretroviral therapy. *AIDS Research and Treatment,* 2012(1), 1-5.

Payne, S., Gibson, G., Wynne, A., Hudspith, B., Brostoff, J. & Tuohy, K. (2003). *In vitro* studies on colonization resistance of the human gut microbiota to *Candida albicans* and the effects of tetracycline and *Lactobacillus plantarum* LPK. *Current Issues in Intestinal Microbiology,* 4(1), 1-8.

Pedersen, A.B. & Fenton, A. (2007). Emphasizing the ecology in parasite community ecology. *Trends in Ecology and Evolution,* 22(3), 133-139.

Peleg, A.Y., Hogan, D.A. and Mylonakis, E., (2010). Medically important bacterial–fungal interactions. *Nature Reviews Microbiology*, 8(5), 340-349.

Peleg, A.Y., Tampakakis, E., Fuchs, B.B., Eliopoulos, G.M., Moellering, R.C., Jr. & Mylonakis, E. (2008). Prokaryote-eukaryote interactions identified by using *Caenorhabditis elegans*. *Proceedings of the National Academy of Sciences USA,* 105(38), 14585-14590.

Peña-Miller, R., Fuentes-Hernandez, A., Reding, C., Gudelj, I. & Beardmore, R. (2014). Testing the optimality properties of a dual antibiotic treatment in a two-locus, two-allele model. *Journal of The Royal Society Interface,* 11(96), 1-13.

Pereira-Cenci, T., Deng, D.M., Kraneveld, E.A., Manders, E.M., Del Bel Cury, A.A., Ten Cate, J.M. & Crielaard, W. (2008). The effect of *Streptococcus mutans* and *Candida glabrata* on *Candida albicans* biofilms formed on different surfaces. *Archives of Oral Biology,* 53(8), 755-764.

Perlin, D.S. (2007). Resistance to echinocandin-class antifungal drugs. *Drug Resistance Updates,* 10(3), 121-130.

Perlin, D.S. (2011). Current perspectives on echinocandin class drugs. *Future microbiology,* 6(4), 441-457.

Perlin, D. S. (2015). Mechanisms of echinocandin antifungal drug resistance. *Annals of the New York Academy of Sciences*, 1354(1), 1-11.

Perlman, R.L. (2009). Life histories of pathogen populations. *International Journal of Infectious Diseases,* 13(2), 121-124.

Perumal, P., Mekala, S. & Chaffin, W.L. (2007). Role for cell density in antifungal drug resistance in *Candida albicans* biofilms. *Antimicrobial Agents and Chemotherapy,* 51(7), 2454-2463.

Pfaller, M., Messer, S., Hollis, R., Boyken, L., Tendolkar, S., Kroeger, J. & Diekema, D. (2009). Variation in susceptibility of bloodstream isolates of *Candida glabrata* to fluconazole according to patient age and geographic location in the United States in 2001 to 2007. *Journal of Clinical Microbiology,* 47(10), 3185-3190.

Pfaller, M.A., Castanheira, M., Lockhart, S.R. & Jones, R.N. (2012). *Candida glabrata*: multidrug resistance and increased virulence in a major opportunistic fungal pathogen. *Current Fungal Infection Reports,* 6(3), 154-164.

Pfeiffer, T., Schuster, S. & Bonhoeffer, S. (2001). Cooperation and competition in the evolution of ATP-producing pathways. *Science,* 292(5516), 504-507.

Pham, C.D., Iqbal, N., Bolden, C.B., Kuykendall, R.J., Harrison, L.H., Farley, M.M., Schaffner, W., Beldavs, Z.G., Chiller, T.M., Park, B.J., Cleveland, A.A. & Lockhart, S.R. (2014). Role of *FKS* Mutations in *Candida glabrata*: MIC values, echinocandin resistance, and multidrug resistance. *Antimicrobial Agents and Chemotherapy,* 58(8), 4690-4696.

Pirt, S. (1965). The maintenance energy of bacteria in growing cultures. *Proceedings of the Royal Society of London B: Biological Sciences,* 163(991), 224-231.

Postma, E. R. I. K., Kuiper, A., Tomasouw, W. F., Scheffers, W. A., & Van Dijken, J. P. (1989a). Competition for glucose between the yeasts *Saccharomyces cerevisiae* and *Candida utilis*. *Applied and Environmental Microbiology*, 55(12), 3214-3220.

Postma, E., Verduyn, C., Scheffers, W.A. & Van Dijken, J.P. (1989b). Enzymic analysis of the crabtree effect in glucose-limited chemostat cultures of *Saccharomyces cerevisiae*. *Applied and Environmental Microbiology,* 55(2), 468-477.

Proctor, R.A., Van Langevelde, P., Kristjansson, M., Maslow, J.N. & Arbeit, R.D. (1995). Persistent and relapsing infections associated with small-colony variants of *Staphylococcus aureus*. *Clinical Infectious Diseases,* 20(1), 95-102.

Proctor, R.A., Von Eiff, C., Kahl, B.C., Becker, K., Mcnamara, P., Herrmann, M. & Peters, G. (2006). Small colony variants: a pathogenic form of bacteria that facilitates persistent and recurrent infections. *Nature Reviews Microbiology,* 4(4), 295-305.

Promega. (2009). Wizard® SV Gel and PCR Clean-Up System: Quick Protocol. [pdf]. Madison: Promega Corporation. Available at: https://www.promega.co.uk/resources/protocols/technical-bulletins/101/wizard-sv-gel-and-pcr-cleanup-system-protocol/ [Accessed 20 Jun. 17].

Promega. (2014). GoTaq® G2 Green Master Mix Certificate of Analysis 9PIM782. [pdf]. Madison: Promega Corporation. Available at: https://www.promega.co.uk/resources/protocols/product-information-sheets/g/gotaq-g2-green-master-mix-protocol/ [Accessed 20 Jun. 17].

Pukkila-Worley, R., Peleg, A.Y., Tampakakis, E. & Mylonakis, E. (2009). *Candida albicans* hyphal formation and virulence assessed using a *Caenorhabditis elegans* infection model. *Eukaryotic Cell,* 8(11), 1750-1758.

R Core Team, (2016, 2017). R: A language and environment for statistical computing. R Foundation for Statistical Computing, Vienna, Austria. URL https://www.R-project.org/.

Rainey, P.B., Buckling, A., Kassen, R. & Travisano, M. (2000). The emergence and maintenance of diversity: insights from experimental bacterial populations. *Trends in Ecology and Evolution,* 15(6), 243-247.

Rainey, P.B. & Travisano, M. (1998). Adaptive radiation in a heterogeneous environment. *Nature,* 394(6688), 69-72.

Ramadhan, A. & Hegedus, E. (2005). Survivability of vancomycin resistant enterococci and fitness cost of vancomycin resistance acquisition. *Journal of Clinical Pathology,* 58(7), 744-746.

Ratcliffe, N. A. (1985). Invertebrate immunity—a primer for the non-specialist. *Immunology Letters*, 10(5), 253-270.

Read, A.F., Day, T. & Huijben, S. (2011). The evolution of drug resistance and the curious orthodoxy of aggressive chemotherapy. *Proceedings of the National Academy of Sciences,* 108(Supplement 2), 10871-10877.

Reding-Roman, C., Hewlett, M., Duxbury, S., Gori, F., Gudelj, I. & Beardmore, R. (2017). The unconstrained evolution of fast and efficient antibiotic-resistant bacterial genomes. *Nature Ecology & Evolution,* 1(3), 0050.

Riggsby, W., Torres-Bauza, L., Wills, J. & Townes, T. (1982). DNA content, kinetic complexity, and the ploidy question in *Candida albicans*. *Molecular and Cellular Biology,* 2(7), 853-862.

Ritz, C., Baty, F., Streibig, J.C. & Gerhard, D. (2015). Dose-response analysis using R. *PloS One,* 10(12), e0146021.

Rodaki, A., Bohovych, I.M., Enjalbert, B., Young, T., Odds, F.C., Gow, N.A. & Brown, A.J. (2009). Glucose promotes stress resistance in the fungal pathogen *Candida albicans*. *Molecular Biology of the Cell,* 20(22), 4845-4855.

Rodrigues, C.F., Silva, S. & Henriques, M. (2014). *Candida glabrata*: a review of its features and resistance. *European Journal of Clinical Microbiology and Infectious Diseases,* 33(5), 673.

Roemhild, R., Barbosa, C., Beardmore, R.E., Jansen, G. & Schulenburg, H. (2015). Temporal variation in antibiotic environments slows down resistance evolution in pathogenic *Pseudomonas aeruginosa*. *Evolutionary Applications,* 8(10), 945-955.

Roetzer, A., Gabaldon, T. & Schuller, C. (2011). From *Saccharomyces cerevisiae* to *Candida glabrata* in a few easy steps: important adaptations for an opportunistic pathogen. *FEMS Microbiology Letters,* 314(1), 1-9.

Roetzer, A., Gregori, C., Jennings, A.M., Quintin, J., Ferrandon, D., Butler, G., Kuchler, K., Ammerer, G. & Schuller, C. (2008). *Candida glabrata* environmental stress response involves *Saccharomyces cerevisiae* Msn2/4 orthologous transcription factors. *Molecular Microbiology,* 69(3), 603-620.

Rossoni, R.D., Barbosa, J.O., Vilela, S.F., Dos Santos, J.D., De Barros, P.P., Prata, M.C., Anbinder, A.L., Fuchs, B.B., Jorge, A.O., Mylonakis, E. & Junqueira, J.C. (2015). Competitive interactions between *C. albicans, C. glabrata* and *C. krusei* during biofilm formation and development of experimental candidiasis. *PloS One,* 10(7), e0131700.

Rozen, D.E., Mcgee, L., Levin, B.R. & Klugman, K.P. (2007). Fitness costs of fluoroquinolone resistance in *Streptococcus pneumoniae*. *Antimicrobial Agents and Chemotherapy,* 51(2), 412-416.

Rozpedowska, E., Galafassi, S., Johansson, L., Hagman, A., Piskur, J. & Compagno, C. (2011). *Candida albicans* - a pre-whole genome duplication yeast - is predominantly aerobic and a poor ethanol producer. *FEMS Yeast Research,* 11(3), 285-291.

Saiman, L., Ludington, E., Dawson, J.D., Patterson, J.E., Rangel-Frausto, S., Wiblin, R.T., Blumberg, H.M., Pfaller, M., Rinaldi, M. & Edwards, J.E. (2001). Risk factors for *Candida* species colonization of neonatal intensive care unit patients. *The Pediatric Infectious Disease Journal,* 20(12), 1119-1124.

Saleem, M., (2015). Microbiome Community Ecology: Fundamentals and Applications [online]. Switzerland: Springer International Publishing. Available from: https://books.google.co.uk/books?id=8vVNBgAAQBAJ&pg=PR2&lpg=PR2&dq=Microbiome+Community+Ecology:+Fundamentals+and+Applications&source=bl&ots=ac-_-3YOdt&sig=-yQPuwDksTlPGn_TqMHeM_fP08c&hl=en&sa=X&ei=AugJVbyfN9TVarSjgMAN&ved=0CDsQ6AEwBQ#v=onepage&q=Microbiome%20Community%20Ecology%3A%20Fundamentals%20and%20Applications&f=false [Accessed 18 March 2015].

Samaranayake, L. P., MacFarlane, T. W., & Williamson, M. I. (1987). Comparison of Sabouraud dextrose and Pagano-Levin agar media for detection and isolation of yeasts from oral samples. *Journal of Clinical Microbiology*, 25(1), 162-164.

Samaranayake, Y.H. & Samaranayake, L. (1994). *Candida krusei*: biology, epidemiology, pathogenicity and clinical manifestations of an emerging pathogen. *Journal of Medical Microbiology,* 41(5), 295-310.

Sanglard, D. (2016). Emerging threats in antifungal-resistant fungal pathogens. *Frontiers in Medicine (Lausanne),* 3(1), 1-10.

Sanglard, D., Ischer, F. & Bille, J. (2001). Role of ATP-binding-cassette transporter genes in high-frequency acquisition of resistance to azole antifungals in *Candida glabrata*. *Antimicrobial Agents and Chemotherapy,* 45(4), 1174-1183.

Sanglard, D. & Odds, F.C. (2002). Resistance of *Candida* species to antifungal agents: molecular mechanisms and clinical consequences. *The Lancet Infectious Diseases,* 2(2), 73-85.

Santos, R., Costa, C., Mil-Homens, D., Romão, D., Carvalho, C. C., Pais, P., ... & Teixeira, M. C. (2017). The multidrug resistance transporters CgTpo1_1 and CgTpo1_2 play a role in virulence and biofilm formation in the human pathogen *Candida glabrata. Cellular Microbiology*, 19(5), 1-13.

Santos, J.D., Piva, E., Vilela, S.F., Jorge, A.O. & Junqueira, J.C. (2016). Mixed biofilms formed by *C. albicans* and non-*albicans* species: a study of microbial interactions. *Brazilian Oral Research,* 30(1), 1-8.

Santos, M.A., Gomes, A.C., Santos, M.C., Carreto, L.C. & Moura, G.R. (2011). The genetic code of the fungal CTG clade. *Comptes Rendus Biologies,* 334(8-9), 607-611.

Schmidt, W., Kuhlmann, W. & Schügerl, K. (1985). Automated determination of glucose in fermentation broths with p-hydroxy-benzoic-acid hydrazide (p-HBAH). *Applied Microbiology and Biotechnology,* 21(1), 78-84.

Schwarzmüller, T., Ma, B., Hiller, E., Istel, F., Tscherner, M., Brunke, S., Ames, L., Firon, A., Green, B. & Cabral, V. (2014). Systematic phenotyping of a large-scale *Candida glabrata* deletion collection reveals novel antifungal tolerance genes. *PLoS Pathogens,* 10(6), e1004211.

Scorzoni, L., De Lucas, M.P., Mesa-Arango, A.C., Fusco-Almeida, A.M., Lozano, E., Cuenca-Estrella, M., Mendes-Giannini, M.J. & Zaragoza, O. (2013). Antifungal efficacy during *Candida krusei* infection in non-conventional models correlates with the yeast in vitro susceptibility profile. *PloS One,* 8(3), e60047.

Scully, L. R., & Bidochka, M. J. (2005). Serial passage of the opportunistic pathogen *Aspergillus flavus* through an insect host yields decreased saprobic capacity. *Canadian Journal of Microbiology*, 51(2), 185-189.

Segal, E. (2005). *Candida*, still number one–what do we know and where are we going from there? *Mycoses,* 48(Supplement 1), 3-11.

Shapiro, R.S. & Cowen, L.E. (2012). Uncovering cellular circuitry controlling temperature-dependent fungal morphogenesis. *Virulence,* 3(4), 400-404.

Shapiro, R.S., Robbins, N. & Cowen, L.E. (2011). Regulatory circuitry governing fungal development, drug resistance, and disease. *Microbiology and Molecular Biology Reviews,* 75(2), 213-267.

Shen, J., Cowen, L.E., Griffin, A.M., Chan, L. & Köhler, J.R. (2008). The *Candida albicans* pescadillo homolog is required for normal hypha-to-yeast morphogenesis and yeast proliferation. *Proceedings of the National Academy of Sciences,* 105(52), 20918-20923.

Shields, R. K., Nguyen, M. H., Press, E. G., Kwa, A. L., Cheng, S., Du, C., & Clancy, C. J. (2012). The presence of an *FKS* mutation rather than MIC is an independent risk factor for failure of echinocandin therapy among patients with invasive candidiasis due to *Candida glabrata*. *Antimicrobial Agents and Chemotherapy*, 56(9), 4862-4869.

Sibley, C.D., Duan, K., Fischer, C., Parkins, M.D., Storey, D.G., Rabin, H.R. & Surette, M.G. (2008). Discerning the complexity of community interactions

using a *Drosophila* model of polymicrobial infections. *PLoS Pathogens,* 4(10), e1000184.

Silva, S., Henriques, M., Hayes, A., Oliveira, R., Azeredo, J. & Williams, D.W. (2011). *Candida glabrata* and *Candida albicans* co-infection of an in vitro oral epithelium. *Journal of Oral Pathology & Medicine,* 40(5), 421-427.

Silva, S., Henriques, M., Hayes, A., Oliveira, R., Azeredo, J. & Williams, D.W. (2011). *Candida glabrata* and *Candida albicans* co-infection of an *in vitro* oral epithelium. *Journal of Oral Pathology and Medicine,* 40(5), 421-427.

Singh, R., Ray, P., Das, A. & Sharma, M. (2009). Role of persisters and small-colony variants in antibiotic resistance of planktonic and biofilm-associated *Staphylococcus aureus*: an *in vitro* study. *Journal of Medical Microbiology,* 58(8), 1067-1073.

Singh-Babak, S.D., Babak, T., Diezmann, S., Hill, J.A., Xie, J.L., Chen, Y.L., Poutanen, S.M., Rennie, R.P., Heitman, J. & Cowen, L.E. (2012). Global analysis of the evolution and mechanism of echinocandin resistance in *Candida glabrata*. *PLoS Pathogens,* 8(5), e1002718.

Smith, K., Mccoy, K.D. & Macpherson, A.J. (2007). Use of axenic animals in studying the adaptation of mammals to their commensal intestinal microbiota. *Seminars in Immunology*, 19(2), 59-69.

Smith, V.H. & Holt, R.D. (1996). Resource competition and within-host disease dynamics. *Trends in Ecology and Evolution,* 11(9), 386-389.

Sokol-Anderson, M., Sligh, J. E., Elberg, S., Brajtburg, J., Kobayashi, G. S., & Medoff, G. (1988). Role of cell defense against oxidative damage in the resistance of *Candida albicans* to the killing effect of amphotericin B. *Antimicrobial Agents and Chemotherapy,* 32(5), 702-705.

Soll DR. Mixed Mycotic Infections. In: Brogden KA, Guthmiller JM, editors. Polymicrobial Diseases. Washington (DC): ASM Press; 2002. Chapter 17. Available from: https://www.ncbi.nlm.nih.gov/books/NBK2485/ [Accessed 22 September 2017].

Stewart, F. M., & Levin, B. R. (1973). Partitioning of resources and the outcome of interspecific competition: a model and some general considerations. *The American Naturalist*, 107(954), 171-198.

Sudbery, P.E. (2011). Growth of *Candida albicans* hyphae. *Nature Reviews Microbiology,* 9(10), 737-748.

Sugita, T. & Nakase, T. (1999). Non-universal usage of the leucine CUG codon and the molecular phylogeny of the genus *Candida*. *Systematic and Applied Microbiology,* 22(1), 79-86.

Superti, S.V., Martins, D.D.S., Caierão, J., Soares, F.D.S., Prochnow, T. & Zavascki, A.P. (2009). Indications of carbapenem resistance evolution through heteroresistance as an intermediate stage in *Acinetobacter baumannii* after carbapenem administration. *Revista do Instituto de Medicina Tropical de São Paulo,* 51(2), 111-113.

Tampakakis, E., Peleg, A.Y. & Mylonakis, E. (2009). Interaction of *Candida albicans* with an intestinal pathogen, *Salmonella enterica* serovar *Typhimurium*. *Eukaryotic Cell,* 8(5), 732-737.

Tati, S., Davidow, P., Mccall, A., Hwang-Wong, E., Rojas, I.G., Cormack, B. & Edgerton, M. (2016). *Candida glabrata* binding to *Candida albicans* hyphae enables its development in oropharyngeal candidiasis. *PLoS Pathogens,* 12(3), e1005522.

Thein, Z., Seneviratne, C., Samaranayake, Y. & Samaranayake, L. (2009). Community lifestyle of *Candida* in mixed biofilms: a mini review. *Mycoses,* 52(6), 467-475.

Thein, Z.M., Samaranayake, Y.H. & Samaranayake, L.P. (2007). Characteristics of dual species *Candida* biofilms on denture acrylic surfaces. *Archives of Oral Biology,* 52(12), 1200-1208.

Thompson, G.R., Wiederhold, N.P., Vallor, A.C., Villareal, N.C., Lewis, J.S. & Patterson, T.F. (2008). Development of caspofungin resistance following prolonged therapy for invasive candidiasis secondary to *Candida glabrata* infection. *Antimicrobial Agents and Chemotherapy,* 52(10), 3783-3785.

Thornton, H. (1922). On the development of a standardised agar medium for counting soil bacteria, with especial regard to the repression of spreading colonies. *Annals of Applied Biology,* 9(3-4), 241-274.

Toprak, E., Veres, A., Michel, J.B., Chait, R., Hartl, D.L. & Kishony, R. (2011). Evolutionary paths to antibiotic resistance under dynamically sustained drug selection. *Nature Genetics,* 44(1), 101-105.

Turner, P.E., Souza, V. & Lenski, R.E. (1996). Tests of ecological mechanisms promoting the stable coexistence of two bacterial genotypes. *Ecology,* 77(7), 2119-2129.

Underhill, D.M. & Iliev, I.D. (2014). The mycobiota: interactions between commensal fungi and the host immune system. *Nature Reviews Immunology,* 14(6), 405-416.

United Kingdom National Culture Collection, (2000). Catalogue of the UK National Culture Collection (UKNCC). 1st ed. Available from: http://download.fa.itb.ac.id/filenya/Handout%20Kuliah/Mikrobiologi%20Farmasi%20STF/Katalog%20FUNGI.pdf [Accessed 14 March 2015].

Uppuluri, P., Dinakaran, H., Thomas, D.P., Chaturvedi, A.K. & Lopez-Ribot, J.L. (2009). Characteristics of *Candida albicans* biofilms grown in a synthetic urine medium. *Journal of Clinical Microbiology,* 47(12), 4078-4083.

Valero-Jiménez, C.A., Kan, J.A., Koenraadt, C.J., Zwaan, B.J. & Schoustra, S.E. (2017). Experimental evolution to increase the efficacy of the entomopathogenic fungus *Beauveria bassiana* against malaria mosquitoes: Effects on mycelial growth and virulence. *Evolutionary Applications,* 10(5), 433-443.

Van Urk, H., Postma, E., Scheffers, W.A. & Van Dijken, J.P. (1989). Glucose transport in Crabtree-positive and Crabtree-negative yeasts. *Microbiology,* 135(9), 2399-2406.

Van Urk, H., Voll, W. L., Scheffers, W. A., Van Dijken, J. P., (1990). Transient-state analysis of metabolic fluxes in Crabtree-positive and Crabtree-negative yeasts. *Applied and Environmental Microbiology*, 56(1), 281-287.

Vandermeer, J. (2010) How populations grow: the exponential and logistic equations. *Nature Education Knowledge*, 3(10),15. Available from: https://www.nature.com/scitable/knowledge/library/how-populations-grow-the-exponential-and-logistic-13240157 [Accessed 14 December 2017]

Vasi, F., Travisano, M. & Lenski, R.E. (1994). Long-term experimental evolution in *Escherichia coli*. II. Changes in life-history traits during adaptation to a seasonal environment. *The American Naturalist,* 144(3), 432-456.

Vellend, M., (2010). Conceptual synthesis in community ecology. *The Quarterly Review of Biology*, 85(2), 183-206.

Verduyn, C., Stouthamer, A.H., Scheffers, W.A. & Dijken, J.P. (1991). A theoretical evaluation of growth yields of yeasts. *Antonie van Leeuwenhoek,* 59(1), 49-63.

Verduyn, C., Zomerdijk, T.P., Dijken, J.P. & Scheffers, W.A., (1984). Continuous measurement of ethanol production by aerobic yeast suspensions with an enzyme electrode. *Applied Microbiology and Biotechnology,* 19(3), 181-185.

Verhulst, P.F. (1845). Recherches mathématiques sur la loi d'accroissement de la population. *Nouveaux Mémoires de L'académie Royale des Sciences et Belles-lettres de Bruxelles,* 18(1), 14-54.

Vincent, B.M., Lancaster, A.K., Scherz-Shouval, R., Whitesell, L. & Lindquist, S. (2013). Fitness trade-offs restrict the evolution of resistance to amphotericin B. *PLoS Biology,* 11(10), e1001692.

Vogel, H., Altincicek, B., Glöckner, G. & Vilcinskas, A. (2011). A comprehensive transcriptome and immune-gene repertoire of the lepidopteran model host *Galleria mellonella*. *BMC Genomics,* 12(1), 308.

Voyles, J., Johnson, L.R., Briggs, C.J., Cashins, S.D., Alford, R.A., Berger, L., Skerratt, L.F., Speare, R. & Rosenblum, E.B. (2014). Experimental evolution alters the rate and temporal pattern of population growth in *Batrachochytrium dendrobatidis*, a lethal fungal pathogen of amphibians. *Ecology and Evolution,* 4(18), 3633-3641.

Wahyuningsih, R., Freisleben, H.-J., Sonntag, H.-G. & Schnitzler, P. (2000). Simple and rapid detection of *Candida albicans* DNA in serum by PCR for diagnosis of invasive candidiasis. *Journal of Clinical Microbiology,* 38(8), 3016-3021.

Wang, X., Kang, Y., Luo, C., Zhao, T., Liu, L., Jiang, X., Fu, R., An, S., Chen, J. & Jiang, N. (2014). Heteroresistance at the single-cell level: adapting to antibiotic stress through a population-based strategy and growth-controlled interphenotypic coordination. *MBio,* 5(1), 1-9.

Watts, G. (2014). UK declares war on antimicrobial resistance. *The Lancet,* 384(9941), 391.

Weber, K., Schulz, B. & Ruhnke, M. (2010). The quorum-sensing molecule E,E-farnesol--its variable secretion and its impact on the growth and metabolism of *Candida* species. *Yeast,* 27(9), 727-739.

Weger, S., Ganji, A., Clemons, K., Byron, J., Minn, Y. & Stevens, D. (2002). Correlation of the frequency of petite formation by isolates of *Saccharomyces cerevisiae* with virulence. *Medical Mycology,* 40(2), 161-168.

Whelan, W., Simon, S., Beneke, E. & Rogers, A. (1984). Auxotrophic variants of *Torulopsis glabrata. FEMS Microbiology Letters,* 24(1), 1-4.

Whiley, R.A., Sheikh, N.P., Mushtaq, N., Hagi-Pavli, E., Personne, Y., Javaid, D. & Waite, R.D. (2014). Differential potentiation of the virulence of the *Pseudomonas aeruginosa* cystic fibrosis liverpool epidemic strain by oral commensal *Streptococci*. *Journal of Infectious Disease,* 209(5), 769-780.

Wiederhold, N. P. (2009). Paradoxical echinocandin activity: a limited in vitro phenomenon? *Medical Mycology*, 47(Supplement 1), S369-S375.

Williamson PR (1994) Biochemical and molecular characterization of the diphenol oxidase of *Cryptococcus neoformans*: identification as a laccase. *Journal of Bacteriology*, 176(3), 656–664.

Wisplinghoff, H., Bischoff, T., Tallent, S.M., Seifert, H., Wenzel, R.P. & Edmond, M.B. (2004). Nosocomial bloodstream infections in US hospitals: analysis

of 24,179 cases from a prospective nationwide surveillance study. *Clinical Infectious Diseases,* 39(3), 309-317.

World Health Organisation (WHO), (2016). Global Report on Diabetes. 1st ed. [pdf] France: WHO, p.6. Available at http://www.who.int/diabetes/global-report/en/ [Accessed 1 Jul. 2017].

World Health Organisation Committee On Diabetes Mellitus. Second Technical Report, Geneva: World Health Organisation, 1980, Series 646: 10.

Yapar, N. (2014). Epidemiology and risk factors for invasive candidiasis. *Therapeutics and Clinical Risk Management,* 10(1), 95-105.

Yin, Z., Wilson, S., Hauser, N.C., Tournu, H., Hoheisel, J.D. & Brown, A.J. (2003). Glucose triggers different global responses in yeast, depending on the strength of the signal, and transiently stabilizes ribosomal protein mRNAs. *Molecular Microbiology,* 48(3), 713-724.

Ying, B.-W., Honda, T., Tsuru, S., Seno, S., Matsuda, H., Kazuta, Y. & Yomo, T. (2015). Evolutionary consequence of a trade-off between growth and maintenance along with ribosomal damages. *PloS One,* 10(8), e0135639.

Zaiontz C. (2015) Real Statistics Using Excel. www.real-statistics.com [Accessed 21 April 2017].

Zakrzewska, A., Van Eikenhorst, G., Burggraaff, J.E., Vis, D.J., Hoefsloot, H., Delneri, D., Oliver, S.G., Brul, S. & Smits, G.J. (2011). Genome-wide analysis of yeast stress survival and tolerance acquisition to analyze the central trade-off between growth rate and cellular robustness. *Molecular Biology of the Cell,* 22(22), 4435-4446.

Zhou, P. B., & Thiele, D. J. (1991). Isolation of a metal-activated transcription factor gene from *Candida glabrata* by complementation in *Saccharomyces cerevisiae*. *Proceedings of the National Academy of Sciences*, *88*(14), 6112-6116.

Zimbeck, A.J., Iqbal, N., Ahlquist, A.M., Farley, M.M., Harrison, L.H., Chiller, T. & Lockhart, S.R. (2010). *FKS* mutations and elevated echinocandin MIC

values among *Candida glabrata* isolates from US population-based surveillance. *Antimicrobial Agents and Chemotherapy,* 54(12), 5042-5047.